Quantification of substrate metabolism in endurance athletes using microscopy techniques.

Emily F P Jevons

A thesis submitted in partial fulfilment of the requirements of Liverpool John Moores University for the degree of Doctor of Philosophy

November 2020

Abstract

Carbohydrate and lipid are important substrates during exercise, and their relative contribution is heavily dependent on exercise intensity and duration. Not only this, but it now appears that the utilisation of muscle glycogen and lipid (intramuscular triglyceride; IMTG) is specific to muscle fibre type and/or the subcellular location of these substrates. However, to date, our understanding of muscle substrate use stems largely from lab-based research. The first aim of this thesis was, therefore, to investigate muscle glycogen and IMTG utilisation on a fibre type and subcellular-specific basis in exercise undertaken in the field. The exercise-induced decrease in muscle glycogen and IMTG necessitates a replenishment of these substrates in the post-exercise period, where traditionally carbohydrate ingestion is the focus. However, the mechanisms regulating post-exercise IMTG resynthesis, especially in the face of carbohydrate ingestion is not well understood. Therefore, a second aim of this thesis was to examine the influence of post-exercise carbohydrate consumption on IMTG resynthesis and the muscle mechanisms regulating this.

Study 1 aimed to quantify glycogen and lipid utilisation in the *vastus lateralis* and *gastrocnemius* muscle of 11 recreationally active male runners during either steady state endurance exercise (10-mile trial) or high intensity interval exercise (8x800m trial) in a field-based training environment. Using transmission electron microscopy (TEM), this study identified 1) a preferential use of intramyofibrillar glycogen during exercise, independent of exercise trial, and 2) lipid utilisation occurred primarily in the intermyofibrillar region of type I fibres during steady state exercise. These data highlight a novel pattern of muscle glycogen and lipid utilisation during field-based exercise which is dependent on exercise intensity and duration.

Study 2 aimed to examine if immunofluorescence microscopy could be used to investigate changes in IMTG on a subcellular level, and additionally compared the agreement between immunofluorescence microscopy with TEM. This study continued the field-based 'theme' examining IMTG utilization during a competitive endurance event. ~1 hour of cross-country skiing in a field-based environment reduced IMTG

content in both type I and type IIa fibres, and in both the peripheral and central subcellular regions. When assessing the agreement between the two microscopy methods, it appears that immunofluorescence microscopy provides a suitable method to quantify IMTG content, but not LD morphology. Therefore, these data have important implications for future studies aiming to understand the mechanisms regulating subcellular LD pools. As such, this directly influenced the methodology for study 3 of this thesis.

Finally, study 3 aimed to investigate the hypothesis that post-exercise IMTG resynthesis would be accelerated under conditions of acute CHO restriction in elite endurance athletes, with a secondary aim to investigate changes in the distribution of perilipin proteins relative to LDs during exercise and in the post-exercise period. IMTG resynthesis was shown to occur rapidly by 4 h post-exercise in the central region of type I fibres following prolonged exercise in highly-trained individuals, independent of CHO availability. Further, increases in IMTG content following exercise preceded an increase in the association of LDs with regulatory perilipin proteins. These data, therefore, suggest that the perilipin proteins do not play a key role in the mechanism of IMTG synthesis, as originally believed.

Overall, this thesis expands our knowledge on the effect of exercise intensity and duration on substrate utilisation by investigating this on a fibre and subcellular basis, whilst also providing an insight into the field-based demands of training and competition on substrate utilization. Furthermore, the work deepens our understanding of the proposed role of the LD regulatory perilipin proteins during IMTG breakdown and resynthesis by providing key insights into the mechanisms underpinning IMTG resynthesis. From a research perspective, it is hoped that this thesis will elicit further field-based studies examining substrate utilisation on a fibre and region-specific basis

Acknowledgements

My PhD has been a very challenging and rewarding experience. It would not have been possible without numerous people, their help and support have played a huge part in getting me to where I am today.

Firstly, I would like to thank my Director of Studies Dr Sam Shepherd, I cannot put into words how grateful I am for your supervision over the past 4 years. Thank you for your support and patience, especially in times of self-doubt. Your guidance and knowledge has helped shape me as a researcher and I cannot thank you enough, for not only being a great supervisor but a great friend. I hope we can continue to work together in the future.

To my co-supervisor Dr Jules Strauss, if it wasn't for our conversation back in summer 2016 I would not be where I am now. I was working at my part-time job when I ran into you and we were discussing how much I enjoyed research. You asked "have you ever considered doing an MPhil?". That moment started the snowball that has been this PhD! So I thank you for this and your support throughout my PhD. I would also like to thank my other co-supervisor Prof James Morton, particularly for your guidance in writing up my thesis.

A thank you must go to our collaborators from the University of Southern Denmark, chapter 5 and 6 would not have been possible without them, and thank you to all participants who donated muscle! I also must mention those in the LSB office, there are too many of you to thank individually but thank you all for your company and listening to my numerous break downs, mostly due to the microscope not working! A special mention to Alex and Mark who frequently took me to Starbucks for coffee and cake to try and resolve the microscope meltdowns! Thank you also to the technicians within the LSB, especially Paul.

Thank you Prof Bill Baltzopoulos and Prof David Richardson for believing in me enough to partially support me with the Tom Reilly Memorial fund. Although I have had multiple jobs over the course of this PhD, a special thanks must go to the team at the University of Chester. For the past year being part of the RKTO team has been a life-line during this global pandemic! Providing me a source of normality and structure and the most amazing, supportive team of work colleagues I could have ever asked for whilst trying to balance work and a PhD. You have no idea how much you have helped!

To Jess, Nicky, Rachelle, Ellie, Alice and Lauz, thank you for listening to me get excited about science despite having no idea what I actually do! I could not have got through the last few years without you girls by my side. Kels and Elena, thank you for being there since we were doing our undergraduate degrees! I've enjoyed watching us all grow as academics and I can't wait to see all your success!

Mum, Dad, Nan, Pops, Joes family and of course my step-parents, thank you for your patience and knowing when to stop asking "how's the PhD going?", its ok, you can ask now and I won't look like I'm completely lost!

Joe, your love and support has saved me throughout this PhD and would not have been possible without you. Thank you for even learning what intramuscular triglycerides are so you could try and understand my research! I don't think I would have got here without you and I can't thank you enough.

Declaration

I declare that the work in this thesis, which I now submit for assessment on the programme of study leading to the award of Doctor of Philosophy is entirely my own and was carried out in accordance with the regulations of Liverpool John Moores University. Additionally, all attempts have been made to ensure that the work is original, does not, to the best of my knowledge, breach any copyright laws and has not been taken from the work of others, apart from the works that have been fully acknowledged within the text. Moreover, no portion of the work referred to in the thesis has been submitted in support of an application for another degree or qualification of this or any other university or other institute of learning.

Abstracts, Conference Communications and Publications

During the completion of this PhD at Liverpool John Moores University, data from this thesis resulted in the following abstracts and conference communications:

Jevons EFP, Gejl KD, Hvid LG, Frandsen U, Jensen K, Sahlin K, Strauss JA, Ørtenblad N, Shepherd SO. (2019) Skeletal muscle lipid droplets are resynthesized before being coated with perilipin proteins following prolonged exercise in elite male triathletes. Poster presentation, Copenhagen Biosciences: Central and Peripheral Control of Energy Metabolism, Copenhagen, Denmark.

Jevons EFP, Gejl KD, Hvid LG, Frandsen U, Jensen K, Sahlin K, Strauss JA, Ørtenblad N, Shepherd SO. (2019) Restricting carbohydrate during recovery from prolonged exercise does not affect intramuscular triglyceride resynthesis. Poster presentation, Cell Symposia: Exercise Metabolism, Stiges, Spain.

Jevons EFP, Gejl KD, Hvid LG, Frandsen U, Jensen K, Sahlin K, Strauss JA, Ørtenblad N, Shepherd SO. (2018) Restricting carbohydrate during recovery from prolonged exercise does not affect intramuscular triglyceride resynthesis. Oral presentation, European College of Sports Science, Dublin, Ireland.

Jevons EFP, Gejl KD, Hvid LG, Frandsen U, Jensen K, Sahlin K, Strauss JA, Ørtenblad N, Shepherd SO. (2018) Restricting carbohydrate during recovery from prolonged exercise does not affect intramuscular triglyceride resynthesis. Poster presentation, Womens Research Conference, Liverpool, UK.

Jevons EFP, Koh HCE, Neilsen J, Strauss JA, Morton JP, Holmberg H-C, Ørtenblad N, Shepherd SO. **(**2017) Intramuscular triglyceride utilisation during cross-country skiing: a comparison between immunofluorescence microscopy and transmission electron microscopy. Poster presentation, Graduate School Annual Conference, Liverpool John Moores University, UK.

Jevons EFP, Koh HCE, Neilsen J, Strauss JA, Morton JP, Holmberg H-C, Ørtenblad N, Shepherd SO. **(**2017) Intramuscular triglyceride utilisation during cross-country skiing: a comparison between immunofluorescence microscopy and transmission electron microscopy. Oral Presentation, British Associate of Sport and Exercise Student Conference, Plymouth, UK.

The following papers were published during the period of postgraduate study:

Strauss JA, Shepherd DA, Macey M, **Jevons EFP.** and Shepherd SO. (2020) 'Divergence exists in the subcellular distribution of intramuscular triglyceride in human

skeletal muscle dependent on the choice of lipid dye', *Histochemistry and Cell Biology, 154, 369–382*

Impey SG, **Jevons EFP,** Mees G, Cocks M, Strauss JA., Chester N, Laurie I, Target D, Hodgson A, Shepherd SO. and Morton JP. (2020) 'Glycogen Utilization during Running: Intensity, Sex, and Muscle-specific Responses**',** *Medicine and Science in Sports and Exercise,* 52, 9, 1966-1975.

Jevons EFP, Gejl KD, Strauss JA, Ørtenblad N. and Shepherd SO. (2020) 'Skeletal muscle lipid droplets are resynthesized before being coated with perilipin proteins following prolonged exercise in elite male triathletes', *AJP Endocrinology and Metabolism,* 318(3), E357-E370.

Whytock KL, **Jevons EFP**, Strauss, JA. and Shepherd SO. (2017) 'Under the microscope: Insights into limb-specific lipid droplet metabolism', *Journal of Physiology,* 595, 19, 6229-6230*.*

Contents Listing

Table of Contents

List of Figures

ACL	Acyl-CoA synthase
AGPAT	1-acyl-glycerol-3-phosphate-O-acyltransferase
AMPK	AMP-activated protein kinase
ATGL	Adipose triglyceride lipase
ADP	Adenosine diphosphate
ATP	Adenosine triphosphate
AMP	Adenosine monophosphate
BODIPY	Difluoro{2-[1-(3,5-dimethyl-2H-pyrrol-2-ylidene-N)ethyl]-3,5-dimethyl1H-pyrrolato-N }boron 493/503
CD36	Cluster of differentiation 36
cAMP	Cyclic AMP
CE_{est}	Estimated coefficient of error
CGI-58	Comparative gene-identification-58
CPT1	Carnitine palmitomyltransferase 1
CHO	Carbohydrate
CM	Central myofibrillar
DAG	Diacylglycerol
DD H_2O	Doubly-distilled water
DGAT	Diacylglycerol
DM	Dry mass
EM	Electron microscopy
EMCL	Extramyocellular lipid
FA	Fatty acids
FA-CoA	Fatty acyl-CoA
FAT/CD36	Fatty acid translocase
FFA	Free fatty acids
G1P	Glucose 1 Phosphate
G3P	Glycerol-3-phosphate
G6P	Glucose 6 Phosphate
GPAT	Glycerol-3-phosphate acyltransferase
GI	Glycaemic index
GLUT4	Glucose transporter 4

GLY	Glycogen
H-MRS	Proton magnetic resonance imaging
HR	Heart rate
H_2O	Water
HSL	Hormone sensitive lipase
IMCL	Intracellular lipid
IMF	Intermyofibrillar
IMTG	Intramuscular triglyceride
INTRA	Intramyofibrillar
LCC	Lin's concordance coefficient
LCFA	Long chain fatty acids
LD	Lipid droplet
LPA	Lysophosphatidic acid
MAG	Monoacylglyceride
MHC	Myosin heavy chain
MITO	Mitochondria
MRI	Magnetic resonance imaging
mRNA	Messenger RNA
MRS	Magnetic resonance spectroscopy
NMR	Nuclear magnetic resonance
ORO	Oil red O
PA	Phosphatidic acid
PAS	Periodic-shift staining
PBS	Phosphate buffer sulphate
PFK	Phosphofructokinase
Pi	Phosphate
PKA	cAMP-dependent protein kinase
PLIN	Perilipin
RER	Respiratory exchange ration
SR	Sarcoplasmic reticulum
SS	Subsarcolemmal
SM	Superficial myofibrillar region
TG	Triacylglycerol
TEM	Transmission electron microscopy

Chapter 1 – General Introduction

1.1 Overview

In 1967, a seminal study by Bergstrom *et al*, (1967) first reported that a carbohydrate (CHO)-rich diet enhanced muscle glycogen concentration to twice that observed following a normal mixed-macronutrient diet, and that the muscle glycogen stores were directly related to time-to-exhaustion during prolonged exercise using their novel muscle biopsy technique. Since then, the muscle biopsy technique has been heavily-utilised to demonstrate the importance of muscle glycogen in determining exercise capacity. Enhancing exogenous CHO availability (through gels, bars or drinks) can augment exercise performance (Cermak & Van Loon, 2013), mediated by liver (Gonzalez *et al*, 2015) and/or muscle glycogen sparing (Yasperlkis *et al*, 1993), maintaining plasma glucose and CHO oxidation rates (Coyle *et al*, 1986; McConell *et al*, 2000) and through direct effects on the central nervous system (Jeukendrup *et al*, 1997). Whilst high CHO diets may lead to greater rates of CHO oxidation, they also lead to reductions in fat oxidation (Coyle *et al*, 2001), which can be attributed to a decrease in the oxidation of both plasma-derived fatty acids and intramuscular triglyceride (IMTG) stores. IMTG are an important substrate during moderate-intensity exercise, particularly in the overnight fasted state, due to their close proximity to muscle mitochondria (Hoppeler *et al*, 1985). Further to this, research has demonstrated that diets high in CHO and low in fat can reduce IMTG storage after 1 week (Coyle *et al,* 2001), 48 h (Johnson *et al,* 2003) or 12 h (Startling *et al,* 1997). Taken together, it is evident that nutritional status influences intramuscular substrate turnover.

Since these studies in the 1960-1970's, various methods have been used to analyse muscle biopsies which have become the standard approach to examine glycogen

utilisation during exercise and can also be used to examine net changes in IMTG content. Multiple biopsies can be taken from one subject, quickly and safely when the correct preparation is in place (Shanely *et* al, 2014) and allows for direct measures of glycogen and IMTG to be examined pre, mid and post-exercise. As well as substrate utilisation, biopsies allow the assessment of muscle damage, mitochondrial biogenesis, enzyme activity, shifts in metabolites, protein synthesis and fibre typing (Shanely *et al*, 2014). Due to the insights provided by the data generated by muscle biopsy studies, current sports nutrition guidelines highlight the importance of CHO consumption 1) before exercise to optimise endogenous CHO stores, 2) during exercise to support fuelling and performance, and 3) after exercise to promote resynthesis of muscle glycogen stores. The overall effect of high CHO availability on endurance exercise performance has been well documented (Cermak & Van Loon 2013; Hawley *et al*, 1997), thereby leading to the practice of CHO loading to super-compensate muscle and liver glycogen stores in the days prior to an endurance event. Specifically, with the days prior to aiming to maximise muscle glycogen stores, whilst the CHO intake a few hours before an event will optimise liver glycogen.This became the foundation on which many additional nutritional strategies to optimise endurance performance are based (Burke *et al*, 2018). Overall, the main aim of the current CHO guidelines is to augment performance via sparing muscle glycogen, maintaining plasma glucose and CHO oxidation rates.

Despite decades of research examining glycogen utilisation during exercise, it is still difficult to provide guidelines for CHO consumption in relation to fuelling exact training sessions due to the varying metabolic demands of training and competition. Burke *et al*, (2018) highlighted that key CHO guidelines being used by athletic populations are

not underpinned by data from field-based environments but rather strict laboratory-based conditions. Subsequently, the majority of studies currently influencing sports nutrition guidelines to date are based on laboratory-based protocols (Burke *et al*, 2011). This restriction in our knowledge also applies to the utilisation of IMTG during exercise with our understanding again being underpinned by data from studies based under strict laboratory-based environments. The primary benefit of the laboratory-based protocols (e.g. fasted exercise at a fixed relative intensity for a given duration, such as 1 h at 70% VO_{2max}) is the rigorous control measures put in place to ensure reproducibility and reliability such as set workloads, intensities and durations. However, this does not take into account factors such as changes in terrain and incline, environmental influences such as wind speed and rain, all of which will influence pace, power, speed, the athlete's rate of perceived exhaustion, heart rate and the intensity of the training. Although an athlete may be prescribed a specific training session, external factors such as those listed will alter the metabolic demand of a training session considerably. Overall, laboratory-based studies provide complete control, which is not representative of training or competition in a field-based environment.

To date, much of the data on substrate utilisation during exercise examines changes in glycogen and IMTG on a whole muscle level. However, substrate availability in muscle is dependent on fibre type, with type I fibres containing three-fold greater lipid content than type II muscle fibres (Essen *et al,* 1975; Malenfant *et al,* 2001, Van Loon *et al,* 2003). Further to this, the subcellular location of substrates within the muscle fibre has been shown to be important in the context of storage and utilisation during exercise (Ørtenblad & Nielsen, 2015). For example, glycogen stored within the myofibrils (intramyofibrillar), rather than glycogen stored between the myofibrils

(intermyofibrillar) or at the outermost part of the myofibril (subsarcolemmal), is preferentially used during high intensity exercise (Nielsen *et al*, 2011). Lipid can also be examined in the subsarcolemmal and intermyofibrillar locations, though it is important to note the location of IMTG-containing lipid droplets is often in close proximity to the mitochondria, which is factor underpinning the importance of IMTG as a fuel source. Overall, fibre type and subcellular location are two important factors that should not be overlooked when investigating the field-based effect of exercise on both glycogen and IMTG utilisation during exercise. Using microscopy techniques such as transmission electron microscopy (TEM) and immunofluorescence confocal microscopy permits investigations of glycogen and lipid utilisation on a fibre-type and subcellular specific basis, though to date, there has been no comparison between the two methods.

CHO guidelines outline the appropriate strategies to maximise glycogen replenishment following exercise. Particularly during moderate-intensity exercise, though, IMTG is a key fuel source, and therefore resynthesis of the IMTG pool is also an important consideration. Moreover, recent proteomic and microscopy-based research has identified a distinct proteome associated with IMTG-containing lipid droplets. This observation has enhanced our understanding of the regulation of IMTG utilisation during exercise (Shaw *et al,* 2009; Shepherd *et al,* 2012; 2013; 2017; Gemmink *et al,* 2016). To date, there is a lack of substantial data on the post-exercise replenishment of IMTG, and as a consequence a lack of understanding of the mechanisms governing IMTG resynthesis following exercise.

1.2 Aims and objectives

Overall, this thesis aims to provides a microscopy-based insight into the field-based demands of training and competition on substrate utilization, whilst also providing key insights into the regulatory mechanisms underpinning IMTG resynthesis.

This aim will be achieved by completion of the following objectives:

a) Using TEM, assess fibre type and subcellular-specific muscle glycogen and lipid utilisation during two field-based training sessions (that differ by exercise intensity) typical of middle-to-long distance runners.

b) Examine fibre type and subcellular-specific muscle lipid utilisation during a field-based competitive cross-country skiing event using immunofluorescence microscopy.

c) Investigate the agreement between TEM and immunofluorescence microscopy techniques for investigating IMTG content and LD morphology on fibre and subcellular-specific basis.

d) Determine the effect of acute carbohydrate restriction on post-exercise IMTG repletion.

e) Examine the role of the perilipin proteins in both IMTG utilization during prolonged exercise and post-exercise IMTG resynthesis.

Chapter 2 – Literature Review

2.1 Background

In humans, the ability to exercise is dependent on the conversion of chemical energy to mechanical energy within skeletal muscle. This chemical energy is known as adenosine triphosphate (ATP), and our ability to resynthesise ATP during exercise relies mainly on the breakdown of carbohydrate (CHO) and fat sources. Indeed, sustaining exercise at a desired intensity depends upon a complex interaction between CHO and fat metabolism. It is now well established that a number of factors influence the relative utilisation of extra- and intramuscular CHO and fat, including exercise intensity, duration, sex, feeding status and training status.

The importance of CHO as a substrate for exercise performance has been recognised for around a century (Henriksson, 1977; Charlton & Crawford, 1997). One of the first studies to highlight this was from Levine *et al,* (1924), who measured blood glucose concentrations of a group of runners participating in the 1923 Boston Marathon and reported hypoglycaemia in most individuals following the race, suggesting that carbohydrate availability may be a cause of fatigue. In the 1924 Boston Marathon, runners were this time encouraged to consume CHO during the event, and this subsequently prevented hypoglycaemia. The development of the muscle biopsy technique in the 1960's was another landmark in understanding the importance of CHO for exercise performance. At this time, it was collectively shown that muscle glycogen is reduced in an intensity-dependent manner, and that a high CHO diet increases muscle glycogen storage and subsequently improves exercise performance (Bergstrom *et al,* 1967). The response of muscle glycogen to exercise and diet are now well established in both humans and animals (Bergstrom *et al,* 1967; Jensen & Richter, 2012). For over half a century it has been understood that glycogen stores

8

and CHO availability can compromise exercise capacity, despite other fuel sources being available (Bergstrom *et al,* 1967). Indeed, Bergstrom and Hultman (1966) demonstrated a strong correlation between endurance capacity during prolonged cycling and the availability of muscle glycogen, and when glycogen stores become exhausted there is an inability to continue exercise (Hermansen *et al,* 1967).

The muscle biopsy technique has not only been used to investigate CHO utilisation during exercise, but also intramuscular triglyceride (IMTG) stores. IMTG-containing lipid droplets are often located close to the muscle mitochondria (Hoppeler *et al*, 1985), but it was initially unclear whether IMTG made a significant contribution as a fuel source during exercise. Through the use of stable isotope methodology and the development of microscopy methods, it is now appreciated that IMTG are an important substrate during moderate-intensity exercise (Van Loon *et al,* 2004). Specifically, the development of immunofluorescence microscopy enabled the quantification of IMTG utilisation on a fibre type-specific basis (Essen *et al,* 1975; Howald *et al,* 1985), and this has now been extended to investigations of glycogen utilisation during exercise (Schaart *et al*, 2004). Moreover, the use of transmission electron microscopy (TEM) has provided additional detail, highlighting that different subcellular pools of lipid and glycogen are preferentially utilised during exercise (Neilsen *et al*, 2009; Ørtenblad *et al*, 2011). Collectively, these techniques have informed our understanding of the relative importance of intramuscular substrates as a fuel source during exercise of varying intensities and durations.

The present chapter aims to provide an overview of the background and key concepts concerning intramuscular substrate turnover during exercise and recovery. In this context, the storage and regulation of carbohydrate metabolism is first introduced,

which provides important background information for Chapter 4. Next, the storage and regulation of fat metabolism is outlined. This section specifically focuses on IMTG and the methods used to determine its role as a substrate during exercise (thereby providing critical background information for Chapters 4, 5 and 6). Moreover, the reader is provided a detailed overview of the regulation of IMTG metabolism, with a specific focus on the role of lipid droplet (LD) proteins, which provides important background information for Chapter 6. The review then closes by highlighting that laboratory-exercise trials which underpin exercise nutrition guidelines are grounded on are often limited in their translation and application to the field-based environment.

2.2 Factors affecting intramuscular substrate turnover

2.2.1 Exercise intensity

It is known that both fat (plasma free fatty acids and IMTG) and CHO (plasma glucose and muscle glycogen stores) are the primary substrates for oxidative phosphorylation and fuel aerobic ATP resynthesis in human skeletal muscle (Hargreaves & Spriet, 2012). Exercise intensity is a key factor in regulating substrate utilisation during exercise. At rest in the overnight fasted state, most energy is derived from the oxidation of adipose tissue-derived plasma free fatty acids (FFA). During low intensity exercise, energy expenditure is increased several fold in comparison to resting conditions. This initiates an increase in both CHO oxidation from plasma glucose and muscle glycogen stores, and fat oxidation from plasma free FA and other fat sources such as IMTG (van Loon *et al,* 2001). During moderate intensity exercise, fat oxidation is maximal (contributing ~50% to total energy expenditure) with an equal contribution from IMTG and plasma free FA. Indeed, maximal rates of lipid oxidation are considered to be around 65% VO_{2max}, although this is dependent on other factors such

as training status and nutritional status of the individual (Achten & Jeukendrup, 2004).

In regard to high-intensity exercise, Van Loon *et al,* (2001) demonstrated male cyclists completing 90 min of cycling in three 30 min stages of increasing exercise intensity (40, 55 and 75%Wmax), will lead to muscle glycogen becoming the major fuel source as exercise intensity increases, with a subsequent decrease in fat oxidation due to reductions in both plasma FFA and IMTG oxidation by 75% Wmax, (Fig. 2.1, Van Loon *et al,* 2001).
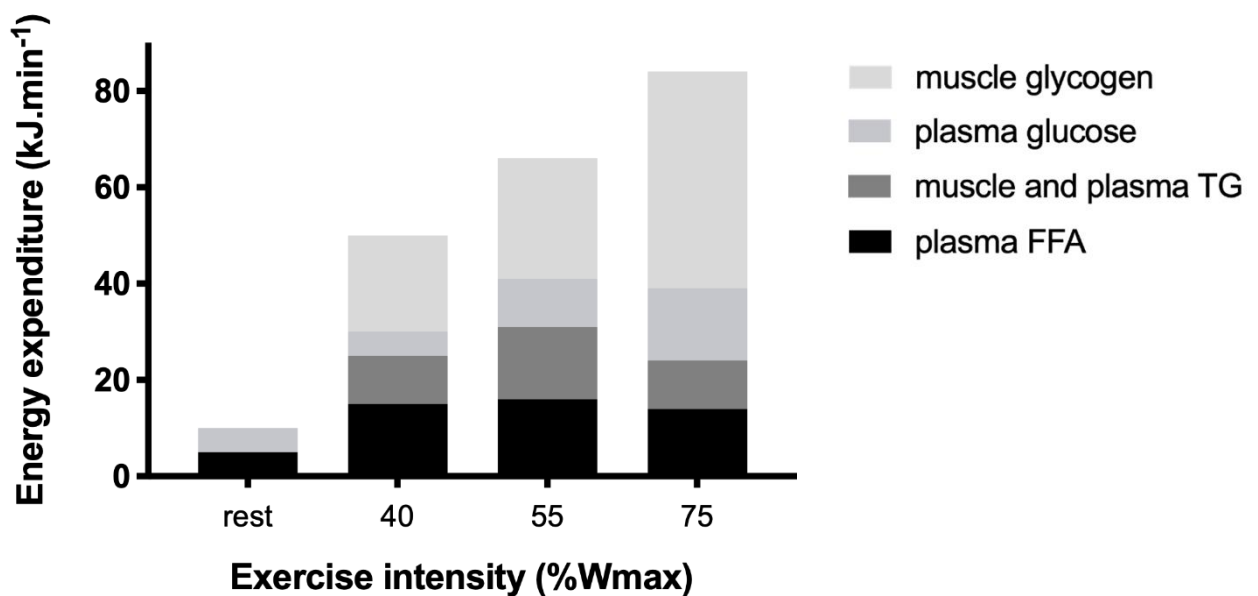
Figure 2.1. Energy expenditure as a function of exercise intensity (expressed as % of maximal workload capacity). The contribution of plasma glucose, muscle glycogen, plasma free fatty acid, and muscle and plasma triglycerides to total energy expenditure. Redrawn from van Loon *et al,* 2001.

Following high intensity exercise, there is a rapid increase in plasma glycerol concentrations suggesting that even during high intensity exercise the rate of adipose tissue lipolysis remains high. This shift between fat and CHO oxidation as exercise intensity increases could therefore be explained by a relative reduction in adipose

tissue blood flow, such that fatty acids liberated from triglyceride remain trapped within adipose tissue. As such, Romijn *et al,* (1993) examined plasma free FA and glycerol during exercise at 25, 65 and 85% VO_{2max}, witnessing reductions in plasma free FA at 85% VO_{2max} alongside increases in plasma glycerol. Stable isotope methodology demonstrated the rate of appearance of glycerol was not reduced at 85% VO_{2max} in comparison to 65% VO_{2max}, therefore suggesting the decrease in plasma FFA was due to a reduction in adipose tissue blood flow rather than a reduction in lipolysis. Further to this, investigations using an intravenous infusion of lipid and heparin during exercise at 85% VO_{2max}, thereby maintaining plasma free FA, was compared to control conditions (Romijn *et al,* 1995). There results indicated that lipid oxidation rates were enhanced with the lipid and heparin infusion in comparison to the control, though not to levels witnessed during exercise at 65% VO_{2max} (Romijn *et al,* 1995). Therefore, only half of the reduced lipid oxidation rates witnessed with increased exercise intensity could be explained by this reduction in FFA availability. A further potential mechanism to explain this shift between fat and CHO oxidation as exercise intensity increases, is that a high glycolytic flux during high-intensity exercise suppress long-chain FA oxidation (Dyck *et al,* 1993; Odland *et al,* 1998). Increases in glycolytic flux lead to an accumulation of acetyl-CoA (Constantin-Teodosiu *et al,* 1991; Dyck *et al,* 1993), subsequently causing increases in malonyl-CoA, which has been proposed to inhibit carnitine palmitomyltransferase I (CPT1), consequently supressing long-chain FA entry into the mitochondria. Though, due to lack of increases in malonyl-CoA in both rat and human skeletal muscle during high intensity exercise (Rasmussen & Winder, 1997; Odland *et al,* 1998; Dean *et al,* 2000), it has been questioned whether this mechanism actually functions as proposed. A further mechanism that could explain the reduction in fat oxidation during high intensity exercise includes the

availability of muscle carnitine. Carnitine is required for the long-chain FA to be transported through the inner mitochondrial membrane (Frtiz *et al*, 1955). The high rate of glycolysis during high-intensity exercise results in an increase in acetyl-CoA, which is then trapped by carnitine (creating acetyl-carnitine), thereby reducing free carnitine availability for long-chain mitochondrial FA transportation (Jeppesen & Kiens 2012).

2.2.2 Exercise duration

The duration of exercise is also known to effect substrate utilisation, even when exercise intensity remains constant. Prolonged exercise of a moderate intensity is associated with time-dependent reduction in CHO oxidation and subsequent increases in fat oxidation (Fig. 2.2, Watt *et al,* 2002; Romijn *et al*, 1993). After 1-2 h of exercise, there is a shift in substrate utilisation, with an increase in the oxidation of plasma FFA due to continuous mobilisation from adipose tissue stores, as shown in figure 2.2. During prolonged exercise, plasma FFA oxidation increases in parallel with decreases in CHO oxidation. This reduction in CHO oxidation in prolonged exercise is likely due to a reduction in muscle glycogen stores (Gollnick *et al*, 1974). The enhanced rate of fat oxidation is due to increases in catecholamine (i.e. adrenaline) and decreases in circulating insulin.
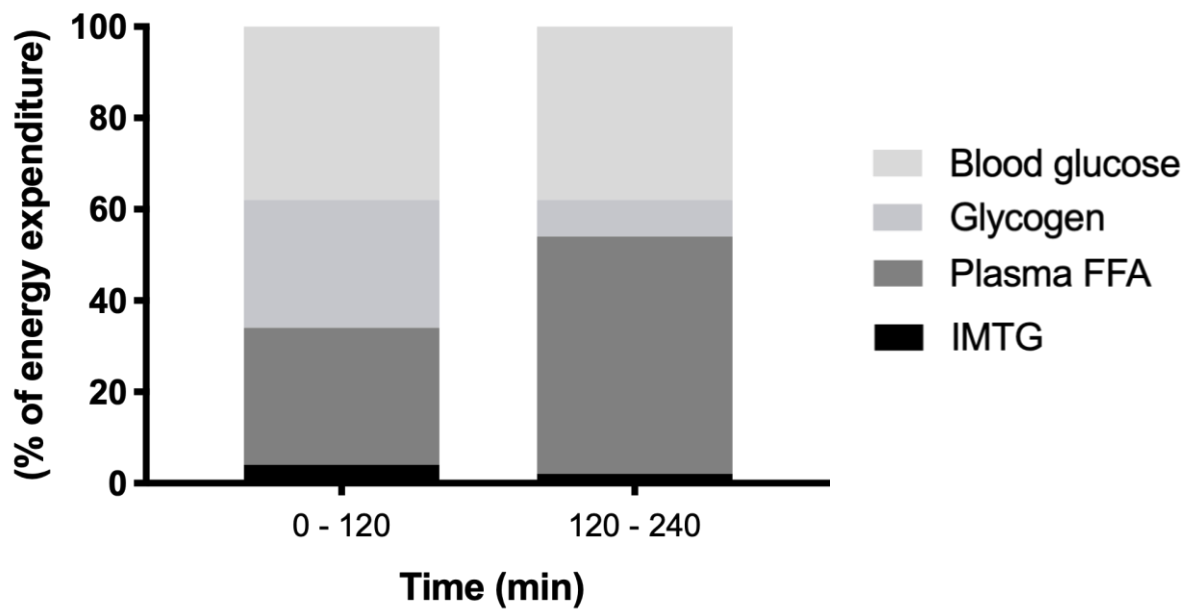
Figure 2.2. The contribution of endogenous and blood-borne substrates to energy production during 240 min of moderate intensity exercise in men. Adapted from Watt *et al,* (2002).

2.2.3 Training and nutritional status

As well as exercise intensity and duration, training status is also known to have an effect on substrate metabolism during exercise due to a number of physiological and metabolic adaptations. The aim of such adaptations is to improve homeostasis for a given exercise intensity and duration, therefore ultimately delaying fatigue. Regular endurance training, will lead to a reduced reliance on CHO as a substrate for exercise, whilst increasing reliance on lipid particularly during moderate-intensity exercise. As the reliance on CHO is decreased with exercise training, fat metabolism is therefore increased to enable this sparing of CHO sources (Henriksson, 1977; Turcotte *et al,* 1992; Kiens *et al,* 1993). Further to this, endurance training will increase the muscles capacity to store muscle glycogen and IMTG, which will thereby increase substrate availability during exercise.

Altering the diet of an individual has also been shown to modify substrate availability, both before, during and after exercise. For example, muscle glycogen availability impacts substrate metabolism, since it has been demonstrated that glycogen utilisation was increased during exercise at 45% VO_{2max} that began with high muscle glycogen concentrations, in comparison to exercise at 70% VO_{2max} started with much lower muscle glycogen concentrations (591 and 223 $mmol.kg^{-1}$ dw, respectively), despite the greater exercise intensity (Arkinstall *et al,* 2004). However, in the same study lipid oxidation was greatest when exercise began with reduced muscle glycogen stores, independent of exercise intensity. The effect of diet on IMTG in particular is discussed in further detail in section 2.10. This shift toward greater lipid oxidation when pre-exercise muscle glycogen levels are low is likely due to a combination of increased plasma FFA oxidation due to reduced glycogen availability, and increased adrenaline concentrations which favour lipid oxidation and lipolysis in comparison to conditions of high glycogen (Arkinstall *et al,* 2004). However, Roepstorff *et al,* (2005) observed minimal differences in plasma FFA availability and adrenaline following a pre-exercise meal and a subsequent glucose infusion during glycogen-depleted exercise, yet lipid oxidation was still enhanced. Therefore, regulation may lie within the muscle cell itself and specifically carnitine availability (since free carnitine levels were increased) may allow greater rates of lipid oxidation to occur (Roepstorff *et al,* (2005).

2.3 Carbohydrate metabolism

2.3.1 Carbohydrate storage

Within the body, CHO is stored as glycogen in the liver (~100g) and skeletal muscle (350 – 700g depending on diet and training status of the individual), and a small

amount (~5g) circulates in the blood as glucose. Hepatic glycogen storage is restricted due to the size of the liver itself. Because human skeletal muscle contributes ~20-30% of total body weight, the amount of glycogen stored in muscle can equate to three-to-four times more than the glycogen stored within the liver. Even so, both of these endogenous CHO stores are considered relatively small (~5% of total energy storage), which underpins the relationship between CHO availability and exercise performance with low carbohydrate availability often leading to reduced exercise capacity and/or performance (Bergstrom *et al,* 1967; Hermansen *et al,* 1967; Jensen & Richter, 2012)

In skeletal muscle, the importance of CHO stored as glycogen lies in its ability to be utilised without the presence of oxygen and its ability to be rapidly mobilised in the presence of elevated energy requirements. Glycogen itself is a branched polymer of glucose, which operates as an energy reserve for adenosine triphosphate (ATP) production within muscle and liver cells. Glycogen granules, also known as "glycosomes", are considered to be an independent metabolic unit. They are composed of protein-glycogen (Meyer *et al,* 1970), and can be found in three forms termed α- and β-granules and γ-particles (Drochmans, 1962; Rybicka, 1996). α-granules are found in the liver and made up of multiple β-granules. The β-granules in muscle are individual glycogen granules, which include several γ-particles (Prats *et al,* 2018), and are considered to be a rapid energy source. The β-granules measure ~20-30nm in diameter, whilst α- granules in the liver are up to 300nm in diameter (Drochmans, 1962; Rybicka, 1996), and are considered a much slower energy source (Sullivan *et al,* 2014). β-granules are known to be organised as concentric layers of glucose chains, also known as tiers. As such, the theoretical; maximum size/capacity

for an individual β-granule is 42nm, or 12 tiers (Shearer & Graham, 2004). The branched structure of glycogen molecules increases the surface area allowing large amounts of glucose to be stored without compromising cellular osmolality. The result is a vast quantity of readily-available substrate to be used to generate energy for the muscle and/or liver (Melendez-Hevia *et al*, 1993).

Beyond the structure of glycogen, it is important to note that the distribution of glycogen may differ between skeletal muscle fibre types. Using biochemical quantification, slow-twitch type I fibres, which are capable of prolonged activity, contain lower glycogen content at rest than type IIa fibres with ~ 303 and ~ 372 mmol.kg DM $^{-1}$ muscle glycogen, respectively (Tsintzas *et al,* 1995). In contrast, through the use of histochemical methodology, muscle glycogen at rest has been determined to not be substantially different between type I and type II fibres (Essen & Henriksson, 1974; Essen *et al,* 1975; Stellingwerff *et al,* 2007). The requirement to identify muscle fibre type is important due to distinct muscle fibre recruitment patterns from changes in exercise intensity and duration (Gollnick *et al,* 1974), as well as different modes of exercise such as running and cycling (Millet *et al,* 2009). In addition, it is now recognised that glycogen is located in distinct subcellular locations or compartments within muscle fibres. Optimal energy production requires a fast, efficient and continuous conversion of glycogen to ATP. The ATP-producing mitochondria are located between the myofibrils and beneath the sarcolemma (Ørtenblad & Stephenson, 2003). As such, glycogen and enzymes of the glycolytic pathway are localised in these specific regions of the muscle fibre. Evidence for compartmentalised glycogen metabolism first became apparent when studies demonstrated simultaneous synthesis and utilisation of glycogen through Carbon-13

nuclear magnetic resonance (^{13}C NMR) with infusion during aerobic contractions (Shulman & Rothman, 2001), and a preferential need for glycolytic ATP to support the activity of the Na$^+$-K$^+$ pumps within skeletal muscle (James *et al*, 1999).

Through the use of transmission electron microscopy (TEM), it is now known that glycogen particles are located in three distinct subcellular locations: 1) the intermyofibrillar (IMF) region, located between the myofibrils in close proximity to the sarcoplasmic reticulum and mitochondria, which contributes to ~75% of the cells total glycogen store, 2) the intramyofibrillar (INTRA) region, which is located within the myofibrils interspersed within the contractile filaments, and 3) the subsarcolemmal (SS) region of the cell which is located just beneath the surface membrane in close association with mitochondria, lipids and nuclei (Nielsen and Ørtenblad, 2011). The INTRA and SS regions account for the remaining 5 to 15% of the cell's total glycogen respectively (Figure 2.3).

Each of these glycogen pools may play a specific role in providing a substrate for energy production to fuel distinct processes within the skeletal muscle (Nielsen *et al*, 2009; Ørtenblad, *et al*, 2011), although at present this concept is not completely understood. Neverthless, it is now believed that the link between glycogen concentrations and muscle fatigue likely originates from an association specifically between INTRA glycogen and sarcoplasmic reticulum calcium release (SR Ca^{2+}) (Nielsen *et al*, 2009; 2014; Ørtenblad *et al*, 2011). Further to this, INTRA glycogen is preferentially depleted during prolonged exercise (Marchand *et al,* 2007; Nielsen *et al*, 2011), thus suggesting a potential explanation for the glycogen-dependent component in muscular fatigue (Ørtenblad *et al*, 2015). In support, Jensen *et al,* (2020) recently

showed that INTRA glycogen is the best predictor of time to exhaustion, but that SS glycogen was also reduced during exercise. SS glycogen may contribute energy to support Na^+-K^+ pump activity at the sarcolemma (Nielsen & Ørtenblad, 2013), and in this way spare the utilisation of INTRA glycogen to support SR Ca^{2+} release (Ørtenblad *et al,* 2015).
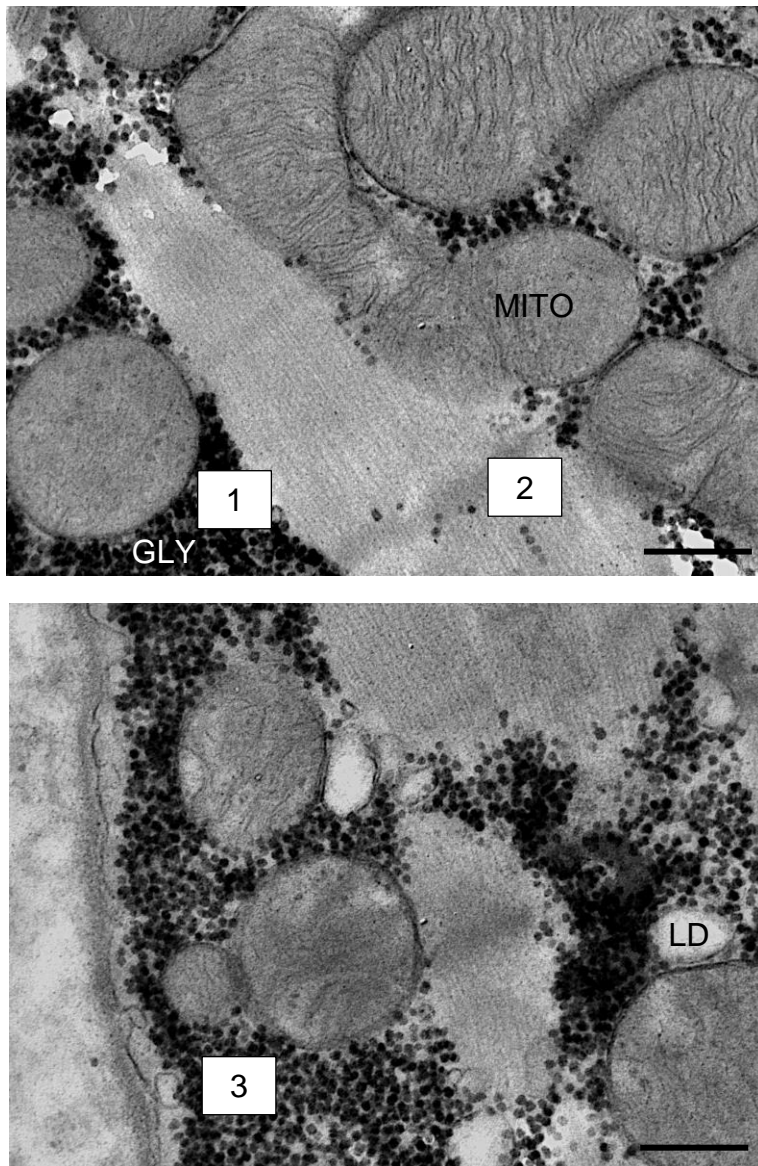
Figure 2.3. Images of a muscle fibre from the vastus lateralis muscle to demonstrate compartmental glycogen distribution. 1. Intermyofibrillar, 2. Intramyofibrillar and 3. Subsarcolemmal. Image taken at 36,000x. Scale bar = 0.5µm. MITO – mitochondria, GLY – glycogen granules, LD – lipid droplet.

2.3.2 Factors influencing carbohydrate storage

Diet and training status will greatly impact CHO storage. As already mentioned, low glycogen availability before exercise compromises exercise capacity, despite other fuel sources being available (Bergstrom *et al*, 1967). Adequate CHO consumption is now considered fundamental in the preparation for an event, with the days prior aiming to maximise muscle glycogen stores, whilst CHO intake a few hours before an event will optimise liver glycogen. When considering the days leading up to an event, the overriding message from the large number of studies investigating pre-exercise CHO consumption and/or CHO loading over the last 40 years, is that purposely consuming a large amount of CHO can improve exercise performance and capacity, particularly when exercise is longer than 90 min in duration by increasing glycogen storage (Hawley *et al*, 1997). More specifically, the exact amount of CHO in the diet will reflect clearly on resting muscle glycogen concentrations. For example, when deliberately withholding CHO after an evening training session, and completing a fasted training session the following morning in a model known as 'sleep low, train low', muscle glycogen concentrations can be <200 mmol/kg dw (Bartlett *et al,* 2013), in comparison to muscle glycogen concentrations of 600 mmol/kg dw on a high CHO diet (8 g kg^{-1} BM) the day before exercise (Impey *et al,* 2016). Training status will also impact CHO storage, such that regular endurance training enhances the capacity for muscle glycogen storage (Greiwe *et al,* 1999). As a training adaptation, trained athletes can have more than twice the amount of glycogen than untrained individuals.

2.4 Lessons from microscopy studies: Muscle glycogen utilisation during exercise

As discussed in detail above, glycogen utilisation during exercise is now well-established to be affected by exercise intensity (Figure 2.1, Van Loon *et al,* 2001) and duration (Figure 2.2, Watt *et al,* 2002), as well as being affected by the nutritional (Arkinstall *et al,* 2004) and training status of the individual (Saltin *et al,* 1976; Henriksson, 1977). It is now also acknowledged that glycogen utilisation during exercise is not only dependent on muscle fibre type (Gollnick *et al,* 1974), but also on the specific subcellular location of glycogen within the muscle fibres (Marchand *et al,* 2007; Nielsen *et al*, 2011; Nielsen and Ørtenblad, 2011), thereby adding another layer of complexity in understanding glycogen metabolism during exercise (Ørtenblad & Nielsen, 2015).

Glycogen can be measured using biochemical techniques on muscle homogenates, though this method cannot discriminate between muscle fibre types. To examine glycogen utilisation on a fibre-specific basis histochemical methods have been used, providing a highly valuable research tool that enables the collection of (semi)quantitative data alongside informative visual images exhibiting spatial distributions of cellular structures. To examine glycogen periodic acid-schiff (PAS) staining has been used, the validity of which has been investigated by Van Der Laarse *et al,* (1992). PAS staining is based on the reaction of periodic acid with the diol functional groups found in glucose and other sugars, causing oxidation to form aldehyde. This reacts with the Schiff reagent to produce a purple/magenta stain (Prats *et al,* 2013). Though, this means that the PAS stain is not exclusive to glycogen and also will stain glycoproteins and proteoglycans. However, glycogen can be singled out

by pre-treating the cryosections with the glycogenolytic enzyme diastace (Baba, 1993). Despite this, many published studies have not used this process, therefore glycogen content can be overestimated (Prats *et al,* 2013). Research using PAS staining has allowed the identification of differences in muscle glycogen depletion dependent on muscle fibre type (Vollestad *et al,* 1984) and demonstrated that in endurance trained males only 1 day of CHO (10 g.day$^{(-1)}$.kg$^{(-1)}$) is required to maximise CHO storage in type I, IIa and IIb muscle fibres (Bassau *et al,* 2002).

There have been reports going back to the 1960's of electron microscopy being utilised to examine glycogen (Revel, 1963) and TEM has enabled direct and detailed information to be gathered showing glycogen particles and their localisation in relation to the mitochondria and within the muscle fibres (see Figure 2.3). TEM provides great detail with regards to the location of muscle glycogen, and using this technique, INTRA glycogen has been demonstrated to be preferentially depleted during prolonged exercise (Marchand *et al,* 2007; Nielsen *et al,* 2011), thus suggesting a potential explanation for the glycogen-dependent component in muscular fatigue (Ørtenblad *et al,* 2015). In addition, Jensen *et al,* (2020) recently showed that INTRA glycogen is the best predictor of time to exhaustion. However, TEM investigations rely on morphological factors to identify fibre type (z-line width and mitochondria), and analysis is only limited to a small number of fibres (~4-8 fibres) due to the time-consuming procedure which is related to the magnification required to obtain measures of glycogen volume fraction, which requires 20 – 30 images per fibre. Further to this when identifying fibre type using morphological factors, images of many fibres (~10-12 fibres) are collected, though only a few of these fibres which represent type I or type II fibres will be used (more on this procedure is included in 3.4.4). This

means many more fibres will be imaged than the amount that can actually be analysed for glycogen or lipid. There is also a limited number of fibres to image due to the ultrathin sections used for TEM analysis. Overall, when choosing methodology to examine glycogen utilisation during exercise, both fibre and region-specific analysis should be considered.

2.5 Regulation of carbohydrate metabolism during exercise

There are a number of key processes that govern the regulation of CHO metabolism. Muscle glycogen breakdown occurs through the process of glycogenolysis, where glycogen is first broken down into glucose-1-phosphate (G1P) by glycogen phosphorylase, and is then transformed into glucose-6-phosphate (G6P) by the enzyme phosphoglucomutase. Glycogen phosphorylase is considered the rate-limiting enzyme in the process of glycogenolysis (Richter *et al,* 1986) and is regulated via hormonal and/or allosteric control. At rest, glycogen phosphorylase is inactive in its b form, though when exercise begins, phosphorylase kinase phosphorylates the b form into the active a form. This process is initiated by the exercise-induced secretion of adrenaline from the adrenal medulla. Adrenaline binds to the β-adrenergic receptors on the sarcolemma, causing the activation of G-protein, which in turn activates adenylate cyclase, thus converting ATP into cyclic AMP (cAMP). cAMP then activates protein kinase A (PKA), which will subsequently activate phosphorylase kinase, resulting in the transformation of glycogen phosphorylase into its active a form. The activity of glycogen phosphorylase a can also be modified by allosteric factors, including Ca^{2+} flux, and the accumulation of adenosine diphosphate (ADP), adenosine monophosphate (AMP) and inorganic phosphate (P_i).

Given that adrenaline leads to phosphorylation and transformation of glycogen phosphorylase from the b to a form, it is reasonable to assume that this may explain the increase in glycogen utilisation with increasing exercise intensity. This would also be in line with the greater sarcoplasmic Ca^{2+} concentrations apparent during high intensity exercise, given the requirement for increased crossbridge cycling, and the fact that Ca^{2+} is a positive allosteric regulator of glycogen phosphorylase activity. However, Howlett *et al,* (1998) observed that glycogen phosphorylase activation was not augmented in line with increasing exercise intensity. In fact, the proportion of glycogen phosphorylase a was actually reduced after 10 minutes of high intensity exercise which was proposed to be due to the reduction in pH associated with higher exercise intensities. Although Ca^{2+}-mediated signalling (leading to glycogen phosphorylase transformation) may occur within seconds of muscle contraction beginning (Parolin *et al*, 1999), it is likely that post-transformational modifications are required during more prolonged high intensity exercise given that glycogenolysis still occurs despite a reduction in transformation. In this regard, it seems that the energy status of the cell may be more of a controlling factor, with increasing exercise intensity augmenting ATP hydrolysis, thereby increasing ADP, AMP and Pi accumulation. Specifically, the increase in Pi, will increase glycogenolysis as it provides greater amounts of substrate for the reaction to take place. Furthermore, whilst it is well-appreciated that glycogen phosphorylase is regulated through hormonal control via adrenaline (Jansson *et al,* 1986; Spriet *et al,* 1988; Febbraio *et al,* 1998), this is not always the case (Chesley *et al,* 1995; Wendling *et al,* 1996).

In addition to muscle glycogen, the contribution of plasma glucose to ATP production is also important. Plasma glucose entering skeletal muscle via GLUT4 is first

phosphorylated by hexokinase to form G6P. As such, G6P generated from both plasma glucose and muscle glycogen enter the process of glycolysis. Glycolysis is the breakdown of glucose leading to the production of pyruvic acid. Once glucose enters the glycolytic pathway, the rate-limiting enzyme in glycolysis is considered to be phosphofructokinase (PFK), which is allosterically regulated via ADP, AMP and Pi. Increased exercise duration will lead to a decrease in CHO metabolism and an increase in lipid metabolism. This is likely due to glycogen depletion and reduction in glycolytic flux through both glycogenolysis and glycolysis, thereby leading to a reduction in pyruvate and therefore the downregulation of pyruvate dehydrogenase activity resulting in decreased CHO oxidation.

2.6 Post-exercise muscle glycogen resynthesis

Many sports need athletes to be able to perform for training or competition on consecutive days, endurance sports such as cycling, distance running, rowing and swimming are prime examples. Therefore, the replenishment of glycogen stores is important in order to maximise recovery and subsequent performance capabilities. CHO is a key substrate in maximising post-exercise muscle glycogen resynthesis, with CHO intake in the first few hours post-exercise being particularly important. During the first 30 – 40 minutes following exercise, glycogen is rapidly resynthesized via exercise-induced translocation of GLUT4 to the cell membrane facilitating glucose uptake. The rate of synthesis is dependent on several factors, including the availability of plasma glucose as a result of hepatic glucose production, the transportation of glucose into the cell via GLUT4, the intramuscular concentration of glucose-6-phosphate (G-6-P), and the activity of enzymes such as glycogen synthase, which is related to the level of glycogen depletion. Due to the changing activity of these enzymes and the

effectiveness of the glucose transportation, there are two different phases of glycogen-synthesis post-exercise. The first phase, occurs independent of a rise in circulating insulin concentrations, and is therefore often referred to as the insulin-independent phase (Piehl, 1974). Glycogen synthase (the rate-limiting enzyme for glycogen synthesis) is present in an inactive or active form. When muscle glycogen is low, both glycogen synthase phosphatase is activated, which triggers the dephosphorylation of glycogen synthase, converting it to an active form and enhancing the rate of glycogen synthesis (Ivy & Kuo, 1998). Further to this, the availability of glucose, which is dependent on GLUT4 at the plasma membrane will affect this phase. For the first hour post-exercise, there is enhanced GLUT4 availability at the cell membrane, thereby facilitating glucose uptake. AMPK activity also elicits greater GLUT4 translocation, though this is partially mediated by muscle glycogen availability due to the glycogen binding domain in AMPK (McBride *et al,* 2009). As such, low glycogen availability has been demonstrated to enhance AMPK signalling responses and adaptations to exercise in rat (Wojtaszewski *et al,* 2002) and human skeletal muscle (Wojtaszewski *et al,* 2003). This phase has been suggested to only occur when post-exercise glycogen concentrations are less than ~ 120 – 150 mmol/kg dw (Price *et al,* 1994).

The insulin-dependent phase which follows supports continued glycogen storage as a result of post-exercise CHO ingestion, and although this phase occurs at a much slower rate, it can last for up to 24 hours (Jenjens and Jeukendrup, 2003). This phase is characterised by an enhanced sensitivity of skeletal muscle to physiological increases in plasma insulin, which can last for several hours depending on the level of glycogen depletion and provision of CHO (Cartee *et al,* 1989). Why this occurs is yet to be elucidated, though it is likely to be due to an interaction between muscle glycogen

concentration, AMPK and insulin signalling molecules (Jensen and Richter, 2012). After glucose enters the cell, the majority will be directed toward glycogen storage rather than oxidation. This is regulated via enhanced glycogen synthase activity, which is activated through insulin, though may also be due to an increase in GLUT4 activity in the cell leading to greater glycogen synthesis rates (Ren *et al,* 1994).

Research has also demonstrated that glycogen resynthesis can differ between the subcellular pools of glycogen. Nielsen *et al,* (2011) observed impaired INTRA glycogen resynthesis during the first 4 h of recovery from high intensity exercise when no CHO was consumed, whereas resynthesis of IMF and SS glycogen was less affected. When CHO is present during recovery, serum levels of insulin increase. Increases in glucose uptake after the initial 1-2 h recovery is only observed when insulin is present (Frosig & Richter, 2009). Interestingly, the T-system has been demonstrated to be a key site for insulin-mediated glucose uptake (Lauritzen *et al*, 2006). The t-tubuli are extensions of the cell membrane that penetrate into the centre of skeletal muscle cells, thus providing direct access for the incoming glucose to the INTRA region of the cell. Therefore, when CHO is withheld during recovery, this will result in impaired insulin-dependent GLUT4 translocation to the T-system rather than to the sarcolemma. Furthermore, research by Nielsen *et al,* (2011) demonstrated that glycogen in the IMF and SS regions was fully resynthesized at 22 h post-exercise, whilst the INTRA glycogen levels had only reached 60% of the respective pre-exercise levels, regardless of CHO availability during the first 4 h post-exercise. This suggests a delay in the recovery of INTRA stores beyond 24 h following exercise, regardless of total post-exercise CHO intake. However, this is in contrast to data by Marchand *et al*,

(2007), who demonstrated a preferential resynthesis of INTRA glycogen following prolonged exercise.

Early work from the late 1980's suggested that consumption of 0.7g CHO/kg BW/h immediately post-exercise could elicit an increase of ~20 mmol/kg dw/h as the maximal rate attainable over 4 h (Ivy *et al,* 1987). However, further work demonstrated that consuming smaller amounts (30 min intervals) of CHO post-exercise, providing 1.2g CHO/kg BW/h further augmented the rate of glycogen synthesis to 44.8 mmol/kg dw/h (Van Loon *et al,* 2000). The highest rate of glycogen resynthesis recorded is 85 mmol/kg dw/h, though this was only attainable through a CHO infusion whilst being in a glycogen depleted state (Bergstrom & Hultman, 1967). The type of CHO and method of consumption should be considered carefully. High glycaemic index (GI) CHO has been demonstrated to produce 61% greater glycogen resynthesis than low GI CHO (Burke, 1993). The effect of GI is likely mediated through an increase in gastric emptying, therefore the concentration of blood glucose available for absorption by skeletal muscle. Practically, a mixture of fluid and solid CHO is recommended to be consumed is recommended to facilitate rehydration and repletion of glycogen following exercise, respectively.

2.7 Lipid metabolism

2.7.1 Skeletal muscle lipid storage

Triacylglycerol (TG) molecules consist of 1 glycerol molecule (backbone) with 3 FA molecules attached. The primary storage site for TG within the body, is within subcutaneous and visceral adipose tissue depots. Here the amount of TG will vary greatly between individuals due to factors such as training status and diet, but the

average healthy male of ~ 70kg will store 9 – 15 kg of TG within adipose tissue, equating to an energy store of ~ 80,000 – 140,000 kcal (Van Loon, 2004). As such, diet leading to caloric excess will result in adipose tissue stores expanding in size, whilst under conditions of caloric deficit will lead to reductions in adipose tissue TG as the hydrolysis of TG will result in FA mobilisation so the body's energy requirements can be met. Therefore, making TG within adipose tissue a dynamic pool for FA storage and release as demand dictates. As introduced above, adipose tissue is the primary storage site for fat, though this means there are others. FA can also be stored as TG within intracellular lipid droplets (LD). In muscle, smaller quantities of TG are seen within muscle fibres, known as IMTG. The concentration of IMTG is generally within the range of 2 and 10 mmol.kg^{-1} wet weight, which equates to mixed muscle TG content of approximately 0.2kg, providing an energy store of ~ 1,850 kcal (Van Loon, 2004; Watt *et al,* 2002; Wendling *et al,* 1996). The concentration of IMTG is heavily influenced by energy intake, diet and training status. Indeed, one of the most prominent adaptations to endurance training is enhanced IMTG storage (reviewed in Shaw *et al,* 2010). Electron microscopy analysis of skeletal muscle tissue has demonstrated IMTG-containing LD are located close to the mitochondria (Hoppeler, 1999; Shaw *et al,* 2008), therefore providing a readily available fuel store of FA for oxidation during exercise. IMTG storage is known to be up to three-fold greater in type I muscle fibres in comparison to type II (Essen *et al,* 1975; Koopman *et al,* 2001; Malenfant *et al,* 2001; Van Loon *et al,* 2003a, 2003b), with exercise causing a preferential reduction in IMTG content of type I fibres (Van Loon *et al,* 2003; Stellingwerff *et al,* 2007). The subcellular distribution of IMTG has been demonstrated using TEM to be in two LD pools, 1) subsarcolemmal LDs, located just beneath the plasma membrane, and 2) intermyofibrillar LDs, located between the myofibrils

(Nielsen *et al,* 2010a). This is important as TEM investigations have demonstrated a reduction in intermyofibrillar, but not subsarcolemmal LDs following 1 h of moderate-intensity exercise in lean, healthy individuals (Chee *et al,* 2016).

2.7.2 Lipid droplets

IMTG is referred to throughout this thesis as a description of the source of FA which contribute to fat oxidation during exercise. Although adipose tissue is the predominant site for TG storage, nearly all cell types can store FA as TG, and TG is typically housed within intracellular LD. For years, LD's were considered to be inert storage depots. However, they are now recognised as functional organelles playing key roles in a number of biological processes (Walther & Farese, 2009). In adipose tissue, LD are unilocular and have one large LD per cell per se, whilst in skeletal muscle there are numerous smaller LD. The structure of LD's is unique, consisting of a neutral lipid core primarily containing TG and cholesterol esters with a surrounding monolayer of phospholipids (Ohsaki *et al,* 2009) that is decorated with integral and peripheral proteins (Fujimoto *et al,* 2011). Proteomic analyses have revealed that there are over 300 proteins either functionally associated with or embedded within the phospholipid monolayer of LD's (Zhang *et al,* 2011). Of these proteins, the most well known are the PAT proteins, or more commonly known as the Perilipin (PLIN) proteins, as well as many other proteins that regulate LD formation, TG synthesis and hydrolysis. The proteome of LD subpopulations likely determines their role in cellular function, as well as their morphology and subcellular location. When considering morphology, the balance between synthesis and breakdown of TG will determine the number and size of LD. Currently though, it is yet to be elucidated whether an increase in LD synthesis

will lead to an increase in individual LD number and/or LD size, with the same also applying to our knowledge on the breakdown of LD during exercise. Nevertheless, what is clear is that although LD are relatively small, there is variation in size (0.20 – 0.50 μm^2, Daemen *et al,* 2018).

2.7.3 IMTG utilisation during exercise

As mentioned previously, whole-body fat oxidation is maximal during moderate-intensity exercise, where fat oxidation rates are increased by ~ 10 fold in comparison to rest in trained individuals (Romijn *et al,* 1993; Van Loon *et al,* 2001). In order to investigate the contribution of IMTG to total fat oxidation during exercise, several studies have used indirect calorimetry measures alongside the infusion of a ^{13}C-labelled FA tracer (Romijn *et al,* 1993; Van Loon *et al,* 2001; Watt *et al,* 2002; Van Loon *et al,* 2003). Stable isotope tracers provide a powerful, unique tool for investigating substrate utilisation at a whole-body level by combining indirect calorimetry with the use of stable and/or radioactive isotope tracers (Rennie, 1999). Using this technique, it is possible to measure total fat and plasma free fatty acid (FFA) oxidation, and subsequently calculate the contribution of other fat sources (i.e. IMTG and lipoprotein-derived TG) to total fat oxidation. However, this method assumes lipoprotein-derived TG oxidation to make a small contribution to total fat oxidation (~5-10%), which it does following an overnight fast under normal dietary conditions (Van Loon, 2004; Watt *et al,* 2002). Overall, it has been concluded that IMTG represents an important substrate during moderate-intensity exercise and the measurement of

plasma FFA oxidation using stable isotopes enables an indirect estimation of both muscle and/or lipoprotein-derived TG oxidation during exercise.

While stable isotopes provide an indirect estimate of IMTG oxidation, directly measuring IMTG content before and after exercise enables net changes in IMTG to be calculated. One such method to achieve this is the use of Proton magnetic resonance imaging ^{1}H-MRS, which provides a non-invasive technique allowing quantification of both intramyocellular and extramyocellular lipid (EMCL) (Boesch *et al*, 1999; Boesch & Kreis, 2000). It enables quantification by measuring the resonances from methyl and methylene groups of muscle triglycerides appearing in multiple peaks on the proton spectrum, such peaks have been linked to either intramyocellular lipid (peak at 1.3 – 1.4 ppm) or EMCL (peak at 1.5 – 1.6 ppm) (Boesch *et al*, 1999; Szczepaniak *et al*, 2001). This was validated via a differentiation in readings of subjects with generalised lipodystrophy (characterised by the absence of interfascial adipose tissue), where no EMCL (peak at 1.5 – 1.6 ppm) was detected in comparison to a strong IMCL signal (peak at 1.3 – 1.4 ppm) (Szczepaniak *et al*, 2001). Using this technique, it has been consistently reported that IMTG concentration is significantly reduced by ~20–40% following moderate-intensity exercise (reviewed by Van Loon, 2004), and therefore provides evidence to support IMTG contributing to total fat oxidation in active individuals during exercise.

Using ^{1}H-MRS it has also been established that short-term, high-fat diets (48 h) enhance IMTG utilisation, which is likely due to the greater pre-exercise IMTG content (Johnson *et al,* 2003; Zderic *et al,* 2004). Further to this, validation for this method was provided by studies observing strong correlations between IMTG content determined

with ^{1}H-MRS and electron microscopy (Howald *et al,* 2002) and immunofluorescence microscopy (Van Loon *et al*, 2003). In summary, ^{1}H-MRS provides a non-invasive method enabling the quantification of IMTG content over time under different conditions i.e. nutritional or exercise, *in vivo* in humans. However, MRI is an expensive technique, and machines are not readily accessible or portable; factors which will preclude its accessibility and feasibility within a field-based sporting environment.

While both stable isotope and ^{1}H-MRS methods provide some evidence of the contribution of IMTG to total fat oxidation during moderate-intensity exercise in active individuals, direct quantification of IMTG concentrations through biochemical extraction in skeletal muscle tissue provide a less clear view. Using the biochemical extraction technique, exercise induces a significant decrease in the concentration of IMTG in skeletal muscle following exercise in numerous studies (Essen-Gustavsson & Tesch, 1990; Phillips *et al*, 1996; Sacchetti *et al,* 2002; Watt *et al,* 2002), whereas others did not observe any significant changes (Kiens *et al*, 1993; Kiens and Richter*,* 1998; Wendling *et al,* 1996). It has been suggested that the equivocal findings using this method could be due to the heterogeneity of research protocols (i.e. duration and/or intensity, mode of exercise) as well as the selected population being examined (Van Loon, 2004). Such factors will likely contribute to some variability, but they do not fully explain such contradictory findings within the literature. Methodological difficulties with the TG extraction technique may also account for some of the variability (Watt *et al,* 2002). For example, the between-biopsy variability has a large coefficient of variation of 20-26% (Wendling *et al*, 1996), meaning that net reductions in IMTG content less than this will not reach statistical significance in such studies (Wendling *et al*, 1996). The source of the variability is likely linked to the presence of EMCL in

muscle samples (Guo, 2001; Watt *et al*, 2002; Wendling *et al*, 1996). Although the removal of EMCL is possible via microdissection (Guo, 2001), the presence of even a few adipocytes will cause a substantial overestimation in total IMTG content. To reduce the impact of EMCL on estimates of IMTG, using only well-trained endurance subjects, who typically have low EMCL, is suggested (Boesch *et al,* 2000; Szczepaniak *et al*, 2001; Wendling *et al*, 1996). Clearly though, this limits the application of this technique to investigate IMTG as a substrate during exercise in more unhealthy or diseased populations.

Using the ^{1}H-MRS or biochemical extraction technique only permits the quantification of mixed-muscle TG concentration, and therefore does not take fibre type or subcellular location of IMTG-containing LDs into account, as well as the subcellular distribution of IMTG. The development of immunofluorescence microscopy methods allowed the discrimination between IMTG content in type I and type II fibres using Oil red O (ORO) staining, thus allowing the quantification of IMTG content on a fibre type-specific basis. This technique has revealed that IMTG content is ~2-3-fold greater in type I fibres compared to type II fibres (Essen *et al,* 1975; Howald *et al,* 1985). Further to this, immunofluorescence microscopy has shown that there are greater amounts of IMTG stored in the peripheral regions of muscle fibres (Van Loon *et al,* 2004; Stellingwerff *et al,* 2007; Shaw *et al,* 2008). On the other hand, it is important to note that immunofluorescence microscopy will only provide a semi-quantitative analysis, and the efficacy of the staining procedure and image acquisition settings will highly influence the area fraction stained. Therefore, controls should be used to minimise variability. When accurately controlled, this technique has been used to show 2 h of moderate-intensity exercise will reduce the intramuscular lipid pool in type I fibres by

>60% (Van Loon *et al*, 2003). Moreover, the reduction in IMTG during exercise appears to be related to pre-exercise IMTG levels (Stellingwerff *et al,* 2007). Interestingly, mixed-muscle IMTG measured using immunofluorescence correlates with IMTG quantification using biochemical extraction techniques, though this relationship disappears when used to quantify utilisation during exercise (Stellingwerff *et al,* 2007). This is predominantly due to the rate of IMTG utilisation being greater in type I fibres than in type II.

It is important to note that when staining for IMTG, ORO is not without experimental disadvantages. To use ORO the tissue requires fixing, thus preventing its use on live cells. Furthermore, completely dissolving ORO into solution has proved difficult and once created, has a limited shelf life (Spangenburg *et al,* 2011). Moreover, there is a high level of background staining observed when using ORO, which due to the efficacy of the staining procedure and image-acquisition settings will highly influence the area fraction stained (outcome variable for quantifying IMTG content using immunofluorescence microscopy). An alternative dye to visualise LD in skeletal muscle is the fluorescent dye BODIPY (493/503), which emits a bright green fluorescence (Listenberger & Brown, 2007). BODIPY (493/503) can be coupled with fluorescence staining of other proteins whilst also not needing to be made "fresh" for each use (Spangenburg *et al,* 2011). When determining protein interactions with LD, immunofluorescence in combination with wide-field or confocal imaging has often been used (Daemen *et* al, 2016). Immunohistochemistry is an irreplaceable method to examine the distribution of LD as it provides a highly valuable research tool that enables the collection of (semi)-quantitative data alongside informative visual images exhibiting spatial distributions of cellular structures. We recently compared BODIPY to

ORO for visualising and quantifying IMTG content (Strauss *et al*, 2020), and showed that the detection and quantification of IMTG content was greater when using BODIPY due to the detection of a larger number of LD, when compared to ORO (Fig. 2.4, Strauss *et al,* (2020).
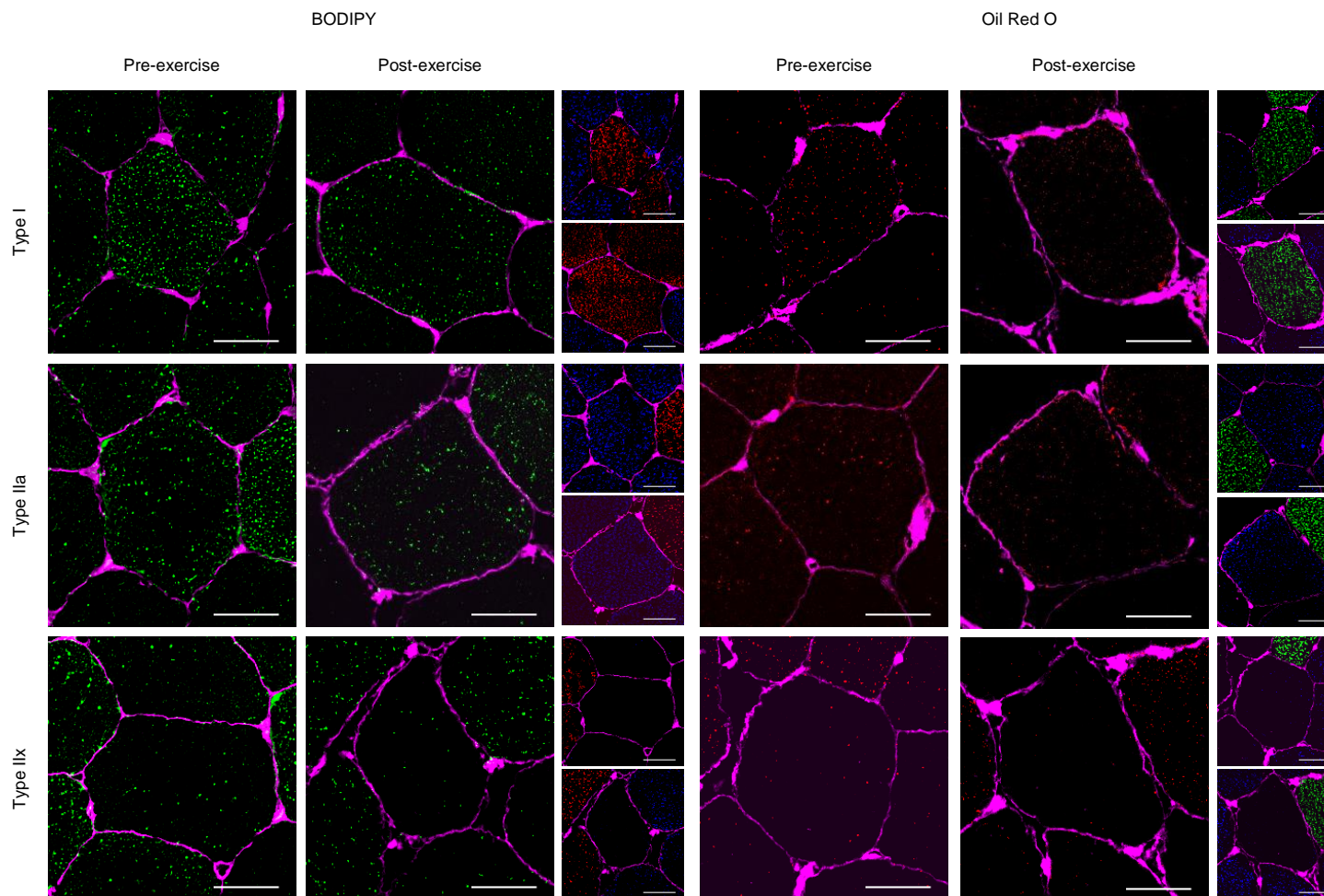
Figure 2.4. Fibre type specific lipid staining using BODIPY and ORO before and after exercise. For BODIPY panel of images, LD's stained before and after exercise using BODIPY (green) and the cell membrane using Laminin (pink) can be seen in the large images for type I (top), type IIa (middle) and type IIx (bottom). The smaller images show the corresponding fibre type staining with MHCI denoting type I fibres (red) and MCHIIa (blue) and no stain showing type IIx fibres. For ORO panel of images, LD's stained before and after exercise using ORO (greyscale for clarity) and cell membrane (pink) can be seen in the large images for type I (top), type IIa (middle) and type IIx (bottom). The smaller images show the corresponding fibre type staining with MHCI denoting type I fibres (green) MCHIIa denotating type IIa fibres (blue) and no stain showing type IIx fibres. taken from Strauss *et al,* (2020) White bar = 30μm.

Moreover, BODIPY was more photostable and had a lower within-sample coefficient of variation than ORO. In summary, there are important differences to consider when deciding which lipid stain to use for quantifying IMTG on a fibre type and subcellular-specific basis. When comparing ORO and BODIPY it has been concluded that BODIPY (493/503), offers a respected alternative to ORO, when examining LD function in skeletal muscle (Spangenberg *et* al, 2011) due to its greater photo-stability and capability to specifically detect IMTG whilst avoiding quantification of membrane structures, compared to ORO (Strauss *et al,* 2020).

Although immunofluorescence microscopy allows quantification on a fibre-specific and subcellular basis, another microscopy technique that can be used to examine IMTG utilisation is transmission electron microscopy (TEM). This technique enables direct and detailed information to be gathered showing LD and their localisations in relation to the mitochondria and spatially within the muscle fibres (see Fig. 2.3). TEM can be used to determine exercise-induced changes in substrate utilisation. By virtue of the greater magnification capabilities and excellent resolution, TEM can be considered the most accurate method to measure changes in LD size and number. Although TEM provides greater detail with regards to the subcellular localisation of LD distribution in muscle, this technique relies on morphological factors to identify fibre type, and analysis is only limited to a small number of fibres per sample (~4-8 fibres). A further disadvantage of TEM, is the ability to only be used on chemically-fixed, and thus material with restricted antigenicity. This complicates the ability to co-stain with specific antibodies in order to examine the interaction of proteins with LDs, for example (Daemen *et al*, 2016). The validity of TEM when examining IMTG has been

investigated by Howald *et al*, (1985), who found a strong correlation between TEM and ^{1}H-MRS. Overall, both immunofluorescence microscopy and TEM provide methods to visualise and quantify IMTG utilisation and changes in LD morphology on a fibre-type and subcellular specific basis, though to date, no direct comparison between the two microscopy methods in quantifying IMTG utilisation has been made.

2.8 Skeletal muscle lipid metabolism

2.8.1 IMTG turnover

IMTG turnover is reflective of the balance between the rate of lipolysis and lipid synthesis, both of which are highly influenced by mitochondrial fat oxidation capacity and plasma FFA availability. FA that are esterified in the IMTG pool are hydrolysed by TG lipases before oxidation, whilst they can be recycled back into the IMTG pool when not oxidised. In healthy individuals, the IMTG pool is in a constant state of flux (due to the regular use of IMTG as a fuel source during exercise) and the major proportion of FA entering the muscle at rest are shunted toward esterification into IMTG (Sacchetti *et al,* 2004). Overall, it is thought that in resting skeletal muscle, the turnover rate of the entire IMTG pool is approximately 29 h (Sacchetti *et al,* 2004). It is thought that lipolysis is hypothetically well-matched to mitochondrial β-oxidation given the location of LD in close proximity to the mitochondria in trained individuals. A potential reduction in the capacity of mitochondrial fat oxidation due the presence of larger LD positioned away from (or without direct contact) to the mitochondria may lead to the promotion of a lower turnover rate of IMTG. Factors that mediate the rate of IMTG turnover include the oxidative capacity of the muscle, the rate of lipolysis i.e. IMTG breakdown, FFA availability and finally, esterification of fatty acids and intermediate products, such as diacylglycerol (DAG).

2.8.2 Lipolysis

Lipolysis is the process of TG breakdown, where the three fatty acids are liberated from the glycerol backbone. Hormone sensitive lipase (HSL) was initially believed to be the the rate-limiting enzyme of lipolysis, with hydrolase activity of HSL at rest accounting for ~ 60% of total neutral hydrolase activity (Watt *et al,* 2004). By inhibiting HSL in rat skeletal muscle, contraction-induced increases in TG lipase activity were eradicated (Langfort *et al,* 2000). Similar to IMTG, the content of HSL is greater in type I fibres compared to type II fibres (Langfort *et al,* 1999). Under conditions that stimulate IMTG breakdown (such as exercise), circulating adrenaline levels are increased and will activate HSL via cAMP-dependent protein kinase (PKA) phosphorylation on HSL Ser^{563} and Ser^{660} (Watt *et al,* 2003; 2006). On the other hand, a postprandial rise in circulating insulin concentrations will inhibit skeletal muscle HSL activity by activating a phosphodiesterase which converts cAMP to inactive $5^{'}$-AMP, therefore meaning there is a reduction in the proportion of HSL that is positively phosphorylated (Enoksson *et al,* 1998). During exercise, muscle contraction also activates HSL through protein kinase C and extracellular signal-related kinase (Donsmark *et al,* 2003), most probably via the phosphorylation at Ser^{600} (Greenberg *et al,* 2001). During higher intensity exercise, AMP-activated protein kinase (AMPK) will increase and subsequently cause the phosphorylation and inhibition of HSL on Ser^{565} which will result in an anti-lipolytic effect (Watt *et al,* 2004; 2006). Further to this, increases in long-chain fatty acyl-CoA, observed during high intensity exercise and also during prolonged steady state exercise (>2 h in duration), may allosterically inhibit HSL activity (Kiens *et al,* 1999; Watt *et al,* 2002). Thus, HSL is upregulated at low-to-moderate exercise intensities, (i.e. 30 and 60% VO_{2peak}) in comparison to higher exercise intensities (90% VO_{2peak}) (Watt *et al,* 2003). In addition to post-

transformational modifications regulating the activity of HSL, another key step is the translocation of HSL from its cytosolic store to the LD. In response to adrenaline or electrically-stimulated muscle contraction, HSL localises to LD in isolated rat skeletal muscle, and actually appears to penetrate the phospholipid monolayer of the LD, therefore gaining access to TG within the core of the LD (Prats *et al,* 2006). Further to this, Whytock *et al,* (2018) recently observed a similar redistribution of HSL to LD specifically within type I fibres of human skeletal muscle in response to 60 min of moderate intensity cycling exercise.

Approximately 20 years ago, evidence began to emerge to suggest that other lipases were also present in adipose tissue and muscle. For example, TG hydrolase activity was only reduced by 50% in adipose tissue of HSL-deficient mice in comparison to wild-type controls (Haemmerle *et al,* 2002b). Furthermore, in skeletal muscle homogenates prepared from resting biopsies and incubated with an antiserum against HSL, there was a decrease in TG hydrolase activity, though this was only reduced by ~25% (Roepstorff *et al,* 2004). Moreover, research in rodent skeletal muscle demonstrated that under either HSL knockout or knockdown conditions contraction-induced lipolysis of IMTG still occurred despite the lack of HSL (Alsted *et al,* 2013). This highlighted the idea that other lipases may be present and subsequently adipose triglyceride lipase (ATGL) was discovered, primarily in adipose tissue but also in skeletal muscle (Villena *et al,* 2004; Zimmermann *et al,* 2004). Overall, ATGL is a relatively new lipase, with research investigating the regulation within skeletal muscle remaining relatively limited. Similar to HSL, ATGL is greater within type I fibres (Jocken *et al,* 2008), with endurance training augmenting ATGL protein expression primarily in type I fibres (Turnbull *et al,* 2016). Overexpression of ATGL in human primary

myotubes initiates an increase in lipolysis and a reduction in TG content (Badin *et al,* 2011). In contrast, under ATGL-knockout conditions, mice demonstrate accumulation of TG in skeletal muscle (Haemmerle *et al,* 2002a), suggesting that ATGL primarily acts on TG rather than DAG. ATGL activation appears to require the co-activator comparative gene-identification-58 (CGI-58) (Schweiger *et al,* 2006). Individuals with a mutation of CGI-58 are known to have greater IMTG content (Lass *et al,* 2006). Overall, when CGI-58 expression is normal it can augment an increase in lipase activity by ~ 20 fold in cultured kidney cells (Lass *et al,* 2006), therefore demonstrating the importance of CGI-58 in ATGL activity. The interaction between ATGL and CGI-58 has also been shown to be increased in rat skeletal muscle through muscle contraction, alongside a decrease in IMTG content (MacPherson *et al,* 2012).

In human adipose tissue, phosphorylation of ATGL on Ser^{404} on ATGL is enhanced through β-adrenergic stimulation and correlates with greater rates of lipolysis (Pagnon *et al,* 2012). However, in skeletal muscle 60 min of moderate-intensity exercise has no effect on ATGL phosphorylation (Mason *et al,* 2012), suggesting that phosphorylation is not vital for ATGL activation. Under basal conditions, the phosphorylation of the Thr^{372} residue on the hydrophobic region in the C-terminus of ATGL inhibits the colocalization with LDs and subsequently reduces ATGL-mediated TG hydrolysis (Xie *et al,* 2014). Several other ATGL phosphorylation sites have been identified, although their function is yet to be elucidated (Xie *et al,* 2014). Opposite to HSL, ATGL is already localised with LD in skeletal muscle, in both resting conditions and following moderate-intensity exercise (Mason *et al,* 2014a). The general consensus is now that ATGL and HSL work in a sequential process, as such ATGL catalyses the initial step of TG lipolysis in human skeletal muscle by causing the

release of one FA molecule and creating DAG, before HSL then becomes crucial for DAG hydrolysis to generate a second FA and monoacylglycerol. Subsequently, final FA liberation from the glycerol backbone is mediated by MGL (Taschler *et al,* 2011). However, as HSL and ATGL equate for ~ 98% of contraction-induced TG lipase activity (Alsted *et al,* 2013), the relative importance of MGL in the process of lipolysis is much lower.

2.8.3 IMTG synthesis

FA uptake into skeletal muscle occurs through the process of facilitated diffusion, mediated by several FA transporter proteins. FAT/CD36 is the primary FA transporter, and at rest resides at the endosomal membrane, but at the onset of exercise it translocates to the plasma membrane (Bonen *et al,* 2000; Bradley *et al,* 2012). FA uptake in FAT/CD36 knockout mice is reduced considerably both at rest and during exercise in comparison to wild-type controls alongside a decrease in fat oxidation (McFarlan *et al,* 2012), thereby demonstrating fat oxidation rates are highly dependent on FA uptake into skeletal muscle. Once FA's enter muscle, they are attached to a coenzyme to form fatty acyl-CoA, catalysed by fatty acyl-CoA synthetase. The first step in TG synthesis is the attachment of a fatty acyl-CoA to glycerol 3-phosphate, resulting in the formation of lysophosphatidic acid (LPA), a reaction catalysed by glycerol-3-phosphate acyltransferase (GPAT). A second fatty acyl-CoA is then attached to LPA to form phosphatidic acid by the enzyme 1-acyl-glycerol-3-phosphate-O-acyltransferase (AGPAT). A phosphate group is then removed from the phosphatidic acid to form DAG. Finally, a third fatty acyl-CoA unit is attached to the

DAG to form TG, a reaction catalysed by diacylglycerol acyltransferase (DGAT). The process of IMTG synthesis can be seen in Figure 2.5.
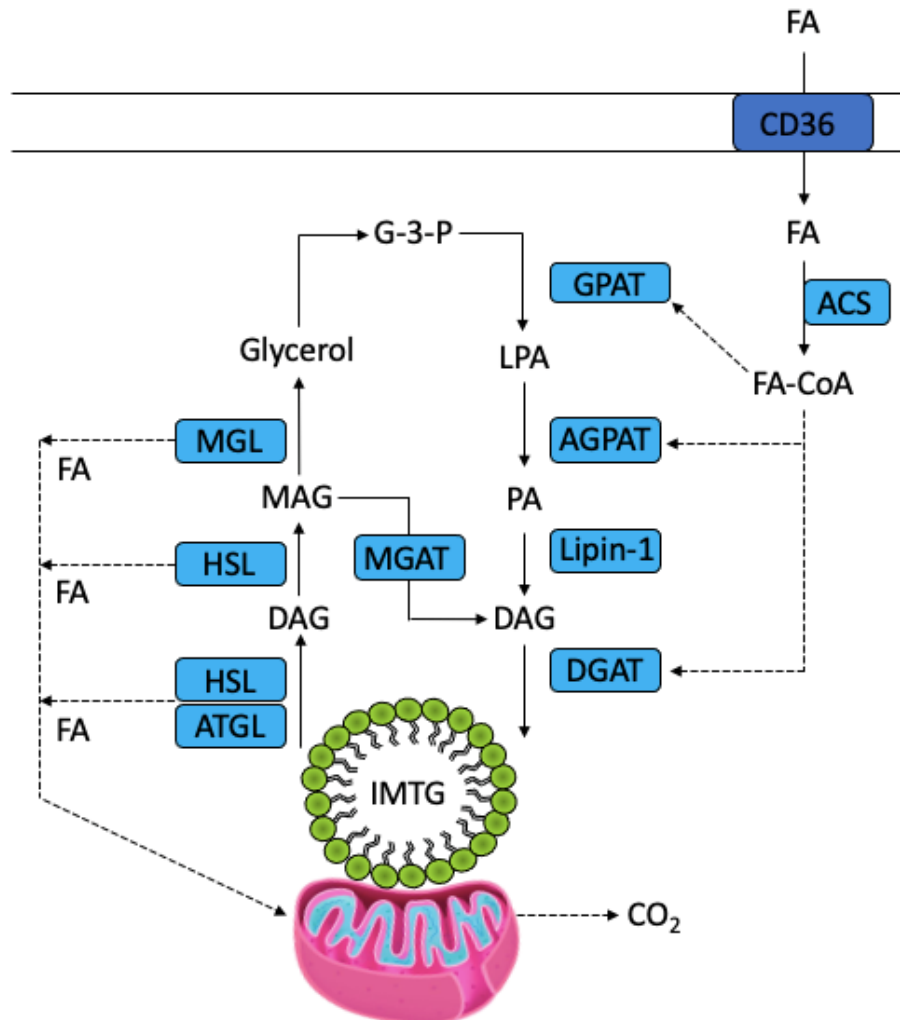
Figure 2.5. IMTG synthesis and hydrolysis in skeletal muscle.
APGAT: 1-aclyglycerol-3-phosphate acyltransferase, ATGL: adipose triglyceride lipase, ACS: acyl-CoA synthase, DAG: diacylglycerol, DGAT: diacylglycerol transferase, FA: fatty acid, FA-CoA: fatty acyl-CoA, CD36: cluster of differentiation 36, G-3-P: glycerol-3-phosphate, GPAT: glycerol-3-phosphate acyltransferase, HSL: hormone sensitive lipase, IMTG: intramuscular triglyceride, LPA: lysophosphatidic acid, MAG: monoacylglycerol, MGAT: monoacylglycerol transferase, PA: phosphatidic acid.

Four different isoforms of GPAT exist, differing in subcellular distribution. As such, GPAT1 and GPAT2 are found localised to mitochondria, whilst GPAT3 and GPAT4 are found localised to the endoplasmic reticulum (Gimeno and Cao, 2008). GPAT is considered to be the rate-limiting enzyme in the IMTG synthesis pathway as it displays the lowest enzyme activity (Coleman & Lee, 2004), and of this activity, 90% of total GPAT activity in skeletal muscle is due to GPAT1 (Park *et al,* 2002). When GPAT1 is overexpressed, FA oxidation is suppressed (Linden *et al,* 2004), whilst in GPAT1 knockout mice, FA oxidation is enhanced (Hammond *et al,* 2005). GPAT1 expression has been examined in human skeletal muscle using western blot methods (Schenk & Horowitz, 2007; Newsom *et al,* 2011), though an understanding of the regulation of GPAT1 in skeletal muscle is currently limited. If GPAT creates lysophosphatidic acid at the mitochondria during IMTG synthesis, it may require transportation to the endoplasmic reticulum where other IMTG-synthesising enzymes are located. In the liver this is facilitated via liver-FA binding protein (Gonzalez-Baro *et al,* 2007), though in skeletal muscle more research is warranted.

DGAT is responsible for the final step of IMTG synthesis (Choi *et al*, 2007), catalyzing the addition of a FA to DAG leading to the formation of TG and subsequently increasing IMTG content. DGAT is known to exist in two isoforms, both expressed in skeletal muscle but localising at different subcellular locations, with DGAT1 localising to the endoplasmic reticulum and DGAT2 localising to the endoplasmic reticulum, mitochondria and LD (Bosma *et al,* 2012). DGAT1 is the primary isoform expressed in skeletal muscle (Cases *et al,* 1998; 2001), suggesting TG synthesis in skeletal muscle will primarily occur in the endoplasmic reticulum. DGAT1 overexpression in C2C12

myotubes leads to a three-to-four fold greater DGAT activity and therefore six-fold greater intracellular TG content and reduced DAG content (Liu *et al,* 2007). Similar to GPAT1, there is limited data available on the regulation of DGAT1 in human skeletal muscle. However, GPAT1 and DGAT1 have been demonstrated to increase following an overnight lipid-heparin infusion, the day after a bout of endurance exercise which consisted of 45 min treadmill running and 45 min cycle ergometer at 65% VO_{2peak} (Schenk and Horowitz, 2007). Thus, GPAT1 and DGAT1 expression is sensitive to exercise, at least in the face of elevated FA availability.

2.9 Perilipin proteins regulating IMTG turnover

2.9.1 Overview

LDs are coated with >300 different LD associated proteins (Zhang *et al,* 2011), of which, the most common and well-known proteins are the perilipin (originally termed the PAT proteins) family (Bickel *et al,* 2009). Of this family, there are five perilipin (PLIN) protein members with proposed roles in the regulation of TG storage and breakdown. PLIN1 was the first member of the family to be identified and is generally believed to be exclusively expressed in adipose tissue and steroidogenic cells (Londos *et al,* 1995), though there is some evidence to suggest that PLIN1 is also expressed in skeletal muscle (Gjelstad *et al,* 2012). In adipose tissue, PLIN1 appears to play a key role in regulating both the storage and hydrolysis of TG stored in LD's (Brasaemle, 2007; Bickel *et al,* 2009; Morales *et al*, 2017). Subsequently, four other members of the PLIN family were identified (their original nomenclature is in parentheses): PLIN2 (adipose differentiation related protein/adipophin), PLIN3 (tail interacting protein of 47kDA), PLIN4 (S3-12) and PLIN5 (OXPAT). PLIN2 and PLIN3 are ubiquitously

expressed, whilst PLIN4 and PLIN5 have a more limited tissue expression, but includes skeletal muscle (Sztalryd & Braseamle, 2017). A feature of many proteins that are associated with LD, including the PLIN proteins, is the similarity of the amino acid sequences predicted to form amphipathic alpha helices to support LD binding (Bussell *et al,* 2003; Krahmer *et al,* 2011). When comparing the amino acid sequences across the PLIN proteins, PLIN2 and PLIN3 have the greatest similarity (Brasaemle, 2007; Miura *et al,* 2002; Kimmel *et al,* 2016), whereas PLIN4 has the most diverse amino acid sequence with very limited similarity to other PLIN proteins. For a summary of the tissues each PLIN is expressed in alongside proposed function see table 2.1. For the purpose of this thesis, there will only be a focus on PLIN's 2, 3, 4 and 5, which are all expressed in skeletal muscle. The following section will focus on the role of each perilipin protein on IMTG turnover and LD regulation, first examining cell-based work, then work conducted in rodent models and human skeletal muscle.

Table 2.1. Basic characteristics of PLIN proteins, adapted from Itabe *et al,* (2017)

Protein	Major site of expression	Other sites of expression	Function
PLIN1	White adipose tissue	Brown adipose tissue, cardiac muscle liposarcoma	Hormone-induced lipolysis Large LD stabilization
PLIN2	Liver	Premature adipocytes macrophages sebocytes mammary gland epithelia choriocarcinoma cells (BeWo) ubiquitously expressed	Adipocyte differentiation Small LD generation LD stabilization
PLIN3	Ubiquitous	skeletal muscle neutrophils, mast cells retinal pigment epithelium sebocytes	LD stabilization (compensation of PLIN2) PGE_2 production intracellular trafficking
PLIN4	White adipose tissue	hMSC (induced during differentiation) skeletal muscle	Human adipocyte differentiation
PLIN5	Cardiac muscle, brown adipose tissue, skeletal muscle	islet β-cells hepatic stellate cells	LD stabilization FA supply to mitochondria

2.9.2 PLIN2

PLIN2 was originally identified to play a role in LD biosynthesis, due to its presence in 3T3-L1 adipocytes and early differentiated adipocytes (Brasaemle *et al,* 1997). Cultured cells exposed to oleic acid show an increase in PLIN2 protein expression alongside an increase in TG stores in Chinese hamster ovary fibroblast cells (Xu *et al,* 2005) and in J774 murine macrophages (Masuda *et al,* 2006). Further to this, oleate treatment in COS-7 cells leads to PLIN2 and DGAT2 colocalising at the LD surface (Stone *et al,* 2009), indicating a role for PLIN2 in TG synthesis. The downregulation of PLIN2 in cultured myotubes led to reduced formation of LD following oleate treatment suggesting a role of PLIN2 in LD stabilisation (Bosma *et al* 2012a). Overall, data from cell studies suggests that PLIN2 is important in the expansion of intracellular TG stores in response to lipid exposure.

The mechanism by which PLIN2 supports IMTG storage is unknown, but one possibility is via suppression of lipolytic enzymes. In support, PLIN2 co-immunoprecipitates with ATGL in rat skeletal muscle under basal conditions, whereas following *ex vivo* electrically-stimulated muscle contraction, this association decreases by 21% (MacPherson *et al,* 2013a). This suggests that PLIN2 enhances lipid accumulation by sequestering ATGL and supressing lipolysis under basal conditions, but releases ATGL enabling it to interact with its co-activator CGI-58 under conditions of lipolytic stimulation (MacPherson *et al,* 2013a). The post-transformational changes that lead to PLIN2 activation though are not known, since work from the same lab was unsuccessful in determining changes in global serine phosphorylation of PLIN2 following adrenaline exposure or electrically-stimulated muscle contraction

(MacPherson *et al,* 2013b). Data from studies in humans does indicate a role for PLIN2 in the expansion of IMTG stores. In human skeletal muscle, IMTG content and PLIN2 protein expression are well-matched (Shaw *et al,* 2009; Peters *et al,* 2012; Shepherd *et al,* 2013), and endurance training enhances IMTG content concomitant with elevated PLIN2 protein expression (Shaw *et al,* 2013; Shepherd *et al,* 2013). Immunohistochemical analysis has shown ~60% of LD are associated with PLIN2 (Shaw *et al,* 2009; Shepherd *et al,* 2013), indicating LD heterogeneity. Thus, using this method it can be inferred that two specific LD pools exist; those associated with PLIN2 (PLIN2+ LD) and those not associated with PLIN2 (PLIN2- LD). When IMTG content is increased via 6 h lipid infusion, the amount of PLIN2+ LD increases significantly without any changes to overall PLIN2 content (Shepherd *et al*, 2017) therefore providing evidence of a subcellular redistribution of PLIN upon expansion of the LD pool.

There is also evidence that PLIN2 may support IMTG breakdown during exercise, since it has been reported that PLIN2+LD are preferentially utilised during 1 h of moderate-intensity exercise in untrained men (Shepherd *et al,* 2012; 2013). However, there was no preferential utilisation of PLIN2+ LD after 6 weeks of endurance or sprint interval training, since both PLIN2+LD or PLIN2-LD utilisation decreasing during 1 h of moderate-intensity exercise (Shepherd *et al,* 2013). Nevertheless, PLIN2 may also interact with HSL, since the cytosolic pool of HSL becomes localised to PLIN2 following adrenaline exposure or electrically-stimulated muscle contraction in rat skeletal muscle (Prats *et al,* 2006). In human skeletal muscle though, Whytock *et al,* (2018) demonstrated no increase in PLIN2 and HSL localisation during 1 h of

moderate intensity exercise. Further research is required to clarify a role of PLIN2 in regulating IMTG breakdown, and whether this involves the regulation of HSL.

2.9.3 PLIN3

The third PLIN to be discovered, PLIN3, was first suggested to play a role in TG synthesis. In non-skeletal muscle cell work, Bulankina *et al,* (2009) observed a reduction in LD maturation and decreased incorporation of TG into LD in HeLa cells when PLIN3 expression was suppressed. Furthermore, in adipocytes incubation with oleic acid, glucose and insulin leads to the localisation of PLIN3 to small LD (Wolins *et al,* 2005). Interestingly though, continued incubation leading to an increase in LD size results in replacement of PLIN3 by PLIN2 (Wolins *et al,* 2005), suggesting a temporal relationship exists between the PLIN protein coat of LDs and the stage of LD growth and expansion. Further to this, knock out models of both PLIN2 and PLIN3 causes reductions in TG storage and the residual LD are fewer but larger in size (Bell *et al,* 2008). Overall, these cell-based studies indicate PLIN3 being of importance in the formation and maturation of LD.

Although it is not known if PLIN3 will display a similar role within skeletal muscle, Kleinert *et al*, (2016) demonstrated that pharmacological activation of AMPK in mice increases PLIN3 gene expression leading to an increase in IMTG content, therefore it has been suggested that PLIN3 may be a factor in IMTG storage. Subcellular localisation may also play a role in the function of PLIN3 as it has been demonstrated that endurance exercise, not short electrically induced contractions, augments PLIN3 expression and its association with mitochondria in rat muscle (Ramos *et al*, 2015).

Whether this is species-specific or due to intracellular localisation is still unknown. There has however, been confirmation that PLIN3 interacts with both ATGL and HSL in rat skeletal muscle, although this is unaffected by lipolytic stimulation (Macpherson *et al*, 2013b). Therefore, the current body of evidence from cell and rodent work suggests PLIN3 may support expansion of TG stores, but the data to support PLIN3 role in IMTG lipolysis is less clear.

In human skeletal muscle, type I fibres are known to display greater PLIN3 protein expression (Shepherd *et al*, 2017b) and there is also evidence of greater PLIN3 expression in females (Peters *et al*, 2012) when overall IMTG content is increased. Prolonged acute exercise at 50% VO_{2max} leads to enhanced PLIN3 expression in human skeletal muscle (Covington *et al*, 2014), though how this is related to IMTG lipolysis is yet to be elucidated. Currently, whether PLIN3 expression is enhanced following endurance exercise training is under debate. PLIN3 expression did not increase after 12 weeks of endurance exercise in neither lean or obese subjects (Peters *et al*, 2012) or after 12 weeks of endurance training combined with strength training in type 2 diabetics (Daemen *et al*, 2018). Conversely when examining fibre-specific changes after 4 weeks of endurance exercise, PLIN3 expression is enhanced in sedentary obese males (Shepherd *et al*, 2017a). Furthermore, after 6 h of lipid infusion, PLIN3+ LD increases alongside increases in IMTG content without changes in overall PLIN3 content (Shepherd *et al*, 2017). There is also an increase in PLIN3 protein expression following 7 days on a high fat, high calorie diet (Whytock *et al,* 2020). Taken together, the current evidence from human studies suggests PLIN3 could exhibit a role in augmenting IMTG stores, but the exact role warrants further investigation.

2.9.4 PLIN4

PLIN4 is expressed in skeletal muscle, heart and also adipose tissue and is preferentially situated in LD with cholesterol esters (Hsieh *et al*, 2012). To date, little is known about PLIN4 in skeletal muscle, though of all the PLIN proteins it is apparently the most highly expressed (Pourteymour *et al*, 2015). The lack of information on PLIN4 is in part, due to the importance of PLIN4 in regulating TG being questioned by Chen *et al*, (2013), who demonstrated that PLIN4 knockout mice had no major alterations in skeletal muscle lipid content. In addition to this, PLIN4 mRNA expression and overall protein content remains unaltered or even reduced following endurance training (Peters *et al*, 2012; Pourteymour *et al*, 2015). However, in more recent years greater PLIN4 protein expressed has been reported in trained compared to sedentary individuals (Shepherd *et al*, 2017b). Like PLIN3, subcellular localisation may be important in defining the role of PLIN4's role, as it was shown that LD located at the periphery of 3T3-L1 adipocytes following oleate treatment were coated with PLIN4 (Wolins *et al*, 2005). In addition, incubation of cultured myotubes with oleic acid enhances PLIN4 mRNA expression (Gjelstad *et al,* 2012), whereas *in vivo* a low-fat diet reduces PLIN4 mRNA expression in human skeletal muscle (Gjelstad *et al,* 2012). Overall, although PLIN4 is expressed in skeletal muscle, there is currently limited and conflicting data on the importance of PLIN4 in IMTG regulation.

2.9.5 PLIN5

Unlike PLIN4, there is much more research concerning PLIN5, which is highly expressed in oxidative tissues such as cardiac tissue and skeletal muscle (Laurens *et al*, 2016). PLIN5 was the final PLIN protein to be discovered with its high expression in tissues that exhibit high rates of lipolysis and β-oxidation (Wolins *et al,* 2006; Peters *et al,* 2012; Shepherd *et al,* 2013). It is found on the LD surface, within the cytosol and at the mitochondria (Bosma *et al*, 2012b; Shepherd *et al*, 2013). Overexpression of PLIN5 in Chinese hamster ovary cells (Dalen *et al*, 2007), in rat skeletal muscle (Bosma *et al*, 2013) and in COS-7 cells (Wolins *et al,* 2006) leads to an increase in TG concentration. PLIN5 overexpression also results in greater interaction between LD and mitochondria (Bosma *et al*, 2012b) and a greater rate of FA oxidation (Wolins *et al*, 2006; Bosma *et al*, 2012b). This interaction may assist in trafficking TG-derived FA to the mitochondria to undergo the process of β-oxidation. However, under PLIN5 knock out conditions, there is a decrease in whole-body FA oxidation observed in mice without any change in the interaction between PLIN5 and mitochondria (Mason *et al*, 2014b). Therefore, the role of PLIN5 in augmenting greater IMTG-derived FA oxidation requires further investigation.

PLIN5 could also provide a functional role as a scaffold protein mediating lipolysis rather than regulating IMTG synthesis. PLIN5 has a conserved N-terminus sequence enabling binding to HSL (Anthonsen *et al*, 1998) and a C-terminus region enabling binding to ATGL or CGI-58 (Granneman *et al*, 2011; Wang *et al*, 2011). CGI-58 is a known co-activator of ATGL, as demonstrated by greater rates of TG hydrolysis when there is an increased interaction between ATGL and CGI-58 (Wang *et al*, 2011). Binding of PLIN5 to ATGL or CGI-58 in Chinese hamster ovary cells suppresses TG hydrolysis under basal conditions (Wang *et al*, 2011). Furthermore, when PKA is

activated under conditions of PLIN5 and ATGL overexpression, there is an increased

rate of lipolysis (Wang *et al*, 2011). From these data, it can be suggested that PLIN5

limits lipolysis under basal conditions via inhibition of ATGL and CGI-58, but enhances

lipolysis by allowing the interaction between ATGL and CGI-58 subsequent to lipolytic

stimuli.

Data from human skeletal muscle also supports a role of PLIN5 in IMTG lipolysis.

Exercise training has been demonstrated to increase PLIN5 expression alongside

increases in IMTG content (Shepherd *et al,* 2013), this increase in PLIN5 expression

indicates a role of PLIN5 in supporting greater IMTG utilisation during exercise. In

untrained individuals, before training and following endurance training, there is a

preferential utilisation of PLIN5+ LD before and after 1 h of moderate-intensity exercise

in human skeletal muscle in comparison to PLIN5- LD (Shepherd *et al*, 2013). Despite

this proposed role, there is a lack of research into the interaction between HSL, ATGL

and PLIN5. Recently though, Whytock *et al,* (2018) demonstrated that HSL relocated

to PLIN5+ LD in response to 1 h of moderate-intensity exercise. Moreover, PLIN5

protein expression also correlates positively with IMTG stores in type I fibres

(Shepherd *et al*, 2013; Shepherd *et al*, 2017b), in endurance trained subjects (Daemen

et al, 2018) or after endurance training (Peters *et al*, 2012; Shepherd *et al*, 2013). In

this way, it is possible that PLIN5 also supports IMTG storage. For example, in human

skeletal muscle, 6 h lipid infusion causes an increase in IMTG with an increase in

PLIN5+ LD in type I fibres (Shepherd *et al*, 2017b). Further to this, a prolonged

exposure to increased lipids via a 5-day high fat diet, will result in greater PLIN5 protein

expression (Gemmink *et al*, 2017a). Whereas, increased IMTG following greater FFA

availability as a consequence of prolonged fasting is entirely attributable to an increase

in PLIN5+ LD (Gemmink *et al*, 2016). Taken together, this data suggests PLIN5 protein expression is often upregulated through enhanced FA availability, and PLIN5 colocalization to LD is enhanced in situations of increased IMTG content, and this may support IMTG storage as well as breakdown when metabolic demands increase. Furthermore, although PLIN5 increases in response to increased FA availability, which is linked to increases in PLIN5+ LD, time-course studies are required to determine whether the increase in PLIN5 labelled LD leads to, or is as a result of, the increase in IMTG.

2.10 Lipid droplet formation

The exact process of LD formation in skeletal muscle is still under debate, and this topic has been extensively reviewed in several recent articles (Pol *et al,* 2014; Henne *et al,* 2018; Goodman *et al,* 2020). For the purposes of this thesis, it is pertinent to provide a brief overview of this process. Currently, the most prevalent hypothesis is that lipid accumulates between two leaflets of the endoplasmic reticulum membrane until this lens of neutral lipid reaches a critical size and is budded into the cytoplasm as a newly formed LD (known as primordial LDs) (Murphy & Vance, 1999). Cultured human macrophages analyzed using freeze-fracture high resolution electron microscopy have provided evidence for this by demonstrating endoplasmic reticulum membranes lie external to and follow the contour of LD, similar to an egg held by an egg cup (Robenek *et al,* 2006). Immunogold labelling has demonstrated PLIN2-enriched domains of the cytoplasmic leaflet of the endoplasmic reticulum are where the LD are located, therefore suggesting a role of PLIN2 in LD biogenesis (Robenek *et al*, 2006).

Several mechanisms have been proposed to explain how LD increase in size, including; 1) the fusion of two LD via pores in the phospholipid monolayer, 2) ripening of one LD through the transfer of lipids and proteins from a LD decreasing in size, and 3) the expansion of pre-existing LD due to increased synthesis of TG from FA (Gemmink *et al,* 2017). Investigations in NIH 3T3 adipocyte cells showed LD growth via fusion to be independent of TG synthesis, but required the presence of microtubules and the motor protein, dynein (Bostrom *et al,* 2005). Microtubules provide a pathway within cells for LD to move to other LD or different organelles altogether (Welte, 2009). Freeze-fracture electron microscopy investigations in macrophages demonstrate close contact between LD and smaller (possibly newly-formed) LD, supporting the concepts of fusion and/or ripening (Robenek *et al,* 2006). The family of SNARE proteins may also play a role in LD fusion, since knockdown of SNAP23, syntaxin-5 and VAMP4 in NIH-3T3 adipocytes reduced the rate of LD fusion leading to an overall decrease in LD size (Bostrom *et al,* 2007). LD can also decrease in size via the processes of fission or fragmentation. The ADP ribosylation factor (ARF)- COPI machinery is known to coat endosomal membranes and Golgi vesicles and is thought to be involved in this process. TG lipolysis in the core of LD by ATGL and HSL is also expected to reduce LD size, though whether fission of LD and TG lipolysis occur together or independently is yet to be elucidated. With regard to LD size and number, it is generally accepted that having a greater number of smaller LD is metabolically advantageous as this provides a greater surface area for regulatory proteins to bind to. This hypothesis stems from the fact that endurance-trained individuals display greater numbers of smaller LD compared to obese individuals and type 2 diabetes patients (Daemen *et al,* 2018).

2.11 Manipulating IMTG content through diet

IMTG content has been demonstrated to be strongly associated with dietary fat intake, with increases of 50-100% following consumption of high-fat diets which provide 40-65% of total energy intake as fat (Hoppeler *et al,* 1999; Helge *et al*, 1998, 2001; Johnson *et al,* 2003; Vogt *et al,* 2003; Zderic *et al,* 2004). Moreover, high fat diets can lead to a shift in fat metabolism. Chronic consumption (4-7 weeks) of a high fat diet increases the capacity for whole-body fat oxidation (Spriet*,* 2014; Volek *et al,* 2015). Adaptations occurring to support this include enhanced carnitine palmitoyl transferase I activity (Fisher *et al*, 1983) and reductions in hexokinase activity (Fisher *et al*, 1983). When combining exercise training with either a low-fat (20%) or high-fat (62%) diet over a 7-week period, whole-body fat oxidation increased by ~80% during exercise after consuming a high-fat diet (Helge *et al,* 2001). This increase during exercise was accounted for via increases in both plasma FFA (~50%) and muscle and/or lipoprotein-derived TG (~100%), though they suggested that IMTG utilisation was of only minor quantitative importance, since they failed to report a significant exercise-induced decrease in IMTG content. There is, however, convincing evidence that a short-term high-fat diet will lead to greater IMTG utilisation during exercise (Johnson *et al,* 2003; Zderic *et al,* 2004). Johnson *et al,* (2003) used ^{1}H-MRS to demonstrate an ~50% increase in resting IMTG content in the *vastus lateralis* following 2 days of a high-fat compared to a low-fat diet, with an exercise-induced reduction of 64% and 57% following each diet, respectively. Zderic *et al,* (2004) also provided evidence to suggest that enhanced fat oxidation following a high-fat diet was largely due to increases in the use of IMTG. Overall, the consumption of fat is important to maintain IMTG stores.

Further to this, there has been great recognition as to the importance of pre-exercise muscle glycogen concentrations being an important factor in mediating endurance performance capacity (Bergstrom *et al,* 1967). Thus, leading to focus on high-CHO dietary recommendations and less focus on the fat component of the diet. High CHO diets, with fat intake varying from 2 – 25% can markedly decrease IMTG storage (Starling *et al,* 1997; Coyle *et al,* 2001; Johnson *et al,* 2003). Furthermore, ^{1}H-MRS studies have observed significant impairments in post-exercise IMTG repletion following consumption of a low-fat, high-CHO diet (Decombaz *et al,* 2000; Decombaz *et al,* 2001; Larson-Meyer *et al,* 2002; Van Loon *et al,* 2003). However, fat intake in these studies was as low as 10–15% total energy intake, which is markedly less than typical fat intake in elite endurance athletes (Van Loon *et al,* 2004). When examining post-exercise IMTG repletion after 3 h of moderate-intensity cycling in well-trained individuals, there was no repletion for at least 48 h when consuming a high-CHO diet containing only 24% of energy from fat (Van Loon *et al,* 2003). In contrast, a moderate-fat diet of ~39% lead to IMTG stores returning to baseline by 24–48 h of recovery. Taken together, it is evident that post-exercise macronutrient intake has an effect on intramuscular substrate replenishment and more research is needed to assess the optimal strategy to support glycogen resynthesis alongside IMTG repletion.

2.12 Demands of field-based training and competition

Despite decades of research examining glycogen utilisation during exercise and resynthesis post-exercise, it is still difficult to provide guidelines for CHO consumption in relation to fuelling exact training sessions due to varying metabolic demands of training and competition. As far back as 2003, recommendations from the international

Olympic committee expert panel acknowledged that fuel demands vary largely based on the type of event, exercise intensity and duration (Burke, 2004). Even among elite endurance athletes, training loads can vary from 10-12 hours per week with key sessions being 60 – 120 min (e.g. track runner), up to 25-30 hours per week with sessions lasting 4-6 hours (e.g. triathletes/cyclists) (Burke *et al,* 2018). This led to a 'sliding' scale of CHO intake targets rather than a universal recommendation for CHO fuelling strategies (Burke *et al,* 2018)*.* The timing and amount of CHO intake should be considered in relation to fuel cost for that days specific training or competition load, with this concept now being referred to as 'fuel for the work required' (Impey *et al,* 2018). Given the variability in training loads discussed above, any given amount of CHO and timing of intake may equal 'high CHO availability' on one specific day or in one specific athlete, whilst in another context e.g. different athlete or different training focus, it may be considered 'low'.

However, Burke *et al*, (2018) highlighted that key CHO guidelines being used by athletic populations are not underpinned by data from field-based environments, but rather strict laboratory-based conditions. Subsequently, the majority of studies currently influencing sports nutrition guidelines, to date, are largely based on laboratory-based protocols (Burke *et al*, 2011). Thus, although the concept of different and/or changing CHO requirements for different training and individuals is now being considered, there is an overall lack of understanding of the fuel costs of these habitual training and field-based competitive environments. This restriction in our knowledge also applies to the utilisation of IMTG during exercise with our understanding being underpinned by data from studies based under strict laboratory-based environments.

The primary issue that arises from the laboratory-based protocols (e.g. fasted exercise at a fixed relative intensity for a given duration, such as 1 h at 70% VO_{2max}), is the rigorous control measures put in place to ensure reproducibility and reliability such as set workloads, intensities and durations. This does not consider factors such as exogenous CHO availability, changes in terrain and incline, and environmental influences such as wind speed and rain, all of which will influence pace, power, speed, the athlete's rating of perceived exertion, heart rate and the intensity of the training. Although an athlete may be prescribed a specific training session, external factors such as those listed will alter the metabolic demand of a training session considerably. Further to this, exercise mode indoors may cause differences in muscle activation and therefore muscle substrate utilisation, in comparison to the same exercise mode outdoors. A review by Hooren *et al,* (2020) demonstrated increased knee flexion at footstrike and contact time, alongside decreases in knee flexion range of motion and foot-ground angle at footstrike when running on a motorised treadmill in comparison to overground running. Such biomechanical differences on a motorised treadmill used in laboratory-based research provide further emphasis as to why more field-based research should be undertaken. Moreover, the physiological demands of treadmill running vs overground running have been demonstrated to differ, with treadmill running requiring a lower rate of oxygen uptake than overground running (Aubry *et al,* 2018), and when running at the same intensity on an outdoor running track, there is greater energy expenditure than a motorised treadmill (Bidder *et al,* 2017). Overall, whilst the laboratory-based studies on which the CHO guidelines are based provide complete control, they are not representative of training or competition in a field-based environment. It has now been highlighted as a key question for future research, that the fuel costs, and particularly glycogen utilisation, are fully understood, in order to

inform CHO requirements of various training sessions commonly undertaken by athletes (Burke *et al,* 2018).

2.13 General Overview

As well as providing an overview of CHO and fat metabolism during exercise, Chapter 2 serves to identify a number of gaps in our knowledge which require further investigation, some of which will be tackled in this thesis. Chapter 3 provides a detailed account of the common methodologies used in each of the experimental chapters, including information on sample collection and detailed protocols for sample staining for both TEM (Chapter 4) and immunofluorescence microscopy (Chapter 5 & 6).

In chapter 4, muscle substrate utilization during two different habitual field-based training sessions in recreationally-active males were investigated using TEM methodology. Specifically, this chapter focused on quantifying fibre type and subcellular-specific glycogen and IMTG utilization in both the *vastus lateralis* and the *gastrocnemius* in response to a 10 mile steady state run and a track interval session (8x800m). Ultimately, the aim of this study was to understand substrate use during field-based training sessions. In chapter 5, we continue to investigate IMTG utilization under field-based conditions, but this time during a cross-country skiing race. This study, aimed to evaluate immunofluorescence microscopy as a suitable method to measure IMTG utilisation and changes in LD morphology on a fibre and subcellular-specific basis during a field-based competitive scenario. It is also important to consider which microscopy method is best suited for our investigations, leading to a secondary aim of chapter 5 to establish the level of agreement between transmission electron

microscopy and immunofluorescence microscopy. This will aid to understanding of whether subcellular-specific data could be generated using immunofluorescence microscopy. Finally, chapter 6 examines IMTG utilisation and also considers the lack of data of post-exercise IMTG resynthesis in comparison to glycogen. Thus, chapter 6 examined the impact of post-exercise CHO availability and the molecular mechanisms underpinning IMTG resynthesis using immunofluorescence microscopy, following on from our findings in chapter 5. As the study aimed to explore potential regulatory mechanisms it was conducted in a more controlled laboratory-based setting than the previous two studies described. In chapter 7 the findings of each of the experimental chapters are discussed and placed within the context of general literature, making proposals for future research directions in light of the findings from this thesis.

Chapter 3 – General methodology

3.1 Overview of chapter

This chapter primarily serves to describe in detail the muscle biopsy procedure, and the theoretical basis and protocols used for the immunofluorescence microscopy and transmission electron microscopy work undertaken across the experimental chapters of the thesis (Chapters 4-6). These methods are cited, where appropriate, within each experimental chapter. Participant characteristics, the study design and experimental protocol is included in each experimental chapter.

3.2 Muscle samples

Percutaneous skeletal muscle biopsies were collected from either the *vastus lateralis,* the lateral head of the *gastrocnemius,* or *triceps brachii* under local anaesthesia (~ 5 ml 1% lidocaine). Following local anaesthesia of the selected site, a small incision was made (~ 1 cm) in the skin and the fascia before the biopsy needle was inserted. Biopsies were collected using either the Bergstrom (Bergstrom *et al,* 1967) needle biopsy technique (Chapters 5 and 6) or the micro-biopsy technique (Bard Monopty Disposable Core Biopsy Instrument 12 guage x 10cm length, Bard Biopsy Systems, Tempre, AZ, USA) (Chapter 4). Under a micro-dissection microscope, muscle samples were blotted of excess blood and any visible fat tissue was removed and discarded. For immunohistochemical analysis, muscle tissue was embedded in Tissue-tek OCT compound (Sakura Finetek Europe, The Netherlands) on a cork board which was subsequently frozen in liquid nitrogen-cooled isopentane (Sigma-Aldrich, Dorset, UK) and stored in cryotubes at – 80°C. The protocol used to preserve muscle samples for subsequent analysis using transmission electron microscopy (TEM) is detailed in section 3.4 of this chapter.

3.3 Immunohistochemical analysis of skeletal muscle sample

3.3.1 Sample preparation and protocol

Immunofluorescence microscopy analyses were used in experimental chapters 5 and 6 of this thesis. Serial 5 µm cryosections were cut at -25°C and mounted onto uncoated, ethanol-cleaned glass slides. Muscle sections from each time-point for the same participant were mounted on to the same slide in order to minimise any difference in the staining process within each subject. Sections were initially fixed to maintain the structural integrity and antigenicity of the muscle samples in 3.7% formaldehyde solution for 1 h followed by three rinses (each for 30 s in doubly-distilled water (dd H_2O)). General membrane permeabilization is then achieved through incubating the slides in 0.5% Triton X-100 for 5 min so that the fluorescent probe can reach the target antigen. Triton-X 100 is a detergent, and aids in partially solvating the cellular membranes without disturbing interactions between proteins, thus improving the penetration of the antibody through the tissue.

Following three 5 min washes in phosphate buffered saline (PBS, 137mM sodium chloride, 3mM potassium chloride, 8 mM disodium hydrogen phosphate and 3 mM potassium dihydrogen phosphate, pH of 7.4), slides were incubated for 60 min with appropriate primary antibodies. Following this incubation period, a further three 5 min PBS washes were completed before the slides were incubated with appropriately-targeted fluorescently-labelled secondary antibodies for 30 min. Three more 5 min washes in PBS preceded a 20 min incubation with BODIPY 493/503 (Invitrogen, Paisley, UK) on occasions when lipid staining was required. Due to the light sensitive nature of BODIPY 493/503, all procedures from this point forward were undertaken in a dark room. Following a final 5 min wash in PBS solution, coverslips were mounted

using Vectashield (H-1000 Vector Laboratories, Burlingame, CA, USA) and sealed with nail varnish before being left to dry overnight.

3.3.2 Antibodies and lipid dye

Primary antibodies were obtained for both experimental chapters 5 and 6 from commercially available sources and diluted in PBS. Details of both primary and secondary antibodies used in chapters 5 and 6 are detailed in Table 3.1. The working dilutions for each of the primary antibodies used are displayed in table 3.1 and were based on previous studies from the laboratory (Shepherd *et* al, 2017; Whytock *et al*, 2018). Alexa Fluor conjugated secondary antibodies were also obtained from commercially available sources and were diluted in PBS at 1:200 unless stated otherwise. To visualise intramuscular triglycerides, a cell permeable lipophilic fluorescence dye Difluoro{2-[1-(3,5-dimethyl-2H -pyrrol-2-ylidene-N)ethyl]-

3,5-dimethyl-1H -pyrrolato-N }boron 493/503 (BODIPY (493/503) was used, which emits a bright green fluorescence. The advantages of BODIPY vs other lipid dyes are discussed in 2.7.3.

Table 3.1. Summary of immunofluorescence staining method for experimental chapter 5 and 6.

Chapter 5			
Target	*Primary antibodies*	*Dilution*	*Commercial source*
Myosin slow twitch fibres	MHCI, host species: mouse	1:100	DSHB, University of Iowa, USA (Cat no. A4.840c)
Myosin fast twitch IIa fibres	MHCIIa, host species: mouse	1:100	DSHB, University of Iowa, USA (Cat no. N2.261c)
Cell membrane	Laminin, host species: rabbit	1:50	
	Secondary antibodies		
Visualization of MHCI	Goat Anti-Mouse IgM 546	1:200	Thermofisher Scientific, Paisley, UK (Cat no. A-21045)
Visualization of MHCIIa	Goat Anti-Mouse IgG 405	1:200	Thermofisher Scientific, Paisley, UK (Cat no. A-31553)
Visualization of the plasma membrane	Goat Anti-Rabbit IgG 633	1:200	Thermofisher Scientific, Paisley, UK (Cat no. A-21070)
	Post staining – also used in chapter 6		
IMTG	Bodipy 493/503	1:100	Invitrogen, Paisley, UK (Cat no. D3922)
Chapter 6			
Target	*Primary antibodies*		
Myosin slow twitch fibres	MHCI, host species: mouse	1:100	DSHB, University of Iowa, USA (Cat no. A4.840c)
Myosin fast twitch IIa fibres	MHCIIa, host species: mouse	1:100	DSHB, University of Iowa, USA (Cat no. N2.261c)
PLIN2	Mouse monoclonal anti-adipophilin	1:50	American Research Products, Waltham MA, USA (Cat no. E-AB-1073)
PLIN3	Rabbit polyclonal anti-perilipin 3/TIP-47	1:50	Novus Biologicals, Cambridge, UK (Cat no. NB110-40764)
PLIN5	Guinea pig polyclonal anti-OXPAT	1:50	Progen Biotechnik, Heidelberg, Germany (Cat no.GP31S)
	Secondary antibodies		
Visualization of PLIN2	Goat anti-Mouse IgG1 633	1:200	Thermofisher Scientific, Paisley, UK (Cat no. A-21126)
Visualization of PLIN3	Goat anti-rabbit IgG 633	1:200	Thermofisher Scientific, Paisley, UK (Cat no. A-21072)
Visualization of PLIN5	Goat anti-guinea pig IgG 633	1:200	Thermofisher Scientific, Paisley, UK (Cat no. A-21105)
Cell membrane	Wheat Germ agglutinin (WGA) Alexa Fluor 633	1:100	Invitrogen, Paisley, UK (Cat no. W21404)

3.3.3 Image capture using confocal microscopy

Images of cross-sectionally orientated muscle fibres were captured using an inverted confocal microscope (Zeiss LSM710; Carl Zeiss AG, Oberkochen, Germany) with a 63x 1.4 NA oil immersion objective with a 1.1x digital zoom. An argon laser was used to excite the Alexa Fluor 488 fluorophore and BODIPY 493/503, a helium-neon laser excited the Alexa Fluor 546 and 633 fluorophores, and a diode laser excited the Alexa Fluor 405 fluorophore. To assess fibre-specific IMTG content, fibres that were positively stained for myosin heavy chain type I were classified as type I fibres, while those that were stained positively for myosin heavy chain type IIa were classified as type IIa fibres. ~20 images were captured per time point aiming for an even split across type I and type IIa fibres. All other fibres were assumed to be type IIx fibres, and though some images were captured, there was an insufficient number of type IIx fibres to perform statistical analysis and therefore the results are not included in chapter 5 or 6. Information on the number of fibres analysed for each fibre type are detailed in the individual experimental chapters.

In chapter 6, to investigate co-localisation between LD and PLIN proteins the same microscope and magnification were utilised to obtain the digital images, but with a 4x digital zoom applied on the straightest edge of an identified cell. This first allowed an image to be taken at the peripheral region of the cell and subsequently the field of view was manually moved to the centre of the cell identified using the cell membrane, to generate an image of the central region of the cell.

3.3.4 Immunofluorescence controls

Before imaging took place, several controls were put in place when staining the muscle samples. First, PBS was used instead of the primary antibody in order to check for non-specific binding of the secondary antibody. For example, using the same fixation and permeabilization method as described in 3.2.1 above, the primary antibody was replaced with PBS, followed by the secondary antibody. The result was extremely low levels of staining (intensity was < 10 AU) in images without the primary antibody. When using the primary antibody, the intensity was considerably more with the typical fluorescence intensity being > 80 AU. Control samples were also generated to check for bleed-through of signal into different colour channels of the microscope. Moreover, the staining procedure was conducted in the absence of any antibodies to check for any autofluorescence of the samples alone that could potentially impact imaging. Further to this, controls where PLIN2 was blocked using a recombinant peptide incubated with the primary antibody, resulting in the fluorescence signal of PLIN2 being removed (Shepherd *et al,* 2012). The concentration of the blocking peptide was titrated to saturating concentrations that would completely block the binding sites for the secondary antibody. This has also been completed for PLIN3 (Shepherd *et al,* 2017) and PLIN5 (Shepherd *et al,* 2013).

3.3.5 Image analysis

Image processing and analysis was completed on a fibre type-specific basis using Image-Pro Plus 5.1 software (Media Cybernetics, Rockville, MD, USA). An intensity threshold was uniformly selected to represent a positive signal for IMTG and/or each PLIN protein. The content of IMTG or PLIN content was expressed as the positively stained area relative to the total area of the peripheral or central region of each muscle

fibre. Using the Image-Pro Plus software the cells were split into two subcellular regions, the peripheral and central regions of the cell. This was completed by using a 2 µm band around the edge of the cell border, identified via the immunofluorescence staining with the appropriate antibody as described in table 3.1, to create the peripheral region to measure subsarcolemmal LD (first 2 µm from the cell border) and the central region to measure intermyofibrillar LD (remainder of the cell). This approach of using a fixed 2 µm distance from the membrane to represent the subsarcolemmal region has been utilised previously to examine IMTG content in differing populations (Van Loon, 2004). LD density was expressed as the number of LD's relative to the area of the peripheral or central region. LD size reflects the average size of all LD's detected in a single image of both the peripheral and central region separately.

3.4 Transmission electron microscopy sample preparation

Fresh muscle samples were fixed with 2.5% glutaraldehyde in 0.1M sodium cacodylate buffer (pH 7.3) for 24 h before being rinsed four times in 0.1M sodium cacodylate buffer. Subsequently, the samples were post-fixed with 1% osmium tetroxide and 1.5% potassium ferrocyanide in 0.1M sodium cacodylate buffer for 90 min at 4°C. Reduced osmium tetroxide containing potassium ferrocyanide was used due to its preference for a high electron density of glycogen particles (De Bruijin, 1973). After post-fixation, the muscle samples were rinsed twice in 0.1M sodium cacodylate buffer at 4°C, and then underwent a graded dehydration using ethanol (30, 50, 70, 90 and 100% concentration). Following two washes with 100% propylene oxide, samples were penetrated with graded mixtures of propylene oxide and epoxy resin (Agar 100 Medium, Agar Scientific, Essex, UK) at 20°C (2:1, 1:1, and 1:2 ratios of propylene oxide to epoxy resin, for 1-2 h each concentration), and finally embedded

in 100% epoxy resin for 12 h at 60°C. Longitudinal orientated ultra-thin (~60 nm) sections were obtained using a ultramicrotome (Reichert Jung Ultracut, Vienna, Austria) fitted with a diamond blade and collected on to formvar coated grids (200 copper mesh size). To obtain as many fibres as possible, sections were collected at three different depths into the tissue block separated by ~150 nm.

3.4.1 Post-staining procedures

Post-staining is advised on samples for TEM to increase the contrast of subcellular structures. Prior to use, stock solutions of both the Reynold's lead citrate and uranyl acetate (UA) (3% by weight in ddH$_2$O) were aliquoted and microcentrifuged for 5 min. Samples were then incubated in UA for 14 min, after which excess UA was removed by manual washing of the sample in ddH$_2$O (only moving the sample in an up and down motion). Subsequently, the sample was incubated in Reynold's lead citrate for 5 min in a dark room at room temperature, followed by washing in ddH$_2$O. Samples were air dried at room temperature for at least 30 min prior to imaging.

3.4.2 Transmission electron microscopy measures of mitochondria and glycogen.

Each muscle sample contained both transverse and longitudinal fibres, but only longitudinally orientated fibres were imaged using a TEM (FEI Morgagni, Field Electron and Ion Company, Oregon, USA), coupled with an Olympus Megaview III camera, which provided an average of 10 fibres per biopsy (range: 6-12 fibres). Each fibre was initially viewed at x1,000 magnification in order to locate the plasma membranes and visually assess the available myofibrillar area (Figure 3.1). For mitochondria and glycogen analysis, images were collected at x36,000 magnification (Figure 3.2), where a total of 24 images were obtained per fibre in a randomized systematic order (Figure 3.1). Of these 24 images collected per fibre, 12 images were

obtained of the subsarcolemmal region (SS), 6 images of the superficial region of the myofibrillar space (superficial myofibrillar) and 6 images of the central region of the myofibrillar space (central myofibrillar, see figure 3.1).
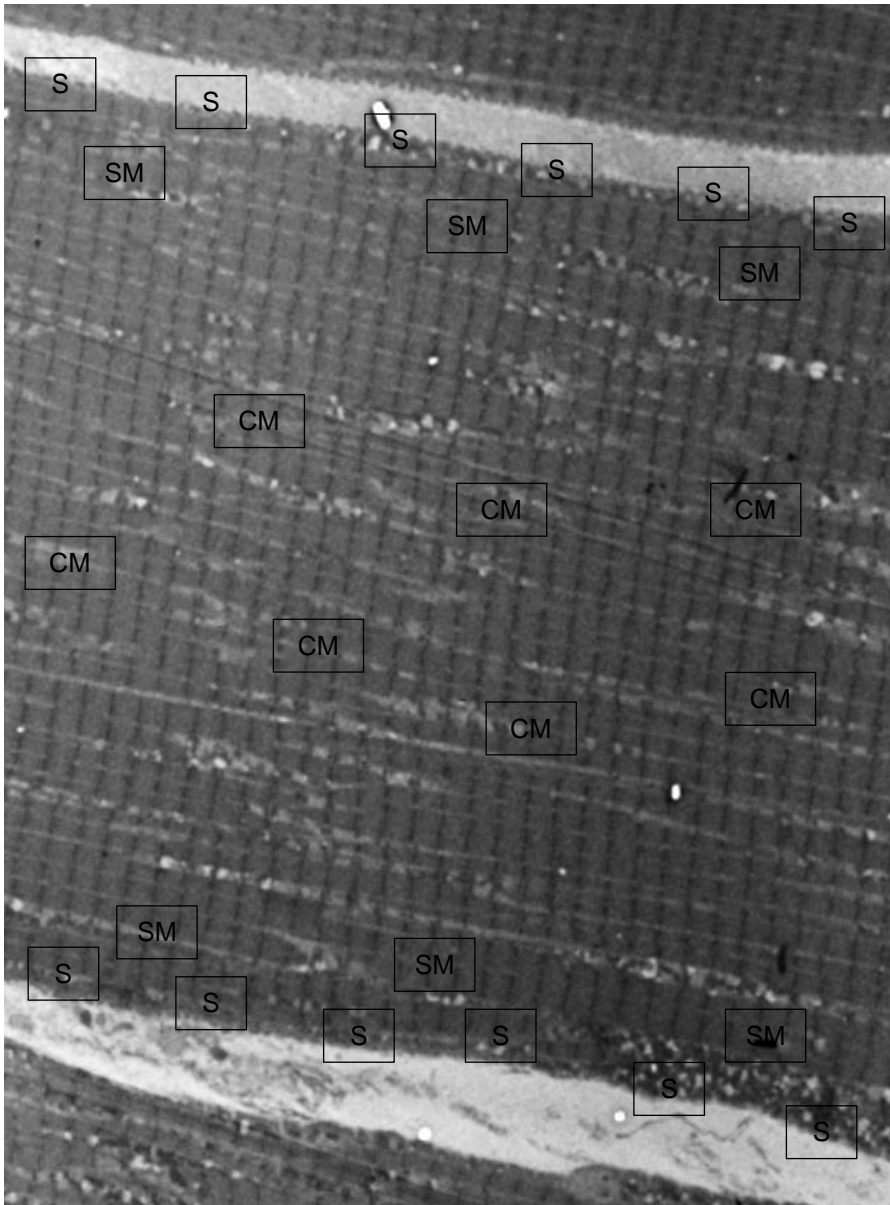
Figure 3.1. Representative location of TEM image locations for glycogen. Representing the subsarcolemmal region (SS), the superficial myofibrillar region (SM) and the central myofibrillar region (CM) of each fibre.
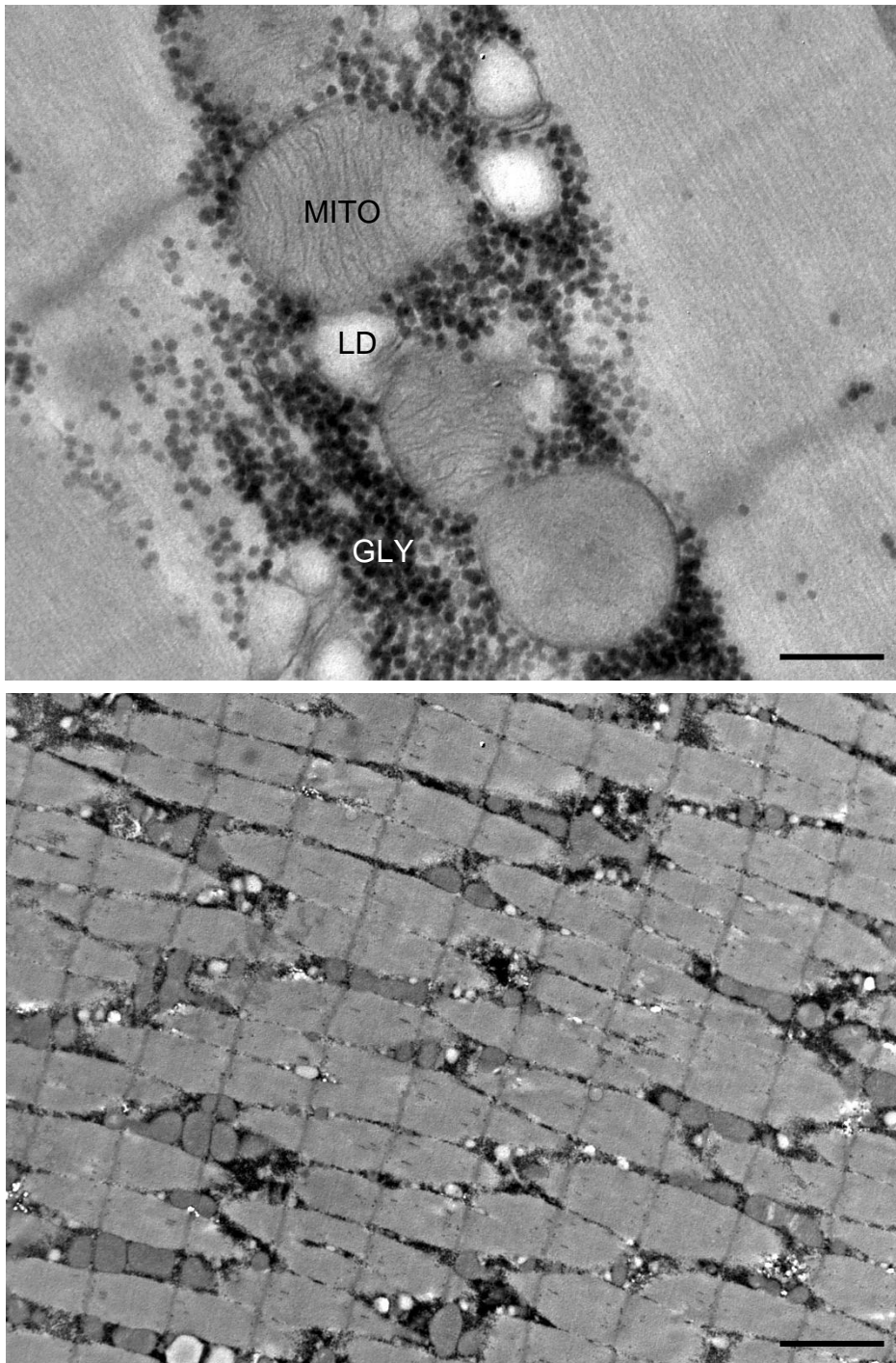
Figure 3.2. Representative TEM images, top image taken at 36,000x scale bar = scale bar = 0.5µm, bottom image taken at 22,000x scale bar = 1µm.

MITO: Mitochondria, GLY: Glycogen granules, LD: Lipid droplet

3.4.3 Overview of stereology

At a practical level, the use of stereological methods enables quantitative information to be gathered on microscopic, 3-D structures, permitting reliable data to be collected from sections (Gundersen *et al,* 1988). Morphometric measurements using stereological methods are often required in muscle-based research with measures such as muscle area, fibre area and number of muscle fibres (Zacharova & Kubinova, 1995). Manual methods or methods that require manual tracing are very time-consuming, whilst automated methods come into difficulty identifying individual fibres. When using such methods, important considerations include any manipulation of the microscope which will alter measurement conditions should be avoided if possible, and when counting, the classification rules must not change throughout. The images collected using transmission electron microscopy were analysed using such methods in order to identify fibre type and subsequently quantify glycogen and lipids.

3.4.4 Fibre type determination

Fibre type differences were assessed through classification of the fibres as either type I or type II by combining measures of IMF mitochondria volume and Z-line width (Sjostrom *et al*, 1982) First, a 135 nm grid was applied to the image (see Figure 3.3 for grid size referencing) before all points of the grid with mitochondria underneath were counted and recorded. The Z-line of each image was then measured twice and recorded. The IMF mitochondria volume fraction was subsequently plotted against the Z-line width for each fibre obtained from each biopsy (Figure 3.4), and the fibres with the greatest IMF mitochondria volume fraction and the thickest Z-line width were classified as type I fibres, with the opposite being true for type II fibres (i.e. lowest IMF mitochondria volume fraction and narrowest Z-line width). Only the 2 most distinct type I or type II fibres were included in the analysis.
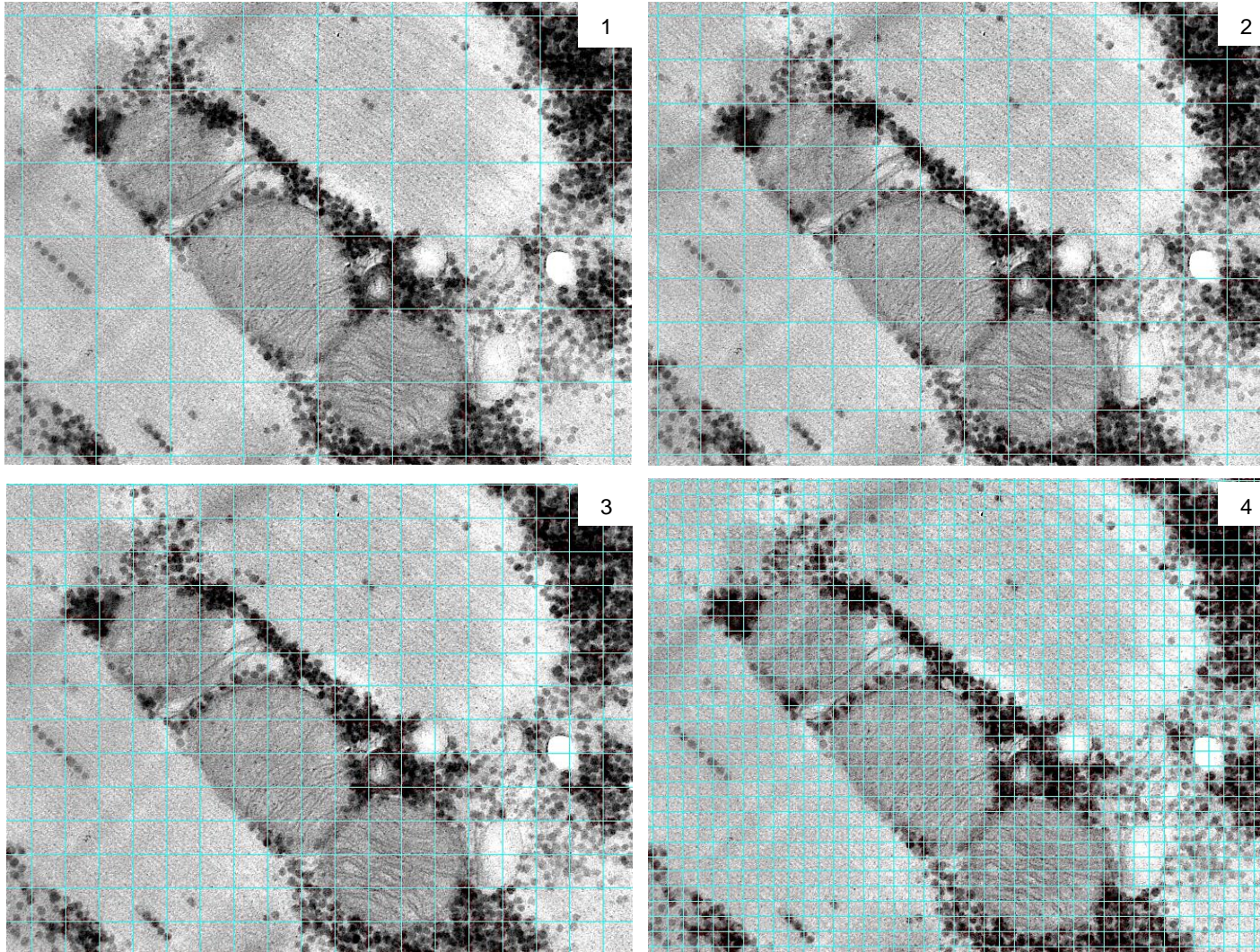
Figure 3.3. The grid sizes used during the quantification of mitochondria, glycogen and lipid. 1. 300nm grid, 2. 180nm grid, 3. 135nm grid and 4. 60nm grid.
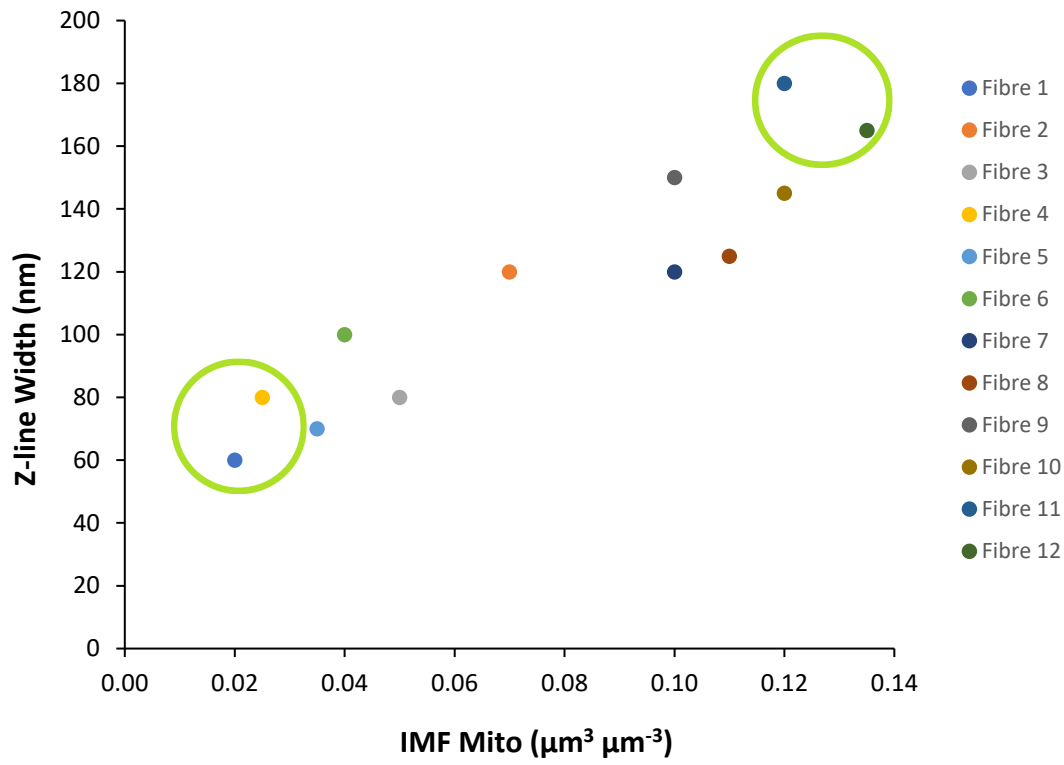
Figure 3.4. Example plot to determine fibre type using Z-line measurement and IMF mitochondria. Green circle represents which fibres would be used.

3.4.5 Image analysis

For each type I and type II fibre, three spatial localizations of glycogen were defined in the following: 1) the subsarcolemmal (SS) space, 2) the intermyofibrillar (IMF) space, and 3) the intramyofibrillar (Intra) space, defined as being inside the myofibrils, between the contractile elements of the fibre. Subsarcolemmal images were used to determine SS glycogen, whereas the combination of superficial and central myofibrillar images were used to determine IMF and Intra glycogen pools.

3.4.6 Glycogen counting

To determine SS glycogen, the length of the subsarcolemmal region was first measured and recorded, and then an 180nm grid (Figure 3.3) was applied to the image for point counting to take place. Point counting refers to the counting of the intersections of the grid with the target, i.e. mitochondria, glycogen, lipid or interspace, directly underneath of the respective grid size. To determine both the IMF and intra glycogen, first the interspace points were counted and recorded using a 300nm grid (Figure 3.3), this measure refers to any part of the image that is myofibrillar space. Glycogen points in the IMF region were then counted using a 180nm grid, whilst the intra glycogen was counted under a 60nm grid (Figure 3.3). These grid sizes have been extensively used in research conducted by our collaborators in experimental Chapter 5 (Nielsen *et al,* 2010, 2013, 2017; Ørtenblad *et al,* 2013, 2018; Koh *et al,* 2017; 2018), and we subsequently adopted these grid sizes for use in Chapter 4. ~ 8 glycogen particles per image were randomly selected and measured to gather particle diameter data for each subcellular location individually.

3.4.7 TEM data calculations – glycogen

In relation to experimental chapter 3 and the TEM comparisons made in chapter 4, the following calculations explain how the absolute and relative distributions of mitochondria, glycogen and lipid in the IMF, intramyofibrillar (intra) and SS locations were calculated.

Absolute and relative glycogen

The glycogen volume fraction (V_v) in each of the three locations was estimated as proposed by Weibel (eq. 4.20, Weibel, 1980), where the effect of section thickness has been taken into account:

$$V_V = A_A - t \left\{ (1/\pi) \right\} B_A - N_A \left[t + H) \right] \}$$

Where A_A is glycogen area fraction, t is section thickness, B_A is the glycogen boundary length density, N_A is the number of particles per area and H is the average profile diameter.

It was assumed that the particles were spherical (Melendez-Hevia *et al,* 1993) and the fibres were cylindrical with a diameter of 80 µm (Saltin & Gollnick, 1983). Since IMF and intra volume fractions are expressed as densities and SS as volume per surface area, total glycogen values were obtained by recalculating IMF and intra data to volume per fibre surface area. Assuming fibres are of a cylindrical shape, the volume beneath the surface area of the fibre (V_b) is:

$$V_B = R \cdot 0.5 \cdot A$$

Where R is fibre radius and A is the fibre surface area. Therefore, when the radius is assumed to be 40 µm and the fibre surface area is 1 µm², the volume beneath the

surface area of fibre is 20 μm^3. Therefore, the V$_V$ of IMF and intra regions are multiplied with a factor of 20 when relative comparison with SS region is conducted and total values are calculated (Neilsen *et al*, 2010).

The relative contribution of glycogen in each subcellular location to total glycogen per fibre is then calculated using the following equations:

$$IMF \rightarrow IMF \; glycogen \; V_V \; / \; Total \; glycogen$$

$$Intra \rightarrow (Intra \; glycogen \; * \; Interspace) \; / \; Total \; glycogen$$

$$SS \rightarrow (SS \; glycogen \; / \; 20) \; / \; Total \; glycogen) \; / \; 20 \; in \; order \; to \; correct \; for \; unit \; difference \; of \; absolute \; data$$

Absolute mitochondria in the intermyofibrillar region

IMF mitochondrial volume fraction was calculated using point counting. The sum of IMF mitochondria is then divided by this to give us the area fraction of IMF mitochondria in the superficial region. As the superficial region of a cylinder occupies 3 times more volume than the central region, volume estimates from the superficial region were weighted 3 times more than those from the central region. Thus, to calculate IMF mitochondrial volume fraction the following equation was used:

$$(3 * IMF \; mitochondria \; in \; the \; superficial + central \; region \; equivalent)/4$$

Absolute Mitochondria in the subsarcolemmal region

In the SS region, mitochondria is not expressed as volume fraction, but is instead expressed as volume per surface area of the fibre. The volume of the image is multiplied by the volume fraction to obtain an absolute volume. The absolute volume

per length of fibre is divided by the thickness of the section to obtain an estimate per surface area of the fibre. The SS mitochondria count is then divided by the grid reference space for mitochondria divided by the length of the fibre available to give the area fraction of SS mitochondria. This then is divided by the image volume which, then gives us the absolute volume to be divided by the thickness of the section. The total mitochondria is calculated by:

$$IMF\ mitochondria\ volume\ fraction + (SS\ mitochondria\ volume\ fraction\ /\ 20)$$

3.5 Transmission electron microscopy measures of lipid.

3.5.1 Imaging

For lipid analysis, the magnification was X11,000 and ~16 (10 – 18) images were collected of the SS and superficial IMF locations, with ~24 (20 – 28) images being taken of the central IMF location. This magnification allowed three specific locations to be defined and analysed: SS, central IMF and superficial IMF. IMF lipid was expressed relative to the myofibrillar space whilst, the SS lipid was relative to the surface area of the fibre through calculating the available length. Within these images, two pools of lipid droplets were identified: IMF LD and SS LD. The fibre typing was undertaken as described in section 3.3.4.

3.5.2 Image analysis for lipid

Our criteria for identifying LD included having a circular white/greyish appearance, lacking a distinct membrane as seen with mitochondria. In agreement with previous research, LD also needed to have a minimum diameter of 200 µm, if smaller than this, they were excluded from the analysis (Koh *et al,* 2017). To count SS lipid, the image

was zoomed in to 200% to ensure accuracy in the counts and measurements, then the available length of the subsarcolemmal region was measured before applying the 180nm grid (Figure 3.2). The LD were measured, both in width and height of the maximum points to generate an average LD diameter. To calculate the myofibrillar lipid, a 200% zoom was applied on the superficial myofibrillar region and the central myofibrillar region separately before point counting occurred.

3.5.3 TEM data calculations – Lipid

Absolute and relative lipid

The same calculations for absolute and relative glycogen were applied to the absolute and relative lipid data. However, the reference grid points were adapted accordingly, using the 180nm grid to count lipid and mitochondria (Figure 3.3). There was no intra data collected meaning no interspace counts were required.

Lipid droplet size and number estimations

LD size was calculated by measuring and averaging the major and minor diameters of each individual LD recorded. The aspect ratio of the LD reflects the "length-to-width ratio" (calculated as major diameter/minor diameter). LD number was calculated by dividing the subcellular LD volume fraction by the mean individual LD volume of the respective subcellular region. The LD were assumed to be spherical in shape and the volume (V) was calculated using the following equation:

$$V = {}^3\!/_4 \; \pi \, r^3$$

Where r is the radius based on the average of the major and minor diameters of each individual LD.

3.5.4 Precision estimates

The precision of stereological estimates, represented by the estimated coefficient of error (CE_{est}), for mitochondria, glycogen and lipid was calculated as proposed by Howard and Reed (2005).

$$\text{CE}\left(\frac{\Sigma y}{\Sigma x}\right) = \sqrt{\frac{n}{n-1}\left(\frac{\Sigma x^2}{\Sigma x \times \Sigma x} + \frac{\Sigma y^2}{\Sigma y \times \Sigma y} - \frac{2 \times \Sigma(x \times y)}{\Sigma x \times \Sigma y}\right)}$$

For each estimate, n = the number of micrographs, x is the total points per micrograph and y is the points crossing the objects of interest. The CE_{est} value examines the variation in the parameters between images and allows the quality of quantitative estimates gathered from stereological methods such as point counting used in this TEM analysis to be estimated. By definition the CE is the standard error of the mean of repeated estimates divided by the mean. The CE_{est} values are reported within experimental chapter 4. Inter-investigator and intra-investigator correlation coefficients for all analyses were > 0.96. Inter-investigator correlation coefficient was calculated through each researcher analysing the same muscle fibre, then values from each researcher were compared. Intra-investigator correlation coefficients were calculated from the same investigator analysing the same muscle fibre on at least two occasions.

Chapter 4 - A microscopy-based investigation into subcellular substrate utilisation during field-based habitual training sessions in male runners.

4.1 Abstract

To date, comparisons of exercise intensity on muscle substrate utilisation at both a fibre type and subcellular-specific level, have not yet been simultaneously examined within the same study in a field-based training environment. This study aimed to quantify glycogen and lipid utilisation on a fibre type and subcellular-specific basis during two field-based training sessions using TEM. In a randomised, repeated measures cross-over design, 11 male runners (age 25 $\pm$ 3 years, body mass 76.2 $\pm$ 7.6 kg, height 178.5 $\pm$ 5.4 cm) completed a 10-mile road run performed at lactate threshold or an 8x800m high-intensity interval track session at VO_{2peak} under standardised nutritional conditions, with muscle biopsies obtained from the *vastus lateralis* and *gastrocnemius* before and after exercise. Overall, glycogen was reduced regardless of fibre type across all subcellular locations following exercise with a preferential use of intramyofibrillar glycogen. In the *vastus lateralis*, INTRA glycogen utilisation was greater following the 8x800 trial (P = 0.002) in comparison to the 10 mile trial (P = 0.061). Lipid utilisation, however, occurred primarily in the IMF region of type I fibres, particularly during the 10-mile trial (P = 0.001). Furthermore, there was a tendency for LD number to be reduced during the 8x800m trial (P = 0.071), whereas there was a tendency for LD size to be reduced during the 10-mile trial (P = 0.067). These data highlight the interaction between muscle fibre recruitment, relative exercise intensity and training duration in modulating subcellular-specific glycogen and lipid utilisation within specific exercise protocols. Being the first to investigate on a subcellular-basis using TEM in running and allowing us to identify a preferential use of INTRA glycogen during exercise, independent of intensity. Furthermore, lipid utilisation occurs primarily in the IMF region of type I fibres, but changes in LD morphology maybe related to exercise intensity and duration. The pattern of glycogen

and lipid utilisation here, specific to the training status of the participants and exercise intensities compared, may aid practical guidelines in relation to fuelling strategies to promote training intensity and metabolic adaptations by providing field-based data to add to the laboratory-based literature on the substrate demands of habitual training.

4.2 Introduction

As outlined in Chapter 2, despite the emphasis on the importance of understanding nutrition to optimise performance in endurance events, there is a considerable lack of data that has been collected in a field-based training or competitive environment. Indeed, the majority of studies influencing sports nutrition guidelines have used laboratory-based protocols (e.g. fasted exercise at a fixed relative intensity for a given duration, such as 1 h at 70% VO_{2max}), which although have the benefits of being able to implement strict control measures, may not always be representative of field-based training due to the lack of physiological responses to changes in changing weather and terrain. Moreover, laboratory-based research often uses motorised treadmills or cycle ergometers. The physiological demands of treadmill running have been demonstrated to require a lower rate of oxygen uptake than overground running (Aubry *et al,* 2018), and when running at the same intensity on an outdoor running track, there is greater energy expenditure than a motorised treadmill (Bidder *et al,* 2017). In addition to this, differences between specific muscles (Koh *et al,* 2017) and specific muscle fibre types (Pendergast *et al,* 2000) are also likely to affect both CHO and lipid utilisation during field-based training sessions at different intensities and durations. To address this, Impey *et al,* (2020) recently undertook a comprehensive study that aimed to assess sex and muscle differences in glycogen utilisation in the *vastus lateralis* and *gastrocnemius* during different typical run training sessions completed in a field-based training environment. Overall, by assessing glycogen concentration using the biochemical extraction technique, they reported a greater utilisation of glycogen in the *gastrocnemius* in comparison to the *vastus lateralis*, and a greater glycogen requirement during a prolonged moderate-intensity run compared to a shorter, interval

running session. Within muscle though, glycogen content varies depending on fibre (type I, type IIa and type IIx fibres) and subcellular region (subsarcolemmal (SS), intermyofibrillar (IMF) and intramyofibrillar regions (INTRA)). Whilst IMF glycogen stores are the largest, it is the INTRA glycogen stores (Marchand *et al,* 2007, Nielsen *et al,* 2011), and the SS glycogen stores that are preferentially utilised during exercise (Jensen *et al,* 2020). This is important, because it has been shown that glycogen and muscular fatigue likely originates via a connection between INTRA glycogen and sarcoplasmic reticulum (SR) Ca^{2+} release (Ørtenblad *et al,* 2011). Thus, when examining muscle substrate utilisation, it would be preferable to use a method that allows assessment on both a fibre type and subcellular-specific basis. Currently, such comparisons of exercise intensity, muscle and substrate utilisation at both a fibre and subcellular region-specific basis, have not yet been simultaneously examined within the same study in a field-based training environment.

Similar to glycogen, intramuscular triglyceride (IMTG)-containing lipid droplets (LD) are also distributed on a fibre and subcellular specific basis (Nielsen *et al,* 2010; Koh *et al,* 2017; 2018). Importantly, transmission electron microscopy (TEM) allows the identifiation and quantification of exercise-induced changes in LD content and morphology (number and size). It is now well known that moderate-intensity exercise leads to a decrease in IMTG content specifically in type I fibres (reviewed by Van Loon, 2004), and there is some evidence that IMF LDs are specifically reduced (Chee *et al,* 2016; Koh *et al,* 2017). However, the effect of exercise intensity on fibre and subcellular-specific changes in both LD content and morphology are yet to be investigated, especially within a field-based setting.

Consequently, the aim of the present study was to quantify glycogen and lipid utilisation of the *vastus lateralis* and *gastrocnemius* muscle of recreationally active male runners during either steady state endurance training or high intensity interval training in a field-based training environment. This was achieved using TEM, which by virtue of its high magnification and resolution capabilities, is considered the gold-standard method for investigating changes in the quantity and morphology of substrates at the subcellular level. Therefore, we quantified glycogen and lipid utilisation on a fibre and subcellular-specific basis during both a 10-mile road run at lactate threshold or an 8x800m track interval session at VO_{2peak}. We hypothesised glycogen utilisation would be preferential to the INTRA glycogen stores, whilst lipid utiisation would be specific to the IMF region and that overall, substrate utilisation would differ between exercise trials, with greater glycogen utilisation following the 8x800m trial and greater lipid utilisation following the 10 mile trial.

4.3 Methods

Participants and ethics

Eleven male competitive and recreational runners were recruited as part of a larger study (Impey *et al,* 2020). Participant's anthropometric and physiological profiles are presented in Table 4.1. All participants had at least 5 years of competitive running experience and were training routinely ≥3 times a week, with a best 10km race time of ≤45 min. Following a detailed explanation of the nature of the study, all participants provided written informed consent. All procedures conformed to the standards set by the *Declaration of Helsinki* and the study was approved by the NHS Research Authority (West Midlands, Black Country Research Ethics Committee, REC reference 15/WM/0428).

Table 4.1. Anthropometric profile, training history and physiological profile.

	Participants (n = 11)
Anthropometric profile	
Age (years)	25 ± 3
Body mass (kg)	76.2 ± 7.6
Height (cm)	178.5 ± 5.4
Fat Free Mass (kg)	59.0 ± 6.1
Training profile	
Weekly distance (km)	34.9 ± 21.2
Weekly duration (hours)	4.6 ± 2.0
Physiological profile	
VO_{2peak} (L/min)	4.2 ± 0.4
VO_{2peak} (mL.kg^{-1}.min^{-1})	53.9 ± 4.7
VO_{2peak} (mL.kg^{-1} FFM.min^{-1})	69.7 ± 6.1
vVO_{2peak} (km.h^{-1})	16.5 ± 0.7
Lactate Threshold (%VO_{2peak})	68.6 ± 6.3
Lactate Threshold (km.h^{-1})	12.5 ± 0.7
Lactate Turnpoint (%VO_{2peak})	76.4 ± 6.1
Lactate Turnpoint (km.h^{-1})	13.6 ± 0.7

P < 0.05. values are presented in means $\pm$ SD. Adapted from Impey *et al,* (2020), Table 1.

Design

In a randomised, repeated measures cross-over design participants took part in two different training sessions at different exercise intensities which are representative of those used to prepare for a 10km race (Spillsbury, personal communication, English Institute of Sport). These sessions consisted of 1) a steady state trial of 10 miles performed at lactate threshold, or 2) a high-intensity intermittent training session of 8 x 800m performed at maximal oxygen uptake (VO_{2peak}). Muscle biopsies were taken from the *vastus lateralis* and the lateral head of the *gastrocnemius* immediately before (pre) and after (post) exercise. The corresponding running speeds for each trial were individual to each participant, and determined on a separate occasion through completion of a graded exercise test to establish VO_{2peak} lactate threshold and lactate turn-point. 48 hours prior to the main experimental trials, participants completed a glycogen-depletion protocol before subsequently receiving a standardised diet in an attempt to normalise pre-exercise muscle glycogen values between participants prior to both exercise trials.

Pre-experimental assessment

All participants reported to the exercise physiology laboratories at Liverpool John Moores University in an overnight fasted state between 07:00h – 08:00h. Participants were given a standardised breakfast (CHO 2 g.kg^{-1} body mass, protein 25g, fat 10g) 3 hours before starting the graded exercise test in the form of incremental running on a treadmill (HP Cosmos, Germany). A resting finger-tip blood sample was collected (Lactate Plus, Nova Biomedical USA) before completing a self-selected warm up. During the graded exercise test, oxygen uptake was measured during exercise via breath-by-breath measurements using a CPX Ultima series online gas analysis

system (Medgraphics, Minnesota, USA). This was calibrated with internal standard of known gases and volumetric syringe.

The graded exercise test commenced with the treadmill at a speed of 10 km.h^{-1} and 1% incline, and the speed increased by 1 km.h^{-1} every 3 min. At the end of each stage blood lactate was assessed via finger-prick capillary blood sampling (Lactate Plus, Nova Biomedical, USA). Participants continued to run until both lactate threshold and lactate turn-point had been achieved. Lactate threshold was expressed as an increase in blood lactate above the resting value by 0.4mmol.L^{-1}, and lactate turn-point was expressed as an increase in blood lactate of ≥ 1.0 mmol.L^{-1} above resting (Winter *et al*, 2007). Part 2 of the test began at a speed 2 km.h^{-1} below the speed reached at lactate turn-point, and the speed was then increased by 1 km.h^{-1} every minute until volitional fatigue or until 16 km.h^{-1} was reached, where the incline was then increase by 1% every minute until volitional fatigue. VO$_{2peak}$ was determined as the greatest VO$_2$ value obtained in any 10 sec period if meeting two of the following criteria: heart rate within 10 beats per min of age-predicted maximum, respiratory exchange ration (RER) > 1.1 or plateau of oxygen consumption despite greater workload. Thus, to calculate the speed at VO$_{2peak}$ the final treadmill speed was used if this was ≤16 kph. For those participants who had reached the incline stages of the test the following equation was used to calculate velocity at VO$_{2max}$:

$$\text{Speed at } \dot{V}O_{2peak} = (\dot{V}O_{2max} \times 60) / \text{Running economy}$$

$\Rightarrow$ $\quad$ $Kph = (ml.kg^{-1}.min^{-1} \times 60) / ml.kg^{-1}.km^{-1}$

$\Rightarrow$ $\quad$ $\text{Running economy} = \dot{V}O_2 / (16 / 60)$

$\Rightarrow$ $\quad$ $VO_{2max} (ml.kg^{-1}.km^{-1}) = ml.kg^{-1}.min^{-1} / (16 / 60)$

Experimental protocol

Days 1 and 2: Participants arrived at the laboratory on the evening of the first experimental day after avoiding alcohol and vigorous physical activity for 24 h prior. A heart rate (HR) monitor (Polar FT1, Finland) was fitted and body mass (BM) was recorded before participants commenced an intermittent glycogen-depleting running protocol on a manually operated treadmill (HP, Cosmos, Germany). Particpants performed 90-min of high-intensity interval running (or to exhaustion if this occurred first). First they completed a self-selected 5 min warm up, and then commenced running for 2 min bouts at 100% VO_{2max}, interspersed with 2 min recovery at 60% VO_{2max}. When participants could no longer complete the 2 min bouts at 100% VO_{2max}, the work-rest ratio was reduced to 1.5 min – 2 min and then finally, reduced to 1 min – 2 min. Once unable to complete 1 min bouts at 100% VO_{2max} the intensity was reduced to 90% VO_{2max} and completed in the same pattern of work-rest ratio as described above. The protocol was chosen to maximally diminish muscle glycogen in both type I and type II muscle fibres. This protocol has been successfully used previously in our laboratory (Bartlett *et al*, 2013; Impey *et al*, 2016; Taylor *et al*, 2013). For both experimental trials, water was consumed ad libitum throughout exercise and total time to exhaustion. Subsequent to completing the glycogen depletion, participants were given 1.2 g CHO.kg^{-1} BM through a sports drink and bar (Lucozade, UK) and 25g whey protein (Science in Sport, UK) to be consumed within the first hour post-depletion. The evening meal provided to the participants included 2 g CHO.kg^{-1} BM, 15g fat and 40 g protein. For the next 36 h participants were provided with food and drink containing 6 g CHO.kg^{-1} BM per 24 h, 2 g protein.kg^{-1} BM per 24 h, and 1 g fat.kg^{-1} BM per 24 h. All food was prepared by a SENr registered sport nutritionist and was in line with dietary preferences of the participants. During this 36 h period,

participants were also advised to avoid caffeine and alcohol as well as strenuous physical exertion.

Day 3: On the afternoon of day 3, participants either arrived at the Tom Reilly building at Liverpool John Moores University to complete the 10-mile trial, or at an outdoor running track (Wavertree Athletics Centre, Liverpool, UK) to complete the 8x800m trial. Trials were separated by a minimum of 7 days and were completed in a randomised order. Skeletal muscle biopsies of the *vastus lateralis* and *gastrocnemius* were collected at rest and preserved for TEM analysis, described in more detail below. Participants were fitted with a GPS watch (Garmin Forerunner 620) before commencing each exercise trial. The 10-mile trial was a supervised road run from and returning to Liverpool John Moores University at a speed corresponding to lactate threshold. Heart rate (HR) and rating of perceived exertion (RPE) were recorded at rest and at the end of every mile. During the 8x800m trial, participants completed 8 repetitions of 800m with 2 min recovery between repetitions at a speed corresponding to VO_{2peak}. HR and RPE were recorded at rest and at the end of each interval. Muscle biopsies were collected after each trial 2 cm distal to the pre-exercise biopsy, and a post-exercise venous blood sample was also obtained.

Muscle biopsies

Skeletal muscle biopsies were collected from the *vastus lateralis* and the lateral head of the *gastrocnemius* before and after exercise. Muscle biopsies were collected under local anaesthesia (0.5% Marcaine) from separate incision sites approximately 2 – 3 cm apart using a Bard Monopty Disposable Core Biopsy Instrument (Bard Biopsy Systems, Tempe, AZ, USA). The muscle samples were prepared for TEM according

to the protocol described in section 3.5 and 3.5.1. They were then imaged according to the description in section 3.6.1, and fibre type was determined as described in section 3.6.2, see figure 4.1 (glycogen) and 4.2 (lipid) for examples of micrographs,. Representative images of glycogen and lipid can be seen in figure 4.1 and 4.2, respectively. Finally, mitochondria, glycogen and lipid analysis were then undertaken as described in section 3.6.3. Approximately 14,000 electron micrographs were analysed from 58 muscle biopsies (30 pre-exercise, 28 post-exercise) for glycogen and mitochondria. For lipid, ~ 18,000 electron micrographs were analysed from 45 biopsies (23 pre-exercise, 22 post-exercise). The coefficient of error (CE_{est}), calculated as explained in section 3.4.4 for mitochondria was 0.119 ± 0.028 and 0.176 ± 0.055 in the IMF and SS regions, respectively. Glycogen and lipid CE_{est} values are displayed in Table 4.2.

Table 4.2. The precision of stereological estimates represented as coefficient of error (CE_{est}).

CE_{est} for volume fraction		Pre-exercise	Post-exercise
Glycogen	IMF	0.070 ± 0.019	0.078 ± 0.036
	INTRA	0.101 ± 0.045	0.139 ± 0.133
	SS	0.101 ± 0.032	0.125 ± 0.082
Lipid	IMF	0.153 ± 0.046	0.159 ± 0.035
	SS	0.329 ± 0.079	0.315 ± 0.055

Values are presented as mean $\pm$ SD including data from both exercise trials, both muscles and both fibre types.
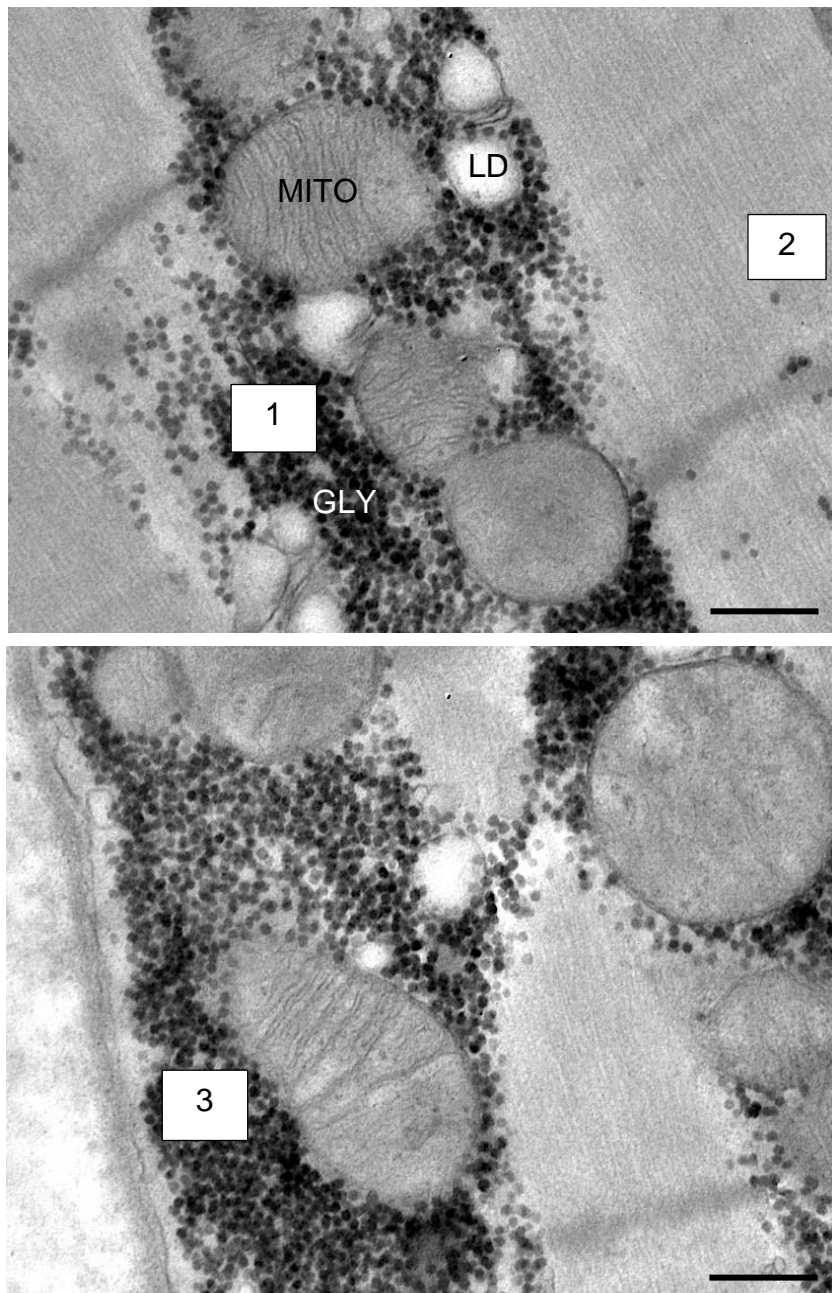
Figure 4.1. Transmission Electron Micrographs for glycogen analysis

Images taken at x 36,000, scale bar = 0.5µm showing 1. Intermyofibrillar, 2. Intramyofibrillar and 3. Subsarcolemmal pools of glycogen. Full description can be found in chapter 3.6.1. MITO: Mitochondria, GLY: Glycogen granules, LD: Lipid droplet
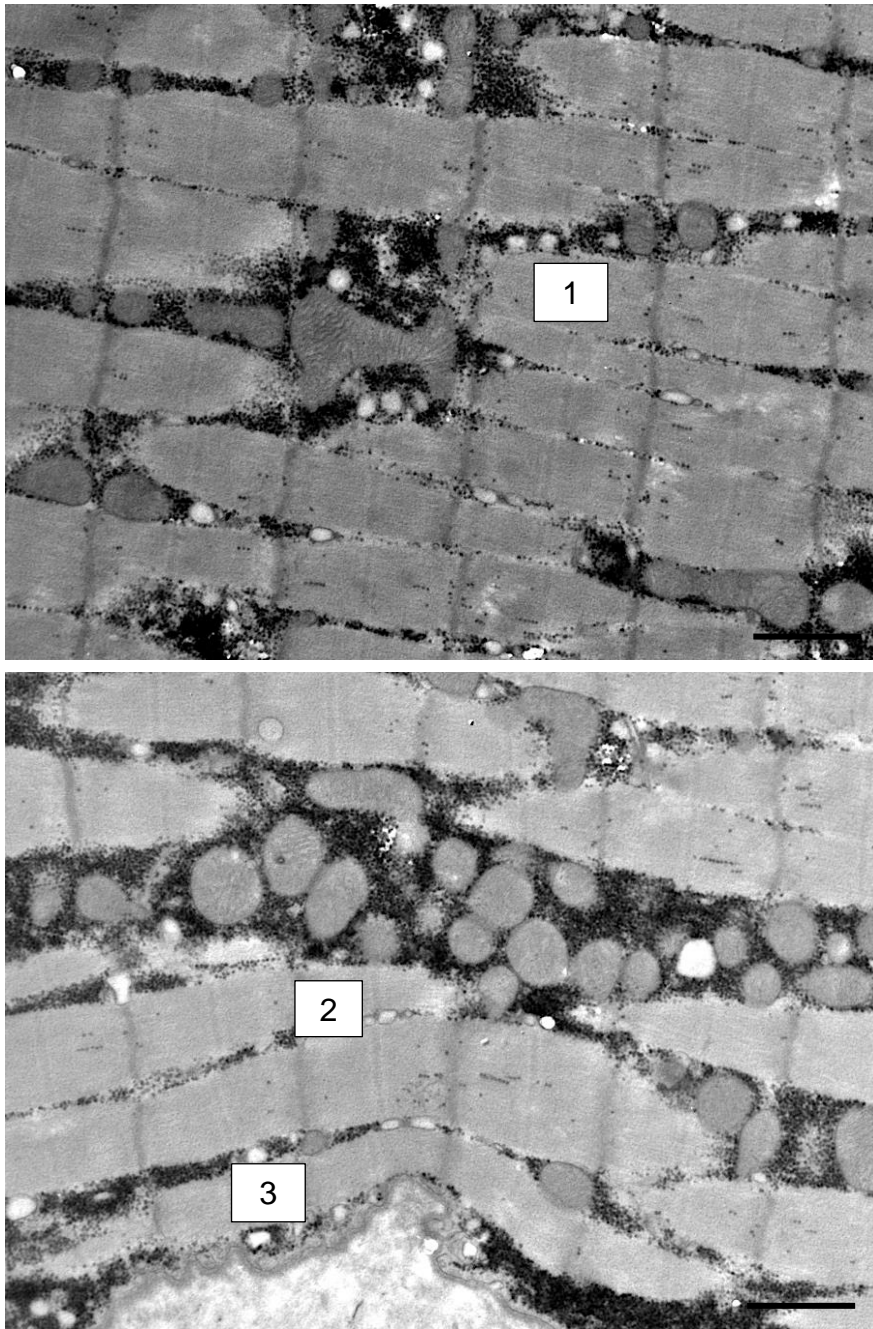
Figure 4.2. Transmission Electron Micrographs for lipid analysis

Images taken at x 11,000 showing, scale bar = 2µm 1. Central myofibrillar, 2. Superficial myofibrillar 3. Subsarcolemmal area of the cell. Full description can be found in chapter 3.7.1.

Statistical analysis

Statistical analyses were performed using SPSS (SPSS; version 23, IBM, USA). Linear mixed modelling was used to examine all dependent variables (glycogen, mitochondria and lipid) pre and post-exercise for both the 10-mile and 8x800m trial, with data separated into the two different muscles, *vastus lateralis* and *gastrocnemius*. All main effects and interactions were tested using a linear mixed-effects model, with random intercepts to account for repeated measurements within subjects to examine differences between exercise trial, muscle, fibre type and subcellular region. Subsequent Bonferroni adjustment post-hoc analysis was used to examine main effects and interactions. Data is presented as mean ± SD. Significance was accepted at $P < 0.05$.

4.4 Results

Fibre-type dependent distribution of mitochondria, glycogen and lipid pre-exercise.

Total mitochondria volume fraction was 51% and 61% greater in type I compared to type II fibres in the *vastus lateralis* and *gastrocnemius*, respectively ($P < 0.05$). There was no difference between muscles in the total mitochondria volume fraction ($P = 0.241$). When considering subcellular region, mitochondria volume fraction was fibre type dependent in both the IMF ($P < 0.05$) and SS subcellular locations of the *vastus lateralis* ($P = 0.017$), with type I fibres containing 51% and 47% more mitochondria in each subcellular location, respectively, compared to type II fibres (Table 4.3). However, in the *gastrocnemius* this fibre-type dependent distribution was only evident in the IMF location ($P < 0.05$), with type I fibres containing 64% more mitochondria than type II fibres. In contrast, the SS mitochondria volume fraction was not different in the *gastrocnemius* between type I and II fibres. The relative distribution of total mitochondria between the IMF and the SS locations was not different when comparing the *vastus lateralis* to the *gastrocnemius* ($P > 0.05$). In type I fibres, $89 \pm 2\%$ of mitochondria was located in the IMF region, whilst $11 \pm 2\%$ was located in the SS region. In type II fibres, $85 \pm 1\%$ of mitochondria was located in the IMF, whilst $15 \pm 1\%$ were located in the SS region.

102

Table 4.3. Subcellular mitochondrial content in the *vastus lateralis* and *gastrocnemius*

	Vastus Lateralis		*Gastrocnemius*	
	Type I	Type II	Type I	Type II
Mitochondria				
IMF $\mu m^3 \cdot \mu m^{-3}$ myofibrillar space$\cdot 10^3$	0.117 ± 0.049	0.057 ± 0.018*	0.154 ± 0.026	0.055 ± 0.008*
SS $\mu m^3 \cdot \mu m^{-2}$ fibre surface area$\cdot 10^3$	0.336 ± 0.191	0.179 ± 0.119*	0.322 ± 0.146	0.219 ± 0.143
Total $\mu m^3 \cdot \mu m^{-3}$ myofibrillar space$\cdot 10^3$	0.134 ± 0.056	0.066 ± 0.023*	0.170 ± 0.031	0.066 ± 0.012*

IMF, intermyofibrillar; SS, Subsarcolemmal. Values are means $\pm$ SD. * $P < 0.05$ vs type I fibres

Pre-exercise, in the *vastus lateralis*, there were no fibre-specific differences in glycogen in the IMF or INTRA locations, however there was a trend for SS glycogen to be greater in type I fibres compared to type II fibres (P = 0.094, Figure 4.3c). The relative distribution of glycogen across subcellular locations was not different between fibre types, with IMF, INTRA and SS glycogen contributing 84%, 5% and 11% of total glycogen in type I fibres, respectively, and 83%, 5% and 12% of total glycogen in type II fibres, respectively (Figure 4.4). However, the location of glycogen in the *gastrocnemius* was found to be highly dependent on fibre type. IMF glycogen was 16% greater in type I fibres compared to type II fibres (P = 0.011, Figure 4.3a), whereas INTRA glycogen was 80% higher in type II fibres compared to type I fibres (P = 0.049, Figure 4.3b). No fibre type differences were observed for SS glycogen (P = 0.382, Figure 4.3c). Thus, IMF glycogen contributed 85% of total glycogen in type I fibres, but only 82% of total glycogen in type II fibres (P = 0.018, Figure 4.4). In contrast, INTRA glycogen contributed only 3% of total glycogen in type I fibres, which increased to 5% in type II fibres (P = 0.019). SS glycogen contributed 12% and 13% of total glycogen in type I and type II fibres, respectively (P = 0.149). When comparing the two muscles, INTRA glycogen was greater in the *vastus lateralis* compared to the *gastrocnemius*, which was true across both type I and type II fibres (P = 0.006).
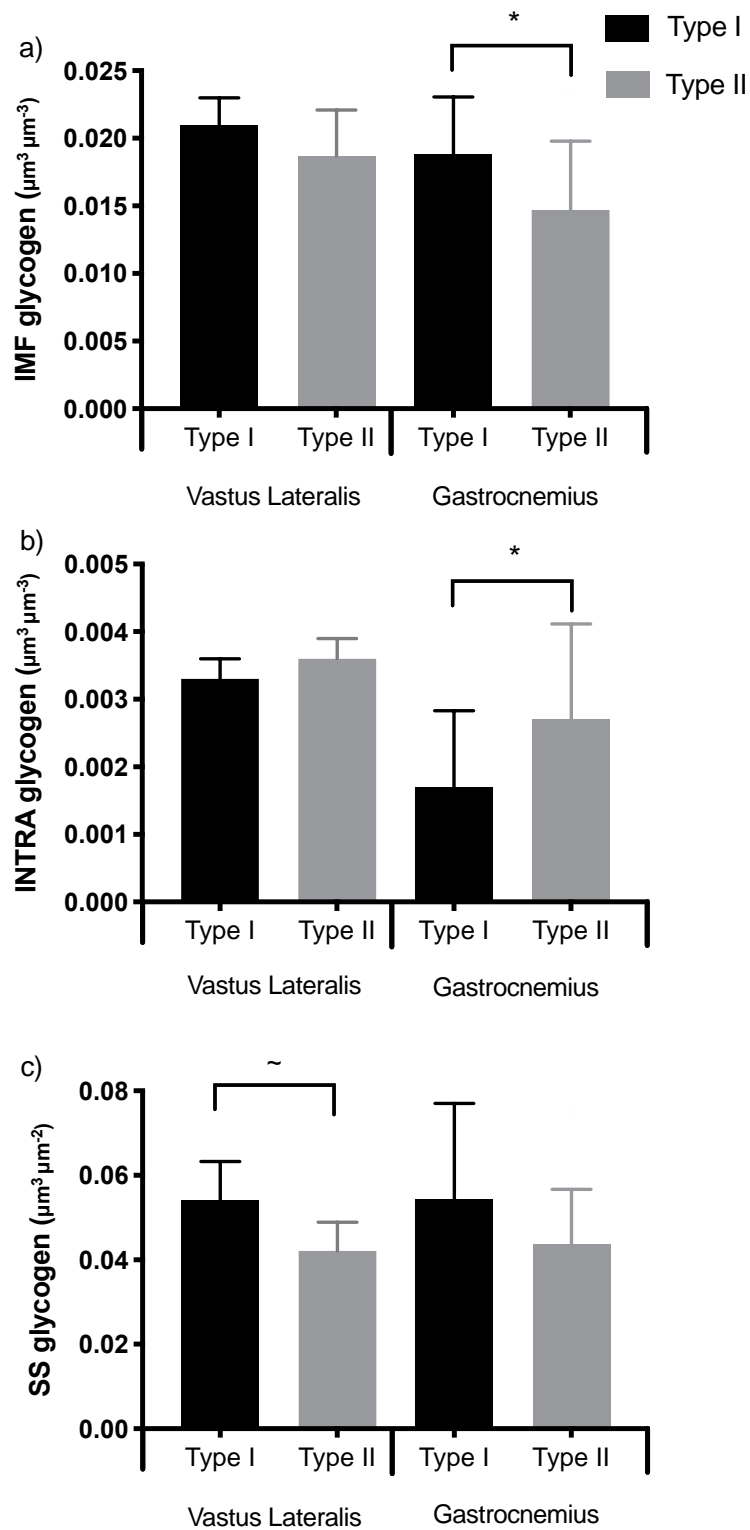
Figure 4.3. Glycogen content in the IMF, INTRA and SS locations before exercise.

Glycogen content in the *vastus lateralis* and *gastrocnemius* in a) intermyofibrillar, b) intramyofibrillar and c) subsarcolemmal locations. Values are means ± SD. * $P < 0.05$ significant fibre type differences, ~ $P < 0.094$ trend for significant fibre type differences.

105
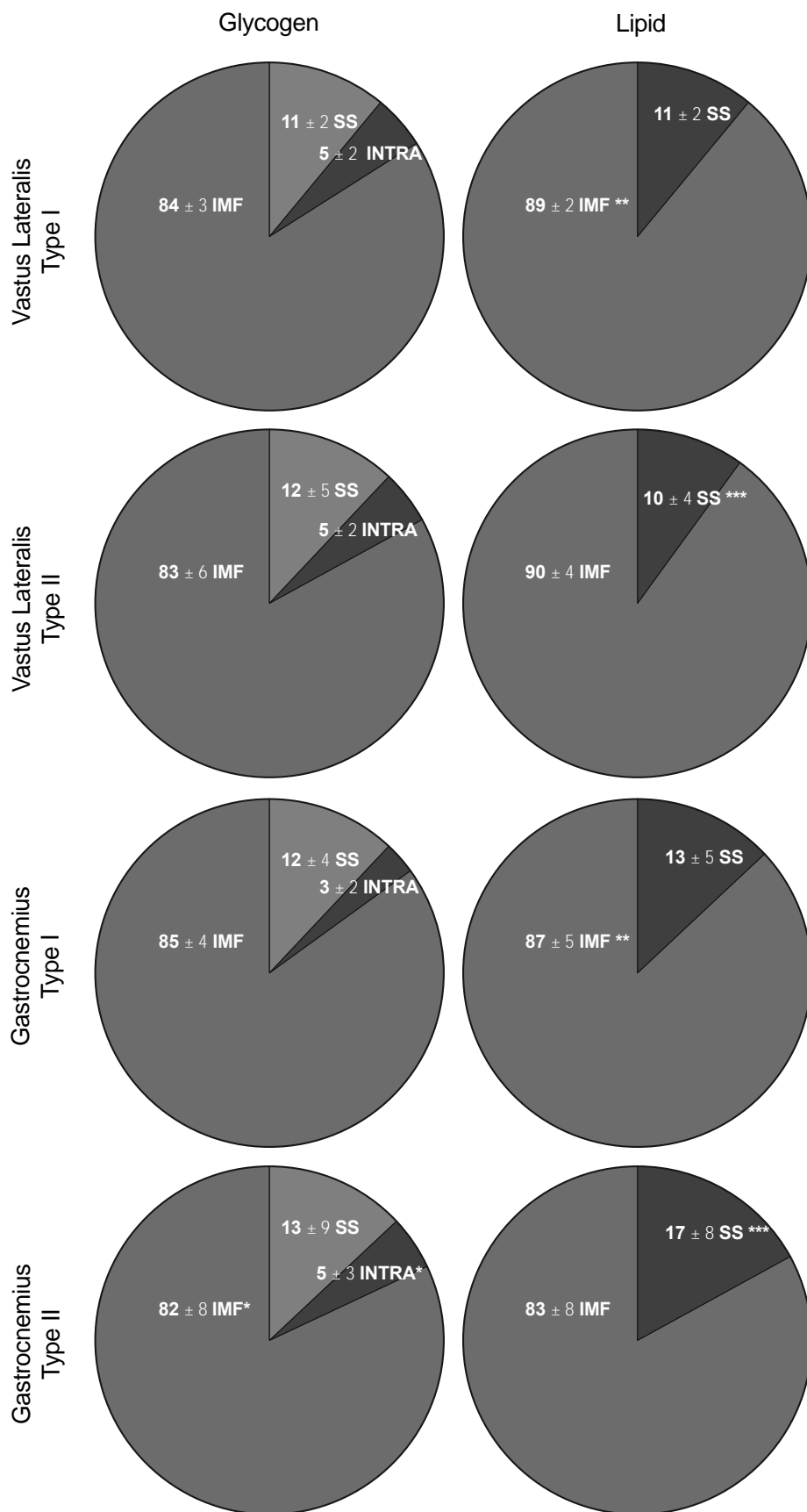
Figure 4.4. Relative distribution of glycogen and lipid across subcellular locations.

Values are mean % ± SD * $P < 0.05$ vs type I fibres of the respective muscle. ** $P < 0.01$ vs type II fibres irrespective of muscle, *** vs type I fibres irrespective of muscle.

At rest, LD volume fraction was not different between muscles in either the IMF (P = 0.752, Figure 4.5a) or SS region (P = 0.241 Figure 4.5b). Overall though (i.e. across muscles), LD volume fraction in the IMF region was 26% greater in type I fibres compared to type II fibres (P = 0.012). In the SS region there were no fibre-specific differences (P = 0.889). Similarly, the relative distribution of lipid was not different between muscles in either the IMF (P = 0.131, Figure 4.4) or SS region (P = 0.131, Figure 4.4). There was, however, a tendency for IMF lipid to be greater in type I compared to type II fibres (P = 0.074), whereas SS lipid tended to be greater in type II when compared to type I fibres (P = 0.059). When considering LD morphology, IMF and SS LD number was also unaffected by muscle or fibre type (P > 0.05, Figure 4.5c and d) Further to this, IMF and SS LD size did not differ by muscle or fibre type (P > 0.05, Figure 4.5e and f). It is important to note, however, that although differences in LD size and number were not significantly different between fibre types, the overall fibre difference in IMF LD volume fraction is likely due to a combination of small non-significant differences between fibre types for both LD size (LDs in type I fibres being 4% greater than LDs in type II fibres) and LD number (29% more LDs in type I compared to type II fibres).

In summary, the pre-exercise data showed mitochondria to be greater in type I fibres with no differences between muscles. Fibre type differences in the IMF region of both muscles, but only in the *vastus lateralis* for the SS region. In regard to glycogen, in the *vastus lateralis*, no fibre differences were seen within the IMF or INTRA regions, but there was a trend for SS glycogen to be greater in type I fibres. In the *gastrocnemius*, glycogen was highly dependent on fibre

type in the IMF and INTRA region, with no differences within the SS region. LD volume fraction was unaffected by muscle, with type I fibres having greater IMF LD. LD size and number unaffected by muscle, fibre or region though the overall fibre difference in IMF LD volume fraction is likely due to a combination of small non-significant differences between fibre types for both LD size and LD number.
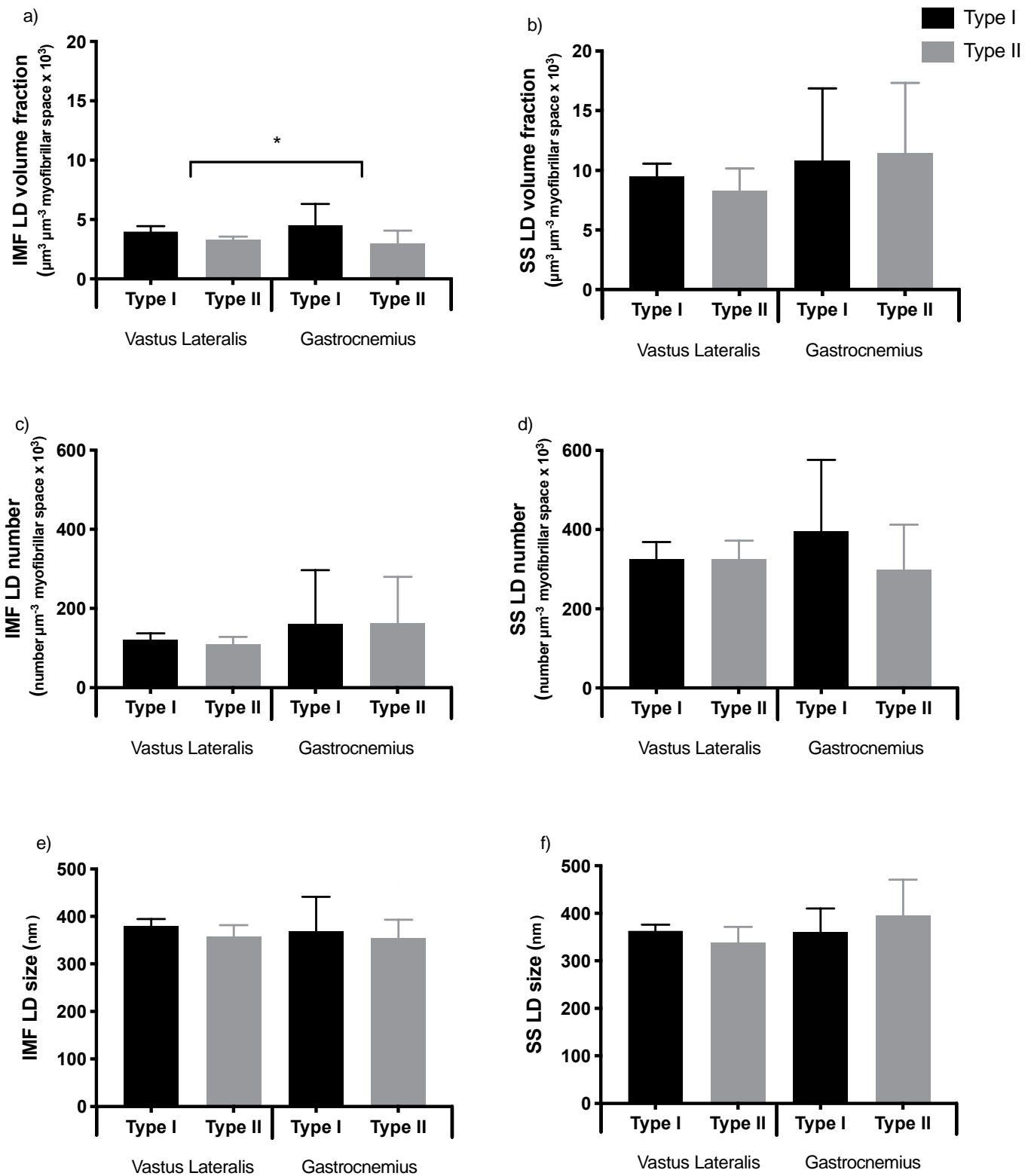
Figure 4.5. LD volume fraction, number and LD size before exercise.

Lipid pre-exercise in the *vastus lateralis* and *gastrocnemius*. LD volume fraction a) IMF and b) SS. LD number c) IMF and d) SS, LD size e) IMF and f) SS. Values are means ± SD * $P < 0.05$ significant fibre type differences irrespective of muscle.

In the *vastus lateralis*, INTRA glycogen decreased by 30% and 31% in type I and type II fibres, respectively following the 8x800m trial ($P = 0.002$, Figure 4.6d). There was also a tendency for INTRA glycogen to be reduced following the 10-mile trial ($P = 0.061$, Figure 4.6c). Consequently, the utilisation of INTRA glycogen in the *vastus lateralis* was greater in the 8x800m trial in comparison to the 10-mile trial ($P = 0.041$). In the *gastrocnemius*, INTRA glycogen decreased by 38% and 26% in type I and II fibres, respectively, following the 8x800m trial ($P = 0.005$, Figure 4.7d). Although pre-exercise INTRA glycogen was greater in the 10-mile trial compared with the 8x800m trial, similar reductions were also observed in the 10-mile trial, with INTRA glycogen decreasing by 31% and 44% in type I and II fibres, respectively ($P < 0.001$), with no difference between fibres.

Overall, exercise reduced SS glycogen in both type I (-27%) and type II fibres (-20%, main effect of time; $P < 0.05$, Figure 4.6e/f and 4.7e/f) but there were no differences between trials ($P = 0.596$) or between muscles ($P = 0.651$). The overall reduction in IMF glycogen (main effect of time; $P = 0.014$) was also not specific to either muscle ($P = 0.254$) or trial ($P = 0.573$), but the reduction in IMF glycogen tended to be greater in type I (-17%) compared to type II fibres (-7%, $P = 0.054$, Figure 4.6a/b and 4.7a/b). When examining the reduction in total glycogen there were no significant differences between muscles, with total glycogen being reduced by 16% in the *vastus lateralis* and 20% in the *gastrocnemius* ($P = 0.606$). Equally, there was no difference in total glycogen

utilisation between trials (P = 0.260).   When considering fibre-specific responses, there was a trend for total glycogen utilisation to be greater in type I fibres (-25%) compared to type II fibres (-12%, P = 0.058) in the 10-mile trial.
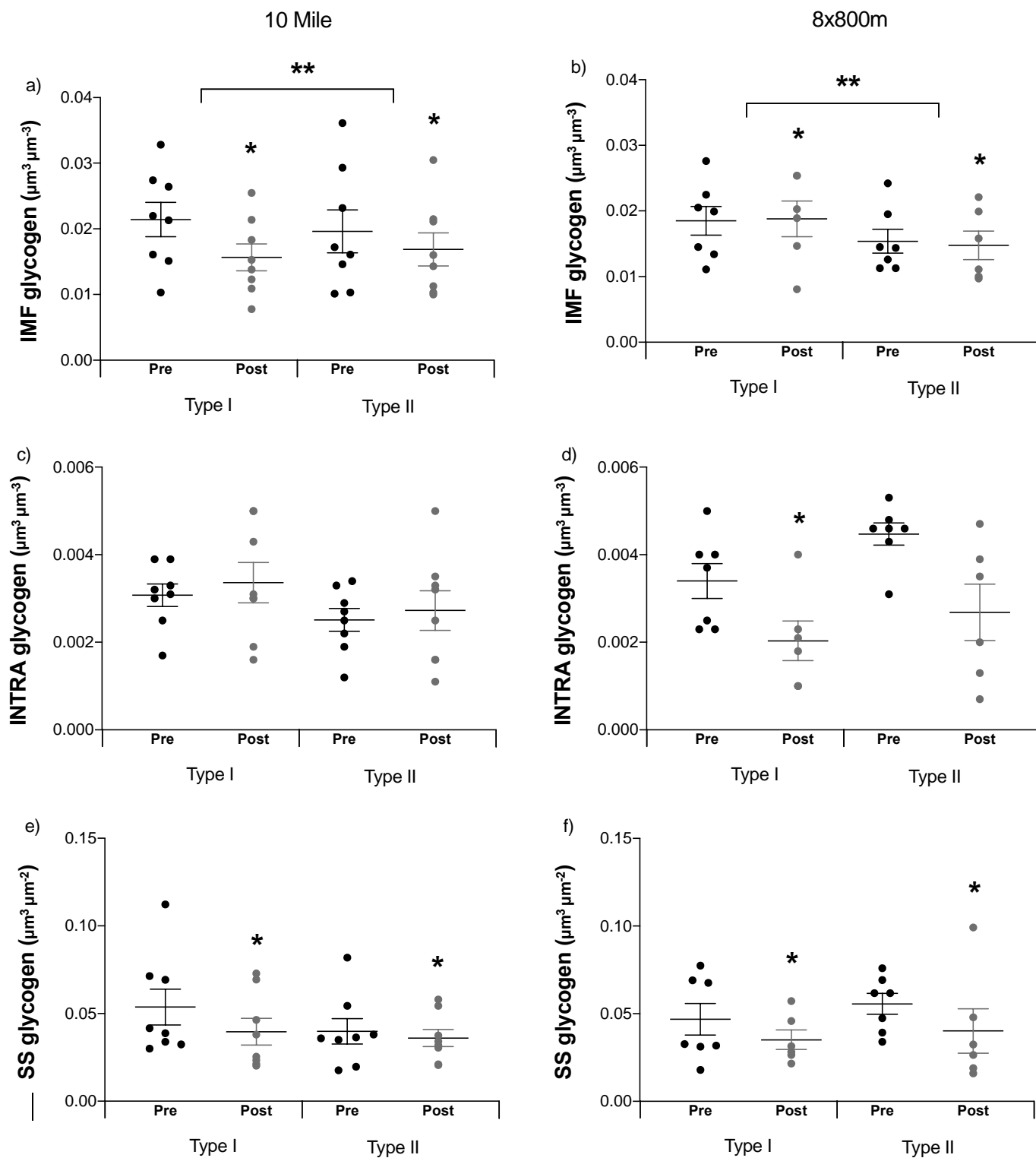
Figure 4.6. Glycogen content before and after each exercise trial in the v*astus lateralis*

The effect of the 10 mile trial on the a) IMF, c) INTRA and e) SS. The effect of the 8x800m trial on the b) IMF, d) INTRA and f) SS. Values are means ± SD. * $P < 0.05$ significant difference to pre exercise, ** $P < 0.054$ trend for type I reductions (-17%) to be greater than type II reductions (-7%).

112
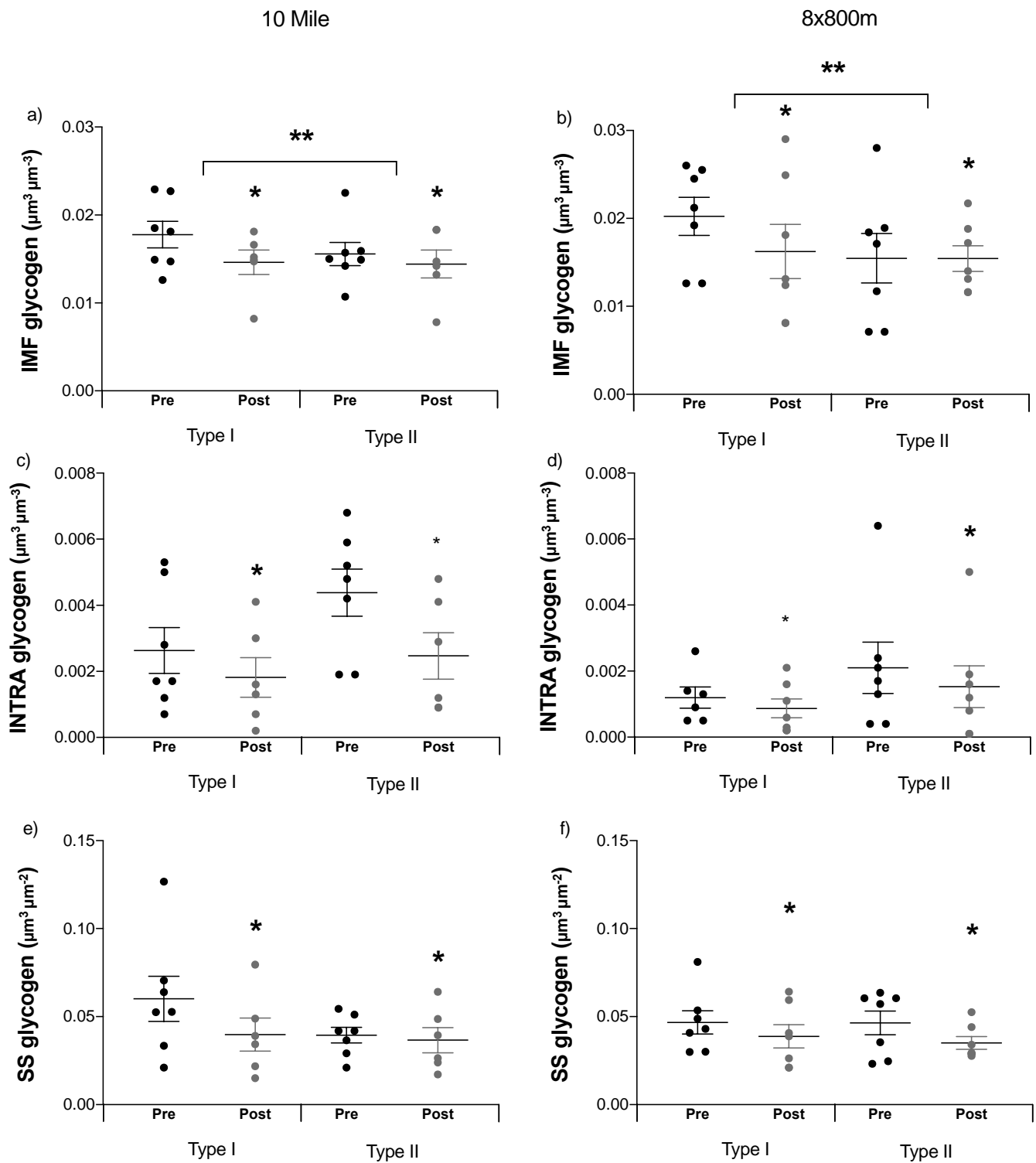
Figure 4.7. The effect of exercise on absolute glycogen values in the *gastrocnemius*.

The effect of the 10 mile trial on the a) IMF, c) INTRA and e) SS. The effect of the 8x800m trial on the b) IMF, d) INTRA and f) SS. Values are means ± SD. * *P* < 0.05 significant difference to pre exercise, ** *P* = 0.054 trend for type I reductions (-17%) to be greater than type II reductions (-7%).

Given the differences in INTRA glycogen in the *gastrocnemius* between trials (described above), there was a greater proportion of total glycogen was located in the INTRA location both pre and post-exercise in the 10-mile trial when compared to the 8x800m trial (P = 0.007, Table 4.4). Importantly though, the contribution of INTRA glycogen to total glycogen content in the 8x800m trial was decreased in both the *gastrocnemius* (P = 0.004) and the *vastus lateralis* (P = 0.023) in both type I and type II fibres. In contrast, there only tended to be a reduction in the contribution of INTRA glycogen to total glycogen content in response to the 10-mile trial in both the *gastrocnemius* (P = 0.052) and the *vastus lateralis* (P = 0.068). There was no change in the contribution of SS glycogen to total glycogen content in either muscle (P = 0.651) across both trials (P = 0.549). Consequently, the relative contribution of IMF glycogen to total glycogen content increased in both the *gastrocnemius* (P = 0.033) and the *vastus lateralis* (P = 0.019) across both trials. Taken together, this suggests that overall in both muscles and trials there was a preferential utilisation of the INTRA glycogen pool.

Table 4.4. Relative distribution (%) of glycogen in human skeletal muscle before and after each exercise trial.

Glycogen Gastrocnemius	IMF		INTRA [#]		SS	
Fibre type	Pre	Post	Pre	Post	Pre	Post
10 Mile						
Type I	82 ± 4	85 ± 6	4 ± 2	4 ± 3	13 ± 5	11 ± 5
Type II	83 ± 5	84 ± 3	6 ± 2	5 ± 3	11 ± 4	11 ± 4
8x800m						
Type I	88 ± 3	86 ± 2	2 ± 1 †	2 ± 2 †	10 ± 2	12 ± 3
Type II	81 ± 10	86 ± 4	3 ± 2 †	2 ± 2 †	16 ± 11	12 ± 4

Vastus Lateralis	IMF		INTRA [#]		SS	
Fibre type	Pre	Post	Pre	Post	Pre	Post
10 Mile						
Type I	84 ± 3	84 ± 6	5 ± 2	4 ± 1*	10 ± 2	11 ± 5
Type II	86 ± 5	86 ± 4	5 ± 2	4 ± 2*	9 ± 3	10 ± 3
8x800m						
Type I	84 ± 2	87 ± 6*	6 ± 2	4 ± 2*	11 ± 2	15 ± 4*
Type II	79 ± 6	85 ± 6*	6 ± 2	4 ± 2*	15 ± 5	11 ± 5*

IMF, intermyofibrillar glycogen; INTRA, intramyofibrillar glycogen; SS, Subsarcolemmal glycogen. Values are expressed as %, and represent mean $\pm$ SD. * $P < 0.05$ vs pre exercise. † $P < 0.05$ differences between exercise trial. [#] $P < 0.05$ difference between muscle.

Exercise caused a 51% reduction in IMF LD volume fraction in type I fibres during the 10-mile trial ($P = 0.001$), and IMF LD volume fraction also tended to decrease in type II fibres (-34%, $P = 0.084$, Figure 4.8). There also tended to be a small reduction in IMF LD volume fraction following the 8x800m trial of 22% across both type I and type II fibres ($P = 0.093$, Figure 4.8), and regardless of muscle ($P = 0.471$). In contrast, SS LD volume fraction was not reduced in response to exercise ($P = 0.645$, Figure 4.8), regardless of muscle ($P = 0.931$) or fibre type ($P = 0.877$). Overall though, there was a significant difference between exercise trials, with post-exercise LD volume fraction being 66% lower in the 10-mile trial compared to the 8x800m trial ($P = 0.019$). Thus, overall lipid utilisation was greater in the 10-mile trial compared to the 8x800m trial. With regards to the relative distribution of lipid, exercise caused the distribution of lipid in the *vastus lateralis* to decrease in the IMF region ($P = 0.006$), consequently causing an increase in the SS region ($P = 0.028$, Table 4.5). In the *gastrocnemius*, the relative distribution of lipid in both the IMF and SS regions were unaffected by trial, muscle or fibre-type (all $P > 0.05$).
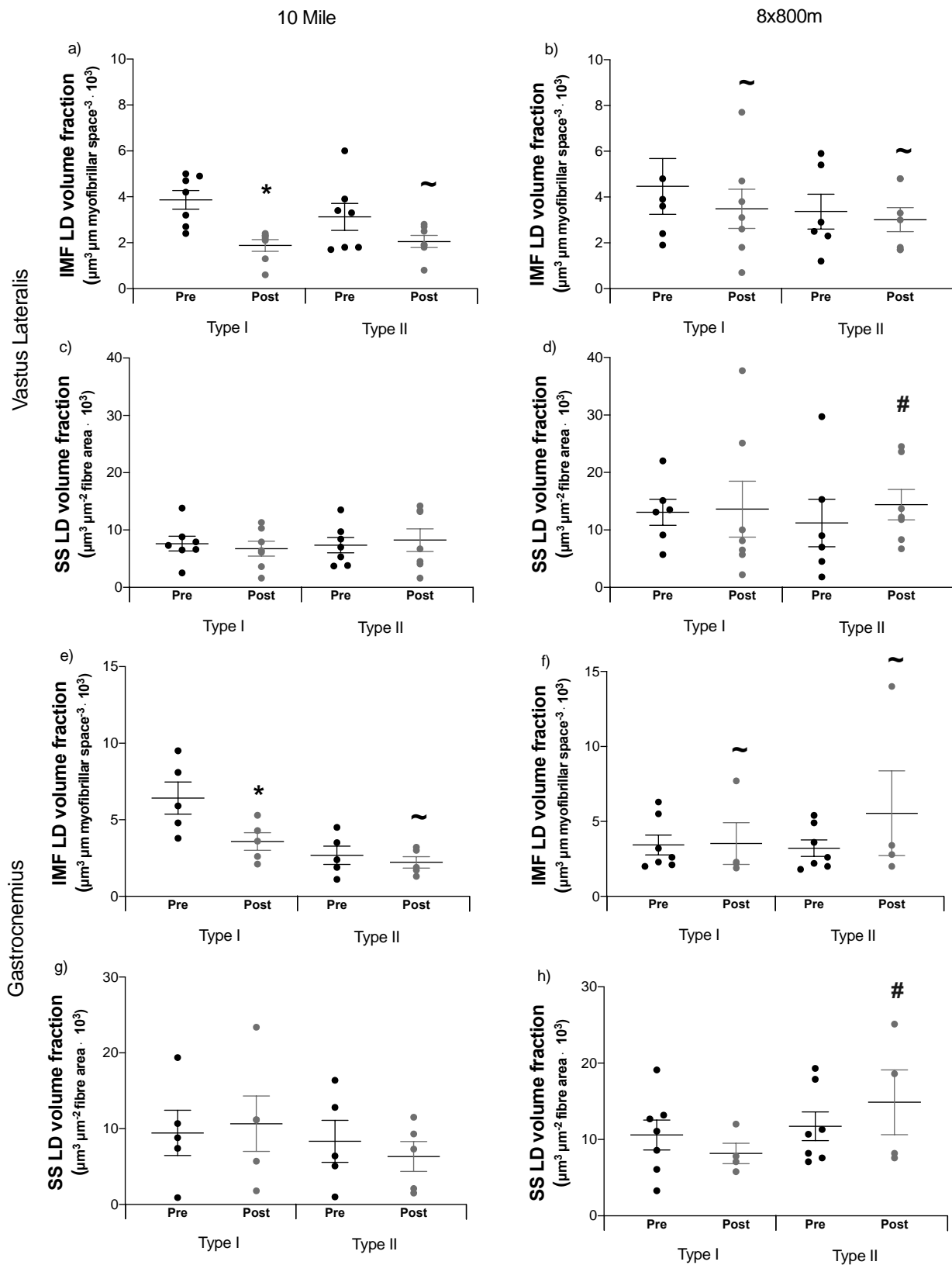
Figure 4.8. The effect of exercise on LD volume fraction in the *vastus lateralis* and *gastrocnemius.*

The effect of the 10 mile trial on a/e) IMF and c/g) SS. The effect of the 8x800 trial on b/e) IMF and d/h) SS. Values are means ± SD. * $P < 0.05$ significant difference to pre exercise, # $P = 0.019$ significant difference to 10 mile trial. ~ $P = 0.084$ and $P = 0.093$ for 10 mile and 8x800 trial, respectively, trend of reductions from pre exercise.

117

Table 4.5. The effect of exercise on the relative distribution (%) of lipid in human skeletal muscle.

Gastrocnemius	Pre exercise		Post exercise	
Fibre type	IMF	SS	IMF	SS
10 Mile				
Type I	91 ± 3	9 ± 3	86 ± 13	14 ± 13
Type II	85 ± 9	13 ± 9	86 ± 7	14 ± 7
8x800m				
Type I	86 ± 6	14 ± 6	83 ± 8	17 ± 8
Type II	85 ± 8	15 ± 8	81 ± 9	19 ± 9
Vastus Lateralis	Pre exercise		Post exercise	
Fibre type	IMF	SS	IMF	SS
10 Mile				
Type I	92 ± 3	8 ± 3	86 ± 3*	14 ± 3*
Type II	88 ± 4	12 ± 4	85 ± 5*	15 ± 5*
8x800m				
Type I	86 ± 6	14 ± 6	82 ± 12*	18 ± 12*
Type II	88 ± 7	12 ± 7	80 ± 9*	20 ± 7*

IMF, intermyofibrillar glycogen; SS, Subsarcolemmal glycogen. Values are expressed as %, and represent mean $\pm$ SD. * $P < 0.05$ vs pre exercise.

In terms of LD morphology, there was a tendency for IMF LD size to decrease by 12% following the 10-mile trial ($P = 0.067$, Figure 4.9), although this was not specific to fibre type or muscle. SS LD size was unaffected by exercise, trial, muscle or fibre ($P > 0.05$). When examining LD number, there was a tendency for IMF LD number to be reduced following the 8x800m trial (-5%; $P = 0.071$, Figure 4.10), although this was not specific to fibre type or muscle. SS LD number decreased by 38% in type I fibres in the *gastrocnemius* following exercise ($P = 0.030$, Figure 4.10), with similar, but not quite significant decreases in the type I fibres of the *vastus lateralis* (-32%, $P = 0.068$, Figure 4.10). Trial alone did not significantly effect LD number in response to exercise ($P = 0.248$).

Figure 4.9. The effect of exercise on LD size in the *vastus lateralis* and *gastrocnemius*.

The effect of the 10 mile trial on a/e) IMF and c/g) SS. The effect of the 8x800m trial on b/f) IMF and d/h) SS. Values are means ± SD. ~ *P* = 0.067 trend of reductions from pre exercise.

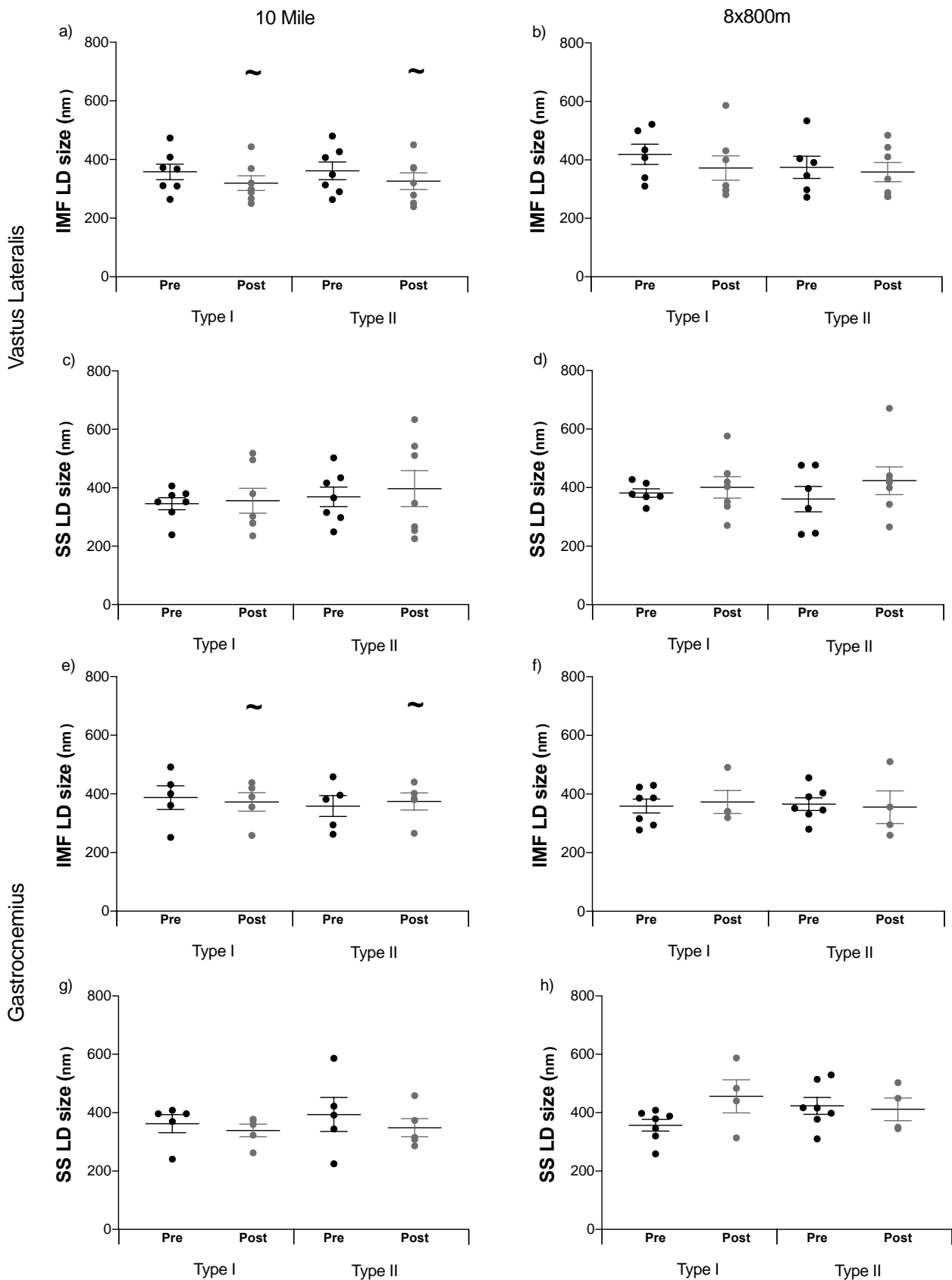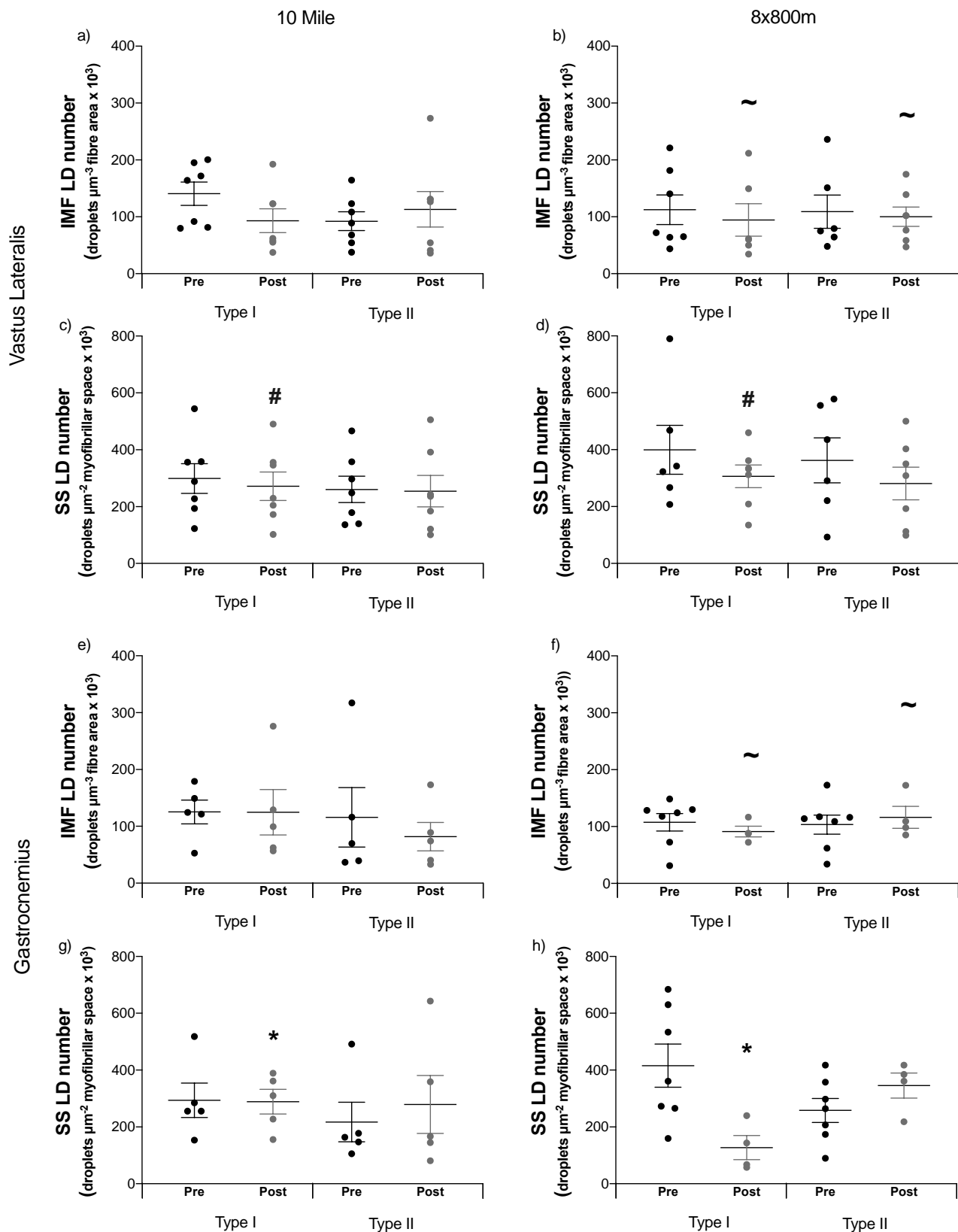**Figure 4.10.** The effect of exercise on LD number in the *vastus lateralis* and *gastrocnemius*.

.

The effect of the 10 mile trial on a/e) IMF and c/g) SS. The effect of the 8x800 trial on b/f) IMF and d/h) SS. Values are means ± SD. # *P* = 0.068 reduction from pre exercise, ~ *P* = 0.071 trend of reductions from pre exercise.

4.5 Discussion

The aim of the present study was to quantify glycogen and lipid utilisation on a fibre and subcellular level in the *vastus lateralis* and *gastrocnemius* muscle of recreationally active male runners during either steady state endurance running (10-mile trial) or high intensity interval exercise (8x800m trial) in a field-based training environment. The key findings of this study were that 1) INTRA glycogen was preferentially utilised in both type I and type II fibres from both muscles during both exercise trials, 2) IMF lipid droplets in both muscles were preferentially reduced in type I fibres in comparison to type II fibres during the 10-mile trial, and 3) changes in LD morphology were dependent on trial, with LD size being reduced following the 10-mile trial, whereas LD number was reduced following 8x800m trial.

Pre exercise mitochondria, glycogen and lipid

In the present study, total mitochondrial volume fraction was greater in type I compared to type II fibres, irrespective of the muscle studied. More specifically, in the *vastus lateralis*, both the IMF and SS mitochondria pool was greater in type I fibres compared type II fibres, which is in agreement with a previous study in highly-trained cross country skiers (Ørtenblad *et al,* 2018). In contrast, in the *gastrocnemius,* only the IMF mitochondria pool, and not the SS mitochondria pool, was greater in type I compared to type II fibres. However, when examining the relative distribution of mitochondria between the IMF and SS regions, there was no differences between muscles with 87% in the IMF and 13% in the SS region, similar to that reported by Ørtenblad *et al.* (2018) who stated 83–86%

and 11-14% of mitochondria were present in the IMF and SS pools, respectively.

Before exercise, the relative proportion of glycogen in each of the subcellular locations was similar across muscles and fibre types, with IMF glycogen contributing ~83%, SS glycogen contributing ~12% and INTRA glycogen contributing ~4%. When considering the volume fraction of glycogen, both IMF and INTRA glycogen were similar in type I and type II fibres within the *vastus lateralis*; that is, there was no fibre-specific distribution of either the IMF or INTRA glycogen pools. This is in agreement with previous research in sedentary obese subjects (Nielsen *et al,* 2010a) and recreationally active young and elderly males (Nielsen *et al,* 2010b). However, in the present study SS glycogen tended to be greater in type I compared to type II fibres in the *vastus lateralis*. It has been suggested that fibre type differences in each of the subcellular glycogen pools emerge as a training adaptation (Nielsen & Ørtenblad, 2013), since in highly-trained individuals SS and INTRA glycogen pools are both greatest in type I fibres, whereas IMF glycogen is greatest in type II fibres (Nielsen *et al*, 2011). If this is true, the data from the present study in moderately-trained individuals would suggest that this fibre type adaptation first occurs in the SS region. The reason for this is unknown, but could be related to the higher Na^+-K^+ pump energy requirements of trained muscle fibres (Nielsen & Ørtenblad, 2013), and the fact that Na^+-K^+ pump activity is greater in type I compared to type II fibres during repetitive contractions (Everts & Clausen, 1992). This adaptation would support the classical adaptation of enhanced endurance capacity following endurance training. The present data

also provides novel insight into the subcellular distribution of glycogen in the *gastrocnemius*. In this muscle, fibre type-specific differences in glycogen appear to be dependent on the specific glycogen pool; that is, IMF glycogen was greater in type I compared to type II fibres, whereas INTRA glycogen was greater in type II compared to type I fibres. When compared to the *vastus lateralis*, these differences could simply be due to the muscle being studied. However, previous qualitative data has reported glycogen particles in the *vastus lateralis* to be more frequently observed in the INTRA space of type II fibres (Sjostrom *et al,* 1982b; Friden *et al,* 1989). Finally, in the *gastrocnemius*, SS glycogen was not different between fibre types. Building on the hypothesis outlined above regarding the adaptation of specific glycogen pools along the aerobic training continuum, it could be that the adaptation is not only fibre-specific, but also muscle-specific too. This hypothesis requires investigation though in a separate study employing a longitudinal training programme. In addition to this, when comparing the two muscles, INTRA glycogen in general was greater in the *vastus lateralis* compared to the *gastrocnemius*. This could be due to the size of individual muscle fibres being larger in the *vastus lateralis*, compared to the *gastrocnemius*, therefore providing 'more room' to store INTRA glycogen (Edstrom & Nystrom, 1969).

With regards to muscle lipid, we observed a fibre type dependency for IMF LD volume fraction, with type I fibres containing 26% more IMF LDs than type II fibres, an observation consistent across both muscles. This is in agreement with previous research by Koh *et al,* (2017), who at rest, also saw fibre-specific differences (albeit larger than those reported in the present study), with IMF LD

volume fraction being 3-fold greater in type I compared to type II fibres. In the present study, the fibre type difference in IMF LD volume fraction is likely due to a combination of small, non-significant differences in IMF LD number and size (i.e. more and larger LDs in type I compared to type II fibres). In contrast, SS LD volume fraction was not different between type I and type II fibres, which is in line with previous work in highly-trained athletes (Koh *et al*, 2017). Thus, it is possible that SS LDs are less dependent on the oxidative properties of muscle fibres. Moreover, it appears that unlike the muscle-specific differences in subcellular glycogen distribution between type I and type II fibres, the distribution of subcellular LD is more consistent across muscles.

Subcellular glycogen utilisation during exercise.

Overall, our results displayed a tendency for greater glycogen utilisation in type I compared to type II fibres during the 10-mile trial. This is in line with Henneman's size principle (Henneman and Olson, 1965), i.e. smaller motor units that are often associated with type I fibres are recruited at lower intensities, whilst larger motor units, are often associated with type II fibres and higher intensities. Indeed, previous research has also reported greater glycogen utilisation in type I compared to type II fibres during exercise (Gollnick *et al,* 1973; 1974; Stellingwerff *et al,* 2007; Branth *et al,* 2009; Jensen *et al,* 2020). A key observation of the present study was that INTRA glycogen was preferentially used during both the 8x800m and 10-mile trials, compared to IMF and SS glycogen. This is evidenced by the decrease in the relative contribution of INTRA glycogen to total glycogen following exercise. Moreover, this

observation is is line with previous research in moderately or well-trained subjects during either prolonged cycling or cross-country ski racing (Marchand *et al,* 2007; Nielsen *et al,* 2011). Due to the design of the current study, whereby participants undertook exercise trials of two different intensities, and two muscles were sampled, we can now extend previous observations regarding INTRA glycogen utilisation; that is, we show that INTRA glycogen utilisation in the *gastrocnemius* was similar between exercise trials, whereas INTRA glycogen utilisation in the *vastus lateralis* was greater in the 8x800m trial compared to the 10-mile trial. Interestingly, mechanistic investigations have identified a link between INTRA glycogen content and SR Ca^{2+} release in skinned rat muscle fibres (Nielsen *et al,* 2009), isolated human SR vesicles (Ørtenblad *et al,* 2011) and intact mouse muscle fibres (Nielsen *et al,* 2014). Therefore, INTRA glycogen likely plays a key role in energy provision for muscle contraction. The proposed relationship between INTRA glycogen and SR Ca^{2+} release may help explain why INTRA glycogen use was greatest in the *vastus lateralis* during the 8x800m trial. This is because the high intensity nature of the 8x800m trial (compared to the 10-mile trial) requires recruitment of a greater total muscle mass in the legs, which would in-turn require greater rates of SR Ca^{2+} release to support the high frequency of muscle contraction. Together with previous literature, these results suggest that the preferential utilisation of INTRA glycogen could be key to understanding the glycogen-dependent influence on muscle fatigue and performance.

IMF and SS glycogen were also decreased in response to exercise, although this wasn't fibre type or muscle-specific and was similar between the exercise

trials. Specifically, exercise reduced SS glycogen in both type I (-27%) and type II fibres (-20%), and although exercise also reduced IMF glycogen, this tended to be greater in type I (-17%) compared to type II fibres (-7%). Previous research has also observed utilisation of SS and IMF glycogen in response to 30km cross-country running (Sjostrom *et al,* 1982a). The reduction in IMF, and particularly SS glycogen, might be related to the concept of glycogen sparing, such that utilisation of these two pools of glycogen increases endurance capacity potentially by sparing INTRA glycogen in order to maintain muscle contraction capabilities, due to the proposed relationship between INTRA glycogen and SR Ca^{2+} release (Nielsen *et al,* 2009; Ørtenblad *et al,* 2011; Nielsen *et al,* 2014). In support, Jensen *et al,* (2020) recently showed that that INTRA glycogen is the best predictor of time to exhaustion, but that SS glycogen was also reduced during exercise. As noted earlier, SS glycogen may contribute energy to support Na^+-K^+ pump activity at the sarcolemma (Nielsen & Ørtenblad, 2013), and in this way spare the utilisation of INTRA glycogen which is also proposed to provide energy for the activity of the Na^+-K^+ pump (Ørtenblad *et al,* 2015). Furthermore, the IMF glycogen pool may act as a reserve that can be utilised as fuel for Ca^{2+} re-uptake into the sarcoplasmic reticulum, thereby allowing muscle contraction to continue. Identifying the role of the IMF glycogen pool should be a focus of future work. Taken together with our results, these observations suggest that INTRA glycogen is preferentially utilised during both prolonged moderate intensity and intermittent high-intensity exercise.

Subcellular lipid utilisation during exercise

Overall, lipid utilisation was apparent in both exercise trials, with a 51% reduction in LD volume fraction following the 10-mile trial and a smaller reduction of 22% following the 8x800m trial. In the 10-mile trial, this was specifically from the IMF region in type I fibres, although there also tended to be a reduction in IMF LD volume fraction in type II fibres. In the SS region, there was no significant reductions in LD volume fraction in response to exercise. This supports the concept of there being a compartmentalised energy demand for lipid utilisation in skeletal muscle. Given the spatial arrangement of LD in close proximity to the mitochondria (Hoppeler *et al,* 1985), and that IMF mitochondria supports ATP production for the contracting myofibrils (Hood, 2001), this would explain the preferential use of IMF lipid during exercise. Our results are in agreement with data in elite cross country skiers who completed a field-based competitive time trial and showed reductions in IMF lipid (Koh *et al,* 2017), and also results from young subjects who completed a 1 h moderate-intensity cycling bout, which augmented a 40% reduction in IMF lipid with no change in SS lipid (Chee *et al,* 2016). Thus, it would seem that regardless of training status, there is a preferential utilisation of IMF lipid during exercise. Though, Chee *et al,* (2016) also found that older lean active and older overweight inactive individuals did not display any change in IMF lipid with exercise. Therefore, in populations that would elicit a decrease in IMTG content during exercise (Van Loon & Goodpaster, 2006), it is typically due to reductions in IMF LD volume fraction (Chee *et al,* 2016; Koh *et al,* 2017).

The utilisation of IMF lipid in type I fibres during the 10-mile trial can be attributed to reductions in LD size. This finding opposes earlier research attributing reductions in IMF lipid to reductions in LD number in elite cross-country skiers completing a 1 h high-intensity time trial (Koh *et al,* 2017). We did, however, observe a tendency for IMF LD number to be reduced in the 8x800m trial. Taken together, these data suggest that exercise that is of a higher intensity (8x800m trial in the present study, and 1 h cross-country skiing time trial in Koh et al, 2017) may specifically result in a reduction in LD number, whereas moderate-intensity exercise (10-mile trial) may induce reductions in LD size. During the 10 mile trial, which was longer in duration, the continuous state of LD turnover as FA entering the muscle alongside FA utilisation may explain why LD number was not decreased in response to exercise, as the utilised LD are replaced with newly-formed LD. However, when considering the reduction in LD number that is present following the 8x800m trial, it is well-established that exercise training augments protein content of PLIN2, PLIN3 and PLIN5 (Shaw *et al,* 2012; Shepherd *et al,* 2013), and LD with PLIN2 or PLIN5 associated are preferentially utilised during exercise (Shepherd *et al,* 2012; 2013). PLIN are able to relocate from the cytosol to the LD (Gemmink *et al*, 2016), and potentially between LDs (Shepherd *et al*, 2017). During higher intensity exercise (i.e. 8x800m trial) when metabolic demand is high, it could be speculated that from an efficiency perspective the movement of PLIN3 and PLIN5 would be limited; that is, these proteins may locate to a LD and remain in situ at that LD until all IMTG contained within that LD has been broken down. If this is true, this would explain the decrease in LD number observed during the 8x800m trial.

When specifically examining LD volume fraction in the SS region, there were no significant reductions in response to exercise. However, we did observe a decrease in SS LD number. Whilst changes in LD size were not apparent, there were small (albeit non-significant) increases in LD size in both type I (6%) and type II (3%) fibres. These opposing changes in SS LD size and number may explain why there was no reduction in overall SS LD volume fraction. It was notable though that the reduction in SS LD number was observed in both muscles and during both trials, and in fact, Koh *et al.* (2017) also reported a decrease in SS LD number in the absence of a reduction in SS LD volume fraction. Thus, exercise-induced decreases in LD number appear to be a consistent finding, although the importance of this is yet to be determined. It is possible that the close proximity of SS LD to nuclei means that this pool of LDs supports nuclear processes. For example, it is known that IMTG-derived fatty acids can act as ligands to support transcriptional processes, thereby supporting the adaptive response to exercise (Seibert *et al,* 2020). To reconcile the lack of a change in overall SS LD volume fraction, it could be speculated that FA coming into the muscle during exercise may subsequently be directed to pre-existing SS LD, thereby resulting in small increases in LD size. Future work should aim to identify the roles that each LD pool play in cell function.

Implications for lipid and glycogen use during exercise

We previously reported that whole muscle glycogen utilisation, as assessed by biochemical assay, was greater during the 10-mile trial compared to the 8x800m trial, and that glycogen utilisation was greater in the *gastrocnemius* compared to the *vastus lateralis* (Impey *et al*, 2020). In contrast to these

observations, using TEM the present study found that glycogen utilisation during exercise was not different between the two trials or the two muscles. The advantage of TEM though is the ability to investigate glycogen at the fibre type and subcellular specific level. Consequently, we found that glycogen utilisation tended to be greater in type I compared to type II fibres during the 10-mile trial, whereas glycogen utilisation was similar in type I and type II fibres in the 8x800m trial. Further to this, we now provide unique insight into how the different subcellular pools of glycogen are used depending on exercise intensity.   Both IMF and SS glycogen were similarly reduced in the g*astrocnemius* and *vastus lateralis* following both trials. Furthermore, INTRA glycogen was reduced to a similar degree following both trials in the *gastrocnemius*, but the reduction in INTRA glycogen was greater in the 8x800m trial compared to the 10-mile trial in the *vastus lateralis*. Thus, greater use of the INTRA glycogen pool appears to be required to meet the elevated metabolic demand during high intensity exercise.

Total LD volume fraction was similar before exercise between trials and across both muscles. However, post-exercise LD volume fraction was lower following the 10-mile trial when compared to the 8x800m trial. This suggests that the oxidation of FA derived from IMTG stored in LD made a larger contribution to overall energy expenditure in the 10-mile trial, which is is in line with the classical literature demonstrating that IMTG utilisation is greatest during moderate-intensity exercise (Van Loon *et al,* 2001; Romijn *et al,* 1993). Furthermore, the decrease in lipid was entirely due to a reduction in the IMF LD pool, which occurred predominantly in type I fibres during the 10-mile trial.

There was a tendency for IMF LD volume fraction to be reduced following the 8x800m trial, suggesting that IMTG may also partly contribute to energy provision during higher intensity exercise (although the magnitude of the decrease was smaller than that for the 10-mile trial). Taken together, it appears that INTRA glycogen was a key substrate during the 8x800m trial, which aligns with previous research demonstrating INTRA glycogen to be the best predictor of time to exhaustion (Jensen *et al,* 2020). In contrast, the lower exercise intensity of the 10-mile trial means that more energy can be derived from IMTG located in IMF LDs.

When comparing muscles, we did not see any differences in total glycogen or lipid utilisation between muscles in either the 10-mile or 8x800m trial. Nielsen *et al.* (2011) and Koh *et al.* (2017) did observe differences in the utilisation of glycogen and lipid, respectively, between muscles from different limbs (*triceps brachii* vs. *vastus lateralis*) during a cross-country skiing time trial. Glycogen utilisation occurred in type I and type II fibres in the triceps brachii, but only in type I fibres in the *vastus lateralis* (Nielsen *et al*, 2011). Lipid utilisation was specific to the *triceps brachii*, with no reduction in LD volume fraction observed in the *vastus lateralis* (Koh *et al*, 2017). We examined two muscles from the same limb, both of which are highly activated in running regardless of exercise intensity, and despite differences in the overall size of the muscles we were investigating, there is evidence demonstrating that both muscles have a relatively similar distribution of fast and slow twitch muscle fibres (Johnson *et al,* 1973; Staron *et al,* 2000). Thus, similarities in fibre type distribution and overall activation when running could provide an explanation for why we did not

observe any differences in total muscle glycogen or lipid utilisation between muscles.

The present study provides a unique insight into substrate utilisation under field-based conditions using TEM. Importantly, the CE_{est} values (as seen in Table 4.2) are similar to those reported in other studies (Nielsen *et al,* 2010; 2011; Koh *et al,* 2017; 2018), thereby demonstrating the validity of the data in the present study and the conclusions drawn herein. However, field-based data collection does have its limitations, i.e. not being able to control variables such as weather conditions altering pace and RPE. Further to this, individual differences in running style i.e. forefoot vs. heel-strike runners and muscle length may be factors to consider in future research, in order to assess if these factors may alter the activation of the *vastus lateralis* and *gastrocnemius*, and therefore influence muscle-specific substrate utilisation.

In conclusion, the present study highlights the interaction between muscle fibre type, relative exercise intensity and training duration in modulating the subcellular specific-glycogen and lipid requirement with specific exercise protocols. This research provides a unique insight into subcellular substrate utilisation in field-based habitual training sessions, being the first to investigate on a subcellular-basis using TEM in running and allowing us to identify a preferential use of INTRA glycogen during exercise, independent of intensity. Furthermore, lipid utilisation occurs primarily in the IMF region of type I fibres, but changes in LD morphology maybe related to exercise intensity and duration. The pattern of glycogen and lipid utilisation here, specific to the training status of the participants and exercise intensities compared, may aid

practical guidelines in relation to fuelling strategies to promote training intensity and metabolic adaptations by providing field-based data to add to the laboratory-based literature on the substrate demands of habitual training.

Chapter 5 – Quantification of exercise-induced changes in IMTG content and lipid droplet morphology on a fibre type and subcellular region-specific basis using immunofluorescence microscopy.

5.1 Abstract

Until recently, the role of intramuscular triglyceride (IMTG) as a substrate during exercise was controversial due to discrepancies in the literature stemming from methodological differences. Now, Transmission Electron Microscopy (TEM) has shown that exercise reduces IMTG content and alters lipid droplet (LD) morphology in a fibre type and subcellular-specific manner. Immunofluorescence microscopy may provide an alternative, more cost-effective method to measure exercise-induced changes in IMTG content. The aim of this study was to evaluate immunofluorescence microscopy as a suitable method to measure IMTG utilisation and changes in LD morphology on a fibre and subcellular-specific basis during a field-based competitive scenario, and evaluate the agreement with TEM. Ten elite male cross-country skiers completed a ~20km (~1h) cross-country skiing time trial with muscle biopsies collected pre and post-exercise from both the arm (*triceps brachii*) and leg (*vastus lateralis*). Across both muscles, IMTG content tended to reduce in both type I (-28%) and type IIa (-50%, $P = 0.071$). In both fibre types there was a tendency for IMTG content to be reduced more in the peripheral region (-40%) compared to the central region (-36%; $P = 0.080$). This was due to both reductions in LD size ($P = 0.004$) and number ($P = 0.064$); specifically, reductions in the number of moderately size LD, 400 and 600 nm^2 ($P < 0.05$). There were significant correlations between immunofluorescence microscopy and TEM methods when examining IMTG content, but not LD size or number, likely due to greater magnification and resolution capabilities of TEM. In conclusion, ~1 hour of cross-country skiing in a real-world environment reduced IMTG content in both type I and type IIa fibres, and in both subcellular regions,

136

which was due to a reduction in both LD size and number. In the first comparison between TEM and immunofluorescence, we demonstrated immunofluorescence provides an alternative method to quantify IMTG content but not LD size and LD number. Therefore, these data have important implications for future studies aiming to understand the mechanisms regulating LD pools. As such, immunofluorescence microscopy analysis should be considered when the aim is to understand the mechanisms regulating the utilisation of specific subcellular LD pools, such as investigations examining the association of LD with PLIN proteins.

5.2 Introduction

Fat is predominantly stored as triacylglycerol (TG) in white adipose tissue, and to a lesser extent in skeletal muscle as intramuscular triglycerides (IMTG). During moderate-intensity exercise in healthy individuals, the rate of whole-body fat oxidation is increased ~10-fold (Van Loon *et al,* 2001), and stable isotope tracer studies estimate that ~50% of oxidised fatty acids are derived from IMTG (Havel *et al,* 1967; Oscai *et al,* 1990; Frayn *et al,* 1996; Helge *et al,* 2001). However, studies that have sampled skeletal muscle tissue before and after exercise to investigate net changes in IMTG have produced equivocal findings with some reported a decrease (Bergstrom, Hultman & Saltin, 1973; Carlson, Ekelund & Froberg, 1971; Cleroux *et* al, 1989; Essen-Gustavsson & Tesch, 1990; Froberg *et al* 1971; Hurley *et al*, 1986; Phillips *et al*, 1996), and other reporting no change in IMTG (Bergman *et al,* 1999; Guo *et al,* 2000; Kiens *et al*, 1993; Kiens *et al,* 1998; Starling *et al*, 1997; Wendling *et al,* 1996). Measuring IMTG concentrations through biochemical extraction of TG is problematic, since any extramyocellular lipid that is present in a sample will interfere with the measurement of IMTG (Guo, 2001; Watt *et al*, 2002; Wendling *et al*, 1996). To address this, studies employed immunohistochemical staining of muscle cross-sections with a lipid dye (e.g. oil red O), which permits exclusion of extramyocellular lipids from IMTG in the quantification process. Combining oil red O staining with an antibody targeting slow myosin heavy chain type I, led to the finding that IMTG content was reduced specifically in type I compared to type II fibres following 2 h of moderate-intensity exercise (Van Loon *et al*, 2003). Although a number of studies have since replicated this observation (Van Proeyen *et al,* 2011; Shepherd *et al*, 2013), to the best of

our knowledge, none have made the distinction between type IIa and IIx fibres. This is important, because type IIa fibres are reported to have a similar oxidative capacity to type I fibres, at least in highly-trained individuals (Boushel *et al,* 2014; Ørtenblad *et al,* 2018).

Transmission electron microscopy (TEM) can also be used to examine IMTG-containing LD, and this method has revealed that two pools of LDs exist in muscle: 1) subsarcolemmal (SS) LDs, located just beneath the plasma membrane, and 2) intermyofibrillar (IMF) LDs, located between the myofibrils (Nielsen *et al,* 2010a). This finding was made possible by virtue of the greater magnification capabilities of TEM, which also permits the most accurate measures of LD morphology (size and number). Using TEM, it has been shown that IMF, but not SS LDs were reduced following 1 h of moderate-intensity exercise in lean, healthy individuals (Chee *et al,* 2016). Thus, TEM could be considered the gold standard method to investigate subcellular-specific changes in LD content and morphology in response to exercise. However, TEM relies on morphological factors such as mitochondria and Z-line band width within the skeletal muscle fibre to identify fibre type, cannot distinguish between type IIa and type IIx fibres, and analysis is only limited to a small number of fibres (~2-3 fibres per sample). Given these limitations, coupled with the relatively slow and technical nature of sample processing and imaging for TEM, it is important to determine whether immunofluorescence microscopy is also capable of detecting exercise-induced changes in LD content and LD morphology at the subcellular level, due to its ability to overcome such issues by enabling labelling of fibre types and analysis of a greater number of fibres.

Cross-country skiing is considered one of the most challenging endurance sports due to the combined metabolic requirements of upper and lower body muscles. Events often also include varied terrain at moderate altitudes over different durations. The energy supply for cross-country skiing is primarily through the aerobic catabolism of CHO stores, thus resulting in an emphasised depletion of intracellular glycogen stores (Ørtenblad *et al,* 2011). However, using TEM it was recently shown that the IMF LD pool is preferentially used in the *triceps brachii* muscle during a ~1h cross-country skiing time trial in comparison to the *vastus lateralis*, which was attributed to a decrease in LD number rather than size (Koh *et al,* 2017). Thus, IMTG also contributes to energy expenditure in highly trained athletes during relatively high intensity exercise (competitive time trial). Using immunofluorescence microscopy to also assess IMTG utilization in the same muscle samples as used by Koh *et al.* (2017) would enable a comparison to be made between the two methods.

The primary aim of this study was to investigate IMTG utilisation on a fibre type and subcellular-specific basis during a field-based competitive scenario in elite cross-country skiers using immunofluorescence microscopy. The secondary aim was to evaluate the association and agreement between the two microscopy techniques; TEM and immunofluorescence microscopy, to compare, for the first time, the two methods for the investigation of fibre and region specific IMTG use during exercise. We hypothesise that a good level of agreement exisits between the two methods. If this hypothesis is true, immunofluorescence microscopy may be the preferred technique to investigate

exercise-induced changes in IMTG content and LD morphology in skeletal muscle.

5.3 Methods

Participants and ethical approval

The muscle samples used for this study were part of a larger study to investigate subcellular-specific glycogen utilisation during exercise and the effect of carbohydrate availability on glycogen resynthesis (Nielsen *et al*, 2011) and the link to sarcoplasmic reticulum calcium handling (Ørtenblad *et al.* 2011). The original project was approved by the Regional Ethical Review Board in Umea ̊, Sweden (no.07-076M). All participants gave informed consent to participate after being fully informed about the risks involved and any possible discomfort that could be caused. They could withdraw from the study at any time and the study conformed to the standards set out by the Declaration of Helsinki.

Ten Norwegian elite male cross-country skiers volunteered to participate in the study, with a mean (± SD) age, weight, height and maximal oxygen uptake (VO_{2max}) of 22 ± 1 years, 80 ± 9 kg, 182 ± 8 cm and 68 ± 5 ml.kg^{-1}. min^{-1}, respectively. Participants trained approximately 700 hours per year and had an average of 11 years experience competing and training in cross country skiing.

Experimental procedures

Prior to the day of the performance test, maximal heart rate (HR_{max}) and VO_{2max} were examined through an incremental exercise test using diagonal stride techniques on a modified treadmill allowing skiing uphill with roller skis (Calbet *et al,* 2005). On the day of the performance test skiers performed an individualised warm-up and ski preparation. The snow conditions on the day

favoured the diagonal stride technique and a high degree of double poling, i.e. upper body exercise. For the performance test, skiers were required to perform a ~20km cross-country skiing time trial. It took on average 57 min to complete (range 52-63 min). Muscle biopsies were obtained pre and post-exercise from both the arm (*triceps brachii*) and leg (*vastus lateralis*). The biopsies were taken by the same person to minimise variations in location and depth before (pre) and immediately (1-2 min) after exercise (post) when the skier had crossed the finish line. These muscles were selected as data has shown that they are highly active during cross-country skiing (Holmberg *et al*, 2005). One specimen of the muscle samples was fixed in glutaraldehyde for transmission electron microscopy (TEM) analysis, whereas another specimen was frozen directly in isopentane and stored for immunofluorescence microscopy (as outlined in 3.3).

Image capture using immunofluorescence microscopy, image processing and data analysis

Full details of the immunofluorescence staining procedures (3.2), including the antibody information (3.3.1), and the image capture process (3.4.2) are detailed in Chapter 3. A representative image including individual channels can be seen in Figure 5.1.

Image processing was completed using Image-Pro Plus 5.1 software (Media Cybernetics, Rockville, MD, USA). IMTG content and LD morphology was investigated on a fibre type-specific basis. Fibres stained positive for MHC I were classified as type I fibres, and those stained positive for MHC IIa were classified as type IIa fibres. Any fibres with no staining were classified as type

IIx fibres. An intensity threshold was uniformly selected to represent a positive signal for IMTG and IMTG content expressed as the positively stained area fraction relative to the total area of each muscle fibre. The cell membrane staining enabled the calculation of individual cell areas. LD density was expressed as the number of LDs relative to area. Data on the area (size; μm^2) of each individual LD were collected per image and used to calculate the frequency of LD's over a range of sizes (100 nm) groups. The mean area of individual LD's in an area of interest, such as the peripheral or central region, was also calculated. At pre-exercise 8 ± 1 type I and 6 ± 1 type IIa fibres were analysed per participant from n=5 arm and n=8 leg samples and at post exercise, 7 ± 2 type I and 5 ± 1 type IIa fibres were analysed per participant from n=4 arm and n=4 leg samples giving an overall total of ~ 300 fibres. Using the Image-Pro Plus software LD were identified as objects and their number and size was then measured. Using Image-Pro, the cells were split into two subcellular regions; the peripheral and central regions of the cell. Representative images of this process can be seen in Figure 5.2 and detailed in section 3.4 of Chapter 3.
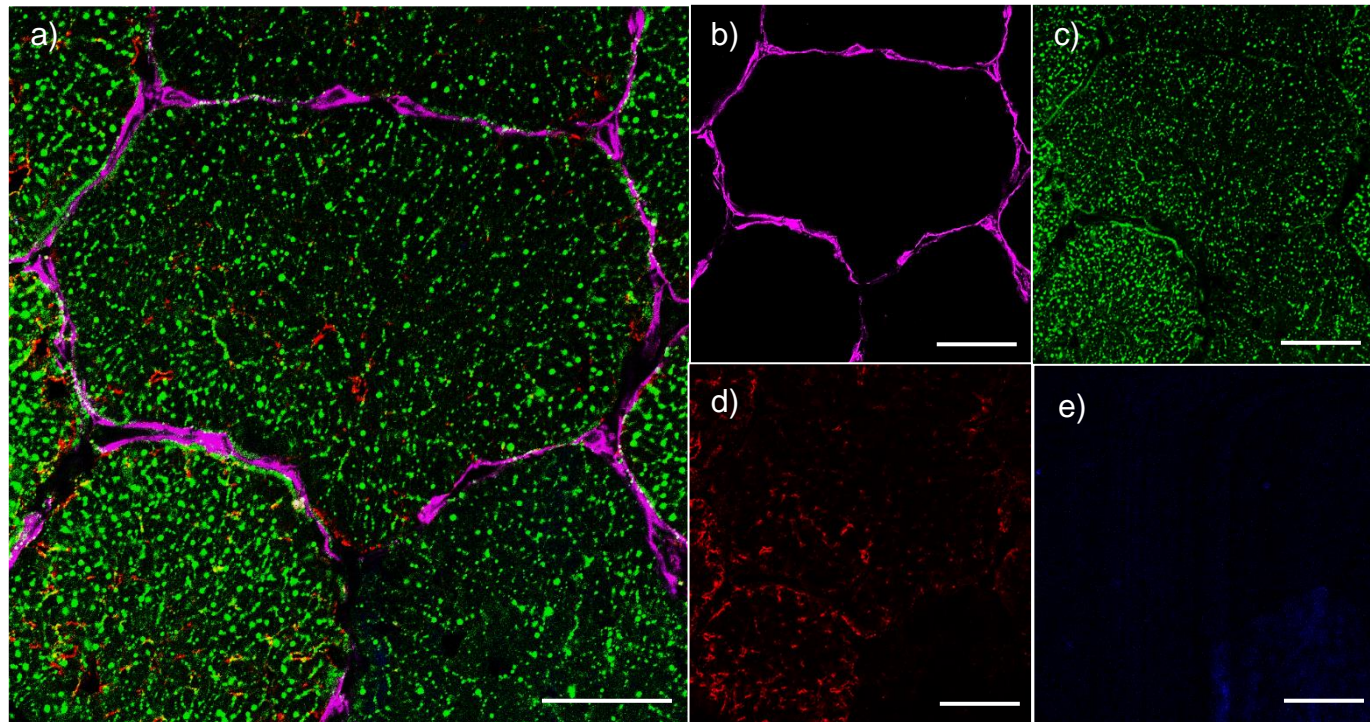
Figure 5.1. Immunofluorescence Confocal microscopy images.
Images taken using an inverted confocal microscope (Zeiss LSM710; Carl Zeiss AG, Oberkochen, Germany) with a 63x 1.4 NA oil immersion objective with a 1.1x digital zoom.

(a) Full image displaying all staining channels, (b) Cell membrane stained with Laminin displaying in pink, (c) BODIPY lipid stain in green, (d) MHCI staining in red and (e) MHCII staining in blue. Scale bar = 30 µm
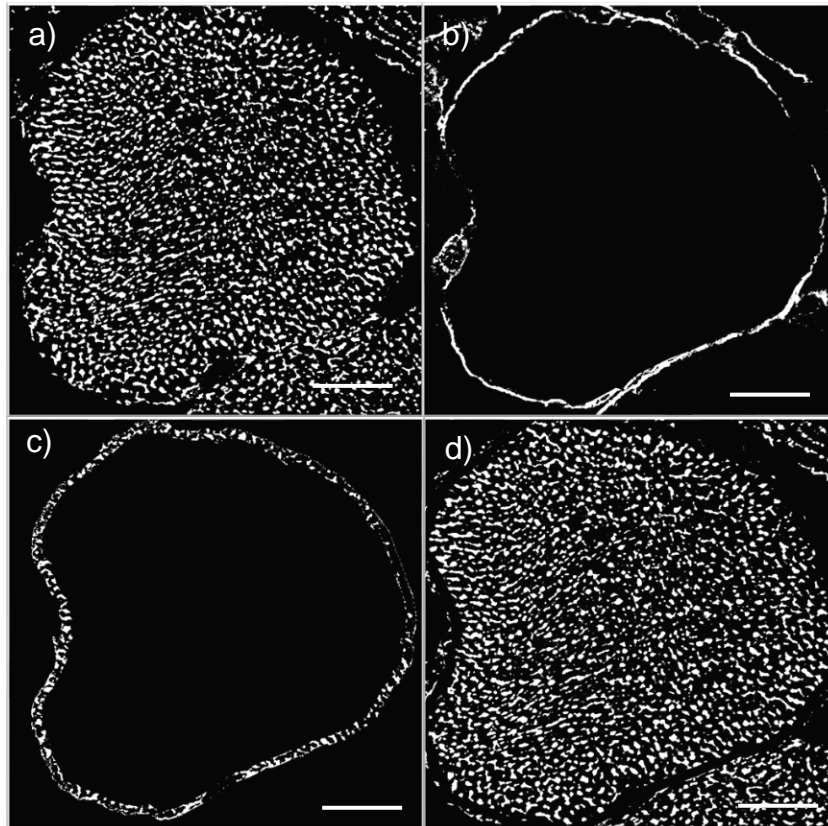
Figure 5.2. Image processing in order to measure IMTG content and LD morphology in the two subcellular regions.

Region-specific image analysis. A grey scale image was created of both BODIPY staining (a) and the cell membrane stained using Laminin (b). A 2 µm region was identified within the inside of the membrane and used to visualise the LDs in the peripheral region (c) and central region was identified as the remaining portion of the cell (d). Scale bar = 30 µm

Transmission Electron Microscopy

Our collaborators at the University of Southern Denmark (Odense, Denmark) completed TEM analysis of the muscle samples as described in Koh *et al.* (2017). The raw data obtained through TEM was shared by the authors, thus enabling a direct comparison with the data generated through immunofluorescence microscopy. The TEM method is described in detail in Koh *et al.* (2017) and in chapter 3.6. Briefly, electron micrographs of 8-9 longitudinally orientated muscle fibres were imaged per biopsy. Overall 80 electron micrographs were obtained in a systematic random order per fibre at a magnification of x10,000. Based on the minimal electron micrographs required, the 80 micrographs collected were made up of 40 from the subsarcolemmal region, 20 from the superficial region and 20 from the central region of the myofibrillar space. Exercise-induced changes in subcellular-specific LD volume fraction, LD size and LD number were calculated as described in chapter 3.6.3.

Statistics

Statistical analyses were performed using SPSS (SPSS; version 26, IBM, USA). A three-factor within-subjects repeated measures ANOVA was used to examine IMTG content, LD number and LD size in relation to the effect of time, fibre type and subcellular region. Linear mixed modelling was used to examine the frequency and changes of LD's of specific sizes ranging from 100 to 1000 nm^2. Significant main effects and interactions were assessed using Bonferroni adjustment post hoc analysis. Pearson correlation coefficients were calculated to investigate the correlation between the two methods in terms of the absolute

values. Alongside this, Lin's concordance coefficient test (LCC; Lin, 1989) was performed, which defines the level of agreement between two variables relative to a line through the origin at an angle of 45 degrees (slope = 1). Thus, this analysis was performed using relative data; individual values were related to one particular subject who had the median values for IMTG content in type I fibres using immunofluorescence microscopy. LCC (R_c) has a scale between 0 and 1 where 0.21 – 0.40 denotes fair concordance, 0.41 – 0.60 moderate concordance, 0.61 – 0.80 substantial concordance and finally 0.81 – 1.00 would show almost perfect concordance (Lin 1989). Data is presented as mean ± SD. Significance was accepted at $P < 0.05$.

5.4 Results

Following the immunofluorescence staining and imaging procedures it became apparent that there was a limited number of viable samples due to frost damage which could be included for analysis. Thus, the viable arm and leg samples were pooled, and as a result the pre-exercise dataset sample size was n=13 (n=5 arm, n=8 leg), whereas the post-exercise dataset had a sample size of n=8 (n=4 arm, n=4 leg).

Using immunofluorescence microscopy to investigate resting IMTG content, distribution and LD morphology

IMTG content (expressed as % area stained, Table 5.1) was 19% greater pre-exercise in type I fibres in comparison to type IIa fibres (P = 0.049). However, there was no difference in IMTG content in the central region of the cell in comparison to the peripheral region (P = 0.144). Fibre had no significant effect on the relative distribution of IMTG content at rest in the peripheral region and central region, with ~12% and ~88% of total IMTG content, respectively (P = 0.173). Only one or two type IIx fibres were observed per muscle section for each participant, and therefore were not included in the analysis for IMTG content and LD morphology.

With regards to LD morphology, LD number pre-exercise the peripheral region contained 13% more LDs than the central region (Table 5.1, P = 0.003) regardless of fibre type. On average, LD in the peripheral region were smaller

than those in the central region (P = 0.027). However, mean LD size was not different between type I and type IIa fibres (Table 5.1, P = 0.156). Thus, the greater IMTG content in type I fibres was predominantly attributed to a higher number of LDs. We further investigated the difference in LD size between subcellular regions across both type I and type IIa fibres by assessing the frequency of LD detected over a range of LD sizes from 100 – 1400 nm^2. Across both fibre types, there was a greater frequency of LD ≤100 nm^2 in the central compared to the peripheral region (P < 0.01), but conversely there was a greater frequency of LD 200 nm^2 in size in the peripheral region compared to the central region (Figure 5.3, P <0.05).

Table 5.1. IMTG content, LD number and size before exercise.

	Type I	Type IIa
IMTG content (% area stained)		
Peripheral	0.434 ± 0.252 *	0.347 ± 0.242
Central	3.774 ± 2.082 *	2.974 ± 2.206
LD number (LD.μm^{-2})		
Peripheral	0.014 ± 0.006 †	0.011 ± 0.006 †
Central	0.010 ± 0.045	0.093 ± 0.057
LD size (μm^2)		
Peripheral	0.281 ± 0.072 †	0.269 ± 0.064 †
Central	0.313 ± 0.079	0.285 ± 0.069

Values reported as mean ± SD. *P = 0.049 Significantly different from type IIa fibres. † P < 0.05 Significantly different from the central region.
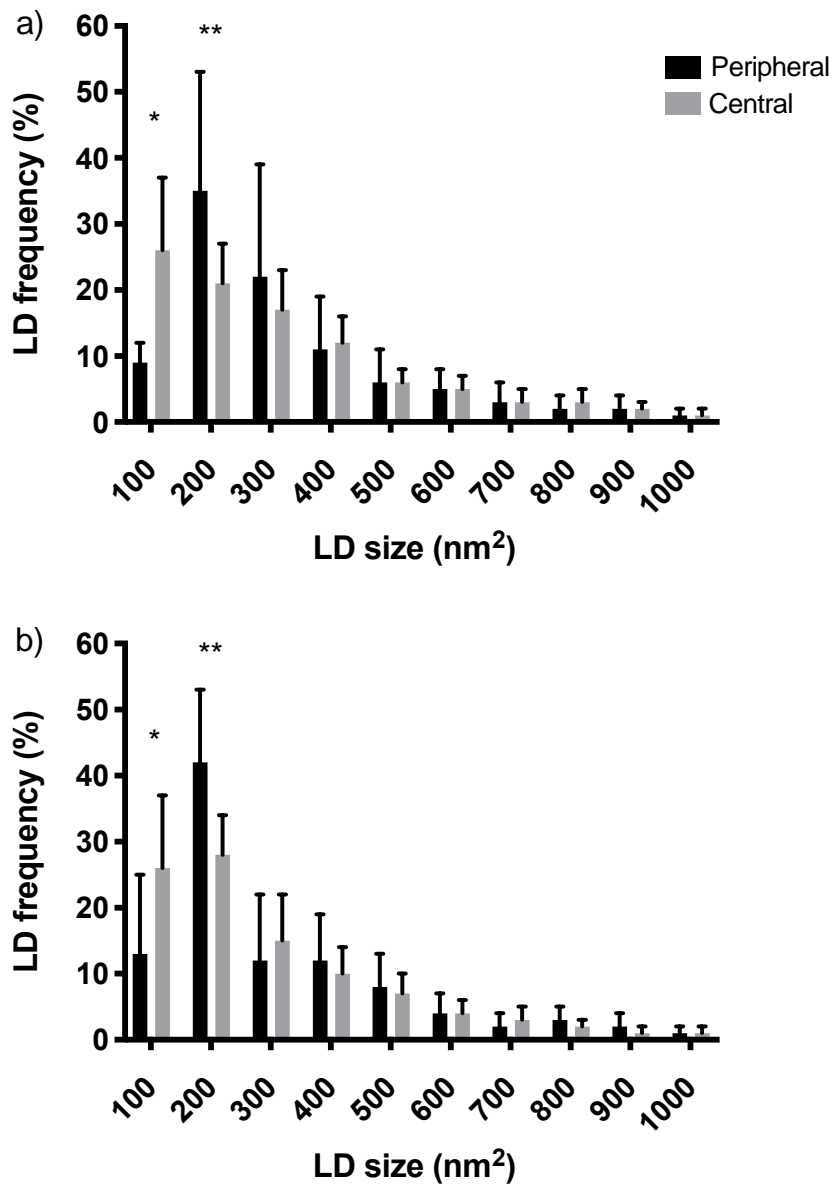
Figure 5.3. LD frequency in type I and type II fibres before exercise.

Difference in LD size and number between the two regions by determining the frequency of LDs detected in each region over a range of LD sizes in type I (a) and type IIa fibres (b). * $P < 0.01$ LD in the central region to be greater than in the peripheral, ** $P < 0.05$ LD in the peripheral region greater than in the central. Values are means ± S.D.

Using immunofluorescence microscopy to investigate exercise-induced changes in IMTG content, distribution and LD morphology

Exercise tended to reduce IMTG content (Figure 5.4a, $P = 0.071$), although this was not fibre type-specific, with IMTG content being reduced by 28% and 50% in type I and type IIa fibres, respectively. Moreover, across both fibres there was a tendency for IMTG content to be reduced more in the peripheral region (-40%) compared to the central region (-36%; $P = 0.080$). Across both fibre types, the relative distribution of IMTG content was not significantly affected by exercise, with ~12% and ~88% of total IMTG content in the peripheral region and central region, respectively (Table 5.2, $P = 0.576$).

Exercise also tended to reduce LD number (Figure 5.4b, $P = 0.064$), regardless of fibre-type, with reductions of ~35% in both type I and type IIa fibres ($P = 0.004$). Further to this, across both fibre types there was a greater reduction in the number of LD from the peripheral region where there are a greater number of smaller LD < 200 μm^2 (- 35%, $P = 0.028$), than in the central region, where there is a tendency of a greater number of larger LD > 200 μm^2 (- 33%, $P = 0.070$, Figure 5.5).

When considering LD size, there was a significant reduction in response to exercise, with LD's shrinking by 14% from pre to post exercise (Figure 5.4c, $P = 0.019$). Although this was not fibre-specific, with reductions in LD size of ~14% in both type I and type IIa fibres, respectively ($P = 0.031$). Exercise had no effect on LD size in relation to subcellular region ($P = 0.112$). When

examining the frequency of LD over a range of LD sizes we found that exercise

caused a significant decrease in the number of LD sized 400 and 600 nm^2

(Figure 5.5, $P < 0.05$), across both fibres and regions.

Table 5.2. Relative distribution of lipid across the peripheral and central regions.

		Type I	Type II
Pre-exercise (%)			
	Peripheral	11 ± 2	12 ± 4
	Central	89 ± 2	88 ± 4
Post-exercise (%)			
	Peripheral	13 ± 7	13 ± 9
	Central	87 ± 7	87 ± 9

Values reported as mean ± SD. No significant differences observed following exercise between fibre type.
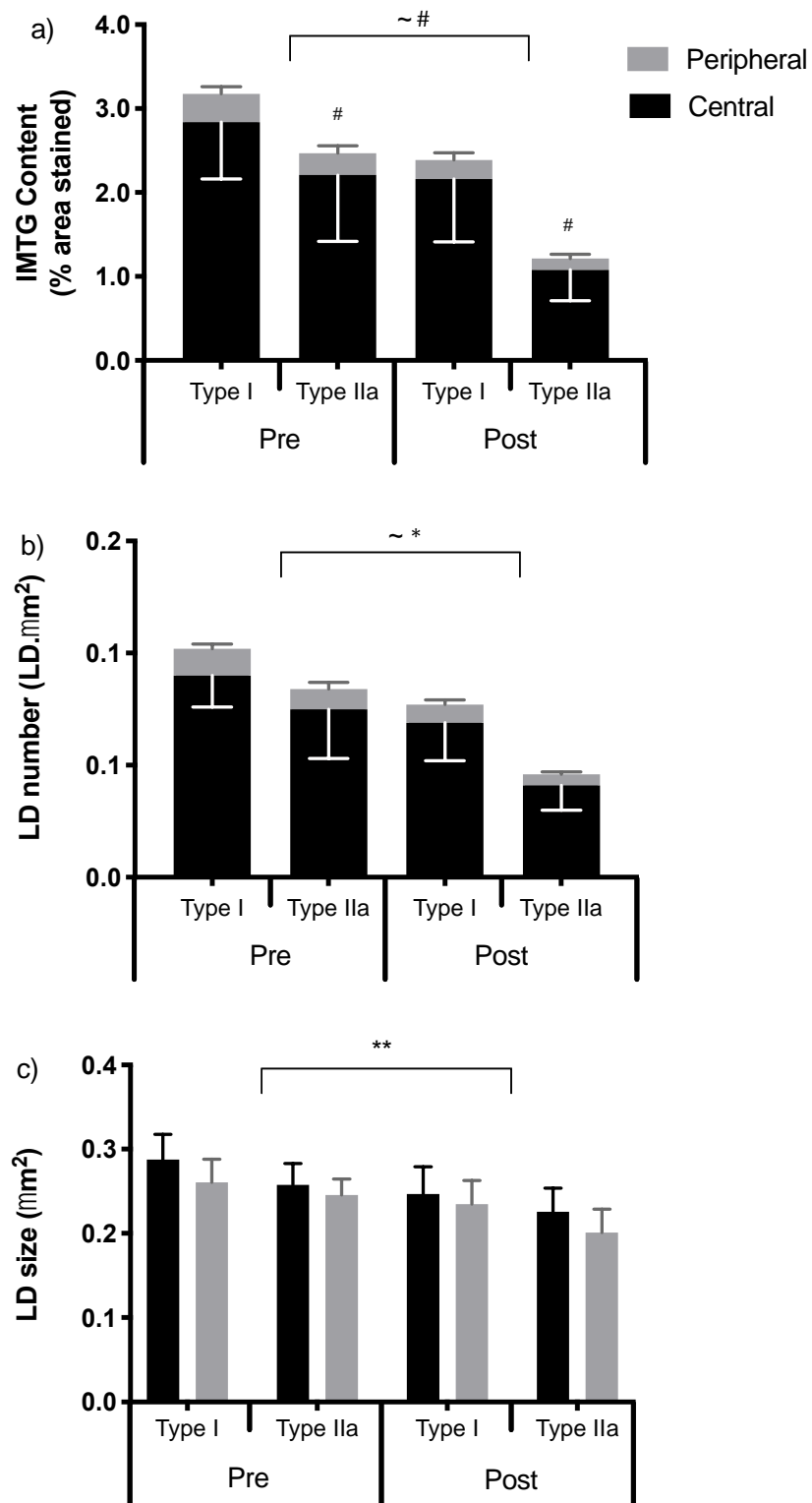
Figure 5.4. Exercise-induced changes in IMTG content, LD number and LD size.

~ $P < 0.1$ tendency for IMTG content and LD number to reduce in response to exercise in both fibre types. # $P < 0.05$ greater reduction in IMTG content from the peripheral region. * $P < 0.05$ greater reduction in LD number from the peripheral region. ** $P = 0.019$ reduction in LD size across both fibre types and regions. Values are mean ± S.D.
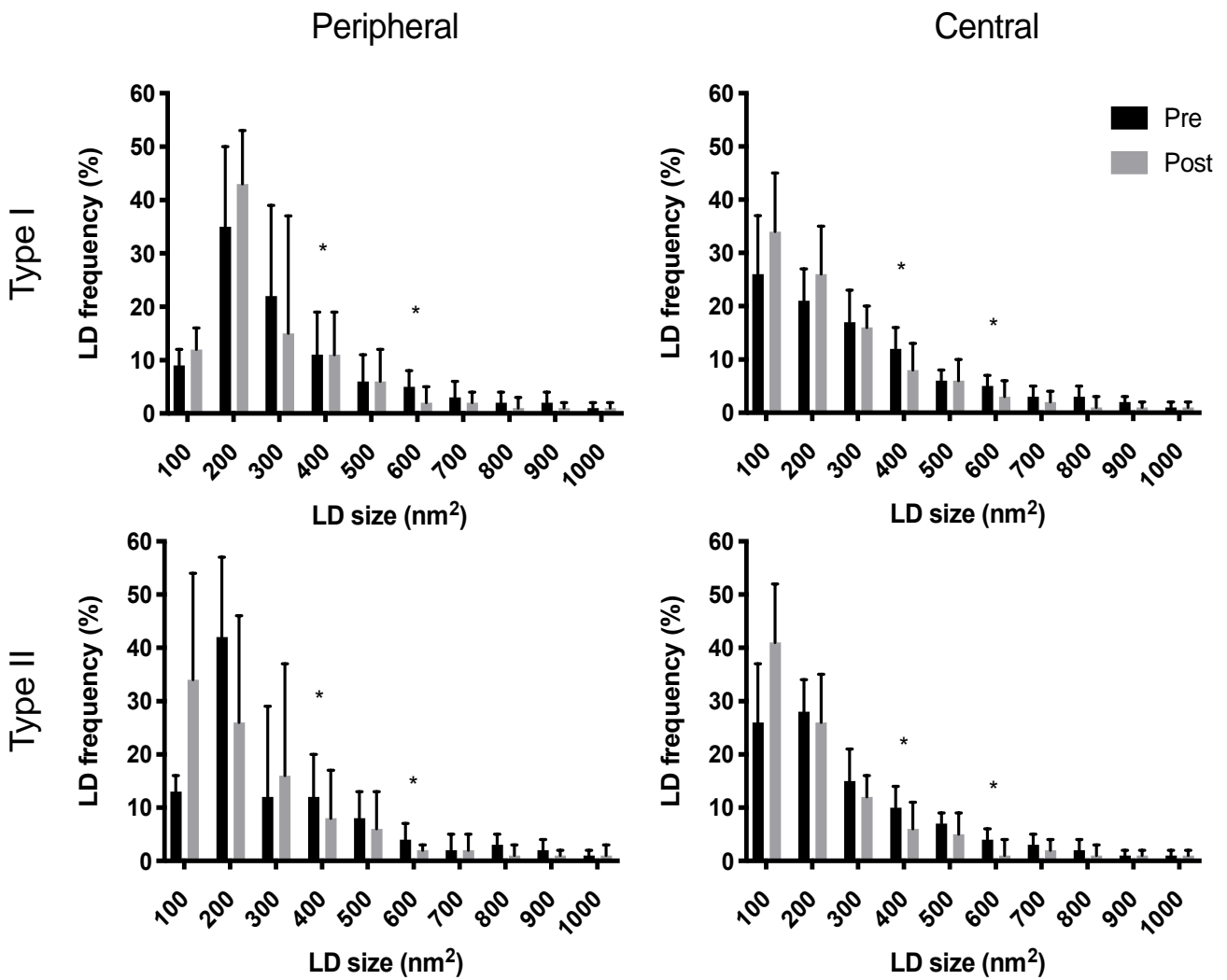
Figure 5.5. Effect of exercise on LD frequency.

The effect of exercise on the difference in LD size and number by determining the frequency of LDs detected at each time point (pre and post) over a range of LD sizes in both fibre types and regions. * $P < 0.05$ reductions in the number of LD sized 400 and 600nm^2. Values are mean ± S.D.

Correlations between immunofluorescence microscopy and transmission electron microscopy (TEM) data

Because TEM and immunofluorescence microscopy can be considered as the gold standard for assessing subcellular LD pools (TEM) and fibre type-specific IMTG content (immunofluorescence microscopy), the two methods were compared across these factors. Thus, for each variable (LD/IMTG content, LD size and number), the data generated using immunofluorescence microscopy was compared to that generated using TEM (as reported in Koh *et al*, 2017) using both Pearson's correlation coefficients and LCC. The Pearson correlation coefficients (*r* values), *P* values and LCC (R_c) are presented in Table 5.3. There was a significant correlation between methods for assessing subcellular-specific LD/IMTG content in both the peripheral/subsarcolemmal (*P* = 0.008, Figure 5.6a) and central/intermyofibrillar regions (*P* = 0.013, Figure 5.6b). Interestingly though, there was only a substantial agreement between methods for LD/IMTG content in the peripheral/subsarcolemmal region when examined using LCC (Rc = 0.660). When comparing fibre types, the correlation between the two datasets for LD/IMTG content was significant for type I fibres (*P* < 0.05, Figure 5.7a), though there was only a trend for a correlation when examining type IIa fibres (*P* = 0.085, Figure 5.7b). Consequently, there was a moderate level of agreement between the two methods for investigating LD/IMTG content in type I fibres when examined using LCC (Rc = 0.542).

With regards to LD morphology, there was significant correlations between the two methods for investigating LD size in both the peripheral/subsarcolemmal

(P = 0.002, Figure 5.6e) and central/intermyofibrillar regions (P = 0.039, Figure 5.6f). However, the level of agreement between methods for investigating LD size in both the peripheral/subsarcolemmal and central/intermyofibrillar region was poor (Table 5.3). Regarding fibre type, there were significant correlations for LD size in both type I (P = 0.009, Figure 5.7e) and type IIa fibres (P = 0.015, Figure 5.7f). Although again, the LCC showed a poor level of agreement between methods for investigating LD size in both fibres (Table 5.3). LD number only tended to be correlated when examined in both the peripheral/subsarcolemmal (P = 0.078, Figure 5.6c) and central regions (P = 0.075, Figure 5.6d). However, there was no correlation between methods for investigating LD number in either fibre type (Figure 5.7 c/d). Moreover, the corresponding LCC values were very low for LD number, overall suggesting that the agreement between the two methods for examining LD size and number is weak.

Table 5.3. Correlation matrix comparing the agreement between TEM and immunofluorescence microscopy for determining IMTG content, LD number and size.

	IMTG content			LD number			LD size		
	r	P	R_C	r	P	R_C	r	P	R_C
Muscle fibre									
Type I	0.710	<0.001*	0.542	- 0.058	0.751	0.237	0.610	0.009*	0.094
Type II	0.320	0.085	0.236	- 0.225	0.251	0.019	0.536	0.015*	0.103
Region									
Peripheral/Subsarcolemmal	0.474	0.008*	0.660	0.327	0.078	0.271	0.466	0.002*	0.105
Central/Intermyofibrillar	0.435	0.013*	0.178	0.319	0.075	0.046	0.647	0.039*	0.086

Correlations are between corresponding variables generated through TEM and immunofluorescence microscopy for IMTG content, LD number and LD size. Significant correlations are denoted as * ($P < 0.05$).

The Lin's concordance coefficient (R_c) is also included. Lin's scale is defined as: 0.21 – 0.40 fair concordance, 0.41 – 0.60 moderate concordance, 0.61 – 0.80 substantial concordance and finally 0.81 – 1.00 would show almost perfect concordance.
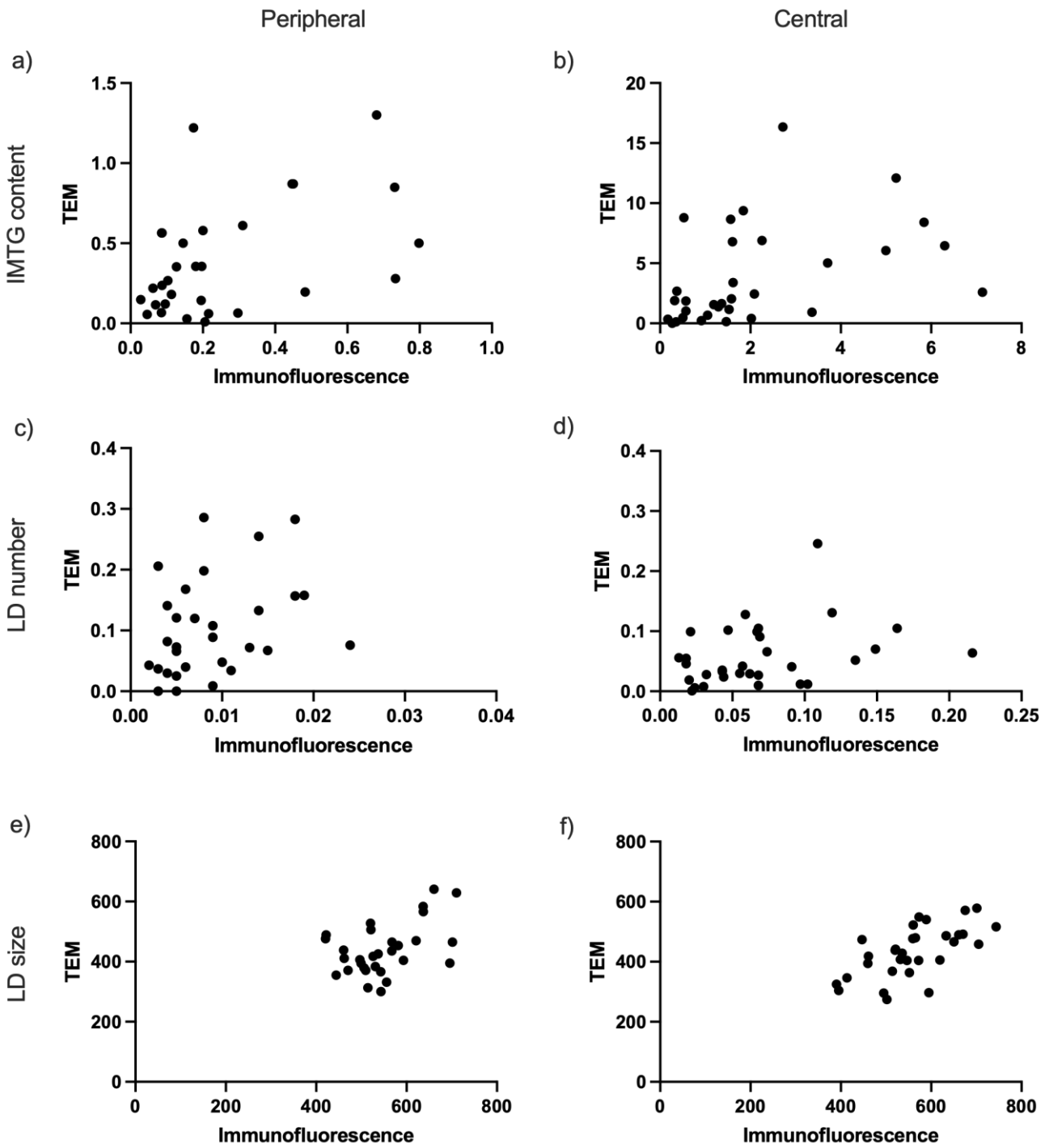
Figure 5.6. Correlations between TEM and immunofluorescence microscopy by subcellular region for IMTG content (a/b), LD number (c/d) and LD size (e/f).

Associated *r, P* and *Rc* values are displayed in the correlation matrix table 5.3.
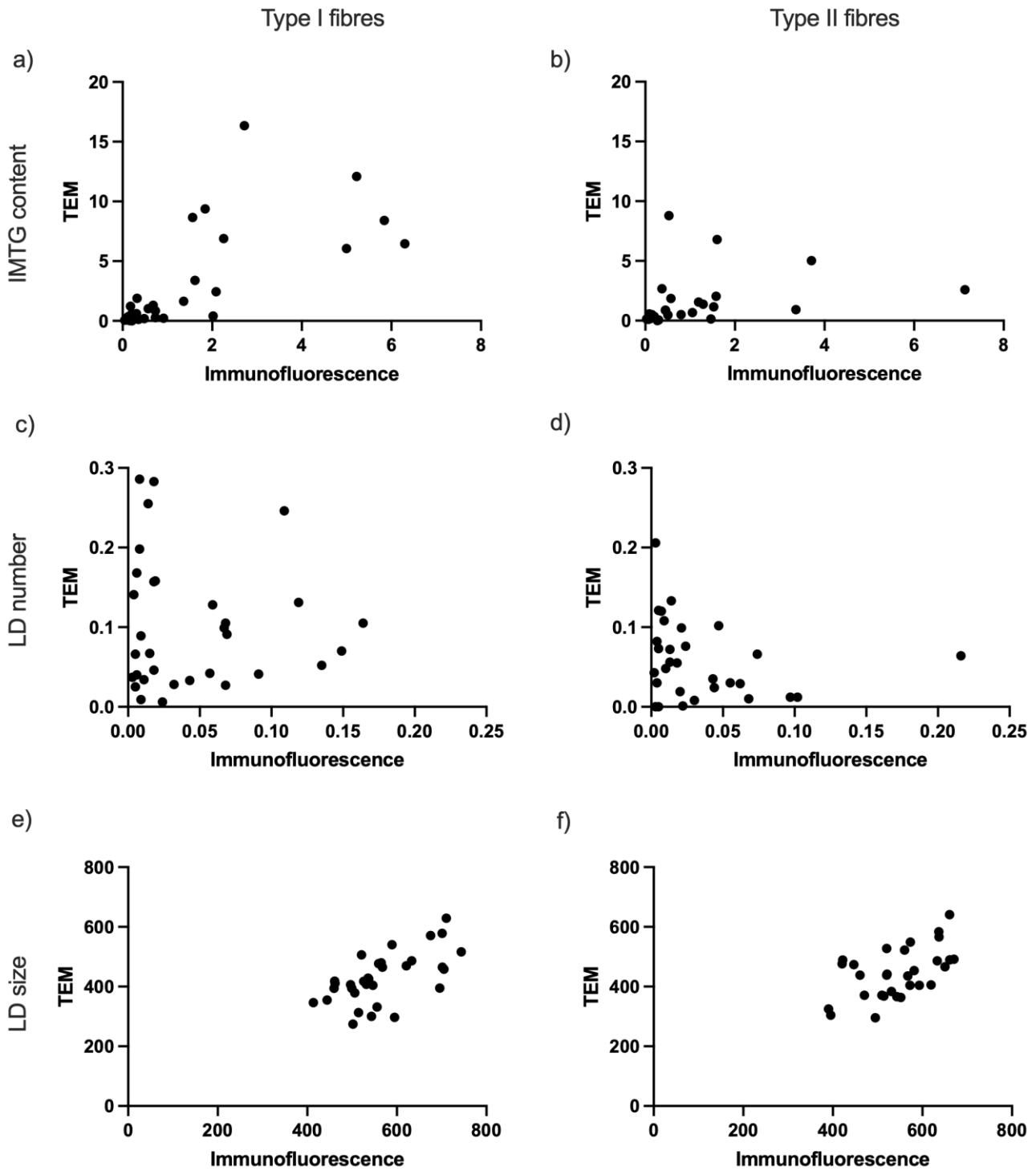
Figure 5.7. Correlations between TEM and immunofluorescence microscopy by fibre type for IMTG content (a/b), LD number (c/d) and LD size (e/f).

Associated *r, P* and *Rc* values are displayed in the correlation matrix table 5.3.

5.5 Discussion

The present study aimed to investigate fibre type and subcellular-specific IMTG utilisation during cross-country skiing using immunofluorescence microscopy, then to evaluate the agreement with TEM. By making a direct comparison with TEM (the gold standard for assessing subcellular LD pools), the study also aimed to determine the suitability of immunofluorescence microscopy for investigating subcellular-specific IMTG utilisation during exercise. The first novel finding was that ~1 hour of cross-country skiing reduced IMTG content in both type I and type IIa fibres, and in both the peripheral and central region of the cell, due to a reduction in both LD size and number. Second, there was agreement between TEM and immunofluorescence microscopy when examining LD/IMTG content, particularly in type I fibres, although there was little agreement when examining LD size and number.

At rest, IMTG content was greater in type I compared to type IIa fibres, which is in agreement with previous literature demonstrating greater IMTG content in type I muscle fibres than in type II fibres (Essen *et al,* 1975; Malenfant *et al,* 2001; Van Loon *et al*, 2003a, Van Loon *et al,* 2003b). IMTG content itself reflects the combination of measures of LD number and size, and therefore these LD characteristics can be examined in order to understand the differences in IMTG content, distribution and morphology. To this end, LD number tended to be greater in type I compared to type IIa fibres, whereas there were no fibre type specific differences in LD size. Therefore, the higher IMTG content in type I fibres

was mainly due to a greater number of LDs, which is consistent with previous observations (Devries *et al,* 2007; Prats *et al,* 2013; Koh *et al,* 2017).

Despite the differences in IMTG content between type I and type IIa fibres, there was no difference in the relative IMTG content when comparing the peripheral and central regions of the cell. This is in agreement with other work using TEM to investigate subcellular-specific LD content in highly-trained individuals (Koh *et al.,* 2017). When considering LD morphology though, we found that there was a greater number of LDs present in the peripheral compared to the central region, whereas LDs in the central region were, on average, larger than those in the peripheral region. The observed region-specific differences in LD morphology are one of few reported in the literature (Strauss *et al,* 2020). Large subsarcolemmal LDs are associated with insulin resistance (Nielsen *et al,* 2017), and therefore maintaining a greater number of small LDs in the peripheral region is likely an adaptation enabling well-trained individuals to possess high IMTG stores while remaining highly insulin sensitive. Although centrally-located LDs had a larger average size than those located in the peripheral region, we also found that the frequency of LDs 100 nm^2 in size was greater in the central compared to the peripheral region. Conversely, there was a greater frequency of LDs 200 nm^2 in size in the peripheral compared to the central region. Together, this suggests that considering the size of individual LDs is more informative than simply measuring average LD size. The general belief is that small LDs have a greater surface area for the interaction of lipolytic enzymes with the IMTG substrate and regulatory proteins located on the LD surface (Bickel *et al,* 2009;

Morales *et al,* 2017). Consequently, the frequency of very small LDs we observed in the central region may be an adaptation underpinning the greater utilisation of IMF LDs during exercise reported in previous studies (Koh *et al,* 2017). Taken together, the novel observations from the current study demonstrate that differences in LD morphology (number and size) can occur independent of differences in IMTG content.

Approximately 1 h of cross-country skiing tended to reduce IMTG content in both type I and type IIa fibres. IMTG utilisation during exercise is most apparent during moderate-intensity exercise (Van Loon, 2004). However, the intensity of the cross-country skiing time trial here was >75% VO_{2max} (Ørtenblad *et al,* 2011), which characteristically relies more heavily on muscle glycogen as a substrate, with less reliance on IMTG (Van Loon *et al,* 2001). Further to this, it is important to note that in the companion study detailing the TEM findings, Koh *et al* (2017) only observed reductions in LD content in the *triceps brachii*, not the *vastus lateralis*. Since in the present study we used a combination of both arm and leg muscle samples, this may also explain why we only observed a trend for a reduction in IMTG content. Typically, exercise-induced reductions in IMTG content are specific to type I fibres (Van Loon *et al,* 2003), but here we report a decrease in both type I and type IIa fibres. Whilst it has been reported that mitochondrial content of type II fibres is lower than type I fibres in highly-trained cross country skiers (Ørtenblad *et al*, 2018), when comparing between arm and leg muscles, there was greater mitochondria reported in the type II fibres of arm muscle than leg (Ørtenblad *et al*, 2018). Furthermore, the mitochondrial content

of those type II fibres is still greater than that reported in healthy untrained individuals (Nielsen *et al,* 2010). Therefore, the high mitochondrial content of the type IIa fibres, in these individuals could explain the reduction in IMTG content in these fibres. On a subcellular level, the decrease in IMTG content occurred in both the peripheral and central regions of the fibres (both type I and type IIa), and on closer inspection there was a tendency for IMTG utilisation to be greater in the peripheral region. In highly-trained cross country skiers mitochondrial content in the arm and leg muscles in type I and type II fibres is similar between the SS and IMF regions (Ørtenblad *et al,* 2018), suggesting the capacity for FA oxidation is similar across both subcellular locations. Combined with the smaller size of LDs in the peripheral region (and therefore a potentially greater surface area for enzyme and protein binding), this could explain the tendency towards greater use of IMTG from the peripheral region.

The exercise-induced decrease in IMTG content can be attributed to reductions in both LD number and size. This is in agreement with previous research in trained individuals (Van Loon *et al,* 2003) and untrained individuals (Shepherd *et al,* 2012), whilst others only observe a decrease in LD number (Koh *et al,* 2017; Devries *et al,* 2007; Shepherd *et al,* 2013). Differences are likely due to different populations studied, duration and intensity of exercise protocol or a combination of both. In the present study, LD number was reduced in both fibre types following 1 h of exhaustive exercise, predominantly in the peripheral region. Li *et al*, (2014), demonstrated the more dominant LD store; IMF (i.e. central region) is not as sensitive to training as the other regions. Koh *et al,* (2017), also reported

reductions in LD number in the SS region of the legs. This is in line with previous data from Devries *et al,* (2007) who demonstrated moderate intensity cycling decreased intramuscular lipid content alongside reductions in LD number. An increase in IMTG content is a consequence of endurance training and can be attributed, in part, to an increase in LD number. This has been found in type I and type II fibres after an acute bout of moderate-intensity exercise following either a period of endurance or sprint interval training by Shepherd *et al,* (2013), though their data showed no reduction in LD size after either exercise protocol. Whereas, when we examined LD size, a decrease was observed in both type I and type IIa fibres within both peripheral and central regions. However, the research from Shepherd *et al,* (2013) was from sedentary males. Therefore, a potential explanation for these differences in results could be the subject population as lipid metabolism is considerably different between sedentary individuals and elite athletes (Bergman *et al,* 1985). In brief, some differences caused by training status include enhanced endogenous substrate concentrations (Shaw *et al,* 2010; Moro *et al,* 2007). As such, endurance training will increase IMTG content in type I fibres as much as three-fold compared with type II fibres. Further to this, regular endurance training will augment the ability to oxidise fat at higher workloads and overall, enhance maximal fat oxidation (Lima-Silva *et al,* 2010; Scharhag-Rosenberger *et al,* 2010).

Further to our observations of overall reductions in LD size, we would speculate that the smaller LD's would be targeted for utilisation first, as they are highly abundant in both the central and peripheral regions of the cell (Figure 5.5).

However, by examining differences in the frequency of specific LDs (based on size), it seems that more moderately sized LD of 400 and 600 nm^2 were reduced from pre to post-exercise. A possible explanation for the smaller LDs not being preferentially targeted for breakdown could be that they are newly-formed or nascent LDs, and are therefore not yet labelled with the appropriate LD-associated PLIN protein isoforms. Alternatively, it could be that the smaller LD (e.g. 100 and 200 nm^2) were in fact targeted for breakdown during exercise, but that at the same time the moderately-sized LD of 400 and 600 nm^2 were also reduced in size, and became LDs of 100 and 200 nm^2 in size. This would then explain why no reduction in smaller sized LD was observed. Irrespective of the pool of LDs that is used, it has been demonstrated that LD with PLIN2 or PLIN5 attached appear to be preferentially utilised during exercise over those LD without these proteins (Shepherd *et al,* 2012; 2013). Further studies are required to explore which particular-sized LDs have PLIN2 and/or PLIN5 located within their phospholipid monolayer meaning that they are targeted for breakdown during exercise.

The data obtained using immunofluorescence microscopy was compared to LD-related data obtained by Koh *et al,* (2017) using TEM in order to determine how appropriate immunofluorescence microscopy may be for measuring IMTG content and LD morphology on subcellular-specific basis. Whilst there was correlation between methods for assessing LD/IMTG content in both subcellular regions, there was only a substantial agreement between methods for examining LD/IMTG content in the peripheral region. The positive aspect of this finding is

that it supports the use of a 2 µm band to represent the peripheral region when using immunofluorescence microscopy. Of course, using this approach does not take into account natural variations in the width of the SS region which are visible when using TEM. However, the relative proportion of IMTG found in the peripheral and central region of the cell as determined through immunofluorescence microscopy is similar to the relative distribution of LD reported in the SS and IMF regions using TEM (Koh *et al*, 2017). TEM is considered the gold standard for examining LD morphology due to the greater magnification and resolution capabilities. When examining LD size in both regions there was significant correlation between methods, however, there was only a trend for a correlation when examining LD number, and the LCC analysis revealed little agreement between methods for examining LD size and number. This likely due to differences in magnification capacity.

Conclusions

In conclusion, ~1 hour of cross-country skiing in a real-world environment reduced IMTG content in both type I and type IIa fibres, across both the peripheral and central regions of the muscle fibres due to a reduction in both LD size and number. Compared to TEM, immunofluorescence microscopy apparently provides a good approach to assess IMTG content, but not LD size and number. Moreover, agreement between methods was good for measuring IMTG content and LD size in the 2 µm peripheral region of the cell, thereby supporting the use of this approach to distinguish subcellular regions using immunofluorescence microscopy. Overall, immunofluorescence provides an alternative method to

quantify IMTG content, but not LD size and number. Therefore, these data have important implications for future studies aiming to understand the mechanisms regulating LD pools. As such, immunofluorescence microscopy analysis should be considered when the aim is to understand the mechanisms regulating the utilisation of specific subcellular LD pools, such as investigations examining the association of LD with PLIN proteins.

Chapter 6 - Skeletal muscle lipid droplets are resynthesized before being coated with perilipin proteins following prolonged exercise in elite male triathletes.

The full version of this chapter is published in the American Journal of Physiology, Endocrinology & Metabolism, as stated below.

6.1 Abstract

Intramuscular triglycerides (IMTG) are a key substrate during prolonged exercise, but little is known about the rate of IMTG resynthesis in the post-exercise period. We investigated the hypothesis that the distribution of the lipid droplet (LD)-associated perilipin (PLIN) proteins is linked to IMTG storage following exercise. 14 elite male triathletes (27 ± 1 y, 66.5 ± 1.3 mL.kg^{-1}.min^{-1}) completed 4 h of moderate-intensity cycling. During the first 4 h of recovery, subjects received either CHO or H_2O, after which both groups received CHO. Muscle biopsies collected pre and post-exercise, and 4 h and 24 h post-exercise were analysed using confocal immunofluorescence microscopy for fibre type-specific IMTG content and PLIN distribution with LDs. Exercise reduced IMTG content in type I fibres (-53%, P=0.002), with no change in type IIa fibres. During the first 4 h of recovery, IMTG content increased in type I fibres (P=0.014), but was not increased further after 24 h where it was similar to baseline levels in both conditions. During recovery the number of LDs labelled with PLIN2 (70%), PLIN3 (63%) and PLIN5 (62%; all P<0.05) all increased in type I fibres. Importantly, the increase in LDs labelled with PLIN proteins only occurred at 24 h post-exercise. In conclusion, IMTG resynthesis occurs rapidly in type I fibres following prolonged exercise in highly-trained individuals. Further, increases in IMTG content following exercise preceded an increase in the number of LDs labelled with PLIN proteins. These data, therefore, suggest that the PLIN proteins do not play a key role in post-exercise IMTG resynthesis.

6.2 Introduction

The location of intramuscular triglyceride (IMTG)-containing lipid droplets (LD) in close proximity to mitochondria underpins the importance of IMTG as a fuel source during prolonged moderate-intensity exercise in trained individuals, particularly in type I muscle fibres (Van Loon *et al,* 2003). Indeed, many studies report a decrease in IMTG content during exercise (Van Loon, 2004; Kiens, 2006), but to date there has been much less focus on post-exercise IMTG resynthesis. This is in contrast to the large body of research that has focused on glycogen use during exercise and dietary strategies to optimise glycogen repletion following exercise (Burke *et al,* 2011). High carbohydrate (CHO) diets, however, are reciprocally low in fat (typically 2-25% of total energy intake) and markedly reduce IMTG storage (Starling *et al,* 1997; Coyle *et al,* 2001; Johnson *et al,* 2003). Indeed, post-exercise IMTG resynthesis is suppressed up to 48 h following 3 h moderate-intensity cycling when consuming a high CHO diet (containing 24% fat) (Van Loon *et al,* 2003). More recently though, post-exercise nutritional strategies have shifted towards CHO- or calorie-restriction in an attempt to augment specific training adaptations in human skeletal muscle. In this respect, limiting CHO or energy intake following glycogen-depleting exercise has been shown to enhance the activation of intracellular signalling pathways compatible with mitochondrial biogenesis (reviewed by Impey *et al,* 2018). Typically, in these studies CHO or energy provision is limited throughout exercise as well as during the first few hours following exercise, after which habitual energy and macronutrient intake are resumed. As mentioned above, high CHO diet's can suppress IMTG resynthesis for up to 48 h (Van Loon *et al,* 2003), but whether

nutritional strategies restricting CHO or energy provision post-exercise, designed to augment skeletal muscle training adaptations, can enhance post-exercise IMTG resynthesis, is yet to be investigated.

Given the paucity of studies investigating post-exercise IMTG resynthesis, it is unsurprising that the mechanisms governing the synthetic response are poorly understood. In skeletal muscle, cytosolic LDs provide a storage depot for IMTG, and given their large proteome (>300 proteins) (Zhang *et al,* 2011) these LDs are now considered a highly active organelle. The perilipin (PLIN) proteins are the most abundant of the LD proteins in skeletal muscle, and are more highly expressed in type I compared to type II muscle fibres thereby mirroring the fibre-specific distribution of IMTG (Shaw *et al,* 2009, 2012; Shepherd *et al,* 2012, 2013). Moreover, exercise training typically augments both the protein levels of PLIN2, PLIN3 and PLIN5 alongside elevations in IMTG content (Shaw *et al,* 2012; Shepherd *et al,* 2013), implying that the increase in PLIN protein content is mechanistically important to facilitate growth of the IMTG pool. This assertion is supported by the observation that muscle-specific PLIN2 (Bosma *et al,* 2012) or PLIN5 overexpression (Bosma *et al,* 2013) in rodents fed a high-fat diet promotes IMTG storage, which may be linked to an ability of the PLIN proteins to restrict basal lipolytic rates (Laurens *et al,* 2016). Recently, Gemmink *et al*. (2016) reported that IMTG storage augmented by prolonged fasting in healthy individuals coincided with an increase in the size and number of LDs containing PLIN5. Because no changes occurred in the protein level of PLIN5, these data suggest that a redistribution of the pre-existing PLIN5 pool occurs when the LD

pool expands. We recently corroborated this finding using an acute lipid infusion to stimulate IMTG accretion, and demonstrated that a redistribution of PLIN3, as well as PLIN5, also occurs across a growing LD pool (Shepherd *et al,* 2017). Whilst the use of both prolonged fasting and lipid infusion has provided insight into the potential role of the PLIN proteins in supporting IMTG storage, these experimental models do not represent the normal physiological milieu; that is, they expose the muscle to excess free fatty acid concentrations and stimulate IMTG accretion starting from a 'resting' level. This physiological state, therefore, is distinct from one in which trained individuals regularly use (and reduce the size of) the IMTG pool during exercise and subsequently resynthesize IMTG in the post-exercise period. Investigating the PLIN proteins under more physiologically dynamic conditions may therefore provide additional insight into their role in skeletal muscle.

In addition to the possible mediation of IMTG storage, the PLIN proteins are suggested to be important in mediating the breakdown and oxidation of IMTG. We have previously shown that LDs containing either PLIN2 (Shepherd *et al,* 2012) or PLIN5 (Shepherd *et al,* 2013) are preferentially used during 1 h of moderate-intensity exercise, and recently reported that HSL targets LDs containing PLIN5 for breakdown during exercise (Whytock *et al,* 2018). PLIN3 is associated with fat oxidation in cultured muscle cells (Covington *et al,* 2015), but whether PLIN3 plays a role in the breakdown and oxidation of IMTG *in vivo* is not known. Therefore, we asked the question whether PLIN3-containing LDs are also preferentially targeted for breakdown during exercise.

CHO consumption post-exercise will increase circulating insulin concentrations which will in turn inhibit systemic lipolysis and reduce plasma free FA concentrations. If no energy is consumed, insulin concentrations will remain low and plasma free FA concentrations will be high, thus providing a source of FA to be used to rebuild IMTG stores. In this context, we first aimed to investigate the hypothesis that post-exercise IMTG resynthesis would be accelerated under conditions of acute CHO restriction in elite endurance athletes. To achieve this, CHO ingestion was restricted during the initial 4 h recovery period following prolonged moderate-intensity exercise. By assessing changes in IMTG content in response to exercise and up to 24 h post-exercise, this provided a physiological model to further clarify the roles of the PLIN proteins in mediating IMTG utilisation and storage. In this respect, we hypothesised that during exercise there would be a preference to use LDs labelled with PLIN proteins, and during recovery from prolonged exercise there would be a preferential increase in LDs labelled with PLIN proteins. Consequently, the secondary aim of this study was to investigate changes in the distribution of PLIN proteins relative to LDs during exercise and in the post-exercise period using our previously described immunofluorescence microscopy methodology (Shepherd *et al*, 2017). Finally, because IMTG utilisation during exercise is specific to the IMF region of the fibre (Koh *et al*, 2017), we determined changes in IMTG content and the PLIN LD distribution on a subcellular-specific basis.

6.3 Methods

Subjects

Fourteen elite male triathletes (27.2 ± 0.9 y, 183 ± 2 cm, 75.3 ± 1.4 kg) that had competed at national and/or international level were recruited as part of a larger study (Gejl *et al,* 2014). Participants had been elite athletes for 4.8 ± 1.4 y and trained on average 16.4 ± 0.9 hours a week. There were no differences between experimental groups, other than VO_{2max} where the participants in the CHO condition had a significantly higher VO_{2max} (CHO: 68.3 ± 1.4 mL.kg^{-1}.min^{-1}, H_2O: 63.5 ± 1.8 mL.kg^{-1}.min^{-1}, $P < 0.05$). All participants were fully informed of any risks associated with the study before providing informed verbal and written consent. Ethical approval was approved by the ethics committee of the Region of Southern Denmark (Project ID: S-20090140) and was conducted according to the Declaration of Helsinki.

Experimental procedures

All experimental procedures have been described previously (Gejl *et al,* 2014; Jensen *et al,* 2015). Briefly, participants completed 4 h of cycling at an average of 73% ± 1% HR_{max} equating to ~56% of VO_{2max} (determined via pre-experimental submaximal incremental test and VO_{2max} test) with an intended HR intensity of ~75% HR_{max}. Subjects were provided a standardised breakfast (see "Dietary Procedures" below) 90 min before completing the cycle in which they used personal equipment of their choice (i.e. bike, shoes and pedals) on mounted turbo trainers (Elite Crono Mag ElastoGel Trainer, Fontaniva, Italy). During exercise participants were only allowed to consume water (minimum of 1 mL water.kg^{-1}.h^{-}

^{1}). Following exercise, participants were randomly selected to receive either CHO ($n = 7$) or H_2O ($n = 7$) during the first 4 h of recovery. For the remaining 20 h period following exercise all participants consumed a CHO-rich diet. Muscle biopsies were collected from participants from the *m. vastus lateralis* before and after exercise, as well as at 4 h and 24 h post-exercise, under local anaesthetic (1% lidocaine; Amgros, Copenhagen, Denmark) using a Bergstrom needle (Bergstrom, 1975) with suction as discussed in section 3.1. All procedures were conducted in laboratories at the Department of Sports Science and Clinical Biomechanics, University of Southern Denmark, Odense.

Dietary procedures

The dietary intake was controlled and corresponded to recommendations provided by the American College of Sport Medicine. A breakfast was provided 90 min prior to exercise and consisted of CHO rich foods (i.e. porridge oats, raisins, skimmed milk, orange juice and energy bar; 82 kJ.kg^{-1} bw). All calorie intake was calculated based upon the participant's body mass and equated to 65% CHO, 25% fat and 10% protein. During the initial 2 h recovery period following exercise, the CHO group consumed a meal consisting of pasta, chicken, vegetables and a CHO beverage (1.07 g CHO.kg^{-1} bw.h^{-1}). and subsequently participants were provided with an energy bar and CHO beverage (1.05 g CHO.kg^{-1} bw.h^{-1}) in the following 2 h. During this 4 h period, the H_2O group remained fasted and only consumed water. After the initial 4 h recovery period, both groups received the same standardised meals for the remaining 20 h of recovery. In addition, the H_2O group received energy corresponding to that of the

CHO group during the 4 h recovery period to ensure that the total energy intake between groups was equal. Thus, the CHO group received dinner and breakfast whereas the H_2O group received lunch, an energy bar, dinner and breakfast. In total, subjects received 264 $kJ.kg^{-1}$ bw (10 g $CHO.kg^{-1}$ bw) on the first experimental day.

Immunofluorescence microscopy

Samples were prepared for immunofluorescence imaging as described in section 3.2. Staining was conducted using appropriate primary antibodies targeting myosin heavy chain type I and myosin heavy chain type IIa alone or in combination with antibodies targeting PLIN2, PLIN3 or PLIN5 (see table in section 3.2.2 for details).

Image capture, image processing and data analysis

Images of cross-sectionally orientated sections, used to investigate fibre type-specific IMTG content and LD morphology, were captured using an inverted confocal microscope (Zeiss LSM710; Carl Zeiss AG, Oberkochen, Germany) with a 63x 1.4 NA oil immersion objective as described in section 3.2.3. ~20 images were captured per time point aiming for an even split across type I and type IIa fibres. All other fibres were assumed to be type IIx fibres, and although some images were captured, in this data set there was an insufficient number of type IIx fibres to perform statistical analysis and therefore the results are not included. Overall ~900 images were analysed, equating to 70-80 images per participant.

To investigate co-localisation between LD and PLIN proteins the same microscope and magnification were utilised to obtain the digital images, but with a 4x digital zoom applied on the straightest edge of an identified cell (Fig. 6.1). This first allowed an image to be taken at the peripheral region of the cell and subsequently the field of view was manually moved to the centre of the cell to generate an image of the central region of the cell. There were ~10 peripheral and ~10 central images obtained for each time point per participant, and each PLIN protein was investigated individually meaning there was up to 240 images taken for each participant.
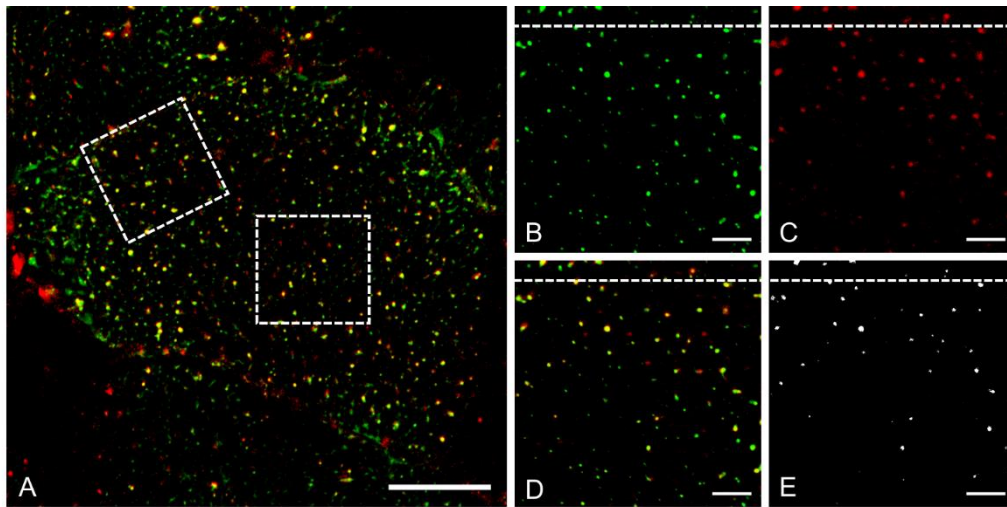
Figure 6.1. Representative colocalisation images of IMTG and PLIN5 visualized using immunofluorescence microscopy.

Confocal immunofluorescence microscopy images were obtained at 4x digital zoom from the central and peripheral region of each cell, as indicated by the two white boxes (A). IMTG were stained with Bodipy 493/503 (green; B), PLIN5 was stained in red (C), and the subsequent co-localisation map (D). The overlapping area of LD and PLIN5 was extracted (D) and used to calculate the fraction of PLIN5 co-localising with LD, and the number of PLIN5+ and PLIN5- LD. The white dotted line in images B-E represents the 2 μm area that was analysed when images at the peripheral region were obtained. White bars represent 25 μm (A) and 5 μm (B-E). The same co-localisation analysis was repeated for PLIN2 and PLIN3.

Image processing was completed using Image-Pro Plus 5.1 software (Media Cybernetics, Rockville, MD, USA) as described in 3.2.5. To assess IMTG content, LD morphology and PLIN protein expression on a fibre type and subcellular-specific basis, each fibre was first separated into a peripheral region to measure SS LD (first 2 μm from the cell border) and the central region to measure IMF LD (remainder of the cell). This approach of using a fixed 2 μm distance from the membrane to represent the subsarcolemmal region has been utilised previously to examine IMTG content in differing populations (Van Loon, 2004) and is now supported by our findings from chapter 5. An intensity threshold was uniformly selected to represent a positive signal for IMTG. The content of IMTG was expressed as the positively stained area relative to the total area of the peripheral or central region of each muscle fibre. LD density was expressed as the number of LDs relative to the area of the peripheral or central region. The area of individual LD's was used to calculate mean LD size in each region.

Because only significant changes in IMTG content were observed in type I fibres (see results), the LD and PLIN co-localisation analysis was only conducted in type I fibres. Co-localisation analysis was performed separately for each PLIN protein with LDs. Briefly, an intensity threshold was uniformly selected to represent a positive signal for IMTG and the PLIN protein of interest. Based on the threshold selected, dual images were generated and subsequently used for co-localisation analysis. The overlapping objects within the images were then extracted creating a separate image of the co-localised areas. This first allowed the identification of the total number of extracted objects, corresponding to the

total number of LDs labelled with PLIN2, 3 or 5 protein (PLIN+ LD). Second, the number of extracted objects was subtracted from the total number of LD in order to quantify the number of LD's with no PLIN protein associated (PLIN- LD). Finally, the number of extracted objects was subtracted from the total number of PLIN objects to determine the number of 'free PLIN' objects. The number of objects identified through each of these analyses were expressed relative to the area of interest, thus providing data on changes in the density of PLIN+ LDs, PLIN-LDs and free PLIN. The peripheral region was identified within the appropriate images by creating a 2 µm wide area of interest, meaning that the above analyses were only conducted in this area of the image. Before conducting this analysis, numerous controls were performed to check for bleed through and non-specific secondary antibody binding before co-localisation analysis was conducted, as previously described (Shepherd *et al*, 2013, 2013   ).

Statistics

Statistical analyses were performed using SPSS (SPSS; version 23, IBM, USA). Linear mixed modelling was used to examine all dependent variables (IMTG content, LD morphology, PLIN protein expression and co-localisation analysis) at the different time points, with data separated into the two different experimental conditions (CHO and H_2O) in the recovery period. All main effects and interactions were tested using a linear mixed-effects model, with random intercepts to account for repeated measurements within subjects to examine differences between experimental condition, fibre type and subcellular region. Subsequent Bonferroni adjustment post-hoc analysis was used to examine main

effects and interactions. Data is presented as mean ± SD. Significance was accepted at $P < 0.05$.

6.4 Results

Lipid analysis:

Pre exercise IMTG content and LD morphology

Before exercise, IMTG content was two-fold greater in type I compared to type IIa fibres (main fibre effect; $P < 0.001$, Table 6.1), and IMTG content was greater in the periphery of the cell (within the 2 μm border) when compared to the central region (main region effect; $P = 0.025$). Overall though, the majority of IMTG was observed in the central compared to the peripheral region of the cell (main region effect; $P < 0.001$, Table 6.2). Considering the number and size of LD´s, there were two-fold greater LD's in type I fibres compared to type IIa fibres ($P = 0.001$). LD's in the central region tended to be 12% larger than in the peripheral region across both fibre types ($P = 0.089$, Table 6.1). Thus, pre-exercise fibre type differences in IMTG content were predominantly explained by differences in LD number, with LD size being similar across fibre types.

Table 6.1. Pre-exercise IMTG content and LD morphology.

	Type I fibres		Type II fibres		*P* value	
	Peripheral	Central	Peripheral	Central	Fibre type	Region
IMTG content (% area stained)	4.63 ± 1.96*	3.93 ± 1.65*	2.42 ± 1.34	1.94 ± 0.91	0.001	0.025
LD size (μm^2)	0.285 ± 0.049	0.321 ± 0.056	0.269 ± 0.062	0.301 ± 0.063	0.500	0.089
LD number (LD.μm^{-2})	0.152 ± 0.057*	0.116 ± 0.036*	0.084 ± 0.043	0.061 ± 0.023	0.001	0.260

IMTG content and LD number are expressed relative to the area of the peripheral or central region. Data are means ± SD.

* Significantly greater in type I fibres (*P* < 0.05).

Effect of exercise on IMTG content and LD morphology

Four hours of steady state moderate-intensity exercise led to a 53% decrease in IMTG content in type I fibres (fibre $\times$ time interaction; P = 0.002, Fig. 6.2a). No significant decrease in IMTG content was observed in type IIa fibres. Moreover, when examining exercise-induced changes in type I fibres on a subcellular-specific basis, IMTG content was reduced by 55% within the central region (time $\times$ region interaction; P < 0.001), whereas IMTG content was not altered in the peripheral region (P = 0.570). Consequently, the relative distribution of IMTG across the subcellular regions decreased from ~87% before exercise in the central region to ~77% after exercise, with a reciprocal increase in the relative distribution of IMTG within the peripheral region from ~13% before exercise to ~23% after exercise (main time effect; P = 0.022, Table 6.2).

When examining changes in LD morphology in response to exercise, LD number was reduced by 46% in type I fibres only (fibre $\times$ time interaction; P = 0.043, Fig. 6.2b). No changes in LD number occurred in type IIa fibres (P = 0.474, Fig. 6.2b), and no changes in LD size were observed in either fibre type (Fig. 6.2c). Thus, IMTG utilization during exercise could be entirely explained by a decrease in LD number.
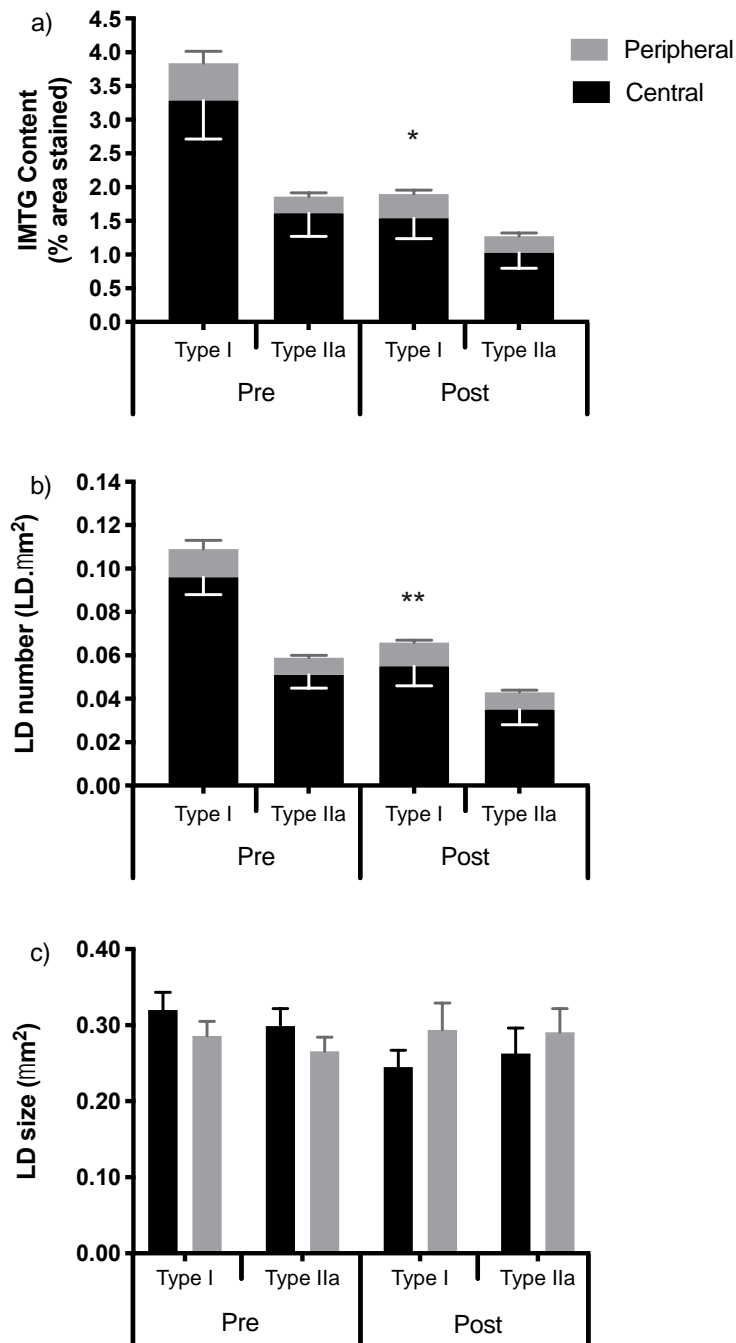
Figure 6.2. Fibre type and subcellular-specific changes in IMTG content and LD morphology in response to prolonged exercise.

IMTG content (a) LD number (b) and LD size (c) in peripheral and central subcellular regions before (pre) and after (post) exercise in type I and type IIa muscle fibres. IMTG content and LD number in each region was normalized to total cell area. *Significant decreases in IMTG content from pre to post exercise in type I fibres only within the central region ($P < 0.05$). **Significant decreases in LD number from pre to post exercise in type I fibres ($P = 0.043$). mean ± SD.

Effect of recovery on IMTG content and LD morphology

During recovery from prolonged exercise IMTG content increased significantly in the central region of type I fibres from post-exercise to 4 h post-exercise, and from post-exercise to 24 h post-exercise (time x fibre x region interaction, $P < 0.001$, Fig. 6.3a). Post-hoc analysis revealed that the increase between 4 h and 24 h post-exercise alone was not significant ($P = 0.160$). No changes in IMTG content occurred in type IIa fibres (Fig. 6.3b). When comparing CHO and H_2O groups, IMTG content was lower post-exercise in the H_2O condition compared to the CHO condition in both fibre types (condition x time interaction; $P = 0.029$). In the H_2O condition, there was an increase in IMTG content from post-exercise to 4 h post-exercise, and from post-exercise to 24 h post-exercise ($P = 0.014$). In contrast, in the CHO condition IMTG content was not significantly changed from post-exercise to 24 h post-exercise ($P = 1.000$). Importantly though, by 24 h post-exercise IMTG content was statistically similar between conditions ($P > 0.05$). When examining subcellular IMTG distribution during recovery, IMTG in the central region increased from ~77% post-exercise to ~82% 4 h post-exercise, finally returning to pre-exercise distribution by 24 h post-exercise with ~86% of IMTG observed in the central region (main time effect; $P = 0.005$, Table 6.2). This was mirrored by changes in IMTG distribution in the peripheral region decreasing from ~23% after exercise to ~18% 4 h post-exercise, and finally to ~14% 24 h post-exercise (main time effect; $P = 0.005$, Table 6.2).

When considering LD number and size, LD number increased in type I fibres from post-exercise to 4 h post-exercise, and from post-exercise to 24 h post-exercise

(time x fibre interaction; P = 0.028). More specifically, LD number significantly increased in the H_2O condition from post-exercise to 4 h post-exercise, and from post-exercise to 24 h post-exercise (condition x time interaction; $P = 0.003$, Fig. 6.3c). No changes in LD number occurred between 4 h post-exercise and 24 h post-exercise. Overall no significant changes were observed in LD size throughout recovery ($P > 0.05$, Fig. 6.3e & f). Thus, changes in IMTG content through recovery could be explained by increases in LD number, with no differences being observed in LD size.

Table 6.2. Relative distribution of IMTG between subcellular regions in response to exercise and during recovery.

		% of IMTG			
		Type I fibres		Type IIa fibres	
		Peripheral	Central*	Peripheral	Central*
Pre		12 ± 1	88 ± 1	14 ± 1	86 ± 1
Post	CHO	$20 \pm 4^{\dagger}$	$80 \pm 4^{\dagger}$	$19 \pm 2^{\dagger}$	$81 \pm 2^{\dagger}$
	Water	$23 \pm 4^{\dagger}$	$77 \pm 4^{\dagger}$	$25 \pm 8^{\dagger}$	$75 \pm 8^{\dagger}$
Post 4 h	CHO	15 ± 2	85 ± 2	16 ± 3	84 ± 3
	Water	22 ± 7	78 ± 7	19 ± 6	81 ± 6
Post 24 h	CHO	13 ± 2	87 ± 2	15 ± 3	85 ± 2
	Water	11 ± 3	89 ± 3	16 ± 4	84 ± 4

Data are means $\pm$ SD. * Significant effect of region across all time points ($P < 0.05$).

† Significantly different from all other time-points within the same condition ($P < 0.05$).
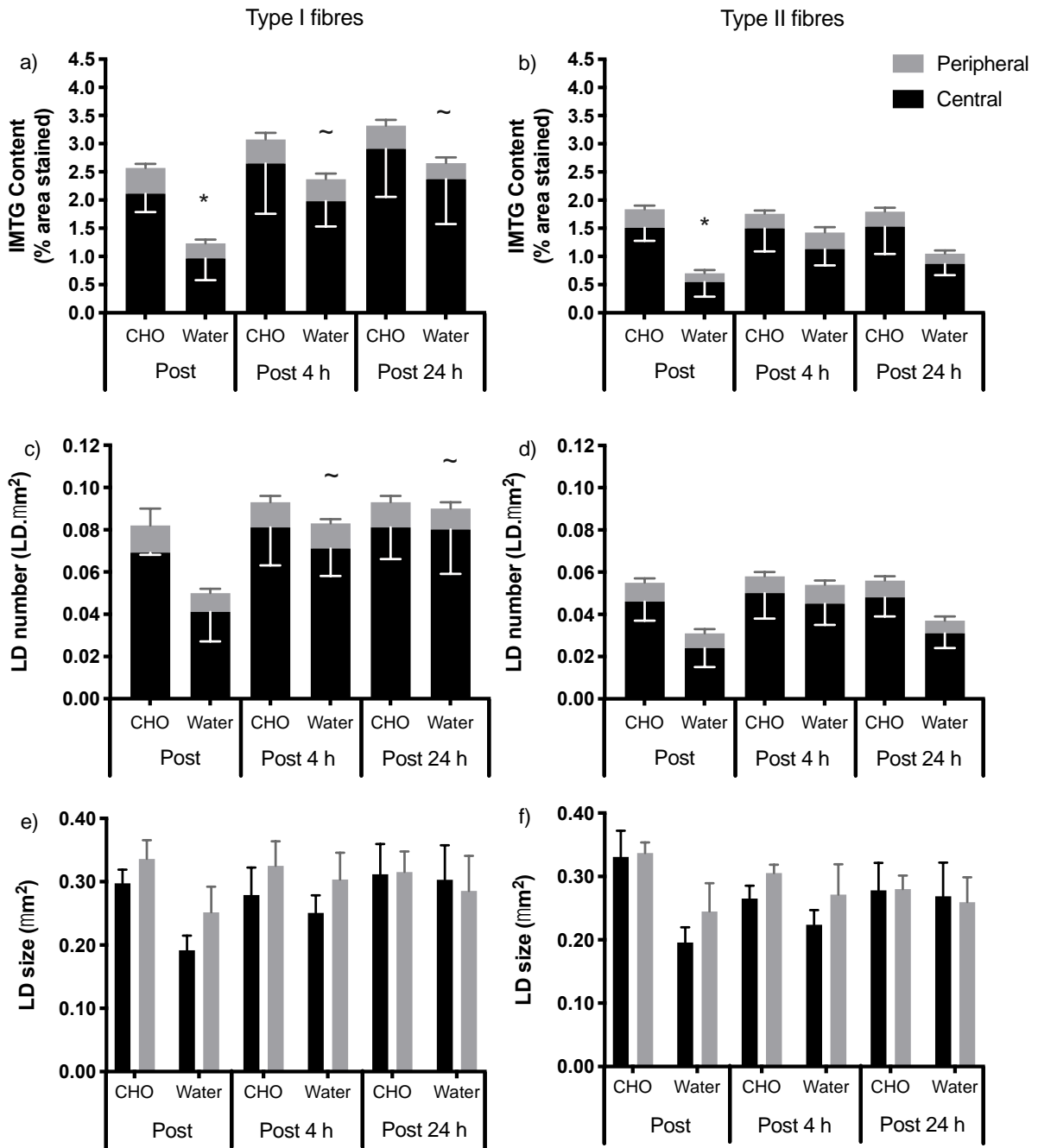
Figure 6.3. Fibre type and subcellular-specific changes in IMTG content and LD morphology during recovery from prolonged exercise.

IMTG content (a, b), LD number (c, d) and LD size (e, f) in peripheral and central subcellular regions during recovery in type I and type IIa fibres. IMTG content and LD number in each region was normalized to total cell area. *IMTG content at post-exercise significantly lower in H_2O vs. CHO ($P = 0.029$). ~Significant increase from post-exercise in the H_2O condition only in type 1 fibres ($P < 0.05$). Values are means ± SD.
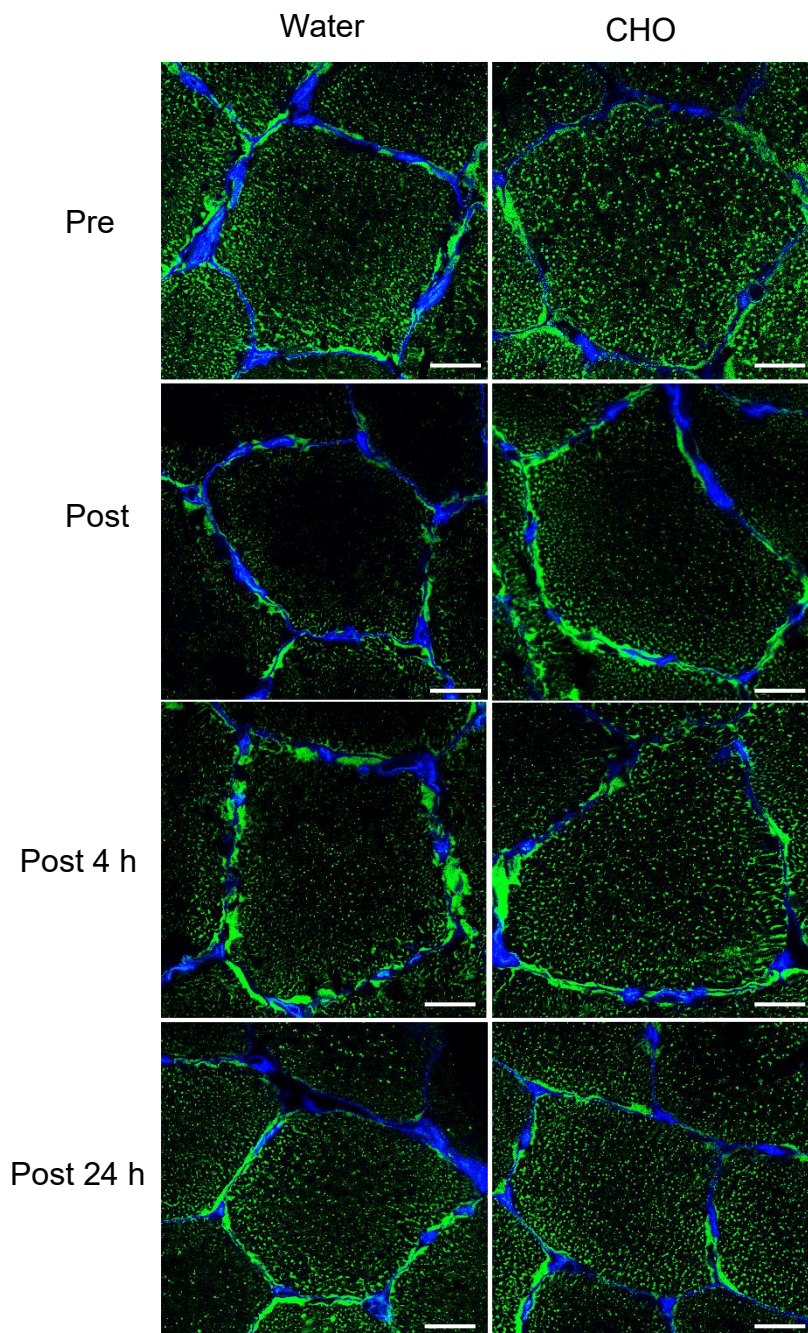
Figure 6.4. Representative immunofluorescence images of IMTG in response to and in recovery from prolonged exercise.

Sections were co-stained for IMTG (stained using Bodipy 493/503; green), fibre type (not shown), and wheat germ agglutinin Alex Fluor 350 (WGA) in order to identify the cell border (stained blue). Images depict IMTG content in type I fibres at pre and post-exercise, and 4 h and 24 h post-exercise in the H_2O and CHO condition. White bars represent 30 µm.

PLIN analysis

Because significant changes in both IMTG content and LD morphology occurred specifically in type I fibres during exercise and recovery, subsequent PLIN protein content and co-localisation analysis was limited to type I fibres. Importantly, the protein expression of PLIN2, PLIN3 and PLIN5 was unaltered by exercise or recovery in either region in both the CHO and H_2O conditions ($P > 0.05$, Fig 6.5 & 6.6). However, there were regional differences in PLIN protein expression, with the central region having greater PLIN content compared to the peripheral region ($P < 0.05$, Table 6.3, Fig 6.5 & 6.6). As well as overall protein content, we examined the co-localisation of PLIN proteins and LD by expressing the number of overlapping objects relative to the total number of PLIN proteins present. Further to this, we examined the number of LD's that either had PLIN (PLIN+ LD), or did not have PLIN associated (PLIN- LD) and also quantified free PLIN (as described previously, Shepherd *et al,* 2013, 2017). The results of these analyses are detailed below.

Table 6.3. Relative distribution of PLIN proteins between subcellular regions in type I fibres.

		% of PLIN					
		PLIN2		PLIN3		PLIN5	
		Peripheral	Central*	Peripheral	Central*	Peripheral	Central*
Pre		13 ± 3	87 ± 9	9 ± 2	91 ± 9	12 ± 1	88 ± 1
Post	CHO	13 ± 3	87 ± 3	10 ± 2	90 ± 2	12 ± 3	88 ± 2
	Water	12 ± 2	88 ± 2	12 ± 3	88 ± 3	25 ± 2	75 ± 2
Post 4 h	CHO	13 ± 2	87 ± 2	11 ± 2	90 ± 1	8 ± 1	92 ± 1
	Water	11 ± 2	75 ± 8	11 ± 2	74 ± 9	19 ± 3	81 ± 4
Post 24 h	CHO	13 ± 2	87 ± 2	11 ± 2	90 ± 2	8 ± 14	92 ± 1
	Water	10 ± 2	78 ± 9	9 ± 2	78 ± 9	19 ± 3	81 ± 3

Data are means $\pm$ SD. * Significant effect of region across all time points ($P < 0.05$).
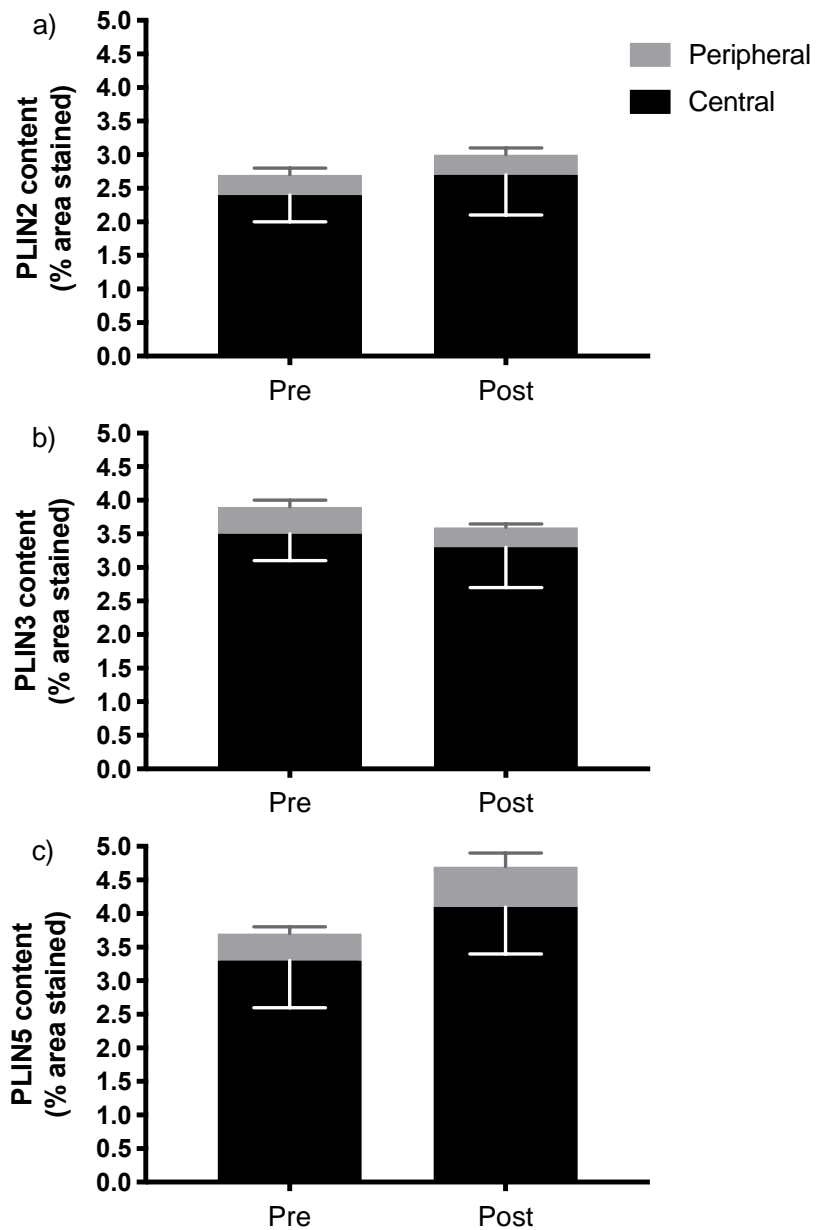
Figure 6.5. PLIN protein expression in response to exercise.

No significant changes in overall PLIN2 (a), PLIN3 (b) and PLIN5 (c) content in response to exercise ($P > 0.05$). Values are means ± SD
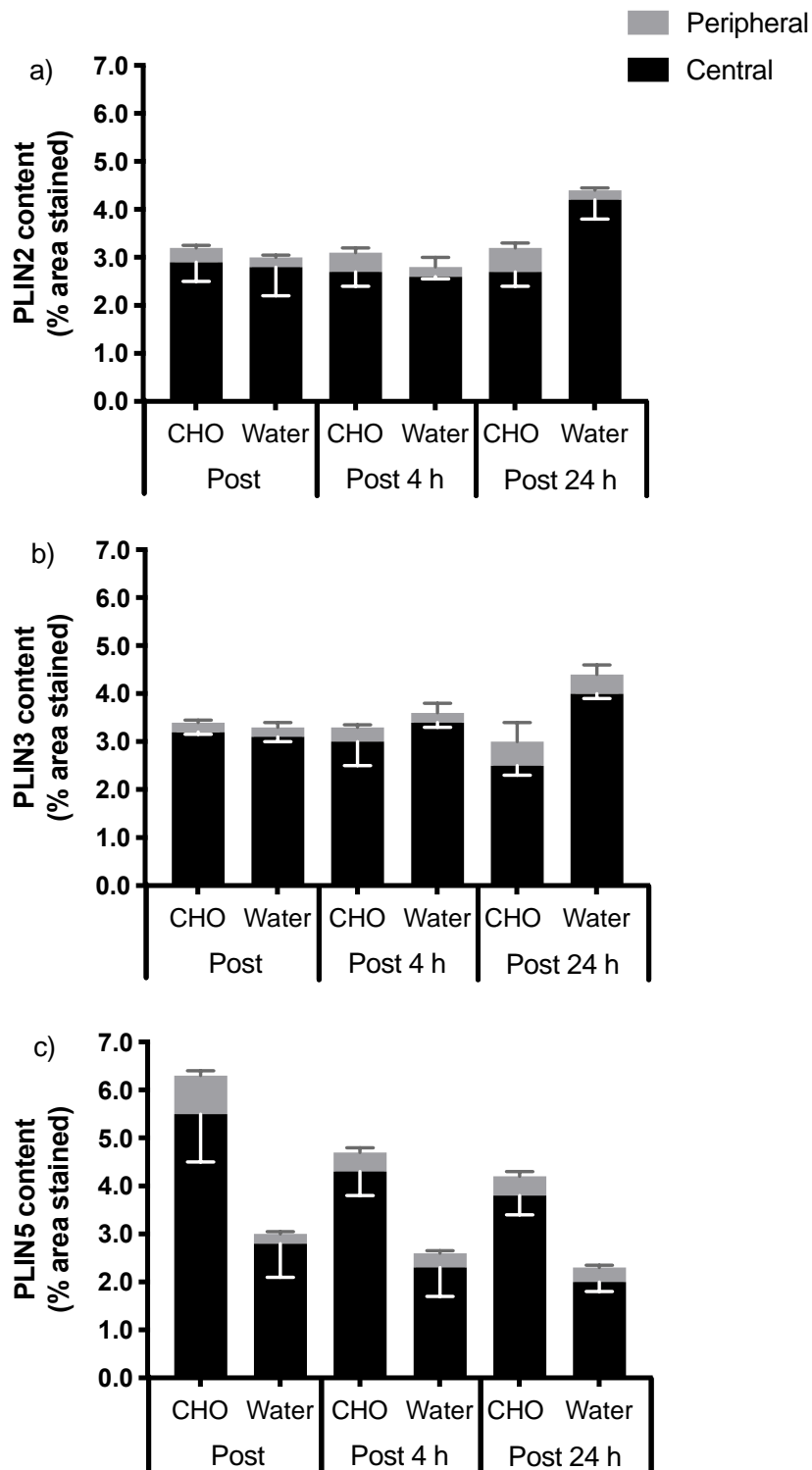
Figure 6.6. PLIN protein expression content during recovery in type I fibres.

No significant changes in overall PLIN2 (a), PLIN3 (b) and PLIN5 (c) content during recovery in either experimental condition ($P > 0.05$). Values are means ± SD.

Effect of exercise on PLIN protein and LD co-localisation

Exercise induced a 62% decrease in the fraction of PLIN2 co-localised with IMTG from pre to post-exercise within the central region (time x region interaction; $P < 0.05$, Table 6.4), although post-hoc analysis revealed that there was also a trend for a decrease of 21% within the peripheral region ($P = 0.060$). Exercise reduced the number of PLIN2+ LD in both the peripheral (-27%; $P = 0.006$) and central region (-71%, $P = 0.001$, Fig. 6.7a). Further to this, the number of PLIN2- LD was also significantly reduced by exercise, which again occurred within both the peripheral (-36%, $P = 0.003$) and central region (-82%, $P < 0.001$, Fig. 6.7b). Free PLIN2 increased by 36% from pre to post-exercise (Pre exercise 0.024 ± 0.005, post-exercise 0.034 ± 0.005, $P = 0.012$).

When examining PLIN3, exercise caused a significant decrease in the fraction of PLIN3 co-localised with LD's within the central region only (-51%, time x region interaction; $P < 0.05$, Table 6.4). Accordingly, the number of PLIN3+ LD's significantly decreased by 67% from pre to post-exercise (main effect of time; $P < 0.001$, Fig. 6.7c). The number of PLIN3- LD's were also reduced by exercise, with a decrease of 56% in the central region and 30% in the peripheral region, specific to the CHO condition (main effect of time; $P = 0.004$, Fig. 6.7d). Free PLIN3 was unaffected by exercise (pre exercise 0.032 ± 0.004, post-exercise 0.031 ± 0.006, $P = 0.699$).

The fraction of PLIN5 co-localised with LD decreased significantly in response to exercise in the central region only (-58%, time x region interaction; $P < 0.001$,

Table 6.4). The number of PLIN5+ LD's decreased by 38% in response to exercise (main effect of time; P = 0.007, Fig. 6.7e), and there tended to be a decrease in the number of PLIN5- LD's (P = 0.071, Fig. 6.7f). Free PLIN5 increased by 20% from pre to post exercise (pre exercise 0.034 $\pm$ 0.004, post-exercise 0.041 $\pm$ 0.006, P = 0.021).

Table 6.4. Changes in PLIN co-localisation with lipid droplets between subcellular regions in response to exercise in type I fibres.

Time Point	Region	PLIN2	PLIN3	PLIN5
Pre	Peripheral	0.61 ± 0.12	0.57 ± 0.06	0.53 ± 0.09
	Central	0.64 ± 0.11	0.53 ± 0.09	0.64 ± 0.10
Post	Peripheral	0.48 ± 0.20	0.51 ± 0.12	0.50 ± 0.17
	Central	0.24 ± 0.15*	0.26 ± 0.12*	0.27 ± 0.09*

Data are means ± SD. * Significant decreases from pre to post-exercise ($P < 0.05$).
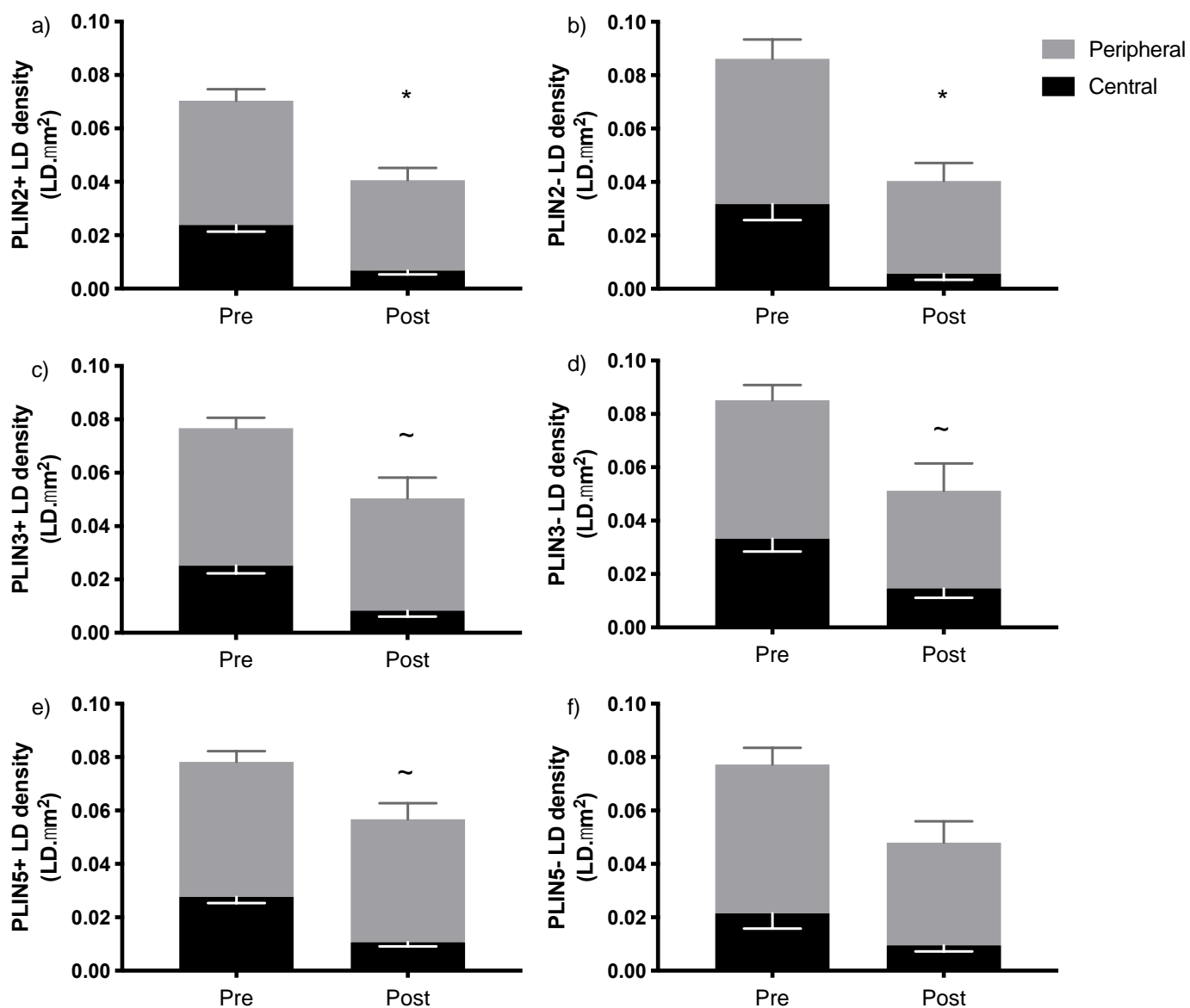
Figure 6.7. Subcellular-specific changes in the number of PLIN+ and PLIN- LDs in type I fibres in response to prolonged exercise.

The effect of exercise on a) PLIN2+ LD, b) PLIN2- LD, c) PLIN3+ LD, d) PLIN3- LD, e) PLIN5+ LD and f) PLIN5- LD. *Significant decrease in PLIN2+ LD and PLIN2- LD in both peripheral and central regions (time x region interaction effect, $P < 0.05$). #Significant decrease in PLIN3+ LD, PLIN3- LD and PLIN5+ LD in response to exercise (main effect of time, $P < 0.05$). Values are means ± SD.

The fraction of PLIN2 co-localised with LD significantly increased throughout recovery, specifically within the central region by 58% from post-exercise to 24 h post-exercise (time x region interaction; $P < 0.001$, Table 6.5). When considering condition, the increased co-localisation between PLIN2 and LD's occurred primarily in the H_2O condition from post-exercise to 24 h post-exercise (time x condition interaction; $P = 0.001$). PLIN2+ LD's increased throughout the recovery period in the central region only from post-exercise to 24 h post exercise (time x region interaction; $P = 0.001$, Fig. 6.8a). Overall the number of PLIN2+ LD's was 63% greater in the peripheral region compared to the central region across all time points (main effect of region; $P < 0.05$). On the other hand, PLIN2- LD's were unchanged during recovery ($P = 0.611$) and did not differ between conditions ($P = 0.940$). Though when considering region, the number of PLIN2- LD were greater in the peripheral region throughout recovery (main effect of region; $P < 0.05$, Fig. 6.8b). Free PLIN2 was unaffected throughout the recovery period in both conditions (post-exercise 0.032 ± 0.005, post 4 h 0.025 ± 0.005, post 24 h 0.026 ± 0.005, $P = 0.699$).

The fraction of PLIN3 co-localised with LD's increased throughout recovery (Table 6.5) in the central region by 49% from post to 24 h post-exercise (time x region interaction; $P < 0.05$). The number of PLIN3+ LD's increased by 63% from post to 24 h post exercise in the central region ($P = 0.014$), whereas in the peripheral region there was no significant difference from post to 24 h post-

exercise ($P = 0.597$, Fig. 6.8c). In addition, there was a significant difference between regions (main effect of region; $P < 0.05$) with the number of PLIN3+ LDs being ~23% greater in the peripheral region than the central region throughout recovery. Condition had no effect on PLIN3+ LD's during recovery ($P = 0.296$). The number of PLIN3- LD's was significantly different between conditions post-exercise, with the H_2O condition having 68% more PLIN3- LD's than the CHO condition ($P = 0.039$). Overall though, the number of PLIN3- LD did not change during recovery ($P = 0.259$, Fig. 6.8d). When examining region, the number of PLIN3- LD's was greater in the central region compared to the peripheral region throughout recovery ($P < 0.05$). Free PLIN3 was unchanged throughout the recovery period (post-exercise 0.032 ± 0.006, post 4 h 0.034 ± 0.005, post 24 h 0.033 ± 0.004, $P = 0.787$).

The fraction of PLIN5 co-localised with LD's increased significantly in the central region only from post to 24 h post exercise (59%, $P < 0.05$), though was unaffected by condition ($P = 0.167$). There was a significant increase in the number of PLIN5+ LD's in the central region from post to 24 h post-exercise (62%, $P = 0.002$), and in the peripheral region but only from post to 4 h post exercise (20%, $P = 0.016$, Fig. 6.8e). On the other hand, the number of PLIN5- LD's were unchanged during recovery ($P = 0.780$), though PLIN5- LD's were significantly greater in the peripheral region than in the central ($P < 0.05$, Fig. 6.8f). Free PLIN5 decreases significantly throughout recovery (post-exercise 0.041 ± 0.006, post 4 h 0.033 ± 0.004, post 24 h 0.027 ± 0.003, $P = 0.008$).
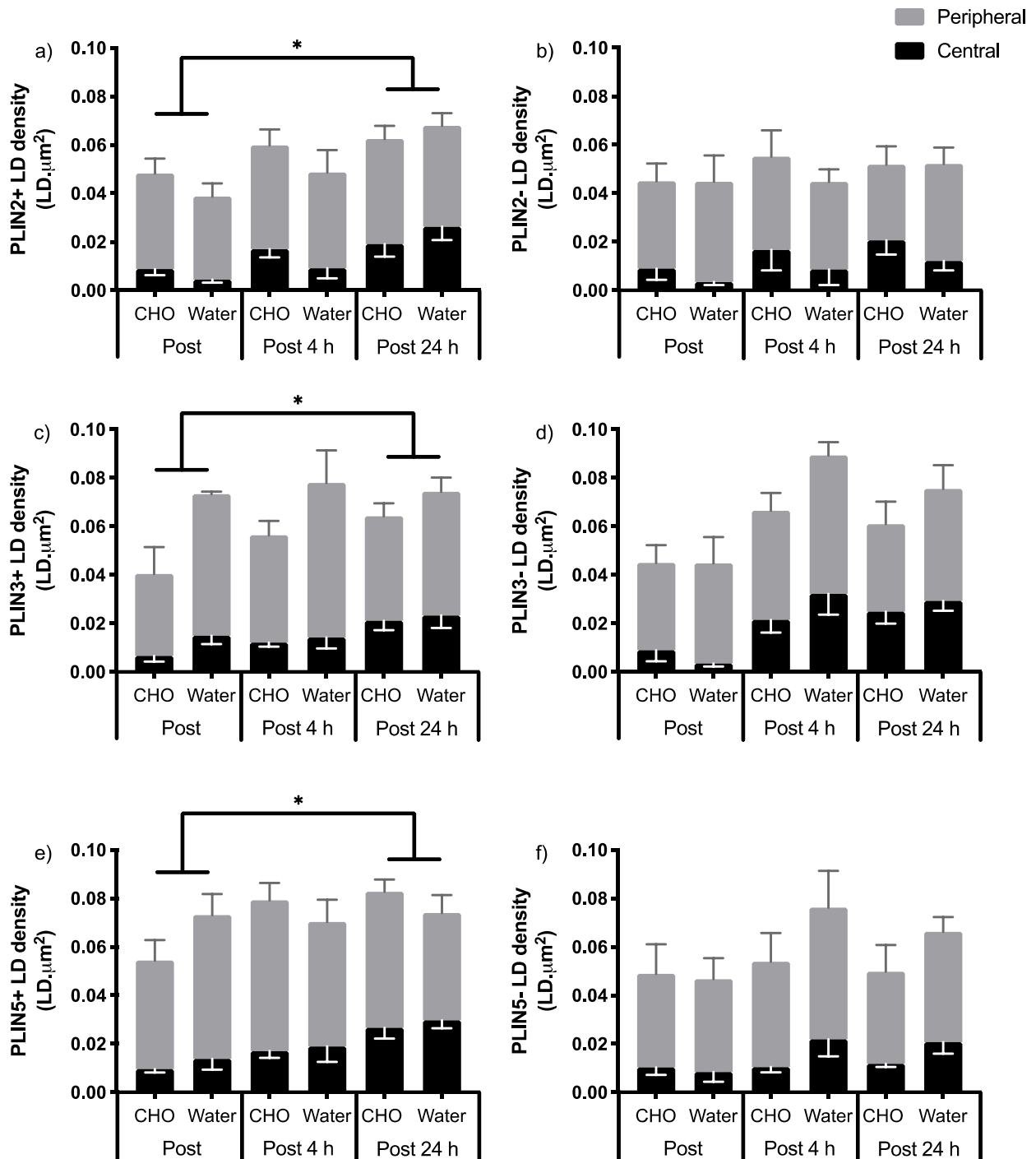
Figure 6.8. Subcellular-specific changes in the number of PLIN+ and PLIN- LDs in type I fibres during recovery from prolonged exercise.

The effect of recovery on a) PLIN2+ LD, b) PLIN2- LD, c) PLIN3+ LD, d) PLIN3-LD, e) PLIN5+ LD and f) PLIN5- LD. *Significant increase during recovery from post-exercise to 24 h post-exercise ($P < 0.05$) with no difference between conditions. Values are means ± SD.

Table 6.5. Changes in PLIN co-localisation with lipid droplets between subcellular regions during recovery in type I fibres.

Time Point	Condition	Region	PLIN2	PLIN3	PLIN5
Post	CHO	Peripheral	0.58 ± 0.22	0.53 ± 0.19	0.42 ± 0.24
		Central	0.31 ± 0.17	0.26 ± 0.09	0.23 ± 0.12
	H_2O	Peripheral	0.46 ± 0.08	0.49 ± 0.06	0.53 ± 0.06
		Central	0.22 ± 0.11	0.36 ± 0.07	0.23 ± 0.07
Post 4 h	CHO	Peripheral	0.71 ± 0.13	0.54 ± 0.07	0.47 ± 0.23
		Central	0.48 ± 0.16	0.35 ± 0.08	0.40 ± 0.20
	H_2O	Peripheral	0.49 ± 0.22	0.62 ± 0.12	0.54 ± 0.11
		Central	0.33 ± 0.26	0.45 ± 0.24	0.41 ± 0.21
Post 24 h	CHO	Peripheral	0.62 ± 0.17	0.58 ± 0.06	0.48 ± 0.22
		Central	0.57 ± 0.21	$0.49 \pm 0.16^*$	$0.58 \pm 0.25^*$
	H_2O	Peripheral	0.62 ± 0.17	0.56 ± 0.08	0.49 ± 0.06
		Central	$0.54 \pm 0.21^*$	$0.50 \pm 0.11^*$	$0.57 \pm 0.21^*$

Data are means $\pm$ SD. * Significant increases from post-exercise ($P < 0.05$).

6.5 Discussion

The present study aimed to investigate the effect of acute CHO restriction on IMTG resynthesis following prolonged exercise, and at the same time explore the dynamic behaviour of LDs and PLIN proteins in order to further clarify the role of these proteins in skeletal muscle. We report for the first time that IMTG resynthesis occurs rapidly in the central region of type I fibres during the first 4 h of recovery following prolonged exercise in highly-trained individuals. With regards to the PLIN proteins, two novel observations were made: 1) during prolonged exercise LD's that had both PLIN associated (PLIN+ LD's) or not associated (PLIN- LD's) were reduced, and 2) during recovery from prolonged exercise only the number of PLIN+ LD's were increased at 24 h post-exercise. Given that significant IMTG resynthesis was apparent by 4 h post-exercise, these data together indicate that the PLIN proteins do not play a key role in post-exercise IMTG resynthesis, but are instead re-distributed to the newly-expanded LD pool during recovery.

In order to investigate post-exercise IMTG resynthesis, we first aimed to reduce IMTG content using 4 h moderate-intensity cycling. As expected, this exercise bout led to a substantial decrease in IMTG content specific to type I fibres, in line with other studies which have also investigated IMTG utilisation using cycling protocols lasting ≥3 h (Van Loon *et al,* 2003; Stellingwerff *et al,* 2006). Moreover, the decrease in IMTG content occurred within the central region of the cell primarily due to a reduction in LD number. This is in line with a recent study employing TEM to demonstrate decreases in LD volume fraction and LD number, but not LD size, in the IMF region of muscle fibres in the arms, but not legs, of elite cross-country skiers in response to 1 h of exhaustive exercise (Koh *et al,* 2017). This is also in agreement with data showing a 40%

decrease in IMF lipid content following 1 h of moderate intensity cycling exercise, whilst SS lipid content did not change (Chee *et al*, 2016). Our data now extend the observed preferential utilisation of the IMF IMTG pool to prolonged cycling, and highlight the capacity for immunofluorescence microscopy-based analysis to detect changes in IMTG content in specific subcellular compartments.

In the present study, we aimed to identify if restricting CHO in the post-exercise recovery period would augment the rate of IMTG resynthesis. On first inspection, the data revealed that the rate of IMTG resynthesis was greatest when only H_2O, and not CHO, was ingested during the first 4 h of recovery from prolonged exercise. This was expected, since CHO ingestion would increase circulating insulin concentrations thereby inhibit systemic lipolysis and reducing free fatty acid availability to the muscle. However, it is important to state that there was a significant difference in post-exercise IMTG content between conditions, despite the experimental treatment only being implemented in the post-exercise period. Since, in this case, the starting IMTG values are different between groups, this precludes our ability to draw a firm conclusion as to whether acute CHO restriction can truly accelerate IMTG resynthesis. In this regard, it should be noted that in the study by Gejl *et al.* (2016) from which these muscle samples were derived, a small, albeit non-significant, difference in glycogen utilisation was observed in the CHO condition (527 mmol/kg dw, 73% reduction) compared to the H_2O condition (421 mmol/kg dw, 63% reduction). Further to this, Gejl *et al.* (2016) also noted a slightly greater exercise intensity in the CHO condition (74% vs 71% HR_{max} in the H_2O condition), although again this was not a significant difference. We believe that the combination of the small differences in exercise intensity and glycogen utilisation between the groups may explain, at least partly, the lower IMTG utilisation

within the CHO condition in the present study. However, despite the differences in IMTG content between conditions at the post-exercise time point, we did observe an increase in IMTG content during the first 4 h of recovery from prolonged exercise independent of experimental group. Importantly, this increase in IMTG content was sustained, but not improved on, at 24 h post-exercise. Furthermore, IMTG content at 24 h post-exercise had returned to baseline levels. Thus together, these data demonstrate that IMTG resynthesis occurs quickly following exercise, at least in highly-trained individuals. Furthermore, this time-course of IMTG resynthesis is the first of its kind to be described in the literature, and importantly provides a dynamic model of IMTG utilisation during exercise and post-exercise resynthesis that can be used to investigate the potential mechanisms underpinning these process.

When investigating changes in IMTG content during the recovery period in more detail, we observed that the increase in IMTG content occurred specifically in type I fibres and within the central region of the fibre. Therefore, not only are intermyofibrillar LDs targeted for breakdown during exercise, we now report for the first time that this subcellular region is an important site for IMTG resynthesis in the post-exercise period. Corresponding to the exercise-induced decreases in LD number, the post-exercise resynthesis of IMTG was driven by increases in LD number rather than LD size. This could be considered to be an advantage as an increase in LD number would provide a greater LD surface area available for the interaction of lipolytic enzymes and regulatory proteins (i.e. PLIN proteins) with IMTG.

Both IMTG content and PLIN protein expression exhibit a fibre-specific distribution, and therefore are closely related such that PLIN2, PLIN3 and PLIN5 content is directly

associated with IMTG content, at least under resting conditions (Amati *et al,* 2011; Minnaard *et al,* 2009; Peters *et al,* 2012; Shepherd *et al,* 2013). By employing subcellular-specific analysis, we are now able to demonstrate an apparent uncoupling of this relationship, since IMTG content is greatest in the peripheral region of the fibre, whereas the PLIN proteins are expressed to a greater extent in the central region of the cell. Importantly though, when considering the relative distribution, the majority of IMTG and PLIN proteins are observed in the central region. This would support the hypothesis that the PLIN proteins play a key role in the utilisation and resynthesis of the IMTG pool, given that changes in IMTG content during exercise and recovery were specific to the central region. Critically, we observed changes in IMTG content during exercise that occurred in the absence of changes in PLIN protein expression, which is in line with previous research (Shepherd *et al,* 2012, 2013), and we extend this observation to the post-exercise recovery period too. This provided the basis to investigate changes in the LD distribution of each PLIN protein under the dynamic state of exercise and recovery in order to further understand the role of these proteins within skeletal muscle.

As reported previously, exercise reduced the number of PLIN2+ LDs and PLIN5+ LDs (Shepherd *et al,* 2012, 2013), and we now report that the number of PLIN3+ LDs also decreases in response to exercise. However, in contrast to our previous studies demonstrating preferential use of PLIN+ LDs in response to 1 h of exercise (Shepherd *et al,* 2012, 2013), we also observed an exercise-induced decrease in the number of PLIN2- and PLIN3- LDs, and PLIN5- LDs also tended to decline. This is likely due to the more prolonged bout of exercise (4 h) employed here than in our previous studies (1 h) (Shepherd *et al,* 2012, 2013), combined with the elite level endurance-trained

population studied who notoriously exhibit high rates of IMTG utilisation during exercise (Stellingwerff *et al,* 2007; Rodriguez *et al,* 2009). Given the decrease in PLIN2+ and PLIN5+ LDs during exercise, combined with no change in PLIN2 and PLIN5 protein expression, it was no surprise to observe an increase in the quantity of (free) PLIN2 and PLIN5 not bound to LDs following exercise. In contrast, the quantity of PLIN3 not bound to LDs was unchanged in response to exercise. Studies in cultured non-muscle cells have demonstrated that PLIN3 is recruited from the cytosolic fraction to LDs upon lipid-loading (Skinner *et al,* 2009; Wolins *et al,* 2001, 2005), suggesting that PLIN3 cycles between the cytosol and LD pool depending on the metabolic state of the cell. Our data now indicates that this 'cycling' may be an important function of PLIN3 to support IMTG utilisation during exercise. In our model, we speculate that PLIN3 may cycle from each LD that is used and be recruited to a PLIN3- LD (and possibly PLIN2- and PLIN5- LDs) to subsequently support continued breakdown of the IMTG pool during exercise.

During recovery, we observed an increase in PLIN and LD co-localisation for all PLIN proteins within the central region of type I fibres at 24 h post-exercise. Consequently, the number of PLIN2+, PLIN3+ and PLIN5+ LDs all increased during recovery, but there was no change in the number of PLIN- LDs. Given that there was no change in the expression of the PLIN proteins during recovery, these data suggest that the pre-existing PLIN protein pool was redistributed across the expanded LD pool during recovery (Figure 6.9). This corroborates previous studies reporting a redistribution of the PLIN proteins in response to prolonged fasting (Gemmink *et al,* 2016) or a lipid infusion (Shepherd *et al,* 2017). In order to determine the location from which the redistributed PLIN proteins originated, it is important to not only consider LDs either

labelled with PLIN or not, but also the cytosolic pool of PLIN proteins. In this regard, when examining the distribution of PLIN2 and PLIN3 throughout recovery increases in PLIN2+ and PLIN3+ LDs occurred in the absence of a change in the quantity of cytosolic PLIN2 or PLIN3. This suggests there is a redistribution of PLIN2 and PLIN3 from pre-existing PLIN2+ or PLIN3+ LD to either newly-synthesised LD and/or pre-existing PLIN- LDs (Figure 6.9). In contrast, PLIN5+ LDs were increased throughout the recovery period with a corresponding decrease in the quantity of cytosolic PLIN5. Therefore, unlike PLIN2 and PLIN3, it is the cytosolic pool of PLIN5 that is redistributed to either newly-synthesised LDs and/or pre-existing PLIN- LDs occurred during recovery (Figure 6.10), underpinning the increased fraction of LDs labelled with PLIN5 at 24 h post-exercise.
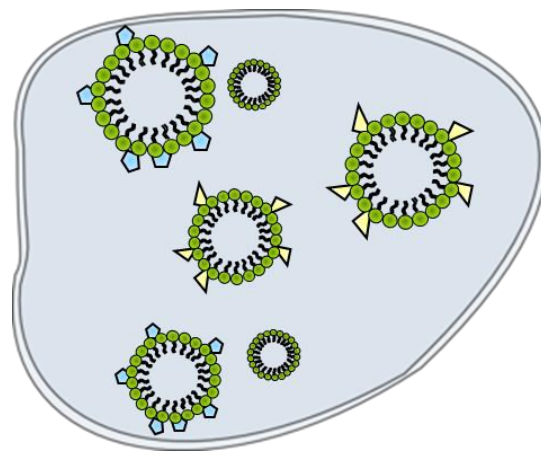
Post exercise PLIN+ and PLIN- LD for both PLIN2 and PLIN3.
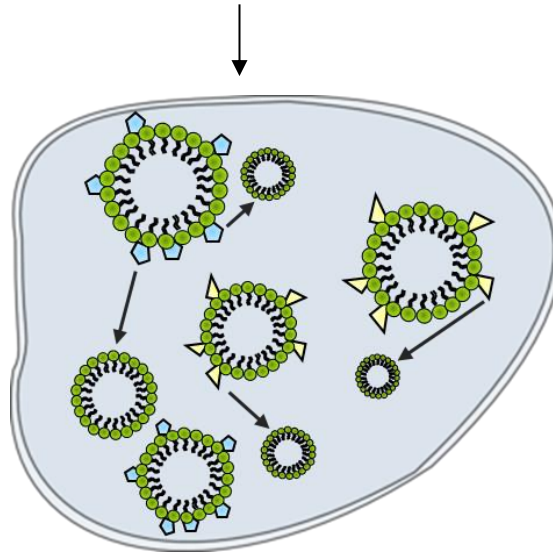
During recovery PLIN redistributes from PLIN+ LD to newly formed LD or previously existing PLIN- LD.
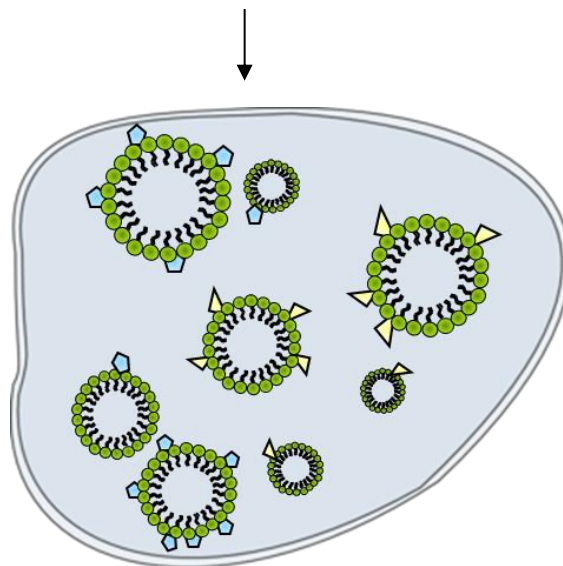
By 24 h post exercise, a greater amount of PLIN+ LD is present from this redistribution.

Figure 6.9. Schematic diagram of the redistribution of PLIN2 and PLIN3 to either newly-synthesised LD and/or pre-existing PLIN- LDs during recovery.
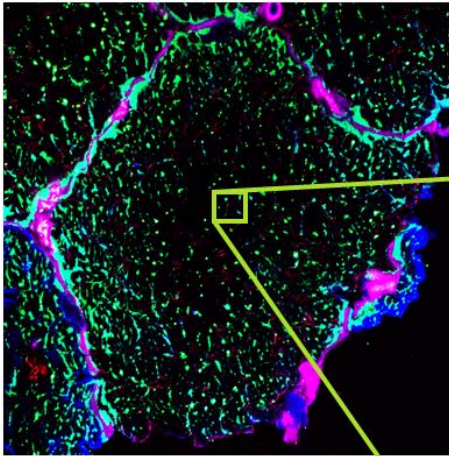
PLIN5- LD with free PLIN5 in the surrounding cytosol.
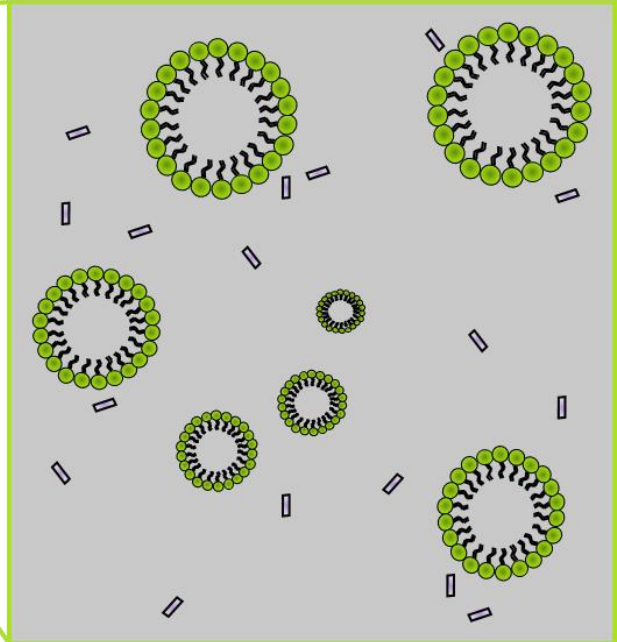
During recovery free PLIN5 in the cytosol decreases as they redistribute to newly synthesized or pre-existing PLIN5- LD.
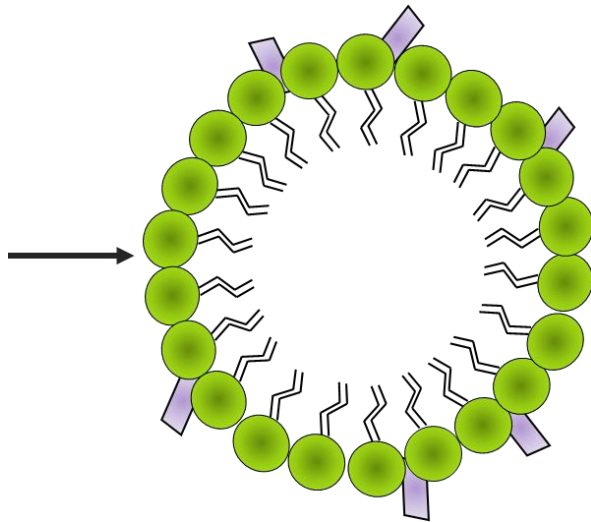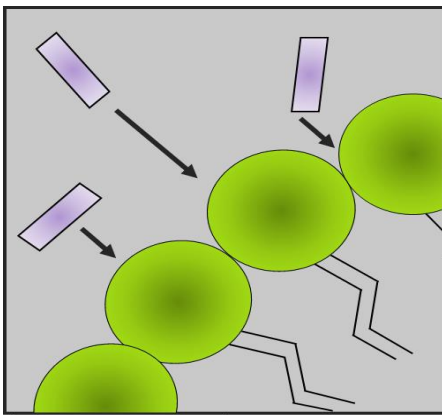
Due to this redistribution of free PLIN5 from the cytosol, by post 24 PLIN5+ LD has increased.

Figure 6.10. Schematic diagram of cytosolic pool of PLIN5 that is redistributed to either newly-synthesised LDs and/or pre-existing PLIN- LDs occurred during recovery.

Previous studies in cultured cells and rodent models have implicated the PLIN proteins in supporting FA incorporation into, and storage as, IMTG in LDs (Bosma *et al,* 2012, 2013; Kleinert *et al,* 2016; Laurens *et al,* 2016). The preferential increase in PLIN+ LDs observed during recovery would theoretically support this concept. However, by obtaining muscle samples at both 4 h and 24 h post-exercise we are able to report for the first time a separation in the time-course between growth of the IMTG pool (at 4 h post-exercise) and increases in coating of LDs with PLIN proteins (at 24 h post-exercise). This suggests that the PLIN proteins don't necessarily play a role in IMTG storage in LD's per se. Rather, the coverage of newly-synthesised LD with PLIN proteins at 24 h post-exercise may be an adaptive response to regulate mobilisation and oxidation of IMTG-derived free fatty acids depending on metabolic demand. In this respect, there is a large evidence-base generated in a number of cell types supporting a role for the PLIN proteins in restricting lipolysis under basal conditions (MacPherson *et al,* 2012). Both PLIN3 and PLIN5 may also play a role in IMTG oxidation. Under stimulated conditions, PLIN5 overexpression in cultured cells augments triacylglycerol hydrolysis and fat oxidation (Laurens *et al,* 2016), through recruitment of LDs to the mitochondrial network (Wang *et al,* 2011). We also recently reported that HSL is targeted to PLIN5+ LDs in response to exercise (Whytock *et al,* 2018). Whole-body fat oxidation (Covington *et al,* 2014) and *ex vivo* palmitate oxidation (Covington *et al,* 2014, 2015) are both positively associated with PLIN3 expression, and PLIN3 is expressed in the mitochondrial fraction of sedentary and endurance-trained rats (Ramos *et al,* 2015). Based on our data, we assert that a redistribution of the PLIN proteins in the post-exercise period is an important adaptation to preserve the flexibility of the intramuscular LD pool to respond appropriately to changes in metabolic demand.

A strength of the present study is the use of validated immunofluorescence microscopy techniques to examine fibre-type specific changes in IMTG content and LD morphology, as well as the associations of PLIN proteins with LDs (Shepherd *et al,* 2012, 2013, 2017). However, the co-localisation assays only enable examination of the association between LDs and a single PLIN protein. A partial overlap between PLIN2 and PLIN5 has been recorded in rat skeletal muscle (MacPherson *et al,* 2012), and both PLIN2 and PLIN5 can be found on the same LD in human skeletal muscle (Gemmink *et al,* 2018). Thus, it is likely that LD's will have more than one PLIN protein associated with the LD surface, meaning that decreases in PLIN- LD we observed during exercise could actually be labelled with an alternative PLIN protein. Alternatively, the observed decrease in PLIN- LD's could be newly-formed LDs that have insufficient PLIN protein associated with the phospholipid monolayer to surpass the lower detection limit of the microscope. In the same context, objects quantified as free PLIN could also be small LDs which do not exceed the lower limits of detection, although it has been established, at least in cultured cells, that cytosolic pools (i.e. non-LD bound) of PLIN proteins do exist (Wolins *et al,* 2005). We also acknowledge that future work should determine whether PLIN4 plays a role in IMTG utilisation and/or resynthesis, given that PLIN4 is highly expressed, at least at the mRNA level, in skeletal muscle of healthy individuals (Pourteymour *et al,* 2015).

In conclusion, this study demonstrates that IMTG resynthesis occurs rapidly in the central region of type I fibres following prolonged exercise in highly-trained individuals. Whilst our previous report of LDs labelled with PLIN proteins being preferentially utilised (Shepherd *et al,* 2012, 2013) is not substantiated when exercise is >1 h in

duration, our data do highlight a novel role of PLIN3 in supporting IMTG utilisation. Moreover, during recovery from prolonged exercise the IMTG pool appears to first be resynthesized, after which PLIN2, PLIN3 and PLIN5 are redistributed to the newly-synthesised LD pool. Given the disparity in the time-course between growth of the IMTG pool and coating of LDs with PLIN proteins, our data do not support a role for the PLIN proteins in mediating IMTG resynthesis.

Chapter 7 – General Discussion

7.1 Overview

It is well-documented that nutritional status influences intramuscular substrate turnover, and to date, the main aim of the current CHO guidelines is to augment performance via sparing muscle glycogen, maintaining plasma glucose and CHO oxidation rates, followed by appropriate strategies to maximise glycogen replenishment following exercise (Burke *et al,* 2018). However, CHO is not the only fuel for exercise, particularly during moderate-intensity exercise where IMTG has been identified as a key fuel source (Van Loon, 2004). Despite this, the importance of post-exercise IMTG repletion to maintain endurance performance, particularly during periods where optimal performance is required on multiple consecutive days of competition has been somewhat overlooked. Overall, there is a lack of data on the post-exercise replenishment of IMTG and therefore, a lack of understanding of the mechanisms governing IMTG resynthesis following exercise. Further to this, substrate availability in muscle is dependent on 1) fibre type, with type I fibres containing three-fold greater lipid content than type II muscle fibres (Essen *et al,* 1975; Malenfant *et al,* 2001, Van Loon *et al,* 2003), and 2) the subcellular location of substrates within the muscle fibre. This has been demonstrated to be important in the context of storage and utilisation during exercise (Ørtenblad & Nielsen, 2015). Microscopy methods can be used to examine both on a fibre and subcellular-specific basis, though the level of agreement between different microscopy methods was not known. Initially this thesis aimed to assess both muscle glycogen and lipid utilisation during two field-based training sessions (that differ by exercise intensity) typical of middle-to-long distance runners. Both confocal immunofluorescence microscopy and TEM were then used to investigate exercise-induced changes in muscle lipids within a competitive endurance event. Finally, as there is considerably more focus in literature to date on the effect of

CHO availability to support glycogen resynthesis post-exercise, the key mechanisms underpinning post-exercise IMTG resynthesis were investigated. Overall, this thesis provides an insight into the field-based demands of training and competition on fibre type and subcellular-specific substrate utilization, whilst also providing key insights into the regulatory mechanisms underpinning IMTG resynthesis.

7.2 Fibre and subcellular-specific substrate utilisation

From laboratory studies it is well-documented that CHO and lipid utilisation is dependent on exercise intensity and duration. With the rationale of aiming to understand more field-based CHO demands during training, Impey *et al,* (2020) recently investigated the utilisation of glycogen during different habitual run training sessions undertaken in a field-based training environment. Overall, they reported a greater utilisation of glycogen in the *gastrocnemius* in comparison to the *vastus lateralis*, and a greater glycogen requirement during prolonged moderate-intensity running compared to a shorter, interval running session. In chapter 4, this thesis now extends such findings examining field-based training substrate utilisation through the use of TEM. First, it was found that glycogen was preferentially utilised from the INTRA region in both type I and type II fibres. Furthermore, glycogen utilisation tended to be greater in type I compared to type II fibres. This was only during the 10-mile trial rather than the 8x800 trial. This is in agreement with previous research also reporting greater glycogen utilisation in type I compared to type II fibres during exercise (Gollnick *et al,* 1973; 1974; Stellingwerff *et al,* 2007; Branth *et al,* 2009; Jensen *et al,* 2020). Further to this, our findings of less glycogen utilisation in the 8x800 trial is in line with whole

muscle homogenate data from Impey *et al,* (2020), demonstrating a lesser requirement for glycogen in the shorter, interval running session.

The preferential utilisation of glycogen in the INTRA region is in line with previous research in moderately or well-trained subjects during either prolonged cycling or cross-country ski racing (Marchand *et al,* 2007; Nielsen *et al,* 2011). However, our data extends such findings to two different exercise intensities and two different muscles. In this regard, we show that INTRA glycogen utilisation in the gastrocnemius was similar between exercise trials, whereas INTRA glycogen utilisation in the vastus lateralis was greater in the 8x800 trial compared to the 10-mile trial. An explanation for the differences in muscle here stems from mechanistic investigations identifying a link between INTRA glycogen and SR Ca^{2+} release in skinned rat muscle fibres (Nielsen *et al,* 2009), isolated human SR vesicles (Ørtenblad *et al,* 2011) and intact mouse muscle fibres (Nielsen *et al,* 2014). Specifically, it seems INTRA glycogen likely has a key role in energy provision for muscle contraction and the high intensity nature of the 8x800 trial (compared to the 10-mile trial) requires recruitment of a greater total muscle mass in the legs, which would in-turn require greater rates of SR Ca^{2+} release to support the high frequency of muscle contraction. Therefore, our data alongside previous literature supports the concept of the relationship between glycogen and muscular fatigue, likely originating through a connection between the INTRA glycogen store and sarcoplasmic reticulum (SR) Ca^{2+} release (Ørtenblad *et al,* 2011; Nielsen *et al,* 2014).

Similar to glycogen, IMTG-containing LD are also distributed on a fibre and subcellular specific basis (Nielsen *et al,* 2010; Koh *et al,* 2017; 2018). It is now well known that

moderate-intensity exercise leads to a decrease in IMTG content specifically in type I fibres (Van Loon, 2004), and there is some evidence that IMF LDs are specifically reduced (Chee *et al,* 206; Koh *et al,* 2017). In chapter 4, we observed lipid utilisation in both exercise trials, with a 51% reduction in LD volume fraction following the 10-mile trial and a smaller reduction of 22% following the 8x800 trial. In the 10-mile trial, this was specifically from the IMF region in type I fibres, although there also tended to be a reduction in IMF LD volume fraction in type II fibres. In the SS region, there was no significant reductions in LD volume fraction in response to exercise. Further to this, in chapter 6, 4 h moderate-intensity cycling bout led to reductions in IMTG content specific to type I fibres specifically from the central region of the cell. This supports the concept of there being a compartmentalised energy demand for lipid utilisation in skeletal muscle. Considering the location of LD in close proximity to the mitochondria, therefore supporting ATP production for the contracting myofibrils (Hood, 2001), this explains why IMF LD may be preferentially used over SS LD during exercise. Our data from chapter 4 using recreationally trained runners and also our data from chapter 6 using elite male triathletes, supports other data collected in a field-based environment, where elite cross-country skiers who completed a time trial demonstrated reductions in IMF lipid, although this was specific to the triceps brachii (Koh *et al,* 2017). Further to this, young subjects who completed 1 h moderate-intensity cycling bout also lead to specific reductions in IMF LD with no change in SS lipid (Chee *et al,* 2016). Together, these data suggest that, at least in healthy individuals, there is a preferential utilisation of IMF lipid during exercise. As such, Chee *et al,* (2016) did not observe a decrease in IMF lipids during exercise in older lean active and older overweight inactive individuals. In addition to this preferential use of IMF lipid in healthy individuals, in chapter 6 we also investigated changes in IMTG content during

recovery, where we observed that the increase in IMTG content occurred specifically in type I fibres and within the central region of the fibre. Therefore, not only are IMF LDs targeted for breakdown during exercise, we can now report for the first time that this subcellular pool of lipid is an important site for IMTG resynthesis in the post-exercise period.

7.3 Lipid droplet morphology and exercise

LDs are known to be distributed between myofibrils as IMF LD or just below the surface membrane as SS LD, both of which are closely associated with muscle mitochondria (Tarnopolsky *et al,* 2007; Shaw *et al,* 2008; Koh *et al,* 2018). Given their location between the myofibrils, IMF LD are likely to be an important energy source to support muscle contraction, an assertion based on reductions in the LD pool during exercise (Chee *et al,* 2016; Koh *et al,* 2017). Reductions in IMF LD volume fraction (or central IMTG content, when determined using immunofluorescence microscopy) can occur via changes in LD number and/or LD size. The size, number and location of LD is heavily influenced by metabolic state and exercise training (Nielsen *et al,* 2010, 2017; Chee *et al,* 2016; Koh *et al,* 2018). In general, the diameter of LD in the muscle of healthy untrained individuals is ~ 500 nm (range 200-1400 nm), with enhanced LD number rather than size, driving the greater IMTG content in type I fibres (Nielsen *et al,* 2017). In chapter 5 the TEM data demonstrates the diameter of LD in highly-trained individuals was ~440 nm before exercise (range 420 – 460 nm), which is as expected to be smaller in highly-trained individuals. However, we also examined the size of individual LD area and observed that the frequency of LDs 100 nm^2 in size to be greater in the central compared to the peripheral region. Conversely, there was a

greater frequency of LDs 200 nm^2 in size in the peripheral compared to the central region. Measuring the frequency of LD across a range of sizes is likely to be more informative as having a large pool of smaller LD is proposed to be a metabolic advantage, due to overall greater surface area of LD providing greater availability for interaction between LD proteins and lipases. Moreover, considering the subcellular location of these LD will likely determine their role in cell function. Together, this suggests that considering the size of individual LDs is more informative than simply measuring average LD size.

In chapter 4, the utilisation of IMF lipid in type I fibres during the 10-mile trial can be attributed to reductions in LD size. This finding opposes other work attributing reductions in IMF lipid to reductions in LD number (Koh *et al,* 2017). However, we also observed a tendency for IMF LD number (but not LD size) to be reduced in response to high-intensity interval running (8x800 trial). Together, these data initially highlight an intriguing possibility that exercise that is of a higher intensity (8x800 trial in chapter 4, and 1 h competitive cross-country skiing time trial in Koh *et al*, 2017) may specifically result in a reduction in LD number, whereas moderate-intensity exercise (10-mile trial in chapter 4) may induce reductions in LD size. However, in chapter 5 the decrease in IMTG content in response to 1 h of a competitive cross-country skiing time trial was attributed to a reduction in both LD number and size, whereas in chapter 6 a decrease in LD number (but not size) was observed during 4 h of moderate-intensity. These contrasting observations could be related to the microscopy method used. Due to the greater magnification capabilities, TEM may be the preferred method to investigate LD morphology. Whereas immunofluorescence microscopy will allow a better estimate of

exercise-induced changes in IMTG content, due to the greater number of fibres that can be analysed.

It should also be considered that these contrasting observations could be related to training status, given that in chapter 4 the subjects were recreationally active, whereas in chapter 6 they were elite level athletes. What appears to be developing from the observations from this thesis, and previously published work, is that exercise-induced changes in LD morphology are at least dependent on exercise intensity, duration, and training status of the individuals being studied. A summary of acute exercise-induced changes in LD morphology of individuals on a subcellular-basis from this thesis and previous literature is presented in table 7.1.

The general belief is that small LDs have a greater surface area for the interaction of lipolytic enzymes with the IMTG substrate and regulatory proteins located on the LD surface (Bickel et al, 2009; Morales et al, 2017). Consequently, the frequency of very small LDs we observed in the central region in chapter 5 may be an adaptation to support the greater utilisation of IMF LDs during exercise reported in previous studies (Koh *et al,* 2017), and in this thesis (chapters 4, 5 and 6). Further to this, we would then speculate that the smaller LD's would be targeted for utilisation first, as they are highly abundant in both the central and peripheral regions of the cell (Chapter 5, Figure 4). However, by examining differences in the frequency of specific LDs (based on size), it seems that more moderately sized LD of 400 and 600 nm^2 were reduced from pre to post-exercise. A possible explanation for the smaller LDs not being preferentially targeted for breakdown could be that they are newly-formed or nascent LDs, and are therefore not yet labelled with the appropriate LD-associated PLIN protein isoforms.

This also supports the decrease in LD size we observed in chapter 4, with the possibility that LD that are larger in size have a greater circumference, therefore providing more space for docking sites for LD-associated proteins, such as the perilipin (PLIN) proteins and therefore increasing their likelihood to be utilised during exercise. However, it could be that the smaller LD (e.g. 100 and 200 nm^2) were targeted for breakdown during exercise, but concomitant decreases in the size of moderately-sized LD of 400 and 600 nm^2 meant that they shrunk to become LDs of 100 and 200 nm^2 in size. This would explain why no reduction in smaller-sized LD was observed.

Table 7.1. Summary of acute exercise-induced reductions of LD on a subcellular basis.

Reference/ Chapter	Participants and training status	Microscopy technique	Exercise protocol	Outcome	Conclusions
Chapter 4	11 male competitive and recreational runners	Transmission Electron Microscopy	10 mile steady state run or 8x800 high intensity intervals.	• 51% reduction in lipid from 10-mile trial, specific to type I fibres, IMF region. Tendency for a 12% reduction in IMF LD size. • 22% reduction in lipid from 8x800 trial. Attributed to a reduction in LD number in IMF (-5%) and SS (-35%) region.	• Lipid utilisation occurs primarily in the IMF region of type I fibres, but changes in LD morphology maybe related to exercise intensity and duration.
Chapter 5	10 elite male cross-country skiers	Immunofluorescence microscopy	~20km high-intensity cross-country skiing time trial.	• Reduction in IMTG content from both the central and peripheral regions in both type I and type II fibres. • Attributed to reductions in both LD number and size of 35% and 14%, respectively.	• ~1 hour of cross-country skiing reduced IMTG content in both type I and type IIa fibres, across both the peripheral and central regions of the muscle fibres due to a reduction in both LD size and number.
Chapter 6	14 elite male triathletes	Immunofluorescence microscopy	4 hr prolonged cycling bout at ~ 56% VO_{2max} with 4 h post-exercise recovery period.	• Reduction in IMTG content in type I fibres, central region, attributed to 46% reduction in LD number. • IMTG repletion specific to central region of type I fibres.	• IMTG resynthesis occurs rapidly in the central region of type I fibres following prolonged exercise in highly-trained individuals. • Highlight a novel role of PLIN3 in supporting IMTG utilisation.
Koh *et al*, 2017	10 elite male cross-country skiers	Transmission Electron Microscopy	~20 km high-intensity cross-country skiing time trial.	• Reduction in IMCL in arms (IMF region) but not legs. • Attributed to 36% reductions in LD number not size.	• Distributions of LD in the muscles of upper and lower limbs differ and LD utilisation differs depending on their subcellular location.
Chee *et al*, 2016	7 young and lean, 7 old and lean, 7 old overweight males	Transmission Electron Microscopy	Cycling at moderate intensity 50% VO_{2max} for 1 h	• Reduction in IMCL attributed to 28% reduction in LD number. • In the overweight/old group, LD size increased by 25% in both the SS and IMF region.	• Increased FA delivery causes increased IMTG in SS region in physically inactive older individuals.

When considering SS LD, they are considered as a supply for SS mitochondria, providing energy for membrane related processes (Hood, 2001). Ferreira *et al,* (2010) separated SS and IMF mitochondria to find proteomic differences and respiratory chain activity between the two subcellular pools of mitochondria. SS mitochondria specifically, had less oxidative phosphorylation proteins, and less activity of the respiratory chain complex than IMF mitochondria (Ferreira *et al,* 2010). This therefore, supports the concept of IMF mitochondria specialising in energy production for muscle contraction and supports the preferential use of IMF LD (or central) during energy demand in this thesis and previous literature (Chee *et al,* 2016; Koh *et al,* 2017). However, overall lipid content is often greater in the SS region (Nielsen *et al,* 2017; Koh *et al,* 2018) and even if training did not significantly change the overall SS or IMF LD volume fraction within muscle, training in general enhances LD number and reduces LD size in the SS region (Nielsen *et al,* 2017). Although the majority of changes observed across all three experimental chapters in this thesis were in IMF lipid, there was a tendency for a reduction in SS LD number in response to exercise in chapter 4. Alongside this slight decrease in LD number, there was also small (albeit non-significant) increases in LD size in both type I (6%) and type II (3%) fibres. These opposing changes in SS LD size and number may explain why there was no reduction in overall SS LD volume fraction. Koh *et al.* (2017) also observed reductions in the number of LD in the SS region, in the absence of a reduction in SS LD volume fraction. Therefore, exercise-induced decreases in SS LD number appear to be a consistent finding, although the importance of this is yet to be determined. It is possible that the close proximity of SS LD to nuclei means that this pool of LDs supports nuclear processes. Much of what is known to date about LD signalling to the nucleus relates to transcriptional regulation of mitochondrial biogenesis and FA oxidation. For

example, it is known that IMTG-derived fatty acids can act as ligands to support transcriptional processes, thereby supporting the adaptive response to exercise (Seibert *et al,* 2020). To reconcile the lack of a change in overall SS LD volume fraction we witnessed in chapter 4, it could be speculated that FA coming into the muscle during exercise may subsequently be directed to pre-existing SS LD, thereby resulting in small increases in LD size. Future work should aim to identify the roles that each LD pool play in cell function.

As discussed in section 2.2.2, both immunofluorescence microscopy and TEM provide methods to visualise and quantify IMTG utilisation and changes in LD morphology on a fibre-type and subcellular specific basis, though to date, no comparison between the two microscopy methods in quantifying IMTG utilisation has been made. In chapter 5, when examining the correlations between TEM and immunofluorescence microscopy, we observed significant correlations for IMTG content in both subcellular regions, though only a substantial agreement according to Lins Concordance coefficient (LCC) within the peripheral/SS region. In this chapter, we used a fixed 2 μm distance from the membrane to represent the SS region, which has been utilised previously to examine IMTG content in differing populations (Van Loon, 2004). Although this 2 μm distance could be considered representative of the SS region, this method does not take into account variations in the width of the SS region which are frequently observed when using TEM. However, the substantial agreement between the two methods we observed in chapter 5 (see table 5.3) strongly supports the use of a 2 μm band around the extracted cell membrane in order to define the peripheral region when using immunofluorescence microscopy. Thus, it does seem to be possible to use immunofluorescence microscopy to investigate changes in IMTG content and LDs at

a subcellular level. This has clear implications for investigating the subcellular distribution of proteins associated with LD.

7.4 Perilipin proteins

The LD coating PLIN proteins are believed to play a key role in LD turnover through the interaction with lipases such as ATGL, HSL and their co-activators (discussed in 2.3.4). PLIN2, PLIN3 and PLIN5 are the main PLINs present in human skeletal muscle (Gemmink *et al,* 2017). PLIN2 negatively regulates ATGL-mediated LD lipolysis by inhibiting ATGL access to the LD surface (Feng *et al,* 2017). PLIN3 coats nascent LD and its expression is associated with fat oxidation rates (Covington *et al,* 2015), and PLIN5 regulates lipolytic rate in an energy-dependent way to match LD FA release with mitochondrial FA oxidation (Gemmink *et al,* 2017). As outlined above, the general belief is that a greater number of small LDs can be seen as a training adaptation, since this leads to a greater surface area for the interaction of lipolytic enzymes with the IMTG substrate and regulatory proteins located on the LD surface, such as the PLIN proteins (Bickel *et al,* 2009; Morales *et al,* 2017). To this end, it is a known endurance training itself augments IMTG content simultaneous to increases in PLIN2, PLIN5 (Shaw *et al*, 2012; Shepherd *et al*, 2013) and PLIN3 expression (Shepherd *et al,* 2017). Our investigations in chapter 6 employing a subcellular-specific analysis, enable us to demonstrate that the majority of IMTG and PLIN proteins are observed in the central region of the cell. We also provided novel data to show that both exercise-induced reductions, and post-exercise increases in IMTG content were specific to the central region. These observations support the hypothesis that the PLIN proteins play a key role in the utilisation and resynthesis of the IMTG pool. The

changes we observed in IMTG content during exercise also occurred in the absence of changes in PLIN protein expression, which is in line with previous research (Shepherd *et al,* 2012, 2013), and we now extend this observation to the post-exercise recovery period too. Our study design provided a novel basis to investigate changes in the LD distribution of PLIN2, PLIN3 and PLIN5 under the dynamic state of exercise and recovery in order to further understand the role of these proteins within skeletal muscle.

Our data extends the findings of previous literature, which reported that exercise augments a reduction in the number of PLIN2+ LDs and PLIN5+ LDs (Shepherd *et al,* 2012, 2013) and now also the number of PLIN3+ LDs. However, the data from chapter 6 opposes previous work demonstrating preferential use of PLIN+ LDs in response to 1 h of exercise (Shepherd *et al,* 2012, 2013), since we also observed an exercise-induced decrease in the number of PLIN2- and PLIN3- LDs, and PLIN5- LDs also tended to decline. The likely explanation for this is the more prolonged bout of exercise (4 h) employed here than in previous studies (1 h) (Shepherd *et al,* 2012, 2013), combined with the elite level endurance-trained population studied who notoriously exhibit high rates of IMTG utilisation during exercise (Stellingwerff *et al,* 2007; Rodriguez *et al,* 2009). Further to this, given the reduction observed in PLIN2+ and PLIN5+ LDs during exercise, and no change in the overall PLIN2 and PLIN5 protein expression, it was no surprise to observe an increase in the quantity of (free) PLIN2 and PLIN5 not bound to LDs following exercise. However, this did not apply to free PLIN3, with no change in response to exercise being observed, despite the reduction in PLIN3+ LDs. A potential explanation for the lack of change in free PLIN3 that we observed stems from research in cultured non-muscle cells which have

demonstrated that PLIN3 is recruited from the cytosolic fraction to LDs upon lipid-loading (Skinner *et al,* 2009; Wolins *et al,* 2001, 2005), suggesting that PLIN3 cycles between the cytosol and LD pool depending on the metabolic state of the cell. Thus, our data could indicate that this 'cycling' of PLIN3 between the cytosol and LDs may be an important function of PLIN3 to support IMTG utilisation during exercise, and may only occur in highly-trained individuals. In our model, we speculate that PLIN3 may cycle from each LD that is used and be recruited to previously PLIN3- LD (and possibly PLIN2- and PLIN5- LDs) to subsequently support continued breakdown of the IMTG pool during exercise.

Previous research in cultured cells and rodent models have implicated the PLIN proteins in supporting fatty acid incorporation into, and storage as, IMTG in LDs (Bosma *et al,* 2012, 2013; Kleinert *et al,* 2016; Laurens *et al,* 2016). The preferential increase in PLIN+ LDs observed during recovery would theoretically support this concept. However, in chapter 6 we gained a novel insight into the time-course of recovery through obtaining muscle samples at both 4 h and 24 h post-exercise. This enabled us to separate the resynthesis of the IMTG pool (at 4 h post-exercise) and increases in coating of LDs with PLIN proteins (at 24 h post-exercise). The findings suggest that the PLIN proteins don't necessarily play a role in IMTG storage in LD's per se. Rather, the coverage of newly-synthesised LD with PLIN proteins at 24 h post-exercise may be an adaptive response to regulate mobilisation and oxidation of IMTG-derived free fatty acids depending on subsequent metabolic demand. Further to this, at this 24 h post-exercise time point, our results demonstrated increases in PLIN and LD co-localisation for all PLIN proteins were specific to the central region of type I fibres. Consequently, the number of PLIN2+, PLIN3+ and PLIN5+ LDs all increased

231

during recovery, but there was no change in the number of PLIN- LDs. Previous literature has suggested the PLIN proteins can re-distribute in response to prolonged fasting (Gemmink *et al,* 2016) or a lipid infusion (Shepherd *et al,* 2017). Our data, demonstrated no change in the expression of the PLIN proteins during recovery, therefore supporting the concept of pre-existing PLIN protein pool being redistributed across the expanded LD pool during the recovery period. Thereby extending the findings from previous literature to include the re-distribution of PLIN post-prolonged exercise in elite athletes. Further to this, to enable the location from which the redistributed PLIN proteins originated, it is important to consider both LDs labelled with PLIN and the cytosolic pool of 'free' PLIN proteins. To this extent, when examining the distribution of PLIN2 and PLIN3 throughout recovery increases in PLIN2+ and PLIN3+ LDs occurred in the absence of a change in the quantity of cytosolic PLIN2 or PLIN3. Thereby suggesting a redistribution of PLIN2 and PLIN3 from pre-existing PLIN2+ or PLIN3+ LD to either newly-synthesised LD and/or pre-existing PLIN- LDs. On the other hand, PLIN5+ LDs were increased throughout the recovery period with a corresponding decrease in the quantity of cytosolic PLIN5. Therefore, unlike PLIN2 and PLIN3, it is likely that the cytosolic pool of PLIN5 that is redistributed to either newly-synthesised LDs and/or pre-existing PLIN- LDs occurred during recovery, underpinning the increased fraction of LDs labelled with PLIN5 at 24 h post-exercise and suggesting that the PLIN proteins act uniquely during resynthesis.

7.5 Future research directions

In summary, this thesis highlights the interaction between muscle fibre recruitment, relative exercise intensity and training duration in modulating the subcellular specific-glycogen and lipid utilisation with specific field-based exercise protocols. We have

highlighted in chapter 4 and 5 that detailed analysis, investigating not only fibre type but subcellular-specific substrate utilisation can be conducted in field-based situations, representing either the training or racing environment. Future research should continue to consider if such approaches are possible, as this as a whole will make the research more applicable to the practice of individuals and/or athletes, that our data informs.

Whilst chapter 4 did highlight differences in intramuscular substrate utilisation dependent on exercise intensity and duration, one factor that was not considered in this thesis was the effect of sex. Indeed, in the original study from which the muscle samples used in chapter 4 were obtained (Impey *et al,* 2020), it was reported that females had reduced resting muscle glycogen concentrations and absolute glycogen utilisation during exercise when compared to males. In response to exercise, it seems females exhibit a lower respiratory exchange ratio, therefore leading to less reliance on CHO metabolism during sub-maximal steady state exercise (Carter *et al*, 2001; Roepstorff *et al,* 2002). Females are also known to have greater IMTG storage in comparison to males (Moro *et al,* 2009) and show greater IMTG utilisation under fasted conditions (Steffensen *et al,* 2002). However due to methodology used in such literature (muscle homogenates or tracers), there is a lack of data on a fibre-type or subcellular basis. As we know subcellular location of glycogen is vastly important, investigations could consider which subcellular regions these gender differences lie.

The field-based theme to this thesis allows data to be more applicable to the habitual fuel utilisation of training and competition, however there are further factors that could be quantified by future research, for example in chapter 4 we examined both the

vastus lateralis and the *gastrocnemius* and found INTRA glycogen utilisation to be greater in the 8x800m trial compared to the 10-mile trial within the *vastus lateralis* only. Suggesting in the *vastus lateralis*, greater use of the INTRA glycogen pool appears to be required to meet the elevated metabolic demand during high intensity exercise. Though, other studies in running specifically, could gain further insight muscle-differences by measuring running style i.e. forefoot vs. heel-strike runners and muscle length in order to assess if these factors may alter the activation of the *vastus lateralis* and *gastrocnemius*, and therefore influence muscle-specific substrate utilisation.

The importance of being able to analyse substrate utilisation on a fibre and subcellular region-specific basis is also highlighted, therefore emphasising the importance of future research being able to use suitable methodology that enables analysis at this level. As such, when evaluating the agreement between immunofluorescence microscopy and TEM (Chapter 5), immunofluorescence microscopy appears to provide an economical option to quantify fibre-specific IMTG content but not necessarily LD size and number. However, the use of immunofluorescence microscopy in Chapter 6 provides valuable insight into the potential role of the PLIN proteins in skeletal muscle. Taken together, it could be suggested that immunofluorescence microscopy is most beneficial when research aims to understand the mechanisms regulating IMTG metabolism on a fibre-specific basis, such as, for example, investigations into proteins related to the regulation of LDs and IMTG turnover. However, research which aims to investigate LD morphology may benefit from using TEM, since the accuracy of LD size and number will be improved at greater magnifications.

Finally, a theme that runs throughout this thesis is the importance of IMTG during exercise, but in Chapter 6, although we were unsuccessful in determining whether CHO feeding immediately post-exercise (in line with current guidelines) would suppress IMTG resynthesis, we do highlight the importance of post-exercise IMTG resynthesis. More specifically, we demonstrate that despite their previously proposed role in the synthesis and storage of IMTG in LD (MacPherson *et al,* 2015; Morales *et al,* 2017), the PLIN proteins do not appear to play a key role in post-exercise IMTG resynthesis.

Based on the observations from the studies in this thesis, there are several potential areas of future research that have emerged, and which are outlined below:

1. Differences in LD morphology in response to exercise were evident throughout this thesis. It seems that a combination or exercise intensity, duration and training status of the individual will directly influence changes in LD morphology (summarised in table 1), though we clearly lack a complete understanding in which factors are most critical in determining changes in LD morphology. In the first instance, further investigations should be conducted to examine changes in LD morphology under more controlled conditions (i.e. within a laboratory) where exercise intensity and duration can be closely monitored. Subsequent studies could also consider how sex and training status influence these responses. Within these studies, a combination of immunofluorescence microscopy (to measure IMTG content) and TEM (to ensure the most accurate measures of both LD number and size) should be employed.

2. In chapter 4, we observed reductions in SS LD number despite no change in overall SS LD volume fraction, as also observed by Koh *et al,* (2017). A possible explanation for these independent observations is that alongside the significant decreases in SS LD number were small (albeit non-significant) increases in LD size, thereby resulting in no significant changes in LD volume fraction. If this is true, it could be that FA coming into the muscle during exercise may subsequently be directed to pre-existing SS LD, thereby resulting in small increases in LD size (rather than being used to create new LD). One possible approach to test this would be to use a pharmacological inhibitor of adipose tissue lipolysis (Acipimox) which would in turn inhibit FA coming into the muscle. As a result, and if the above hypothesis is true, this would preclude pre-existing LD from increasing in size (in comparison to a placebo control trial).

3. In chapter 5, we build on emerging data that LD of certain sizes may be targeted for breakdown during exercise, rather than the LD pool as a whole (which would manifest as a decrease in mean LD size). This adds to the current literature suggesting that LD are heterogenous in nature, and their function may be determined by their individual protein coat. In regard to such proteins, investigations into whether there is a difference in PLIN protein isoforms located on different subpopulations of LD i.e. IMF or SS LD, would enable insights into the specific function of these LD. Such investigations could be done by comparing individual LD size following acute exercise in combination with staining for PLIN proteins in trained individuals and untrained/sedentary and should consider advanced microscopes such as super-resolution microscopy as used by Gemmink *et al,* (2018; 2020). The advantage of using such a

microscope is being able to visualise and quantify the abundance of, and examine the distribution of key proteins such as PLIN or ATGL in individual organelles. As such Gemmink *et al,* (2018) demonstrated PLIN2 and PLIN5 to localise to distinct LD docking sites with greater PLIN5 at LD-mitochondria tethering sites.

4. In chapter 6, we observed IMTG utilisation from both PLIN+ and PLIN- LD following prolonged exercise, which differed from previous literature demonstrating utilisation of PLIN+ LD after 1 h of exercise (Shepherd *et al,* 2012, 2013). In this respect, Watt *et al,* (2002) demonstrated IMTG utilisation to be greatest within the first 1 – 2 h of prolonged exercise, therefore it could be speculated that first PLIN+ LD were utilised, and then as exercise progressed PLIN- LD were targeted. As such, a time-course study, with biopsies obtained during (e.g. after 1 h), as well as before and after prolonged (i.e. 4 h) exercise should be considered in order to generate a more complete understanding of the pattern of PLIN+ and PLIN- LDs during exercise.

5. Further to point 4, another possible explanation for the utilisation on PLIN- LD could be the possibility of more than one PLIN protein being associated with one LD, as demonstrated in human skeletal muscle with PLIN2 and PLIN5 by Gemmink *et al* (2018). The development of an assay which would enable us to identify LD with more than one PLIN attached, would allow investigations into the utilisation of these PLIN+ LD, and would ultimately provide information indicating which PLIN proteins specifically are regulating the breakdown of LD.

7.6 Closing thoughts

In summary, this thesis has leveraged two forms of microscopy in order to generate novel data which first demonstrates a unique insight into fibre type and subcellular-specific substrate utilisation in field-based exercise settings. Specifically, running elicits a preferential use of INTRA glycogen during exercise, independent of intensity, and both running and cross-country skiing stimulate a breakdown of IMF LDs, primarily in type I fibres. Second, this thesis generates novel information concerning the potential role of the PLIN proteins in skeletal muscle, demonstrating that the coating of LDs with PLIN proteins is secondary to the resynthesis of the IMTG pool. This thesis expands our knowledge on the effect of exercise intensity and duration on substrate utilisation through investigations at a fibre and subcellular level, alongside deepening our understanding of the proposed role of PLIN proteins during IMTG breakdown and resynthesis. From a research perspective, it is hoped that this thesis will elicit further field-based studies examining substrate utilisation on a fibre and region-specific basis.

Chapter 8 – References

Achten J and Jeukendrup AE. Optimizing fat oxidation through exercise and diet. Nutrition 20: 716-727, 2004.

Alsted TJ, Ploug T, Prats C, Serup AK, Hoeg L, Schjerling P, Holm C, Zimmermann R, Fledelius C, Galbo H, Kiens B. Contraction-induced lipolysis is not impaired by inhibition of hormone-sensitive lipase in skeletal muscle. J Physiol-London 591: 5141-5155, 2013.

Amati F, Dube JJ, Alvarez-Carnero E, Edreira MM, Chomentowski P, Coen PM, Switzer GE, Bickel PE, Stefanovic-Racic M, Toledo FGS, Goodpaster BH. Skeletal Muscle Triglycerides, Diacylglycerols, and Ceramides in Insulin Resistance Another Paradox in Endurance-Trained Athletes? Diabetes 60: 2588-2597, 2011.

Anthonsen MW, Ronnstrand L, Wernstedt C, Degerman E, Holm C. Identification of novel phosphorylation sites in hormone-sensitive lipase that are phosphorylated in response to isoproterenol and govern activation properties in vitro. J Biol Chem 273: 215-221, 1998.

Arkinstall MJ, Bruce CR, Clark SA, Rickards CA, Burke LM, Hawley JA. Regulation of fuel metabolism by preexercise muscle glycogen content and exercise intensity. J Appl Physiol 97: 2275-2283, 2004.

Baba O. Production of monoclonal antibody that recognizes glycogen and its application for immunohistochemistry. Kokubyo Gakkai zasshi The Journal of the Stomatological Society, Japan 60: 264-287, 1993.

Badin PM, Louche K, Mairal A, Liebisch G, Schmitz G, Rustan AC, Smith SR, Langin D, Moro C. Altered Skeletal Muscle Lipase Expression and Activity Contribute to Insulin Resistance in Humans. Diabetes 60: 1734-1742, 2011.

Bartlett JD, Louhelainen J, Iqbal Z, Cochran AJ, Gibala MJ, Gregson W, Close GL, Drust B, Morton JP. Reduced carbohydrate availability enhances exercise-induced p53 signaling in human skeletal muscle: implications for mitochondrial biogenesis. Am J Physiol-Regul Integr Comp Physiol 304: R450-R458, 2013.

Bassau VA, Fairchild TJ, Rao A, Steele P, Fournier PA. Carbohydrate loading in human muscle: an improved 1 day protocol. Eur J Appl Physiol 87: 290-295, 2002.

Bell M, Wang H, Chen H, McLenithan JC, Gong DW, Yang RZ, Yu DZ, Fried SK, Quon MJ, Londos C, Sztalryd C. Consequences of lipid droplet coat protein downregulation in liver cells: abnormal lipid droplet metabolism and induction of insulin resistance. Diabetes 57: 2037-2045, 2008.

Bergman BC, Butterfield GE, Wolfel EE, Casazza GA, Lopaschuk GD, Brooks GA. Evaluation of exercise and training on muscle lipid metabolism. American journal of physiology Endocrinology and metabolism 276: E106-E117, 1999.

Bergstrom J. Percutaneous needle biopsy of skeletal muscle in physiological and clinical research Scandinavian journal of clinical and laboratory investigation 35: 609 - 616., 1975.

Bergstrom J and Hultman E. A study of the glycogen metabolism during exercise in man. Scandinavian journal of clinical and laboratory investigation 19: 218-228, 1967.

Bergstrom J, Hultman E and Saltin B. Muscle glycogen consumption during cross-country skiing (Vasa Ski Race). Internationale Zetischrift Fur Angewandte Physiologie Einschliesslich Arbeitsphysiologie 31: 71-75, 1973.

Bergstrom JH, L.; Hultman E.; Saltin B. Diet, Muscle Glycogen and Physical Performance. Acta Physiologica Scandinavica 71: 140-150, 1967.

Bickel PE, Tansey JT and Welte MA. PAT proteins, an ancient family of lipid droplet proteins that regulate cellular lipid stores. Biochim Biophys Acta Mol Cell Biol Lipids 1791: 419-440, 2009.

Boesch C and Kreis R. Observation of intramyocellular lipids by H-1-magnetic resonance spectroscopy. AnnNY AcadSci 904: 25-31, 2000.

Bonen A. Skeletal muscle fatty acid transport and transporters. J Aging Phys Act 8: 249-249, 2000.

Bosma M, Hesselink MKC, Sparks LM, Timmers S, Ferraz MJ, Mattijssen F, van Beurden D, Schaart G, de Baets MH, Verheyen FK, Kersten S, Schrauwen P. Perilipin 2 Improves Insulin Sensitivity in Skeletal Muscle Despite Elevated Intramuscular Lipid Levels. Diabetes 61: 2679-2690, 2012a.

Bosma M, Minnaard R, Sparks LM, Schaart G, Losen M, de Baets MH, Duimel H, Kersten S, Bickel PE, Schrauwen P, Hesselink MKC. The lipid droplet coat protein perilipin 5 also localizes to muscle mitochondria. Histochem Cell Biol 137: 205-216, 2012b.

Bosma M, Sparks LM, Hooiveld GJ, Jorgensen JA, Houten SM, Schrauwen P, Kersten S, Hesselink MKC. Overexpression of PLIN5 in skeletal muscle promotes oxidative gene expression and intramyocellular lipid content without compromising insulin sensitivity. Biochim Biophys Acta Mol Cell Biol Lipids 1831: 844-852, 2013.

Bostrom P, Andersson L, Rutberg M, Perman J, Lidberg U, Johansson BR, Fernandez-Rodriguez J, Ericson J, Nilsson T, Boren J, Olofsson SO. SNARE proteins mediate fusion between cytosolic lipid droplets and are implicated in insulin sensitivity. Nat Cell Biol 9: 1286-U1139, 2007.

Bostrom P, Rutberg M, Ericsson J, Holmdahl P, Andersson L, Frohman MA, Boren J, Olofsson SO. Cytosolic lipid droplets increase in size by microtubule-dependent complex formation. Arterioscler Thromb Vasc Biol 25: 1945-1951, 2005.

Boushel R, Ara I, Gnaiger E, Helge JW, Gonzalez-Alonso J, Munck-Andersen T, Sondergaard H, Damsgaard R, van Hall G, Saltin B, Calbet JAL. Low-intensity training increases peak arm VO2 by enhancing both convective and diffusive O-2 delivery. Acta Physiol 211: 122-134, 2014.

Bradley NS, Snook LA, Jain SS, Heigenhauser GJF, Bonen A, Spriet LL. Acute endurance exercise increases plasma membrane fatty acid transport proteins in rat and human skeletal muscle. Am J Physiol-Endocrinol Metab 302: E183-E189, 2012.

Branth S, Hambraeus L, Piehl-Aulin K, Essen-Gustavsson B, Akerfeldt T, Olsson R, Stridsberg M, Ronquist G. Metabolic stress-like condition can be induced by prolonged strenuous exercise in athletes. Ups J Med Sci 114: 12-25, 2009.

Brasaemle DL. The perilipin family of structural lipid droplet proteins: stabilization of lipid droplets and control of lipolysis. J Lipid Res 48: 2547-2559, 2007.

Brasaemle DL, Barber T, Wolins NE, Serrero G, BlanchetteMackie EJ, Londos C. Adipose differentiation-related protein is an ubiquitously expressed lipid storage droplet-associated protein. J Lipid Res 38: 2249-2263, 1997.

Bulankina AV, Deggerich A, Wenzel D, Mutenda K, Wittmann JG, Rudolph MG, Burger KNJ, Honing S. TIP47 functions in the biogenesis of lipid droplets. J Cell Biol 185: 641-655, 2009.

Burke L. The IOC Consensus on Sports Nutrition 2003: New Guidelines for Nutrition for Athletes. Int J Sport Nutr Exerc Metab 13: 549-552, 2004.

Burke LM, Collier GR and Hargreaves M. Muscle glycogen storage after prolonged exercise - effect of the glycemic index of carbohydrate feedings J Appl Physiol 75: 1019-1023, 1993.

Burke LM, Hawley JA, Jeukendrup A, Morton JP, Stellingwerff T, Maughan RJ. Toward a Common Understanding of Diet-Exercise Strategies to Manipulate Fuel Availability for Training and Competition Preparation in Endurance Sport. Int J Sport Nutr Exerc Metab 28: 451-463, 2018.

Burke LM, Hawley JA, Wong SHS, Jeukendrup AE. Carbohydrates for training and competition. J Sports Sci 29: S17-S27, 2011.

Bussell R and Eliezer D. A structural and functional role for 11-mer repeats in alpha-synuclein and other exchangeable lipid binding proteins. J Mol Biol 329: 763-778, 2003.

Calbet JAL, Holmberg HC, Rosdahl H, van Hall G, Jensen-Urstad M, Saltin B. Why do arms extract less oxygen than legs during exercise? Am J Physiol-Regul Integr Comp Physiol 289: R1448-R1458, 2005.

Carlson LA, Ekelund LG and Froberg SO. Concentration of triglycerides, phospholipids and glycogen in skeleatl muscle and of free fatty acids and beta-hydroxybutyric acid in blood in man in response to exercise. Eur J Clin Invest 1: 248-&, 1971.

Cartee GD, Young DA, Sleeper MD, Zierath J, Wallberghenriksson H, Holloszy JO. Prolonged increase in insulin-stimulated glucose-transport in muscle after exercise. Am J Physiol 256: E494-E499, 1989.

Carter SL, Rennie C and Tarnopolsky MA. Substrate utilization during endurance exercise in men and women after endurance training. Am J Physiol-Endocrinol Metab 280: E898-E907, 2001.

Cases S, Smith SJ, Zheng YW, Myers HM, Lear SR, Sande E, Novak S, Collins C, Welch CB, Lusis AJ, Erickson SK, Farese RV. Identification of a gene encoding an acyl CoA : diacylglycerol acyltransferase, a key enzyme in triacylglycerol synthesis. Proc Natl Acad Sci U S A 95: 13018-13023, 1998.

Cases S, Stone SJ, Zhou P, Yen E, Tow B, Lardizabal KD, Voelker T, Farese RV. Cloning of DGAT2, a second mammalian diacylglycerol acyltransferase, and related family members. J Biol Chem 276: 38870-38876, 2001.

Cermak NM and Loon L. The Use of Carbohydrates During Exercise as an Ergogenic Aid. Sports Med 43: 1139-1155, 2013.

Charlton GA and Crawford MH. Physiologic consequences of training. Cardiology Clinics 15: 345-354, 1997.

Chee C, Shannon CE, Burns A, Selby AL, Wilkinson D, Smith K, Greenhaff PL, Stephens FB. Relative Contribution of Intramyocellular Lipid to Whole-Body Fat Oxidation Is Reduced With Age but Subsarcolemmal Lipid Accumulation and Insulin

Resistance Are Only Associated With Overweight Individuals. Diabetes 65: 840-850, 2016.

Chen WQ, Chang B, Wu XY, Li L, Sleeman M, Chan L. Inactivation of Plin4 downregulates Plin5 and reduces cardiac lipid accumulation in mice. Am J Physiol-Endocrinol Metab 304: E770-E779, 2013.

Chesley A, Hultman E and Spriet LL. Effects of Epinephrine infusion on muscle glycogenolysis during intense aerobic exercise. Am J Physiol-Endocrinol Metab 268: E127-E134, 1995.

Choi CS, Savage, D. B., Kulkarni, A., Yu, X. X., Liu, Z-X., Morino, K., Kim, S., Distefano, A., Samuel, V. T., Neschen, S., Zhang, D., Wang, A., Zhang, X-M., Kahn, M., Cline, G. W., Pandey, S. K., Geisler, J. G., Bhanot, S., Monia, B. P. & Shulman, G. I. Suppression of diacylglycerol acyltransferase-2 (DGAT2), but not DGAT1, with antisense oligonucleotides reverses diet-induced hepatic steatosis and insulin resistance. J Biol Chem 282: 22678-22688, 2007.

Cleroux J, Vannguyen P, Taylor AW, Leenen FHH. Effects of beta-1-beta2-blockade vs beta-1+beta-2-blockade on exercise endurance and muscle metabolism in humans. J Appl Physiol 66: 548-554, 1989.

Coleman RA and Lee DP. Enzymes of triacylglycerol synthesis and their regulation. Prog Lipid Res 43: 134-176, 2004.

Constantinteodosiu D, Carlin JI, Cederblad G, Harris RC, Hultman E. Acetyl group accumulation and pyruvate-dehydrogenase activity in human muscle during incremental exercise. Acta Physiologica Scandinavica 143: 367-372, 1991.

Covington JD, Galgani JE, Moro C, LaGrange JM, Zhang ZY, Rustan AC, Ravussin E, Bajpeyi S. Skeletal Muscle Perilipin 3 and Coatomer Proteins Are Increased following Exercise and Are Associated with Fat Oxidation. PLoS One 9: 8, 2014.

Covington JD, Noland RC, Hebert RC, Masinter BS, Smith SR, Rustan AC, Ravussin E, Bajpeyi S. Perilipin 3 Differentially Regulates Skeletal Muscle Lipid Oxidation in Active, Sedentary, and Type 2 Diabetic Males. J Clin Endocrinol Metab 100: 3683-3692, 2015.

Coyle EF, Coggan AR, Hemmert MK, Ivy JL. Muscle glycogen utilisation during prolonged strenuous exercise when fed carbohydrate J Appl Physiol 61: 165-172, 1986.

Coyle EF, Jeukendrup AE, Oseto MC, Hodgkinson BJ, Zderic TW. Low-fat diet alters intramuscular substrates and reduces lipolysis and fat oxidation during exercise. Am J Physiol-Endocrinol Metab 280: E391-E398, 2001.

Daemen S, Gemmink A, Brouwers B, Meex RCR, Huntjens PR, Schaart G, Moonen-Komips E, Jorgensen J, Hoeks J, Schrauwen P, Hesselink MKC. Distinct lipid droplet characteristics and distribution unmask the apparent contradiction of the athlete's paradox. Mol Metab 17: 71-81, 2018.

Daemen S, van Zandvoort M, Parekh SH, Hesselink MKC. Microscopy tools for the investigation of intracellular lipid storage and dynamics. Mol Metab 5: 153-163, 2016.

Dalen KT, Dahl T, Holter E, Arntsen B, Londos C, Sztalryd C, Nebb HI. LSDP5 is a PAT protein specifically expressed in fatty acid oxidizing tissues. Biochim Biophys Acta Mol Cell Biol Lipids 1771: 210-227, 2007.

Dean D, Daugaard JR, Young ME, Saha A, Vavvas D, Asp S, Kiens B, Kim KH, Witters L, Richter EA, Ruderman N. Exercise diminishes the activity of acetyl-CoA carboxylase in human muscle. Diabetes 49: 1295-1300, 2000.

Decombaz J, Fleith M, Hoppeler H, Kreis R, Boesch C. Effect of diet on the replenishment of intramyocellular lipids after exercise. European Journal of Nutrition 39: 244-247, 2000.

Decombaz J, Schmitt B, Ith M, Decarli BH, Diem P, Kreis R, Hoppeler H, Boesch C. Postexercise fat intake repletes intramyocellular lipids but no faster in trained than in sedentary subjects. Am J Physiol-Regul Integr Comp Physiol 281: R760-R769, 2001.

Devries MC, Lowther SA, Glover AW, Hamadeh MJ, Tarnopolsky MA. IMCL area density, but not IMCL utilization, is higher in women during moderate-intensity endurance exercise, compared with men. Am J Physiol-Regul Integr Comp Physiol 293: R2336-R2342, 2007.

Donsmark M, Langfort J, Holm C, Ploug T, Galbo H. Contractions activate hormone-sensitive lipase in rat muscle by protein kinase C and mitogen-activated protein kinase. J Physiol-London 550: 845-854, 2003.

Drochmans P. Morphology of glycogen. Electron microscopic study of the negative stains of particulate glycogen. Journal of ultrastructure research 6: 141-163, 1962.

Dyck DJ, Putman CT, Heigenhauser GJF, Hultman E, Spriet LL. Regulation of fat-carbohydrate interaction in skeletal-muscle during intense aerobic cycling. Am J
Edstrom LN, B. Histochemical types and sizes of fibres in normal human muscles. Acta Neurologica Scandinavica 45: 1969.

Enoksson S, Degerman E, Hagstrom-Toft E, Large V, Arner P. Various phosphodiesterase subtypes mediate the in vivo antilipolytic effect of insulin on adipose tissue and skeletal muscle in man. Diabetologia 41: 560-568, 1998.

Essen B and Henriksson J. Glycogen content of individual muscle-fibres in man. Acta Physiologica Scandinavica 90: 645-647, 1974.

Essen B, Jansson E, Henriksson J, Taylor AW, Saltin B. Metabolic characteristics of fibre types in human skeletal muscle. Acta Physiologica Scandinavica 95: 153-165, 1975.

Essengustavsson B and Tesch PA. Glycogen and triglyceride utilisation in relation to muscle meteabolic characteristics in men performing heavy-resistance exercise. Eur J Appl Physiol 61: 5-10, 1990.

Everts ME and Clausen T. Activation of the NA-K pump by intracellular NA in rat slow-twitch and fast-twitch muscle Acta Physiologica Scandinavica 145: 353-362, 1992.

Farese RV and Walther TC. Lipid Droplets Finally Get a Little R-E-S-P-E-C-T. Cell 139: 855-860, 2009.

Febbraio MA, Lambert DL, Starkie RL, Proietto J, Hargreaves M. Effect of epinephrine on muscle glycogenolysis during exercise in trained men. J Appl Physiol 84: 465-470, 1998.

Fisher EA, Blum CB, Zannis VI, Breslow JL. Independent effects of dietary saturated fat and cholesterol on plasma-lipids, lipoproteins, and apolipoprotein-E. J Lipid Res 24: 1039-1048, 1983.

Friden J, Seger J and Ekblom B. Topographical localization of muscle glycogen - an ultrahistochemical study in human vastus lateralis. Acta Physiologica Scandinavica 135: 381-391, 1989.

Fritz I. The effect of muscle extracts on the oxidation of palmitic acid by liver slices and homogenates. Acta physiologica Scandinavica 34: 367-385, 1955.

Froberg SO and Mossfeldt F. Effect of prolonged strenuous exercise on concentration of triglycerides, phospholipids and glycogen in muscle of man. Acta Physiologica Scandinavica 82: 167-+, 1971.

Frosig C and Richter EA. Improved Insulin Sensitivity After Exercise: Focus on Insulin Signaling. Obesity 17: S15-S20, 2009.

Fujimoto TP, R. G. Not Just Fat: The Structure and Function of the Lipid Droplet. Cold Spring Harb Perspect Biol 3: a004838, 2011.

Gejl KD, Hvid LG, Frandsen U, Jensen K, Sahlin K, Ørtenblad N. Muscle Glycogen Content Modifies SR Ca2+ Release Rate in Elite Endurance Athletes. Med Sci Sports Exerc 46: 496-505, 2014.

Gemmink A, Bakker LEH, Guigas B, Kornips E, Schaart G, Meinders AE, Jazet IM, Hesselink MKC. Lipid droplet dynamics and insulin sensitivity upon a 5-day high-fat diet in Caucasians and South Asians. Sci Rep 7: 9, 2017.

Gemmink A, Bosma M, Kuijpers HJH, Hoeks J, Schaart G, van Zandvoort M, Schrauwen P, Hesselink MKC. Decoration of intramyocellular lipid droplets with PLIN5 modulates fasting-induced insulin resistance and lipotoxicity in humans. Diabetologia 59: 1040-1048, 2016.

Gemmink A, Daemen S, Brouwers B, Hoeks J, Schaart G, Knoops K, Schrauwen P, Hesselink MKC. Decoration of myocellular lipid droplets with perilipins as a marker for in vivo lipid droplet dynamics: A super-resolution microscopy study in trained athletes and insulin resistant individuals. Biochimica et biophysica acta Molecular and cell biology of lipids 1866: 158852-158852, 2020.

Gemmink A, Daemen S, Kuijpers HJH, Schaart G, Duimel H, Lopez-Iglesias C, van Zandvoort M, Knoops K, Hesselink MKC. Super-resolution microscopy localizes perilipin 5 at lipid droplet-mitochondria interaction sites and at lipid droplets juxtaposing to perilipin 2. Biochim Biophys Acta Mol Cell Biol Lipids 1863: 1423-1432, 2018.

Gimeno RE and Cao J. Thematic review series: Glycerolipids - Mammalian glycerol-3-phosphate acyltransferases: new genes for an old activity. J Lipid Res 49: 2079-2088, 2008.

Gjelstad IMF, Haugen F, Gulseth HL, Norheim F, Jans A, Bakke SS, Raastad T, Tjonna AE, Wisloff U, Blaak EE, Riserus U, Gaster M, Roche HM, Birkeland KI, Drevon CA. Expression of perilipins in human skeletal muscle in vitro and in vivo in relation to diet, exercise and energy balance. Arch Physiol Biochem 118: 22-30, 2012.

Gollnick PD, Armstrong RB, Saubert CW, Sembrowich WL, Shepherd RE, Saltin B. Glycogen depletion patterns in human skeletal-muscle fibers during prolonged work. Pflugers Arch 344: 1-12, 1973.

Gollnick PD, Piehl K and Saltin B. Selective glycogen depletion pattern in human muscle-fibers after exercise of varying intensity and at varying pedalling rates. J Physiol-London 241: 45-&, 1974.

Gonzalez JT, Fuchs CJ, Smith FE, Thelwall PE, Taylor R, Stevenson EJ, Trenell MI, Cermak NM, van Loon LJC. Ingestion of glucose or sucrose prevents liver but not muscle glycogen depletion during prolonged endurance-type exercise in trained cyclists. Am J Physiol-Endocrinol Metab 309: E1032-E1039, 2015.

Gonzalez-Baro MR, Lewin TM and Coleman RA. Regulation of triglyceride metabolism II. Function of mitochondrial GPAT1 in the regulation of triacylglycerol biosynthesis and insulin action. American Journal of Physiology-Gastrointestinal and Liver Physiology 292: G1195-G1199, 2007.

Goodman JM. Building the lipid droplet assembly complex. J Cell Biol 219: 2, 2020.
90.   Granneman JG, Moore HPH, Mottillo EP, Zhu ZX, Zhou L. Interactions of Perilipin-5 (Plin5) with Adipose Triglyceride Lipase. J Biol Chem 286: 5126-5135, 2011.

Greenberg AS, Shen WJ, Muliro K, Patel S, Souza SC, Roth RA, Kraemer FB. Stimulation of lipolysis and hormone-sensitive lipase via the extracellular signal-regulated kinase pathway. J Biol Chem 276: 45456-45461, 2001.

Greiwe JS, Hickner RC, Hansen PA, Racette SB, Chen MM, Holloszy JO. Effects of endurance exercise training on muscle glycogen accumulation in humans. Med Sci Sports Exerc 31: S54-S54, 1999.

Guo ZK. Triglyceride content in skeletal muscle: Variability and the source. Anal Biochem 296: 1-8, 2001.

Guo ZK, Burguera B and Jensen MD. Kinetics of intramuscular triglyceride fatty acids in exercising humans. J Appl Physiol 89: 2057-2064, 2000.

Haemmerle G, Zimmermann R, Strauss JG, Kratky D, Riederer M, Knipping G, Zechner R. Hormone-sensitive lipase deficiency in mice changes the plasma lipid profile by affecting the tissue-specific expression pattern of lipoprotein lipase in adipose tissue and muscle. J Biol Chem 277: 12946-12952, 2002b.

Hammond LE, Neschen S, Romanelli AJ, Cline GW, Ilkayeva OR, Shulman GI, Muoio DM, Coleman RA. Mitochondrial glycerol-3-phosphate acyltransferase-1 is essential in liver for the metabolism of excess acyl-CoAs. J Biol Chem 280: 25629-25636, 2005.

Havel R, Pernow, B, and Jones, NL. Uptake and release of free fatty acids and other metabolites in the legs of exercising men. J Appl Physiol 89: 2057-2064, 1967.

Hawley JA, Schabort EJ, Noakes TD, Dennis SC. Carbohydrate-loading and exercise performance - An update. Sports Med 24: 73-81, 1997.

Helge JW, Watt PW, Richter EA, Rennie MJ, Kiens B. Fat utilization during exercise: adaptation to a fat-rich diet increases utilization of plasma fatty acids and very low density lipoprotein-triacylglycerol in humans. J Physiol-London 537: 1009-1020, 2001.

Helge JW, Wulff B and Kiens B. Impact of a fat-rich diet on endurance in man: role of the dietary period. Med Sci Sports Exerc 30: 456-461, 1998.

Henne WM, Reese ML and Goodman JM. The assembly of lipid droplets and their roles in challenged cells. Embo J 37: 14, 2018.

Henneman EO, CB. . Relations between structure and function in the design of skeletal muscles. J Neurophysiol 28: 581-598, 1965.

Henriksson J. Training induced adaptation of skeletal-muscle and metabolism during submaximal exercise. J Physiol-London 270: 661-675, 1977.

Hermansen L, Hultman E and Saltin B. Muscle glycogen during prolonged severe exercise. Acta physiologica Scandinavica 71: 129-139, 1967.

Holmberg HC, Lindinger S, Stoggl T, Eitzlmair E, Muller E. Biomechanical analysis of double poling in elite cross-country skiers. Med Sci Sports Exerc 37: 807-818, 2005.

Hood DA. Plasticity in skeletal, cardiac, and smooth muscle - Invited review: Contractile activity-induced mitochondrial biogenesis in skeletal muscle. J Appl Physiol 90: 1137-1157, 2001.

Hoppeler H. Skeletal muscle substrate metabolism. Int J Obes 23: S7-S10, 1999.

Hoppeler H, Howald H, Conley K, Lindstedt SL, Claassen H, Vock P, Weibel ER. Endurance training in humans - aerobic capacity and structure of skeletal-muscle. J Appl Physiol 59: 320-327, 1985.

Howald H, Boesch C, Kreis R, Matter S, Billeter R, Essen-Gustavsson B, Hoppeler H. Content of intramyocellular lipids derived by electron microscopy, biochemical assays, and H-1-MR spectroscopy. J Appl Physiol 92: 2264-2272, 2002.

Howald H, Hoppeler H, Claassen H, Mathieu O, Straub R. Influences of endurance training on the ultrastructural composition of the different muscle-fiber types in humans. Pflugers Arch 403: 369-376, 1985.

Howlett RA, Parolin ML, Dyck DJ, Hultman E, Jones NL, Heigenhauser GJF, Spriet LL. Regulation of skeletal muscle glycogen phosphorylase and PDH at varying

exercise power outputs. Am J Physiol-Regul Integr Comp Physiol 275: R418-R425, 1998.

Hsieh K, Lee YK, Londos C, Raaka BM, Dalen KT, Kimmel AR. Perilipin family members preferentially sequester to either triacylglycerol-specific or cholesteryl-ester-specific intracellular lipid storage droplets. J Cell Sci 125: 4067-4076, 2012.

Hurley BF, Nemeth PM, Martin WH, Hagberg JM, Dalsky GP, Holloszy JO. Muscle triglyceride utilisation during exercise - effect of training. J Appl Physiol 60: 562-567, 1986.

Impey SG, Hammond KM, Shepherd SO, Sharples AP, Stewart C, Limb M, Smith K, Philp A, Jeromson S, Hamilton DL, Close GL, Morton JP. Fuel for the work required: a practical approach to amalgamating train-low paradigms for endurance athletes. Physiol Rep 4: 15, 2016.

Impey SG, Hearris MA, Hammond KM, Bartlett JD, Louis J, Close GL, Morton JP. Fuel for the Work Required: A Theoretical Framework for Carbohydrate Periodization and the Glycogen Threshold Hypothesis. Sports Med 48: 1031-1048, 2018.

Impey SG, Jevons E, Mees G, Cocks M, Strauss J, Chester N, Laurie I, Target D, Hodgson A, Shepherd SO, Morton JP. Glycogen Utilization during Running: Intensity, Sex, and Muscle-Specific Responses. Med Sci Sports Exerc 52: 1966-1975, 2020.

Ivy JL, Chi MMY, Hintz CS, Sherman WM, Hellendall RP, Lowry OH. Progressive metabolite changes in individual human-muscle fibers with increasing work rates. Am J Physiol 252: C630-C639, 1987.

Ivy JL and Kuo CH. Regulation of GLUT4 protein and glycogen synthase during muscle glycogen synthesis after exercise. Acta Physiologica Scandinavica 162: 295-304, 1998.

James JH, Wagner KR, King J-K, Leffler RE, Upputuri RK, Balasubramaniam A, Friend LA, Shelly DA, Paul RJ, Fischer JE. Stimulation of both aerobic glycolysis and Na+-K+-ATPase activity in skeletal muscle by epinephrine or amylin. American journal of physiology Endocrinology and metabolism 277: E176-E186, 1999.

Jansson E, Hjemdahl P and Kaijser L. Epinephrine-induced changes in muscle carbohydrate during exercise in male-subjects. J Appl Physiol 60: 1466-1470, 1986.

Jensen L, Gejl KD, Ørtenblad N, Nielsen JL, Bech RD, Nygaard T, Sahlin K, Frandsen U. Carbohydrate restricted recovery from long term endurance exercise does not affect gene responses involved in mitochondrial biogenesis in highly trained athletes. Physiol Rep 3: 13, 2015.

Jensen R, Ørtenblad N, Stausholm MLH, Skjaerbaek MC, Larsen DN, Hansen M, Holmberg HC, Plomgaard P, Nielsen J. Heterogeneity in subcellular muscle glycogen utilisation during exercise impacts endurance capacity in men. J Physiol-London 22, 2020.

Jensen TE and Richter EA. Regulation of glucose and glycogen metabolism during and after exercise. J Physiol-London 590: 1069-1076, 2012.

Jentjens R and Jeukendrup AE. Determinants of post-exercise glycogen synthesis during short-term recovery. Sports Med 33: 117-144, 2003.

Jeppesen J and Kiens B. Regulation and limitations to fatty acid oxidation during exercise. J Physiol-London 590: 1059-1068, 2012.

Jeukendrup A, Brouns F, Wagenmakers AJM, Saris WHM. Carbohydrate-electrolyte feedings improve 1 h time trial cycling performance. Int J Sports Med 18: 125-129, 1997.

Jocken JWE, Smit E, Goossens GH, Essers YPG, van Baak MA, Mensink M, Saris WHM, Blaak EE. Adipose triglyceride lipase (ATGL) expression in human skeletal muscle is type I (oxidative) fiber specific. Histochem Cell Biol 129: 535-538, 2008.

Johnson M, Polgar, J., Weightman, D. & Appleton, D. Data on the distribution of fibre types in thirty-six human muscles: an autopsy study. Journal of the neurological sciences 18: 111-129, 1973.

Johnson NA, Stannard SR, Mehalski K, Trenell MI, Sachinwalla T, Thompson CH, Thompson MW. Intramyocellular triacylglycerol in prolonged cycling with high- and low-carbohydrate availability. J Appl Physiol 94: 1365-1372, 2003.

Kiens B. Skeletal muscle lipid metabolism in exercise and insulin resistance. Physiol Rev 86: 205-243, 2006.

Kiens B, Essengustavsson B, Christensen NJ, Saltin B. Skeletal-muscle substrate utilisation during submaximal exercise in man - effect of endurance training J Physiol-London 469: 459-478, 1993.

Kiens B and Richter EA. Utilization of skeletal muscle triacylglycerol during postexercise recovery in humans. Am J Physiol-Endocrinol Metab 275: E332-E337, 1998.

Kiens B, Roemen THM and van der Vusse GJ. Muscular long-chain fatty acid content during graded exercise in humans. American journal of physiology Endocrinology and metabolism 276: E352-E357, 1999.

Kimmel AR and Sztalryd C. The Perilipins: Major Cytosolic Lipid Droplet-Associated Proteins and Their Roles in Cellular Lipid Storage, Mobilization, and Systemic Homeostasis. In: Annual Review of Nutrition. Annual Review of Nutrition, Vol 36, edited by Stover PJ. Palo Alto: Annual Reviews, 2016, p. 471-509.

Kleinert M, Parker BL, Chaudhuri R, Fazakerley DJ, Serup A, Thomas KC, Krycer JR, Sylow L, Fritzen AM, Hoffman NJ, Jeppesen J, Schjerling P, Ruegg MA, Kiens B, James DE, Richter EA. mTORC2 and AMPK differentially regulate muscle triglyceride content via Perilipin 3. Mol Metab 5: 646-655, 2016.

Koh HCE, Nielsen J, Saltin B, Holmberg HC, Ørtenblad N. Pronounced limb and fibre type differences in subcellular lipid droplet content and distribution in elite skiers before and after exhaustive exercise. J Physiol-London 595: 5781-5795, 2017.

Koh HCE, Ørtenblad N, Winding KM, Helisten Y, Mortensen SP, Nielsen J. High-intensity interval, but not endurance, training induces muscle fiber type-specific subsarcolemmal lipid droplet size reduction in type 2 diabetic patients. Am J Physiol-Endocrinol Metab 315: E872-E884, 2018.

Koopman R, Schaart G and Hesselink MKC. Optimisation of oil red O staining permits combination with immunofluorescence and automated quantification of lipids. Histochem Cell Biol 116: 63-68, 2001.

Krahmer N, Guo Y, Wilfling F, Hilger M, Lingrell S, Heger K, Newman HW, Schmidt-Supprian M, Vance DE, Mann M, Farese RV, Walther TC. Phosphatidylcholine Synthesis for Lipid Droplet Expansion Is Mediated by Localized Activation of CTP:Phosphocholine Cytidylyltransferase. Cell Metab 14: 504-515, 2011.

Langfort J, Ploug T, Ihlemann J, Holm C, Galbo H. Stimulation of hormone-sensitive lipase activity by contractions in rat skeletal muscle. Biochem J 351: 207-214, 2000.

Langfort J, Ploug T, Ihlemann J, Saldo M, Holm C, Galbo H. Expression of hormone-sensitive lipase and its regulation by adrenaline in skeletal muscle. Biochem J 340: 459-465, 1999.

Larson-Meyer DE, Newcomer BR and Hunter GR. Influence of endurance running and recovery diet on intramyocellular lipid content in women: a H-1 NMR study. Am J Physiol-Endocrinol Metab 282: E95-E106, 2002.

Lass A, Zimmermann R, Haemmerle G, Riederer M, Schoiswohl G, Schweiger M, Kienesberger P, Strauss JG, Gorkiewicz G, Zechner R. Adipose triglyceridelipase-mediated lipolysis of cellular fat stores is activated by CGI-58 and defective in Chanarin-Dorfman Syndrome. Cell Metab 3: 309-319, 2006.

Laurens C, Bourlier V, Mairal A, Louche K, Badin PM, Mouisel E, Montagner A, Marette A, Tremblay A, Weisnagel JS, Guillou H, Langin D, Joanisse DR, Moro C. Perilipin 5 fine-tunes lipid oxidation to metabolic demand and protects against lipotoxicity in skeletal muscle. Sci Rep 6: 12, 2016.

Lauritzen H, Mug T, Prats C, Tavare JM, Galbo H. Imaging of insulin signaling in skeletal muscle of living mice shows major role of T-tubules. Diabetes 55: 1300-1306, 2006.

Levine SA, Gordon, B. & Derick, C. L. Some changes in the chemical constituents of the blood following a marathon race with special reference to the development of hypoglycemia Journal of the American Medical Association 82: 1778, 1924.

Li Y, Lee, S., Langleite, T. & Norheim, F. Subsarcolemmal lipid droplet responses to a combined endurance and strength exercise intervention. Physiol Rep 2: e12187-e12187, 2014.

Lima-Silva AE, Bertuzzi RCM, Pires FO, Gagliardi JFL, Barros RV, Hammond J, Kiss M. Relationship between training status and maximal fat oxidation rate. J Sport Sci Med 9: 31-35, 2010.

Linden D, William-Olsson L, Rhedin M, Asztely A, Clapham J, Schreyer S. Overexpression of mitochondrial glycerol-3-phosphate acyltransferase in rat hepatocytes leads to decreased fatty acid oxidation and increased glycerolipid biosynthesis. Atherosclerosis Supplements 5: 75-76, 2004.

Listenberger LL and Brown DA. Fluorescent detection of lipid droplets and associated proteins. Current protocols in cell biology Chapter 24: Unit 24.22, 2007.

Liu L, Zhang YY, Chen N, Shi XJ, Tsang B, Yu YH. Upregulation of myocellular DGAT1 augments triglyceride synthesis in skeletal muscle and protects against fat-induced insulin resistance. J Clin Invest 117: 1679-1689, 2007.

Londos C, Brasaemle DL, Gruiagray J, Servetnick DA, Schultz CJ, Levin DM, Kimmel AR. Perilipin - unique proteins associated with intracellular neutral lipid droplets in adipocytes and steroidogenic cells. Biochemical Society Transactions 23: 611-615, 1995.

Macpherson REK, Vandenboom, R., Roy, B. D. & Peters, S. J. Skeletal muscle PLIN3 and PLIN5 are serine phosphorylated at rest and following lipolysis during adrenergic or contractile stimulation. . Phsyiol Rep 1: e00084, 2013b.

MacPherson REK, Herbst EAF, Reynolds EJ, Vandenboom R, Roy BD, Peters SJ. Subcellular localization of skeletal muscle lipid droplets and PLIN family proteins OXPAT and ADRP at rest and following contraction in rat soleus muscle. Am J Physiol-Regul Integr Comp Physiol 302: R29-R36, 2012.

MacPherson REK and Peters SJ. Piecing together the puzzle of perilipin proteins and skeletal muscle lipolysis. Appl Physiol Nutr Metab 40: 641-651, 2015.

MacPherson REK, Ramos SV, Vandenboom R, Roy BD, Peters SJ. Skeletal muscle PLIN proteins, ATGL and CGI-58, interactions at rest and following stimulated contraction. Am J Physiol-Regul Integr Comp Physiol 304: R644-R650, 2013a.

Malenfant P, Joanisse DR, Theriault R, Goodpaster BH, Kelley DE, Simoneau JA. Fat content in individual muscle fibers of lean and obese subjects. Int J Obes 25: 1316-1321, 2001.

Marchand I, Tarnopolsky M, Adamo KB, Bourgeois JM, Chorneyko K, Graham TE. Quantitative assessment of human muscle glycogen granules size and number in subcellular locations during recovery from prolonged exercise. J Physiol-London 580: 617-628, 2007.

Mason RR, Meex RCR, Lee-Young R, Canny BJ, Watt MJ. Phosphorylation of adipose triglyceride lipase Ser(404) is not related to 5 '-AMPK activation during moderate-intensity exercise in humans. Am J Physiol-Endocrinol Metab 303: E534-E541, 2012.

Mason RR, Meex RCR, Russell AP, Canny BJ, Watt MJ. Cellular Localization and Associations of the Major Lipolytic Proteins in Human Skeletal Muscle at Rest and during Exercise. PLoS One 9: 2014a.

Mason RR, Mokhtar R, Matzaris M, Selathurai A, Kowalski GM, Mokbel N, Meikle PJ, Bruce CR, Watt MJ. PLIN5 deletion remodels intracellular lipid composition and causes insulin resistance in muscle. Mol Metab 3: 652-663, 2014b.

Masuda Y, Itabe H, Odaki M, Hama K, Fujimoto Y, Mori M, Sasabe N, Aoki J, Arai H, Takano T. ADRP/adipophilin is degraded through the proteasome-dependent pathway during regression of lipid-storing cells. J Lipid Res 47: 87-98, 2006.

McBride A, Ghilagaber S, Nikolaev A, Hardie DG. The Glycogen-Binding Domain on the AMPK beta Subunit Allows the Kinase to Act as a Glycogen Sensor. Cell Metab 9: 23-34, 2009.

McConell GK, Canny BJ, Daddo MC, Nance MJ, Snow RJ. Effect of carbohydrate ingestion on glucose kinetics and muscle metabolism during intense endurance exercise. J Appl Physiol 89: 1690-1698, 2000.

McFarlan JT, Yoshida Y, Jain SS, Han XX, Snook LA, Lally J, Smith BK, Glatz JFC, Luiken J, Sayer RA, Tupling AR, Chabowski A, Holloway GP, Bonen A. In Vivo, Fatty Acid Translocase (CD36) Critically Regulates Skeletal Muscle Fuel Selection, Exercise Performance, and Training-induced Adaptation of Fatty Acid Oxidation. J Biol Chem 287: 23502-23516, 2012.

Melendezhevia E, Waddell TG and Shelton ED. Optimisation of molecular design in the evolution of metabolism - the glycogen molecule. Biochem J 295: 477-483, 1993.

Millet GP, Vleck VE and Bentley DJ. Physiological Differences Between Cycling and Running Lessons from Triathletes. Sports Med 39: 179-206, 2009.

Minnaard R, Schrauwen P, Schaart G, Jorgensen JA, Lenaers E, Mensink M, Hesselink MKC. Adipocyte Differentiation-Related Protein and OXPAT in Rat and Human Skeletal Muscle: Involvement in Lipid Accumulation and Type 2 Diabetes Mellitus. J Clin Endocrinol Metab 94: 4077-4085, 2009.

Miura S, Gan JW, Brzostowski J, Parisi MJ, Schultz CJ, Londos C, Oliver B, Kimmel AR. Functional conservation for lipid storage droplet association among perilipin, ADRP, and TIP47 (PAT)-related proteins in mammals, Drosophila, and Dictyostelium. J Biol Chem 277: 32253-32257, 2002.

Morales PE, Bucarey JL and Espinosa A. Muscle Lipid Metabolism: Role of Lipid Droplets and Perilipins. J Diabetes Res 2017: 10, 2017.

Moro C, Bajpeyi S and Smith SR. Determinants of intramyocellular triglyceride turnover: implications for insulin sensitivity. Am J Physiol-Endocrinol Metab 294: E203-E213, 2008.

Moro C, Galgani JE, Luu L, Pasarica M, Mairal A, Bajpeyi S, Schmitz G, Langin D, Liebisch G, Smith SR. Influence of Gender, Obesity, and Muscle Lipase Activity on Intramyocellular Lipids in Sedentary Individuals. J Clin Endocrinol Metab 94: 3440-3447, 2009.

Murphy DJ and Vance J. Mechanisms of lipid body formation. Trends BiochemSci 24: 109-115, 1999.

Newsom SA, Schenk S, Li M, Everett AC, Horowitz JF. High fatty acid availability after exercise alters the regulation of muscle lipid metabolism. Metabolism-Clinical and Experimental 60: 852-859, 2011.

Nielsen J, Christensen AE, Nellemann B, Christensen B. Lipid droplet size and location in human skeletal muscle fibers are associated with insulin sensitivity. Am J Physiol-Endocrinol Metab 313: E721-E730, 2017.

Nielsen J, Holmberg HC, Schroder HD, Saltin B, Ørtenblad N. Human skeletal muscle glycogen utilization in exhaustive exercise: role of subcellular localization and fibre type. J Physiol-London 589: 2871-2885, 2011.
Nielsen J, Mogensen M, Vind BF, Sahlin K, Hojlund K, Schroder HD, Ørtenblad N. Increased subsarcolemmal lipids in type 2 diabetes: effect of training on localization of lipids, mitochondria, and glycogen in sedentary human skeletal muscle. Am J Physiol-Endocrinol Metab 298: E706-E713, 2010a.

Nielsen J and Ørtenblad N. Physiological aspects of the subcellular localization of glycogen in skeletal muscle. Appl Physiol Nutr Metab 38: 91-99, 2013.

Nielsen J, Schroder HD, Rix CG, Ørtenblad N. Distinct effects of subcellular glycogen localization on tetanic relaxation time and endurance in mechanically skinned rat skeletal muscle fibres. J Physiol-London 587: 3679-3690, 2009.

Nielsen J, Suetta C, Hvid LG, Schroder HD, Aagaard P, Ørtenblad N. Subcellular localization-dependent decrements in skeletal muscle glycogen and mitochondria content following short-term disuse in young and old men. Am J Physiol-Endocrinol Metab 299: E1053-E1060, 2010b.

Odland LM, Howlett RA, Heigenhauser GJF, Hultman E, Spriet LL. Skeletal muscle malonyl-CoA content at the onset of exercise at varying power outputs in humans. American journal of physiology Endocrinology and metabolism 274: E1080-E1085, 1998.

Ohsaki Y, Cheng JL, Suzuki M, Shinohara Y, Fujita A, Fujimoto T. Biogenesis of cytoplasmic lipid droplets: From the lipid ester globule in the membrane to the visible structure. Biochim Biophys Acta Mol Cell Biol Lipids 1791: 399-407, 2009.

Ørtenblad N and Nielsen J. Muscle glycogen and cell function - Location, location, location. Scand J Med Sci Sports 25: 34-40, 2015.

Ørtenblad N, Nielsen J, Boushel R, Soderlund K, Saltin B, Holmberg HC. The Muscle Fiber Profiles, Mitochondrial Content, and Enzyme Activities of the Exceptionally Well-Trained Arm and Leg Muscles of Elite Cross-Country Skiers. Front Physiol 9: 11, 2018.

Ørtenblad N, Nielsen J, Saltin B, Holmberg HC. Role of glycogen availability in sarcoplasmic reticulum Ca2+ kinetics in human skeletal muscle. J Physiol-London 589: 711-725, 2011.

Ørtenblad N and Stephenson DG. A novel signalling pathway originating in mitochondria modulates rat skeletal muscle membrane excitability. J Physiol-London 548: 139-145, 2003.

Oscai L, Essig, DA. & Palmer, WK. Lipase regulation of muscle triglyceride hydrolysis. J Appl Physiol 69: 1571–1577,, 1990.

Park H, Kaushik VK, Constant S, Prentki M, Przybytkowski E, Ruderman NB, Saha AK. Coordinate regulation of malonyl-CoA decarboxylase, sn-glycerol-3-phosphate acyltransferase, and acetyl-CoA carboxylase by AMP-activated protein kinase in rat tissues in response to exercise. J Biol Chem 277: 32571-32577, 2002.

Parolin ML, Chesley A, Matsos MP, Spriet LL, Jones NL, Heigenhauser GJF. Regulation of skeletal muscle glycogen phosphorylase and PDH during maximal intermittent exercise. American journal of physiology Endocrinology and metabolism 277: E890-E900, 1999.

Pendergast DR, Leddy JJ and Venkatraman JT. A perspective on fat intake in athletes. J Am Coll Nutr 19: 345-350, 2000.

Peters SJ, Samjoo IA, Devries MC, Stevic I, Robertshaw HA, Tarnopolsky MA. Perilipin family (PLIN) proteins in human skeletal muscle: the effect of sex, obesity, and endurance training. Appl Physiol Nutr Metab 37: 724-735, 2012.

Phillips SM, Green HJ, Tarnopolsky MA, Heigenhauser GJF, Grant SM. Progressive effect of endurance training on metabolic adaptations in working skeletal muscle. Am J Physiol-Endocrinol Metab 270: E265-E272, 1996.

Piehl K. Time course for refilling of glycogen stores in human muscle-fibres following exercise-induced glycogen depletion. Acta Physiologica Scandinavica 90: 297-302, 1974.

Pol A, Gross SP and Parton RG. Biogenesis of the multifunctional lipid droplet: Lipids, proteins, and sites. J Cell Biol 204: 635-646, 2014.

Pourteymour S, Lee S, Langleite TM, Eckardt K, Hjorth M, Bindesboll C, Dalen KT, Birkeland AI, Drevon CA, Holen T, Norheim F. Perilipin 4 in human skeletal muscle: localization and effect of physical activity. Physiol Rep 3: 15, 2015.

Prats C, Donsmark M, Qvortrup K, Londos C, Sztalryd C, Holm C, Galbo H, Ploug T. Decrease in intramuscular lipid droplets and translocation of HSL in response to muscle contraction and epinephrine. J Lipid Res 47: 2392-2399, 2006.

Prats C, Gomez-Cabello A, Nordby P, Andersen JL, Helge JW, Dela F, Baba O, Ploug T. An Optimized Histochemical Method to Assess Skeletal Muscle Glycogen and Lipid Stores Reveals Two Metabolically Distinct Populations of Type I Muscle Fibers. PLoS One 8: 9, 2013.

Price TB, Rothman DL, Taylor R, Avison MJ, Shulman GI, Shulman RG. Human muscle glycogen resynthesis after exercise - insulin dependent and insulin independent phases J Appl Physiol 76: 104-111, 1994.

Ramos SV, Turnbull PC, MacPherson REK, LeBlanc PJ, Ward WE, Peters SJ. Changes in mitochondrial perilipin 3 and perilipin 5 protein content in rat skeletal muscle following endurance training and acute stimulated contraction. Exp Physiol 100: 450-462, 2015.

Rasmussen BB and Winder WW. Effect of exercise intensity on skeletal muscle malonyl-CoA and acetyl-CoA carboxylase. J Appl Physiol 83: 1104-1109, 1997.

Ren JM, Semenkovich CF, Gulve EA, Gao JP, Holloszy JO. Exercise induces rapid increase in GLUT4 expression glucose-transport capacity, and insulin-stimulated glycogen-storage in muscle. J Biol Chem 269: 14396-14401, 1994.

Revel JP. Electron microscopy of glycogen. J Histochem Cytochem 12: 104-114, 1964.

Richter EA and Galbo H. High glycogen levels enhance glycogen breakdown in isolated contracting skeletal-muscle. J Appl Physiol 61: 827-831, 1986.

Robenek H, Hofnagel O, Buers I, Robenek MJ, Troyer D, Severs NJ. Adipophilin-enriched domains in the ER membrane are sites of lipid droplet biogenesis. J Cell Sci 119: 4215-4224, 2006.

Rodriguez NR, DiMarco NM, Langley S, Denny S, Hager MH, Manore MM, Myers E, Meyer N, Stevens J, Webber JA, Benedict R, Booth M, Chuey P, Erdman KA, Ledoux M, Petrie H, Lynch P, Mansfield E, Barr S, Benardot D, Berning J, Coggan A, Roy B, Vislocky LM, Amer Dietet A, Amer Coll Sports M, Dietitians C. Nutrition and Athletic Performance. Med Sci Sports Exerc 41: 709-731, 2009.

Roepstorff C, Steffensen CH, Madsen M, Stallknecht B, Kanstrup IL, Richter EA, Kiens B. Gender differences in substrate utilization during submaximal exercise in endurance-trained subjects. Am J Physiol-Endocrinol Metab 282: E435-E447, 2002.

Roepstorff C, Vistisen B, Donsmark M, Nielsen JN, Galbo H, Green KA, Hardie DG, Wojtaszewski JFP, Richter EA, Kiens B. Regulation of hormone-sensitive lipase activity and Ser(563) and Ser(565) phosphorylation in human skeletal muscle during exercise. J Physiol-London 560: 551-562, 2004.

Romijn JA, Coyle EF, Sidossis LS, Gastaldelli A, Horowitz JF, Endert E, Wolfe RR. Regulation of endogenous fat and carbohydrate metabolism in relation to exercise intensity and duration. Am J Physiol 265: E380-E391, 1993.

Romijn JA, Coyle EF, Sidossis LS, Zhang XJ, Wolfe RR. Relationship between fatty acid delivery and fatty acid oxidation during strenuous exercise. J Appl Physiol 79: 1939-1945, 1995.

Rybicka KK. Glycosomes - The organelles of glycogen metabolism. Tissue & Cell 28: 253-265, 1996.

Sacchetti M, Saltin B, Olsen DB, van Hall G. High triacylglycerol turnover rate in human skeletal muscle. J Physiol-London 561: 883-891, 2004.

Sacchetti M, Saltin B, Osada T, van Hall G. Intramuscular fatty acid metabolism in contracting and noncontracting human skeletal muscle. J Physiol-London 540: 387-395, 2002.

Saltin B, Nazar K, Costill DL, Stein E, Jansson E, Essen B, Gollnick PD. Nature of tranining response - peripheral and central adaptations to one-legged exercise. Acta Physiologica Scandinavica 96: 289-305, 1976.

Schaart G, Hesselink RP, Keizer HA, van Kranenburg G, Drost MR, Hesselink MKC. A modified PAS stain combined with immunofluorescence for quantitative analyses of glycogen in muscle sections. Histochem Cell Biol 122: 161-169, 2004.

Scharhag-Rosenberger F, Meyer T, Walitzek S, Kindermann W. Effects of One Year Aerobic Endurance Training on Resting Metabolic Rate and Exercise Fat Oxidation in Previously Untrained Men and Women Metabolic Endurance Training Adaptations. Int J Sports Med 31: 498-504, 2010.

Schenk S and Horowitz JF. Acute exercise increases triglyceride synthesis in skeletal muscle and prevents fatty acid-induced insulin resistance. J Clin Invest 117: 1690-1698, 2007.

Schweiger M, Schreiber R, Haemmerle G, Lass A, Fledelius C, Jacobsen P, Tornqvist H, Zechner R, Zimmermann R. Adipose triglyceride lipase and hormone-sensitive

lipase are the major enzymes in adipose tissue triacylglycerol catabolism. J Biol Chem 281: 40236-40241, 2006.

Seibert JT, Najt, C. P., Heden, T. D., Mashek, D. G., & Chow, L. S. Muscle Lipid Droplets: Cellular Signaling to Exercise Physiology and Beyond. Trends in Endocrinology & Metabolism 2020.

Shanely RA, Zwetsloot KA, Triplett NT, Meaney MP, Farris GE, Nieman DC. Human Skeletal Muscle Biopsy Procedures Using the Modified Bergstrom Technique. J Vis Exp 8, 2014.

Shaw C, Sherlock M, Stewart P, Wagenmakers A. Adipophilin distribution and colocalisation with lipid droplets in skeletal muscle. Histochem Cell Biol 131: 575-581, 2009.

Shaw CS, Clark J and Wagenmakers AJM. The Effect of Exercise and Nutrition on Intramuscular Fat Metabolism and Insulin Sensitivity. In: Annual Review of Nutrition. Annual Review of Nutrition, Vol 30, edited by Cousins RJ. Palo Alto: Annual Reviews, 2010, p. 13-34.

Shaw CS, Clark JA and Shepherd SO. HSL and ATGL: the movers and shakers of muscle lipolysis. J Physiol-London 591: 6137-6138, 2013.

Shaw CS, Jones DA and Wagenmakers AJM. Network distribution of mitochondria and lipid droplets in human muscle fibres. Histochem Cell Biol 129: 65-72, 2008.

Shaw CS, Shepherd SO, Wagenmakers AJM, Hansen D, Dendale P, van Loon LJC. Prolonged exercise training increases intramuscular lipid content and perilipin 2 expression in type I muscle fibers of patients with type 2 diabetes. Am J Physiol-Endocrinol Metab 303: E1158-E1165, 2012.

Shearer J and Graham TE. Novel aspects of skeletal muscle glycogen and its regulation during rest and exercise. Exercise and Sport Sciences Reviews 32: 120-126, 2004.

Shepherd SO, Cocks M, Meikle PJ, Mellett NA, Ranasinghe AM, Barker TA, Wagenmakers AJM, Shaw CS. Lipid droplet remodelling and reduced muscle ceramides following sprint interval and moderate-intensity continuous exercise training in obese males. Int J Obes 41: 1745-1754, 2017a.

Shepherd SO, Cocks M, Tipton KD, Ranasinghe AM, Barker TA, Burniston JG, Wagenmakers AJM, Shaw CS. Preferential utilization of perilipin 2-associated intramuscular triglycerides during 1 h of moderate-intensity endurance-type exercise. Exp Physiol 97: 970-980, 2012.

Shepherd SO, Cocks M, Tipton KD, Ranasinghe AM, Barker TA, Burniston JG, Wagenmakers AJM, Shaw CS. Sprint interval and traditional endurance training increase net intramuscular triglyceride breakdown and expression of perilipin 2 and 5. J Physiol-London 591: 657-675, 2013.

Shepherd SO, Strauss JA, Wang Q, Dube JJ, Goodpaster B, Mashek DG, Chow LS. Training alters the distribution of perilipin proteins in muscle following acute free fatty acid exposure. J Physiol-London 595: 5587-5601, 2017b.

Shulman RG and Rothman DL. The "glycogen shunt" in exercising muscle: A role for glycogen in muscle energetics and fatigue. Proc Natl Acad Sci U S A 98: 457-461, 2001.

Sjostrom M, Angquist KA, Bylund AC, Friden J, Gustavsson L, Schersten T. Morphometric analyses of human-muscle fiber types. Muscle Nerve 5: 538-553, 1982b.

Sjostrom M, Friden J and Ekblom B. Fine-structural details of human-muscle fibres after fiber type specific glycogen depletion. Histochemistry 76: 425-438, 1982a.

Skinner JR, Shew TM, Schwartz DM, Tzekov A, Lepus CM, Abumrad NA, Wolins NE. Diacylglycerol Enrichment of Endoplasmic Reticulum or Lipid Droplets Recruits Perilipin 3/TIP47 during Lipid Storage and Mobilization. J Biol Chem 284: 30941-30948, 2009.

Spangenburg EE, Pratt SJP, Wohlers LM, Lovering RM. Use of BODIPY (493/503) to Visualize Intramuscular Lipid Droplets in Skeletal Muscle. J Biomed Biotechnol 8, 2011.

Spriet LL. New Insights into the Interaction of Carbohydrate and Fat Metabolism During Exercise. Sports Med 44: 87-96, 2014.

Spriet LL, Ren JM and Hultman E. Ephinephrine infusion enhances muscle glycogenolysis during prolonged electircal-stimulation. J Appl Physiol 64: 1439-1444, 1988.

Starling RD, Trappe TA, Parcell AC, Kerr CG, Fink WJ, Costill DL. Effects of diet on muscle triglyceride and endurance performance. J Appl Physiol 82: 1185-1189, 1997.

Staron RS, Hagerman FC, Hikida RS, Murray TF, Hostler DP, Crill MT, Ragg KE, Toma K. Fiber type composition of the vastus lateralis muscle of young men and women. J Histochem Cytochem 48: 623-629, 2000.

Steffensen CH, Roepstorff C, Madsen M, Kiens B. Myocellular triacylglycerol breakdown in females but not in males during exercise. Am J Physiol-Endocrinol Metab 282: E634-E642, 2002.

Stellingwerff T, Boon H, Jonkers RAM, Senden JM, Spriet LL, Koopman R, van Loon LJC. Significant intramyocellular lipid use during prolonged cycling in endurance-trained males as assessed by three different methodologies. Am J Physiol-Endocrinol Metab 292: E1715-E1723, 2007.

Stone SJ, Levin MC, Zhou P, Han JY, Walther TC, Farese RV. The Endoplasmic Reticulum Enzyme DGAT2 Is Found in Mitochondria-associated Membranes and Has a Mitochondrial Targeting Signal That Promotes Its Association with Mitochondria. J Biol Chem 284: 5352-5361, 2009.

Strauss JA, Shepherd DA, Macey M, Jevons EFP, Shepherd SO. Divergence exists in the subcellular distribution of intramuscular triglyceride in human skeletal muscle dependent on the choice of lipid dye. Histochem Cell Biol 154: 369-382, 2020.

Szczepaniak LS, Babcock EE, Schick F, Dobbins RL, Garg A, Burns DK, McGarry JD, Stein DT. Measurement of intracellular triglyceride stores by H-1 spectroscopy: validation in vivo. Am J Physiol-Endocrinol Metab 276: E977-E989, 1999.

Sztalryd C and Brasaemle DL. The perilipin family of lipid droplet proteins: Gatekeepers of intracellular lipolysis. Biochim Biophys Acta Mol Cell Biol Lipids 1862: 1221-1232, 2017.

Taschler U, Radner FPW, Heier C, Schreiber R, Schweiger M, Schoiswohl G, Preiss-Landl K, Jaeger D, Reiter B, Koefeler HC, Wojciechowski J, Theussl C, Penninger JM, Lass A, Haemmerle G, Zechner R, Zimmermann R. Monoglyceride Lipase Deficiency in Mice Impairs Lipolysis and Attenuates Diet-induced Insulin Resistance. J Biol Chem 286: 17467-17477, 2011.

Taylor C, Bartlett JD, van de Graaf CS, Louhelainen J, Coyne V, Iqbal Z, MacLaren DPM, Gregson W, Close GL, Morton JP. Protein ingestion does not impair exercise-induced AMPK signalling when in a glycogen-depleted state: implications for train-low compete-high. Eur J Appl Physiol 113: 1457-1468, 2013.

Tsintzas OK, Williams C, Boobis L, Greenhaff P. Carbohydrate ingestion and glycogen utilisation in different muscle-fiber types in man. J Physiol-London 489: 243-250, 1995.

Turcotte LP, Richter EA and Kiens B. Increased plasma FFA uptake and oxidation during prolonged exercise in trained vs untrained humans. Am J Physiol 262: E791-E799, 1992.

Turnbull PC, Longo AB, Ramos SV, Roy BD, Ward WE, Peters SJ. Increases in skeletal muscle ATGL and its inhibitor G0S2 following 8 weeks of endurance training in metabolically different rat skeletal muscles. Am J Physiol-Regul Integr Comp Physiol 310: R125-R133, 2016.

van Loon LJC. Intramyocellular triacylglycerol as a substrate source during exercise. Proc Nutr Soc 63: 301-307, 2004.

van Loon LJC and Goodpaster BH. Increased intramuscular lipid storage in the insulin-resistant and endurance-trained state. Pflugers Arch 451: 606-616, 2006.

van Loon LJC, Greenhaff PL, Teodosiu DC, Saris WHM, Wagenmakers AJM. The effects of increasing exercise intensity on muscle fuel utilisation in humans. J Physiol-London 536: 295-304, 2001.

van Loon LJC, Koopman R, Stegen J, Wagenmakers AJM, Keizer HA, Saris WHM. Intramyocellular lipids form an important substrate source during moderate intensity exercise in endurance-trained males in a fasted state. J Physiol-London 553: 611-625, 2003a.

van Loon LJC, Saris WHM, Kruijshoop M, Wagenmakers AJM. Maximizing postexercise muscle glycogen synthesis: carbohydrate supplementation and the application of amino acid or protein hydrolysate mixtures. Am J Clin Nutr 72: 106-111, 2000.

van Loon LJC, Schrauwen-Hinderling VB, Koopman R, Wagenmakers AJM, Hesselink MKC, Schaart G, Kooi ME, Saris WHM. Influence of prolonged endurance cycling and recovery diet on intramuscular triglyceride content in trained males. Am J Physiol-Endocrinol Metab 285: E804-E811, 2003b.

Van Proeyen K, Szlufcik K, Nielens H, Ramaekers M, Hespel P. Beneficial metabolic adaptations due to endurance exercise training in the fasted state. J Appl Physiol 110: 236-245, 2011.

Vanderlaarse WJ, Vannoort P and Diegenbach PC. Calibration of quantitative histochemical methods - estimation of glycogen-content of muscle-fibres using the PAS reaction. Biotech Histochem 67: 303-308, 1992.

Villena JA, Roy S, Sarkadi-Nagy E, Kim KH, Sul HS. Desnutrin, an adipocyte gene encoding a novel patatin domain-containing protein, is induced by fasting and glucocorticoids. J Biol Chem 279: 47066-47075, 2004.

Vissing K, Andersen JL and Schjerling P. Are exercise-induced genes induced by exercise? Faseb J 18: 94-+, 2004.

Vogt M, Puntschart A, Howald H, Mueller B, Mannhart C, Gfeller-Tuescher L, Mullis P, Hoppeler H. Effects of dietary fat on muscle substrates, metabolism, and performance in athletes. Med Sci Sports Exerc 35: 952-960, 2003.

Volek JS, Noakes T and Phinney SD. Rethinking fat as a fuel for endurance exercise. Eur J Sport Sci 15: 13-20, 2015.

Vollestad NK, Vaage O and Hermansen L. Muscle glycogen depletion patterns in type I and subgroups of type II fibres during prolonged severe exercise in man. Acta Physiologica Scandinavica 122: 433-441, 1984.

Wang H, Sreenevasan U, Hu H, Saladino A, Polster BM, Lund LM, Gong DW, Stanley WC, Sztalryd C. Perilipin 5, a lipid droplet-associated protein, provides physical and metabolic linkage to mitochondria. J Lipid Res 52: 2159-2168, 2011.

Watt MJ, Heigenhauser GJF, Dyck DJ, Spriet LL. Intramuscular triacylglycerol, glycogen and acetyl group metabolism during 4 h of moderate exercise in man. J Physiol-London 541: 969-978, 2002.

Watt MJ, Heigenhauser GJF and Spriet LL. Effects of dynamic exercise intensity on the activation of hormone-sensitive lipase in human skeletal muscle. J Physiol-London 547: 301-308, 2003.

Watt MJ, Holmes AG, Pinnamaneni SK, Garnham AP, Steinberg GR, Kemp BE, Febbraio MA. Regulation of HSL serine phosphorylation in skeletal muscle and adipose tissue. Am J Physiol-Endocrinol Metab 290: E500-E508, 2006.

Watt MJ, Steinberg GR, Chan S, Garnham A, Kemp BE, Febbraio MA. beta-adrenergic stimulation of skeletal muscle HSL can be overridden by AMPK signaling. Faseb J 18: 1445-+, 2004.

Welte MA. Fat on the move: intracellular motion of lipid droplets. Biochemical Society Transactions 37: 991-996, 2009.

Wendling PS, Peters SJ, Heigenhauser GJF, Spriet LL. Variability of triacylglycerol content in human skeletal muscle biopsy samples. J Appl Physiol 81: 1150-1155, 1996.

Whytock KL, Shepherd SO, Cocks M, Wagenmakers AJM, Strauss JA. Young, healthy males and females present cardiometabolic protection against the detrimental effects of a 7-day high-fat high-calorie diet. European Journal of Nutrition 13, 2020.

Whytock KL, Shepherd SO, Wagenmakers AJM, Strauss JA. Hormone-sensitive lipase preferentially redistributes to lipid droplets associated with perilipin-5 in human skeletal muscle during moderate-intensity exercise. J Physiol-London 596: 2077-2090, 2018.

Winter EM JA, Davidson RCR, Bromley PD, Mercer TH. Sport and exercise physiology testing guidelines: Volume 1 – Sport Testing. UK: Routledge 2007, p. 112.

Wojtaszewski JFP, Jorgensen SB, Hellsten Y, Hardie DG, Richter EA. Glycogen-dependent effects of 5-aminoimidazole-4-carboxamide (AICA)-riboside on AMP-activated protein kinase and glycogen synthase activities in rat skeletal muscle. Diabetes 51: 284-292, 2002.

Wojtaszewski JFP, MacDonald C, Nielsen JN, Hellsten Y, Hardie DG, Kemp BE, Kiens B, Richter EA. Regulation of 5 ' AMP-activated protein kinase activity and substrate utilization in exercising human skeletal muscle. Am J Physiol-Endocrinol Metab 284: E813-E822, 2003.

Wolins NE, Quaynor BK, Skinner JR, Schoenfish MJ, Tzekov A, Bickel P. S3-12, adipophilin, and TIP47 package lipid in adipocytes. J Biol Chem 280: 19146-19155, 2005.

Wolins NE, Quaynor BK, Skinner JR, Tzekov A, Croce MA, Gropler MC, Varma V, Yao-Borengasser A, Rasouli N, Kern PA, Finck BN, Bickel PE. OXPAT/PAT-1 is a PPAR-induced lipid droplet protein that promotes fatty acid utilization. Diabetes 55: 3418-3428, 2006.

Wolins NE, Rubin D and Brasaemle DL. TIP47 associates with lipid droplets. J Biol Chem 276: 5101-5108, 2001.

Wolins NE, Skinner JR, Schoenfish MJ, Tzekov A, Bensch KG, Bickel PE. Adipocyte protein S3-12 coats nascent lipid droplets. J Biol Chem 278: 37713-37721, 2003.

Xie X, Langlais P, Zhang X, Heckmann BL, Saarinen AM, Mandarino LJ, Liu J. Identification of a novel phosphorylation site in adipose triglyceride lipase as a regulator of lipid droplet localization. Am J Physiol-Endocrinol Metab 306: E1449-E1459, 2014.

Xu GH, Sztalryd C, Lu XY, Tansey JT, Gan JW, Dorward H, Kimmel AR, Londos C. Post-translational regulation of adipose differentiation-related protein by the ubiquitin/proteasome pathway. J Biol Chem 280: 42841-42847, 2005.

Yaspelkis BB, Patterson JG, Anderla PA, Ding Z, Ivy JL. Carbohydrate supplementation spares muscle glycogen during variable-intensity exercise. J Appl Physiol 75: 1477-1485, 1993.

Zderic TW, Davidson CJ, Schenk S, Byerley LO, Coyle EF. High-fat diet elevates resting intramuscular triglyceride concentration and whole body lipolysis during exercise. Am J Physiol-Endocrinol Metab 286: E217-E225, 2004.

Zhang HN, Wang Y, Li J, Yu JH, Pu J, Li LH, Zhang HC, Zhang SY, Peng G, Yang FQ, Liu PS. Proteome of Skeletal Muscle Lipid Droplet Reveals Association with Mitochondria and Apolipoprotein A-I. J Proteome Res 10: 4757-4768, 2011.

Zimmermann R, Strauss JG, Haemmerle G, Schoiswohl G, Birner-Gruenberger R, Riederer M, Lass A, Neuberger G, Eisenhaber F, Hermetter A, Zechner R. Fat mobilization in adipose tissue is promoted by adipose triglyceride lipase. Science 306: 1383-1386, 2004.